EARLY-AGE CRACKING OF MASS CONCRETE STRUCTURES

Except where reference is made to the work of others, the work described in this thesis is my own or was done in collaboration with my advisory committee. This thesis does not include proprietary or classified information.

Jason Lee Meadows

Certificate of Approval:

| | |
|---|---|
| G. Ed Ramey<br>Professor<br>Civil Engineering | Anton K. Schindler, Chair<br>Gottlieb Assistant Professor<br>Civil Engineering |
| Robert W. Barnes<br>Associate Professor<br>Civil Engineering | George T. Flowers<br>Interim Dean<br>Graduate School |

# EARLY-AGE CRACKING OF MASS CONCRETE STRUCTURES

Jason Lee Meadows

A Thesis

Submitted to

the Graduate Faculty of

Auburn University

in Partial Fulfillment of the

Requirements for the

Degree of

Master of Science

Auburn, Alabama
May 10, 2007

EARLY-AGE CRACKING OF MASS CONCRETE STRUCTURES

Jason Lee Meadows



_____
Signature of Author

_____
Date of Graduation

THESIS ABSTRACT

EARLY-AGE CRACKING OF MASS CONCRETE STRUCTURES

Jason Lee Meadows

Master of Science, May 10, 2007
(B.C.E., Auburn University, 2005)

252 Typed Pages

Directed by Anton K. Schindler

Early-age cracking is a recurring problem in many mass concrete structures. Currently agencies tend only to limit the maximum temperature difference that may develop in a mass concrete structure in an attempt to mitigate this distress. A maximum temperature difference of 35°F is most often used irrespective of the materials used or placement conditions. Although early-age cracking has been documented since the early 20$^{th}$ century, explorations into this problem have just recently begun in the U.S. The primary objective of this thesis is to evaluate the early-age cracking tendency of mass concrete.

The research presented in this thesis involved implementation of one match-cured rigid cracking frame, one isothermal rigid cracking frame, and a match-cured free shrinkage frame to explore early-age cracking mechanisms of mass concrete. The rigid

cracking frames were used to evaluate the development of restrained stresses due to thermal and autogenous deformations. The free shrinkage frame was used to evaluate the thermal and autogenous deformations under zero stress conditions. The laboratory testing program was designed to evaluate the effects of placement temperature, ambient temperature, cement type, supplementary cementing materials, air entrainment, and water-to-cementitious ratio on the cracking tendency of mass concrete mixtures.

The laboratory testing program revealed that the heat generated during hydration greatly affects the restrained stress development of concrete. Measures such as variations of placement and ambient temperature as well as use of supplementary cementing materials were found to be the most effective means of reducing heat generation in mass concrete thus reducing restraint stresses.

The behavior of concrete under isothermal conditions was also investigated. The isothermal cracking frame was held at a constant temperature for the duration of the test. Water-to-cement ratio was found to be the most significant variable controlling the magnitude of stress development associated with autogenous shrinkage. The use of supplementary cementing materials to partially replace portland cement was found to mitigate autogenous shrinkage deformations.

ACKNOWLEDGMENTS

I sincerely thank my advisor Dr. Anton Schindler. His technical guidance, time, and friendship have been greatly appreciated. Billy Wilson, graduate students, and undergraduate assistants deserve thanks, for without them this project would never have been completed.

I thank Drs. Kevin Folliard and Maria G. C. Juenger from The University of Texas at Austin. Their intellectual interactions with Auburn University and financial support have made this project possible. I thank Kyle Riding and Jon Poole from The University of Texas at Austin for their assistance, time, and energy. I also thank the Texas Department of Transportation for their support and funding, which made this project possible.

I also thank my family and friends. Their support and encouragement have been greatly appreciated. Finally, I would like to thank my wife, Rebecca for all her love, support, and patience. The sacrifices she has made to make this possible are deeply appreciated.

Style manual or journal used Chicago Manual of Style

Computer software used Microsoft® Word, Microsoft® Excel

TABLE OF CONTENTS

LIST OF TABLES

LIST OF FIGURES

# CHAPTER 1

# INTRODUCTION

## 1.1 BACKGROUND

Early-age cracking in mass concrete structures has been a well documented occurrence since the early 1900s (ACI 207.1R 1996). Engineers and researchers began documenting early-age cracking concerns stemming from the generation of heat during hydration. Measures, such as placing pipes with circulated chilled water in the Hoover dam, have long been implemented to counteract the development of thermal gradients (ACI 207.1R 1996).

Large concrete structures such as bridge abutments, foundations, and dam walls are generally considered to be mass concrete. According to the Florida Department of Transportation (FDOT), mass concrete is defined as "any large volume of cast-in place or precast concrete with dimensions large enough to require that measures be taken to cope with the generation of heat and attendant volume change so as to minimize cracking" (FDOT 2002). The Texas Department of Transportation (TxDOT), defines mass concrete as "placements with at least one cross-sectional dimension greater than or equal to 5 ft" (TxDOT 2004).

As young concrete matures, heat is generated due to hydration of the cement and water. As the heat of hydration subsides, the concrete member begins to cool to reach

equilibrium with the ambient conditions. The exterior portion of the member cools much faster than the interior, resulting in thermal gradients. Non-uniform cooling across the cross section of the member produces substantial strains. As the concrete matures, it develops stiffness, which leads to the development of stresses when coupled with restrained deformations. Cracking initiates once stresses exceed the tensile stress capacity of the concrete.

Thermal deformations are important when evaluating the cracking susceptibility of concrete mixtures; however, many other variables may affect the volume change in concrete. Drying, autogenous, and chemical shrinkage have been found to cause early-age volume changes in mass concrete. Autogenous shrinkage was documented for the first time in the 1930s by Lynam (1934). At that time, autogenous shrinkage was thought to only occur at very low water-to-cement ratios that were beyond the practical range of concrete. But with the advancement of chemical admixtures, low water-to-cement ratios are very common in modern construction.

In order to evaluate the cracking sensitivity of concrete mixtures, all of the mechanisms driving early-age cracking must be thoroughly examined. The factors producing early-age volume change must not be assumed to work independently of one another. Early-age cracking has become a recurring problem in many mass concrete structures. Early-age cracking can be found in foundations, large columns, bridge decks, and pavements. It has become a major concern because it may lead to durability problems in severe environments. Increased permeability from cracks decreases the service-life of the concrete. Corrosion of reinforcing steel due to permeability is a major problem in

cold and marine environments. This problem can be aggrevated by early-age cracking and may result in premature failure of the structure.

A survey conducted by the Federal Highway Administration (FHWA) found that more than 100,000 bridges suffered from early-age cracking (FHWA 2005). Cracking originated from restraint conditions at the girder and bridge deck interface which prevented deformations due to thermal movements. The transportation agencies that responded to the poll found that weather conditions during placement greatly influenced cracking (Krauss and Rogalla 1996). Cracking was found to be worse in low humidity conditions and when concrete was cast at low or hot temperatures (Krauss and Rogalla 1996). Thus, there is a great need to investigate the mechanisms creating early-age volume change and restraint stresses.

## 1.2 RESEARCH OBJECTIVE

The objective of this project is to evaluate the effects of placement temperature, ambient temperature, cement type, cementitious materials, air entrainment, and water-to-cementitious ratio on the cracking tendency of concrete mixtures.

## 1.3 RESEARCH APPROACH

This project implements the use of one match-cured rigid cracking frame, one isothermal rigid cracking frame, and a match-cured free shrinkage frame to evaluate the cracking susceptibility of concrete mixtures. The rigid cracking frames were used to evaluate the development of restrained stresses due to thermal and autogenous deformations. The free shrinkage frame was used to evaluate the thermal and autogenous deformation under zero

stress conditions. This study consists of an evaluation of how certain variables affect early-age cracking. This evaluation provides engineers with knowledge of how to mitigate this distress. The research found in this thesis is part of a larger ongoing project. The data obtained from this study will be used to calibrate models as part of the larger project.

## 1.4 SCOPE OF REPORT

Chapter 2 of this report provides a thorough discussion of the early-age cracking phenomenon. The discussion includes development of heat of hydration, maturity concepts, development of mechanical properties, early-age volume change, early-age creep behavior, and the rigid cracking frame as a method of assessing early-age cracking.

Chapter 3 documents and discusses the experimental laboratory testing program. It includes the laboratory testing setup and materials.

Chapter 4 presents all the results obtained from the execution of the laboratory testing program. It presents the development of mechanical properties, results from the rigid cracking frame, and results from the free shrinkage frame.

Chapter 5 provides a thorough discussion of the laboratory testing results presented in Chapter 4. Stress development due to thermal and autogenous deformations is thoroughly discussed.

Chapter 6 offers conclusions and recommendations resulting from the work documented in this thesis.

Appendix A contains additional design drawings of the free shrinkage frame as well as additional testing and preparation pictures.

Appendix B contains fresh concrete properties for each concrete batch. It includes slump, unit weight, air content, temperature, and setting times.

Appendix C contains results obtained from the isothermal rigid cracking frame.

Appendix D summarizes all the hydration parameters used in the temperature development program.

# CHAPTER 2

# LITERATURE REVIEW

Early-age cracking in mass concrete is a severe problem that reduces the structure's functional life. Cracking originates from stresses induced by volume change as a result of thermal, drying, autogenous, and chemical shrinkage coupled with restraint conditions that prevent movement of the concrete. These stresses develop due to strains that are induced by early-age volume change as the concrete stiffness increases. Over time, stresses may exceed the tensile strength of the concrete, which will result in cracking. The mechanisms driving early-age cracking are influenced by many complex variables, and many of these mechanisms are not clearly understood. In order to better understand the mechanisms driving early-age cracking, the variables that influence the cracking sensitivity of the concrete must be studied. The current state of knowledge regarding these mechanisms and variables is reviewed in this chapter.

## 2.1 HYDRATION OF CEMENTITIOUS MATERIALS

The hydration of portland cement is an exothermic chemical reaction. Heat generated from this reaction may affect the in-place characteristics of various structures (Schindler and Folliard 2005). Many variables affect the heat generated during this hydration process. Factors such as cement composition, mixture proportions, replacement of

cement by supplementary cementing materials (SCMs), and curing temperature can increase or decrease the rate of heat generated during hydration. As a result of the excessive heat that can be generated and non-uniform cooling, thermal gradients occur inside massive concrete elements. This uneven distribution of heat can lead to thermal deformations which, when restrained, can introduce cracking long before the structure is exposed to externally applied loads.

### 2.1.1 CEMENT COMPOSITION

Cement composition is a major contributor to heat of hydration. Variables such as chemical composition and fineness affect the temperature rise of concrete. Some of these factors can be varied as temperature control techniques while others must be accepted as given conditions.

#### 2.1.1.1 Chemical Composition

Portland cement is primarily composed of four principle chemical compounds or Bogue compounds. These are tricalcium silicate ($C_3S$), dicalcium silicate ($C_2S$), tricalcium aluminate ($C_3A$), and tetracalcium aluminoferrite ($C_4AF$). The relative proportions of these chemical compounds and their fineness determine the different types of cement as well as the amount of heat they generate during hydration (Bjøntegaard 1999).

The hydration of cement is a mixture of simultaneous and consecutive reactions (Bjøntegaard 1999). $C_3A$, which forms ettringite, is the first Bogue compound to hydrate. The reaction of $C_3A$ is followed by the hydration of $C_3S$. Finally, $C_3A$ and $C_4AF$ react simultaneously after $C_3S$.

Figure 2-1 demonstrates the heat evolution of cement as it hydrates. The initial reaction (I) is caused by the reaction of $C_3A$ forming ettringite. This process is very fast and a dormant period follows. After the dormant period, the second heat peak (II) is the hydration of $C_3S$. The last heat peak (III) is produced by the transformation of ettringite to monosulfate (Bjøntegaard 1999).

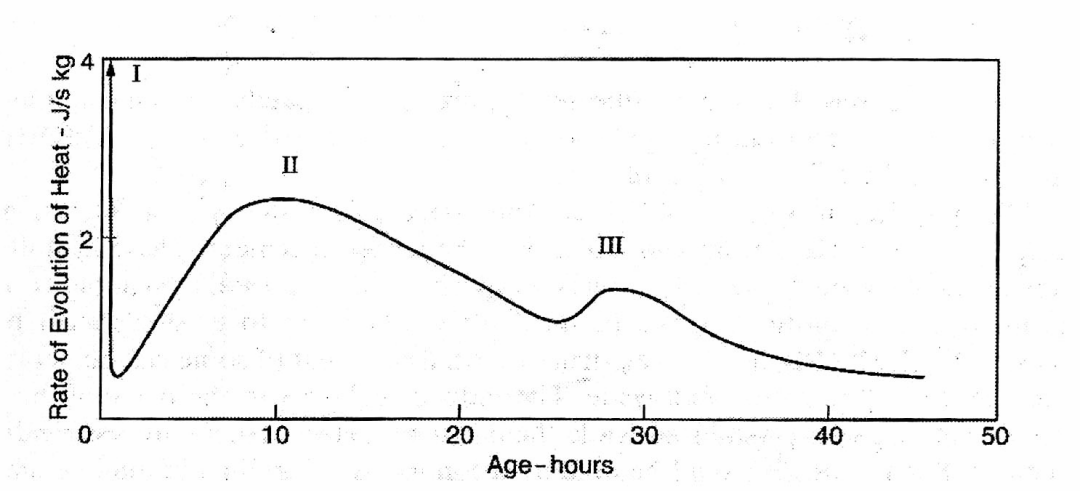


**Figure 2-1:** Heat evolution of hydrating cement (Bjøntegaard 1999)

As discussed above, the chemical reaction between cement and water is highly exothermic. Each of the Bogue compounds when fully hydrated releases relatively large amounts of heat. Table 2-1 describes the heat evolution of the four primary chemical compounds.

**Table 2-1:** Heat evolution of Bogue compounds (Bogue 1929)

| Compound | Heat evolution after complete hydration (J/g) | Rate of reaction with water |
|---|---|---|
| $C_3S$ | 500 | "medium" |
| $C_2S$ | 260 | "slow" |
| $C_3A$ | 866 | "fast" |
| $C_4AF$ | 125 | "medium" |

As shown in Table 2-1, the Bogue compounds generate large amounts of heat. Figure 2-2 demonstrates the effect of cement type on temperature rise due to the variations of the Bogue compounds.

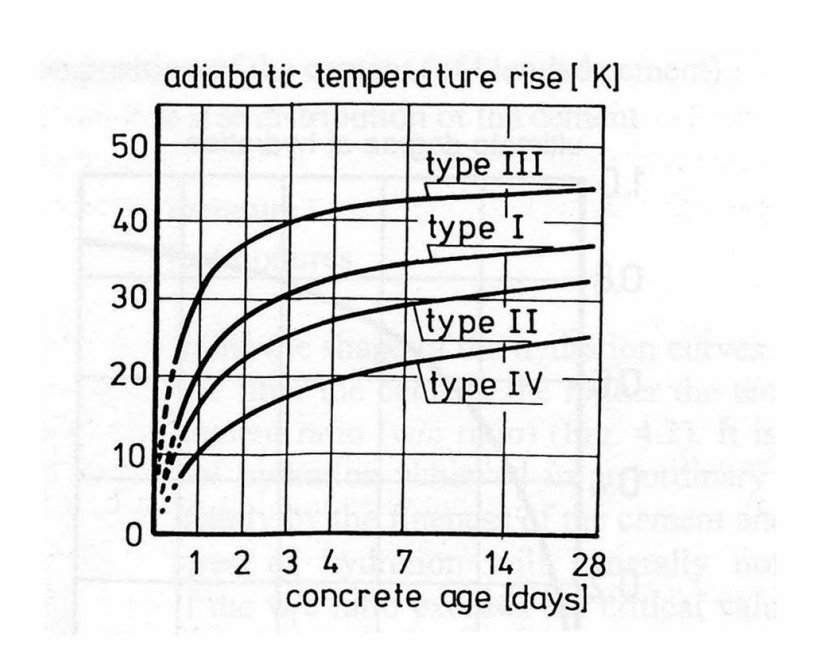


**Figure 2-2:** Adiabatic temperature rise in various types of cement (ACI 207.2R 1973)

Type I cement is the standard cement and is most commonly used in general construction applications in the United States (ACI 116R 1997). Type II and IV cements are low-heat generating cements during early-ages due to relatively low $C_3A$ and high $C_4AF$ content (Townsend 1965). Type III cement is high early-age strength cement due to high $C_3A$ content and fineness, which generates much more heat during hydration than Type I, II, or IV.

#### 2.1.1.2 Fineness

Cement fineness is a variable of hydration that affects the rate of heat generation rather than the magnitude of heat generation (ACI 207.2R 1997). The higher the fineness the more surface area the cement has to react with the water and hydrate as shown in Figure 2-3. The U.S. Bureau of Reclamation states that a "higher fineness increases the rate at which cement hydrates, causing greater early strength and more rapid generation of heat" (USBR 1975). Type III cement is usually associated with a high heat of hydration primarily due to high $C_3A$ content and fineness.

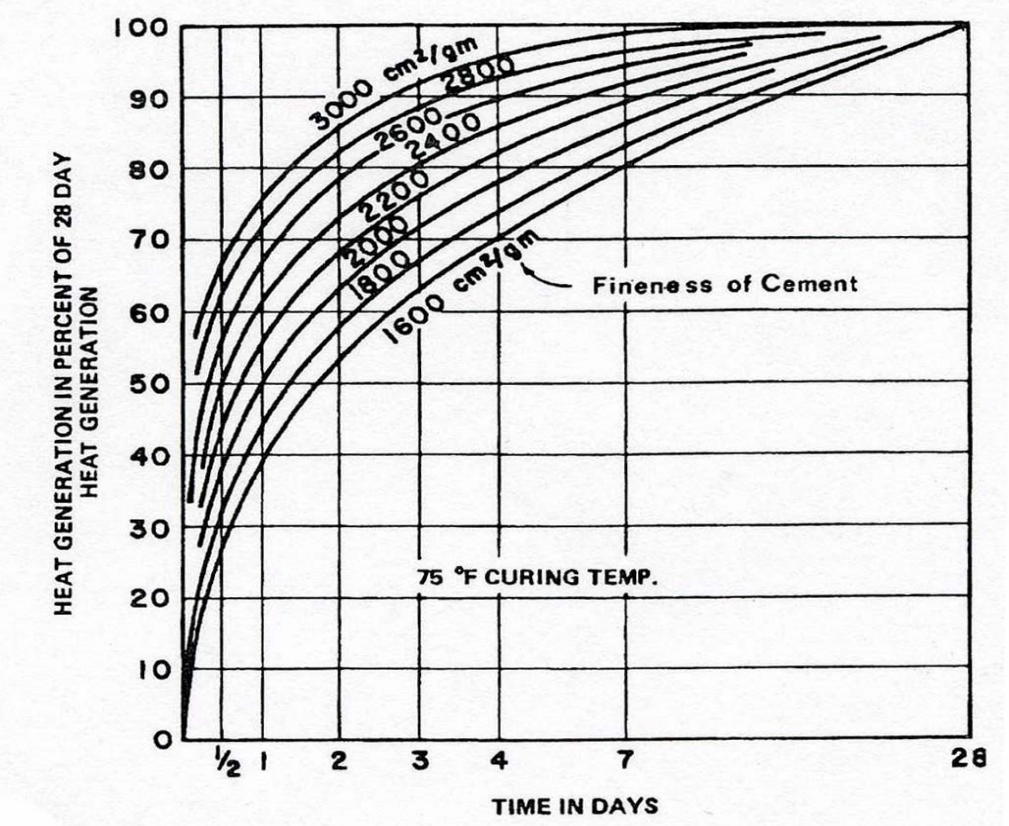


**Figure 2-3:** Effect of fineness of cement on rate of heat generation (ACI 207-2R 1997)

### 2.1.2 MIXTURE PROPORTIONS

The rate and magnitude of heat generation is affected by the quantity of cement used (ACI 207.2R 1997). "It is apparent that the total cement hydration heat of a concrete mix depends on the cement type and content" (Wang and Dilger 1994). This is due to the quantity of reactive products that are available to hydrate and liberate heat. The higher the cement content, the greater the likelihood of temperature rise.

### 2.1.3 REPLACEMENT OF CEMENT WITH SUPPLEMENTARY CEMENTING MATERIALS

To reduce the amount of heat liberated during the hydration of cement, some supplementary cementing materials (SCMs) can be used as a replacement for portland cement. SCMs such as fly ash and ground granulated blast furnace slag (GGBF Slag) have been found to be effective means of reducing the quantity of cement, therefore reducing the heat due to hydration (ACI 207.2R 1997). Springenschmid and Breitenbucher (1998) stated that it is current practice to reduce the cement content as much as possible in order to reduce heat development.

#### 2.1.3.1 Fly Ash

Fly ash is used for mass concrete due to its effect on workability as well as its low heat of hydration (Sakai et al. 2005). Fly ash comes from many different sources. Due to different source locations, the calcium oxide (CaO) content of the fly ash can be used as an indicator of its cementitious nature (Schindler and Folliard 2005).

Class C fly ash is classified as fly ash containing more than 20% of CaO. Class F fly ash contains less than 15% CaO (ACI 232.2R 1997). Class F fly ash is generally more pozzolanic in nature as compared to Class C fly ash, which is more cementitious. Therefore Class F fly ash reduces the total heat of hydration more than Class C. Figure 2-4 and 2-5 demonstrate the reduction in heat liberation due to hydration of cementitious systems containing fly ash and cement-only systems.

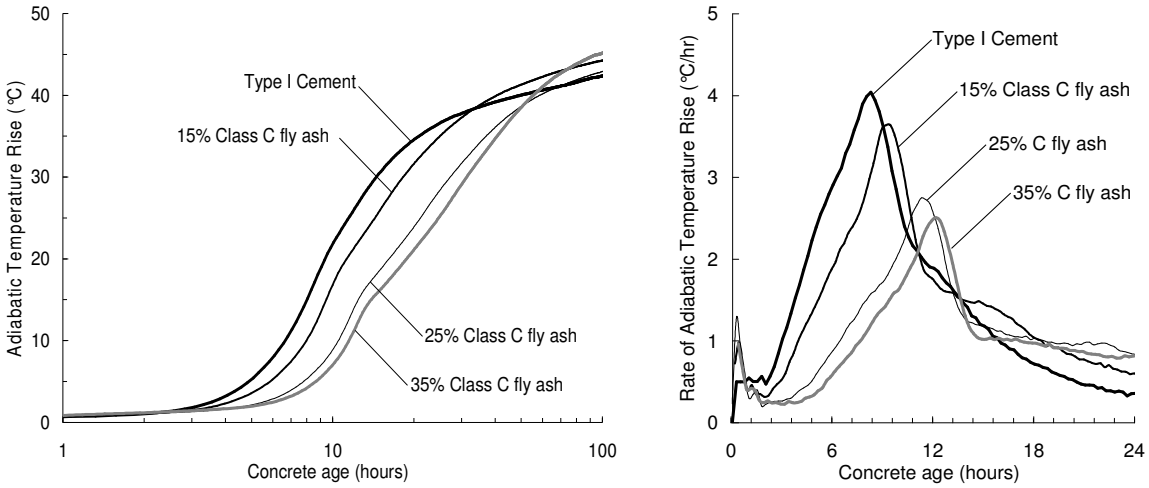


**Figure 2-4:** Total temperature rise and rate of temperature rise using Class C fly ash as a replacement (Schindler and Folliard 2005)

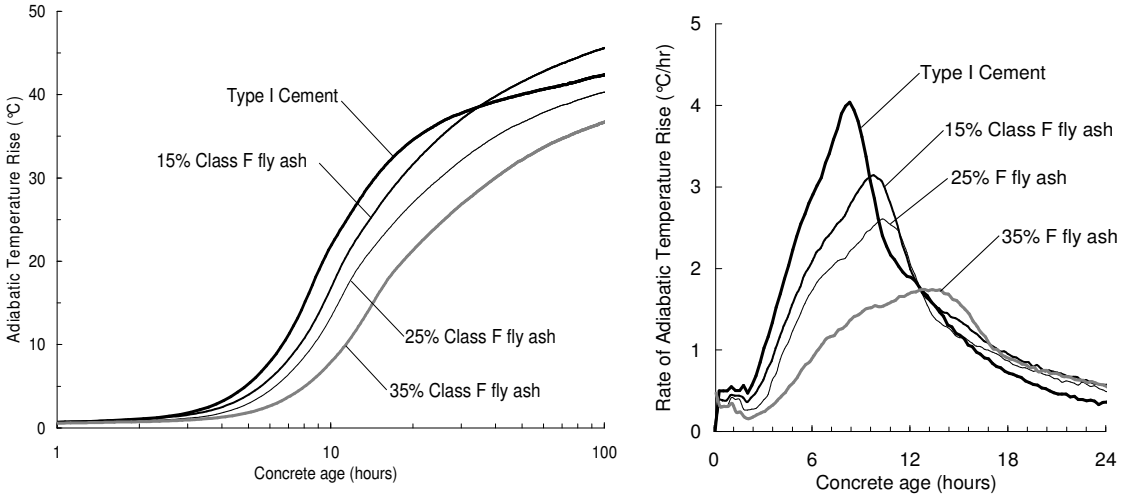


**Figure 2-5:** Total temperature rise and rate of temperature rise using Class F fly ash as a replacement (Schindler and Folliard 2005)

### 2.1.3.2 GGBF Slag

Slag has been used effectively to mitigate the temperature rise in mass concrete (Bamforth 1980 and Fulton 1974). The reduction of early-age heat generation is directly proportional to the slag quantity used (ACI 233R 1997). The peak temperature rise is delayed due to the inclusion of slag (Sioulas and Sanjayan 2000). This is primarily due to the activation energy of the slag which increases or reduces the rate of hydration depending on the curing temperature.

Mixtures containing slag have reduced the heat liberated during hydration. Slag mixtures containing more than 75% slag as replacement liberate approximately the same amount of heat as a 30% Class C fly ash mixture at seven days (Bamforth 1980). The reduction of heat of hydration can be seen in Figure 2-6.

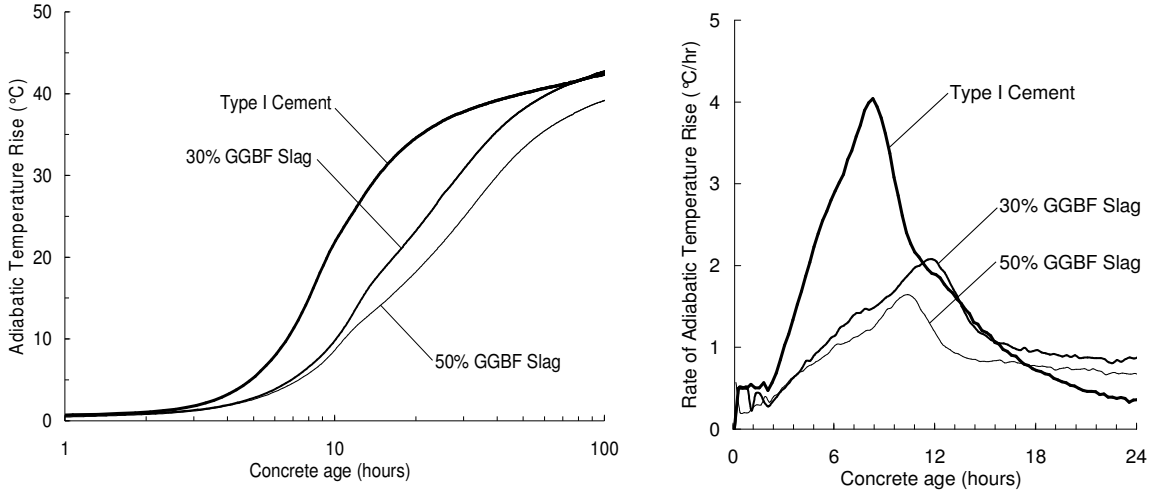


**Figure 2-6:** Total temperature rise and rate of temperature rise using GGBF slag as a replacement (Schindler and Folliard 2005)

### 2.1.4 CURING TEMPERATURE

The curing temperature has a direct influence on the rate of hydration. If the curing temperature is increased, then the rate of hydration is increased. As placement temperatures increase, adiabatic temperature rises faster due to the acceleration of hydration. The effect of placement temperature on heat development can be seen in Figure 2-7.

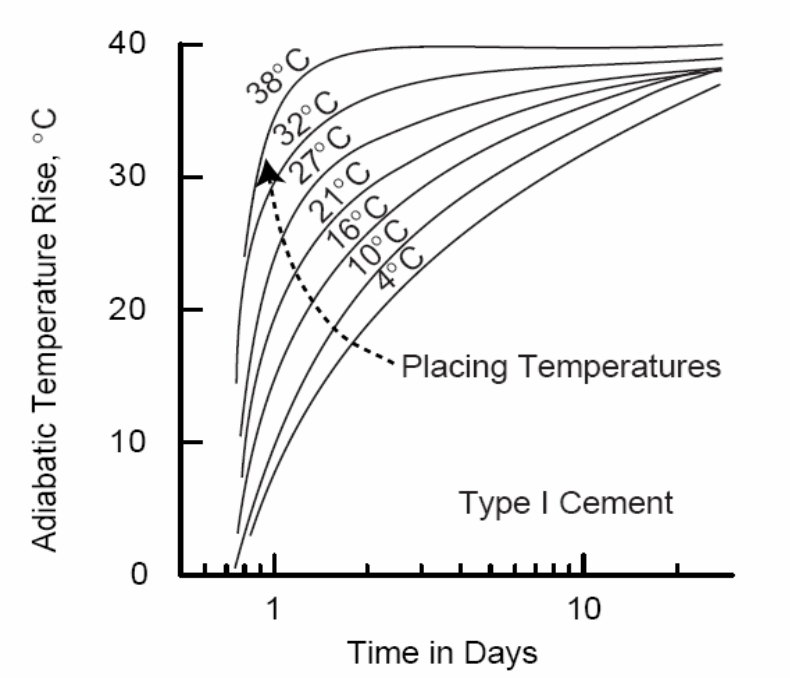


**Figure 2-7:** Effect of placement temperature on temperature rise (ACI Committee 207 1995)

## 2.2 MATURITY CONCEPTS

Carino and Lew (2001) state that "the maturity method is a technique to account for the combined effects of time and temperature on the strength development of concrete". The maturity method is used to estimate in-place strength development of concrete under variable temperature conditions. These variable temperature conditions are a result of heat of hydration, placement temperature, and heat transfer from and to the environment. Therefore, the maturity method can be a useful tool in assessing the in-place strength development of mass concrete structures. It forecasts the evolution of compressive and tensile strength which allows estimation of the correct time of form removal to ensure that the concrete has reached adequate strength to resist early-age cracking.

### 2.2.1 NURSE-SAUL MATURITY FUNCTION

As previously discussed, concrete hydration is a function of time and temperature. Therefore, to determine strength at any given age, time is not sufficient to estimate strength (Waller et al. 2004). This led to the idea of the Nurse-Saul maturity function (ASTM C 1074 2004):

$$M = \sum_{0}^{t} (T - T_0)\Delta t \qquad \textit{Equation 2-1}$$

where,

M = maturity index (°C-hours),

T = average concrete temperature (°C) during the time interval (Δt),

$T_0$ = datum temperature (°C),

t = elapsed time (hours), and

$\Delta t$ = time interval (hours).

The maturity index is a quantitative amount of temperature and time a concrete mixture has accumulated. The datum temperature serves as a reference for the concrete. Anytime that the concrete cures above the datum temperature adds to the maturity index. Figure 2-8 illustrates the Nurse-Saul maturity function.

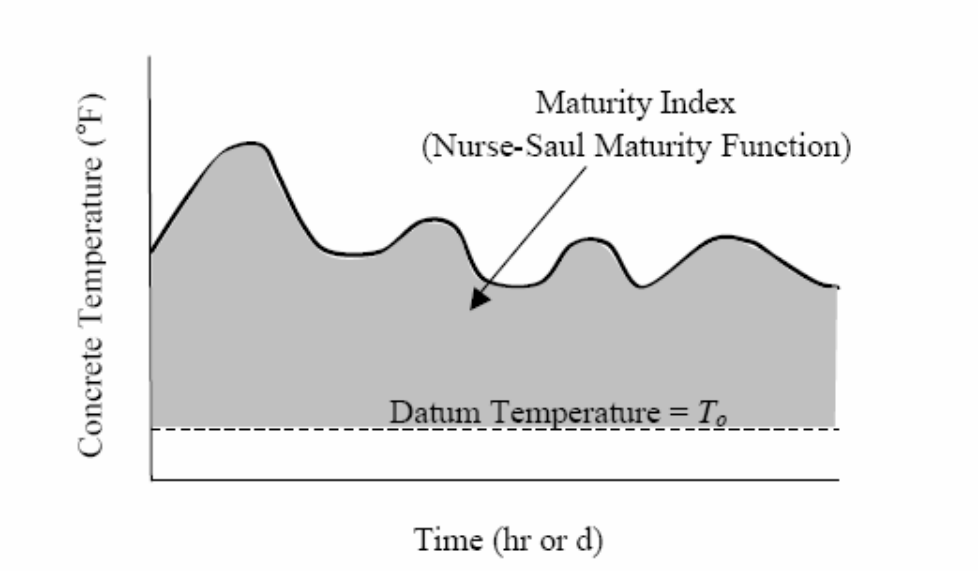


**Figure 2-8:** Concrete maturity diagram using Nurse-Saul maturity function (Wade 2005)

### 2.2.2 ARRHENIUS EQUATION

Another maturity function was developed by Freiesleben Hansen and Pedersen (1977). Unlike the Nurse-Saul maturity function, the Arrhenius maturity function computes the

maturity index in equivalent age. The Arrhenius maturity function is defined in ASTM C 1074 as follows:

$$t_e = \sum_0^t e^{\frac{-E}{R}\left[\frac{1}{273+T_C}-\frac{1}{273+T_r}\right]} \cdot \Delta t \qquad \textit{Equation 2-2}$$

where,

$t_e$ = equivalent age at the reference curing temperature (hours),

$T_c$ = average concrete temperature for the time interval, $\Delta t$, (°C),

$T_r$ = reference temperature, (usually 20°C or 23°C),

E = activation energy (J/mol),

R = universal gas constant (8.314 J/(mol•K)), and

$\Delta t$ = time interval (hrs).

Much like the Nurse-Saul method, the Arrhenius maturity function uses a reference temperature as a neutral point with respect to temperature effects on concrete strength gain. If the concrete cures above the reference temperature, then the concrete will gain strength more rapidly than concrete cured below the reference temperature.

## 2.3. SETTING

Setting is the change in the concrete from a fluid to a rigid state. It is caused by the sufficient formation of hydration products, which is accompanied by a sudden change in temperature rise in the concrete. According to ASTM C 403, initial set is when the concrete paste has reached a bearing pressure of 500 psi. Final set is when the concrete

paste has reached a bearing pressure of 4,000 psi. A plot of penetration resistance over time, like the one shown in Figure 2-9 is used to determine initial and final set.

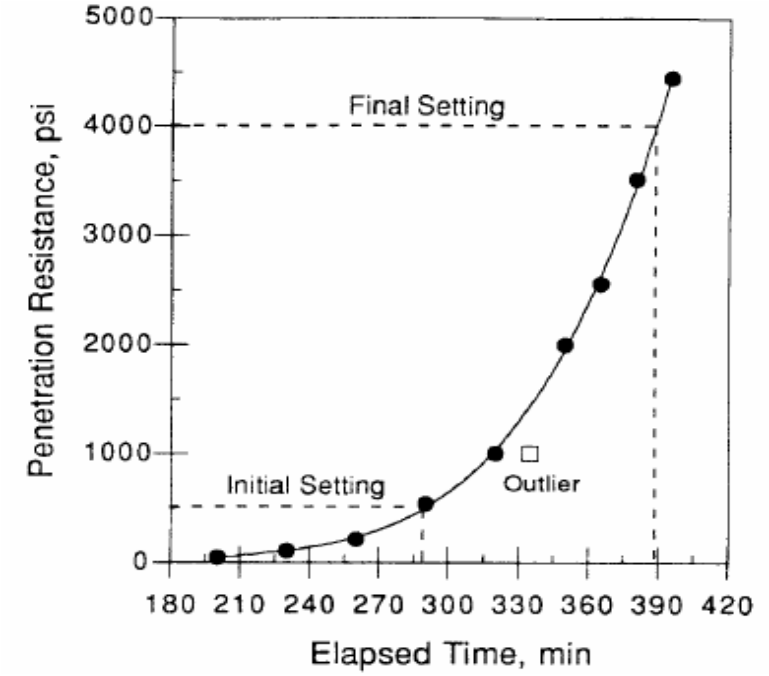


**Figure 2-9:** Typical plot of penetration resistance versus time (ASTM C 403)

## 2.4 DEVELOPMENT OF MECHANICAL PROPERTIES

Cracking in early-age concrete is not just a function of stress development. Cracking is also a function of mechanical properties such as tensile strength and elastic modulus. These properties are time and temperature dependent. The modulus of elasticity relates strains and stresses as discussed in Section 2.4.3. The tensile strength of the concrete resists the stresses from restrained contraction of the concrete as discussed in Section 2.4.2.

### 2.4.1 DEVELOPMENT OF COMPRESSIVE STRENGTH

The development of compressive strength in concrete has been widely studied for many years. Factors such as amount and type of cement and admixtures, temperature, curing conditions, and water-to-cementitious materials ratio affect the development of concrete strength (Emborg 1989).

As discussed in Section 2.1, cement type and amount may affect the amount of temperature developed in the concrete member. Temperature affects the rate at which the cement hydrates. Therefore, early-age and long-term strength can be affected due to changes in these mixture proportions. Variables such as water-to-cementitious ratio (w/cm), air entrainment, and cement type can be varied to increase or decrease strength. Figure 2-10 demonstrates the effect of w/cm on concrete compressive strength. As the w/cm is increased, the compressive strength is decreased. Figure 2-11 illustrates the change in compressive strength as air entrainment is introduced to the mixture proportions. Figure 2-12 demonstrates the effect of cement type on concrete strength.

The curing temperature also affects the rate at which the cement hydrates as discussed in Section 2.1.4. As the curing temperature is increased, the cement hydrates more rapidly. As a result, the concrete develops mechanical properties at a faster pace; however, the long-term strengths are reduced as shown in Figure 2-13.

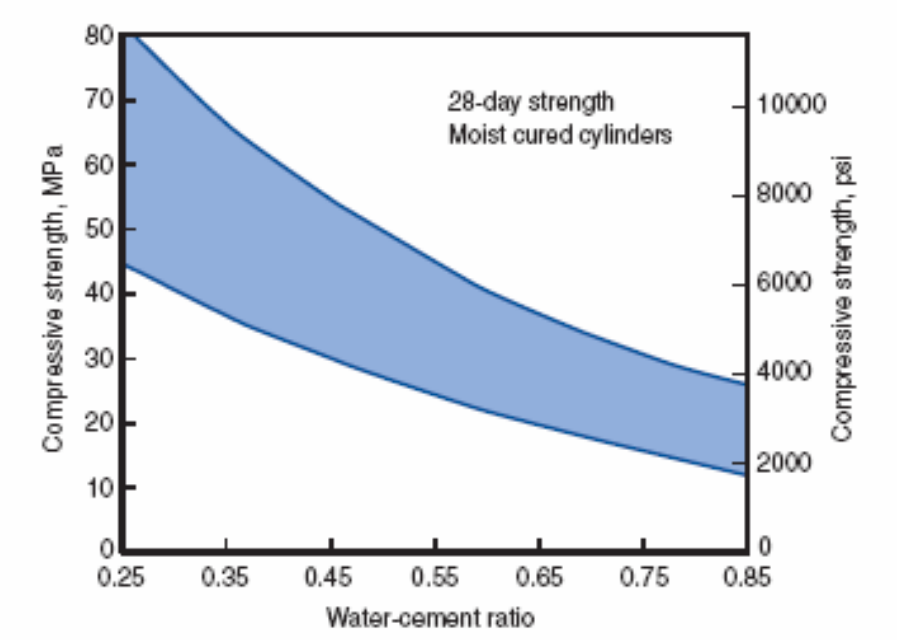


**Figure 2-10:** Effect of water-to-cementitious ratio on concrete strength (Kosmatka et al. 2002)

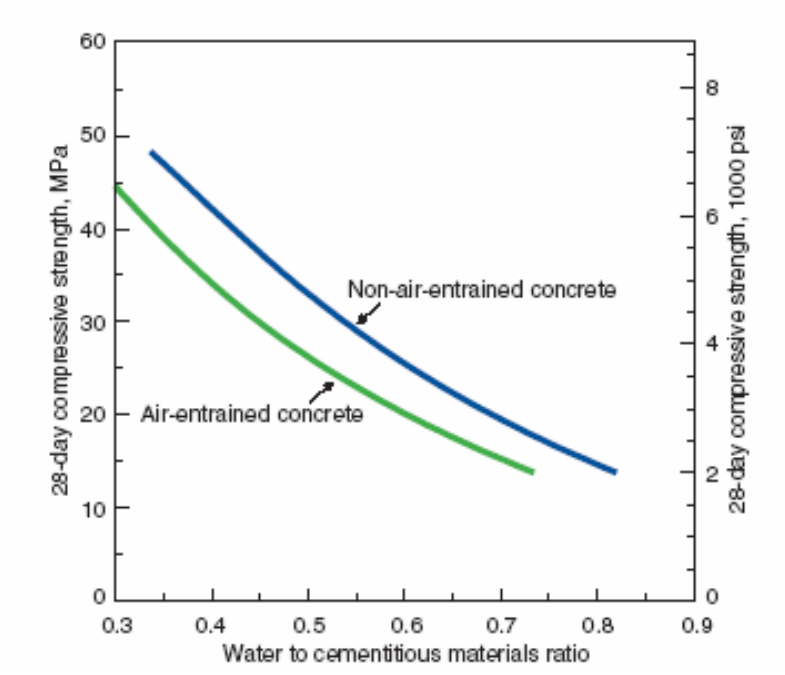


**Figure 2-11:** Effect of air entrainment on concrete strength (Kosmatka et al. 2002)

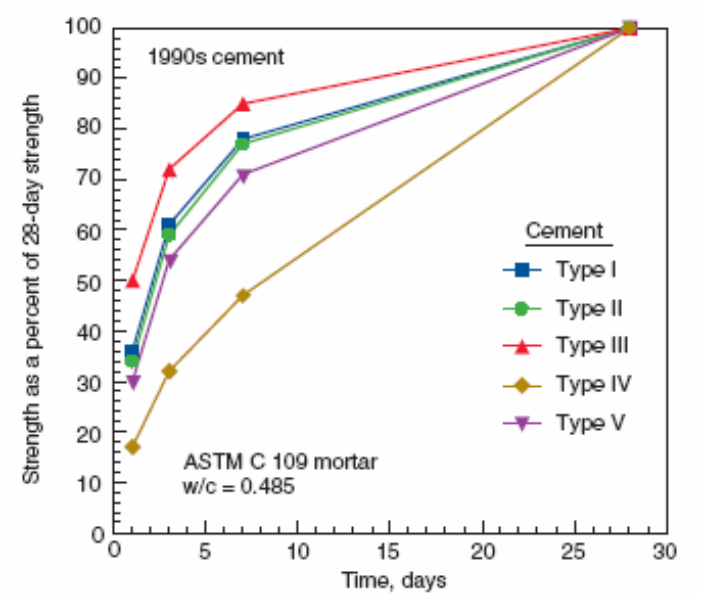


**Figure 2-12:** Effect of cement type on concrete strength (Kosmatka et al. 2002)

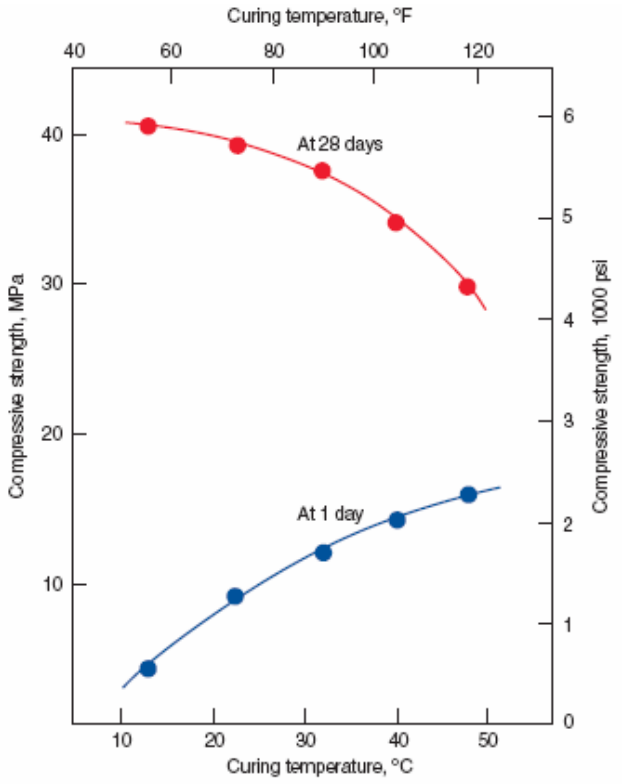


**Figure 2-13:** Effect of curing temperature on concrete strength (Kosmatka et al. 2002)

### 2.4.2 Development of Tensile Strength

Tensile strength of concrete develops due to the same factors as compressive strength; however, tensile strength is much lower due to ease of crack propagation under tensile loads (Mindess et al. 2002). The development of tensile strength is an important property in the mitigation of early-age cracking.

Microcracking originates in the interfacial transition zone (ITZ) and cracking develops as load is applied. The ITZ develops from water films around large aggregate particles as bleeding occurs. As hydration progresses, calcium silicate hydrate (C-S-H) forms to fill the empty voids left behind from the water film. This helps to improve the strength and density of the ITZ (Mehta and Monterio 2006).

The ITZ is the strength-limiting phase in concrete (Mehta and Monteiro 2006). This is primarily due to the microcracking which can be present in the ITZ before the structure is loaded. It is also the reason why concrete displays inelastic behavior while its constituents exhibit elastic behavior until fracture.

Aggregate characteristics influence the tensile strength of concrete (Mehta and Monteiro 2006). Aggregate texture has a substantial impact on the tensile strength of concrete. Rough textured or crushed aggregates have shown higher tensile strengths especially at early ages than smoother aggregates (Mehta and Monteiro 2006).

### 2.4.3 Development of Elastic Modulus

The evolution or development of the elastic modulus of concrete varies in proportion to the square root of the compressive strength gain in concrete (ACI 318 2005). The same factors that alter the development of strength affect the development of the elastic

modulus with some exceptions. The modulus of elasticity is affected primarily by the aggregate type and quantity used in the concrete mixture (Mindess et al. 2002). As the stiffness and amount of the aggregate increases, the stiffness of the concrete increases as shown in Figure 2-14.

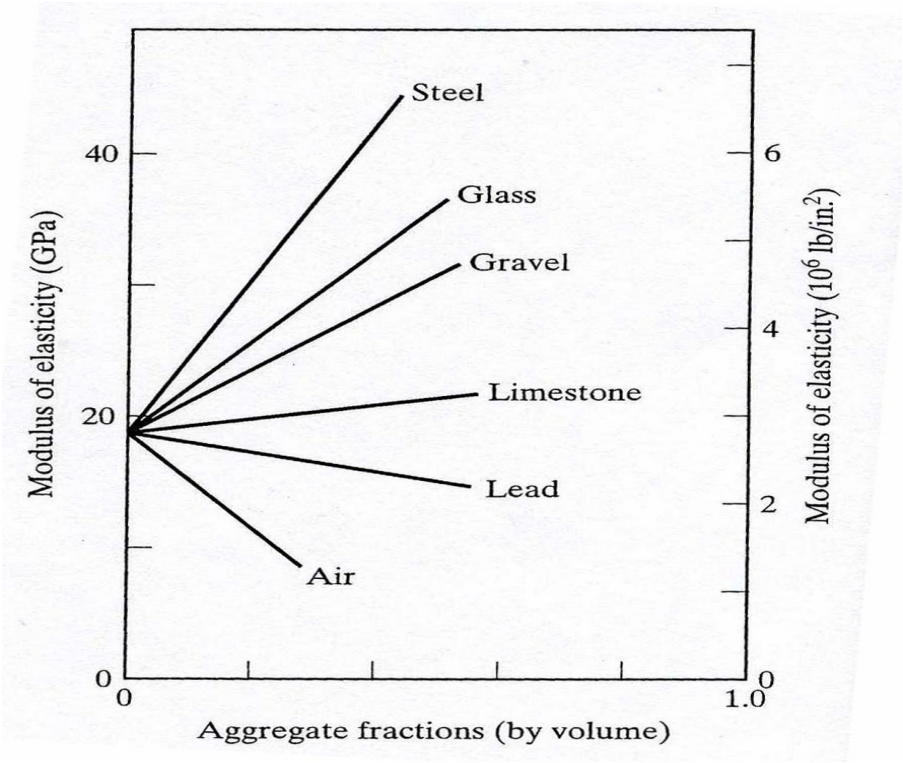


**Figure 2-14:** Effect of aggregates on modulus of elasticity (Mindess et al. 2002)

The modulus of elasticity is also a function of the porosity of the paste fraction of the concrete. As the water-to-cementitious materials ratio is increased, the porosity of the paste fraction is increased. If the porosity is increased, the elastic modulus will decrease. The modulus of elasticity of the paste from Mindess, Young, and Darwin (2002) can be determined as follows:

$$E_p = E_g(1 - P_c)^3 \qquad \textit{Equation 2-3}$$

where,

$E_p$ = elasticity of the cement paste (ksi),

$E_g$ = elasticity of the cement paste at zero porosity (ksi), and

$P_c$ = capillary porosity expressed as a ratio.

Figure 2-15 demonstrates the dependency of the elastic modulus on the porosity of the cement paste. In this figure, E is the modulus of elasticity of the hardened cement paste which is dependent upon the cement porosity and G is the shear modulus. According to Mindess et al. (2002), a similar relationship as in Equation 2-3 holds true for the shear modulus.

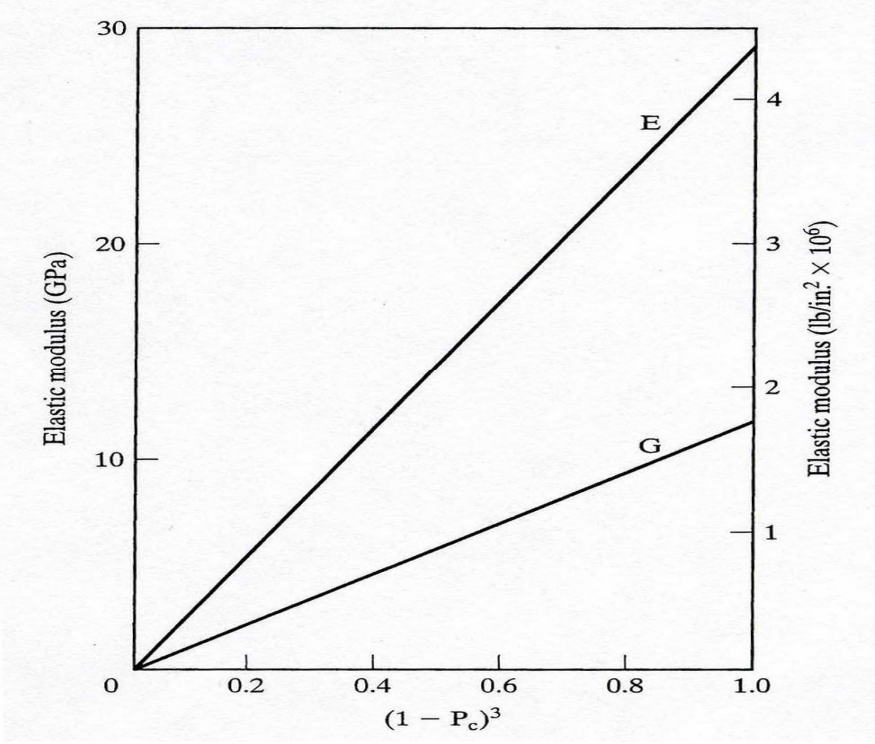


**Figure 2-15:** Dependency of the elastic moduli on the porosity of cement paste (Mindess et al. 2002)

## 2.5 FACTORS THAT PRODUCE EARLY-AGE VOLUME CHANGE

Early-age volume change in concrete is a well known phenomenon that has been studied for many years. Factors such as thermal changes, drying shrinkage, and autogenous shrinkage are known to produce early-age volume change. If the concrete is restrained from movement, the volume changes will induce compressive or tensile stresses. If these stresses are greater than the corresponding strength of the concrete, then cracking may occur. In this section the various factors that contribute to early-age volume changes are discussed.

### 2.5.1 THERMAL EFFECTS

Thermal stresses have been a major cause of early-age cracking of concrete (Lange and Altoubat 2002). Many factors such as heat of hydration (as discussed previously), thermal conductivity, and member size affect the rate of temperature rise. Concrete, like many other materials, expands when it is heated and contracts when it is cooled. If the concrete is restrained from movement, the change in temperature will induce stresses.

Figure 2-16 illustrates the evolution of early-age thermal stresses and mechanical properties under restrained conditions. Due to heat generated during hydration, the temperature of the concrete specimen rises shown in Figure 2-16A. The mechanical properties begin to develop after the concrete has reached final set shown in Figure 2-16C. As the stiffness and temperature of the specimen increases, the concrete experiences compressive stresses shown in Figure 2-16B. As the temperature of the concrete subsides, the compressive stresses diminish and the concrete goes into tension. The concrete experiences tensile stresses at temperatures higher than the placement temperature because the setting temperature is higher than the placement temperature. The concrete also experiences tensile stresses at temperatures higher than the setting temperature because the stiffness increases with time. Once the tensile stresses reach the tensile strength of the concrete, cracking may occur.

Figure 2-16 demonstrates the temperature development of a concrete element that is fully restrained (100%) from movement. The concrete cracked at a temperature change of 8°K (14°F). According to Thielen and Hintzen (1994), if the restraint factor is reduced to 50%, then the temperature change to induce cracking would double. Therefore, the reduction of the degree of restraint will reduce the cracking tendency.

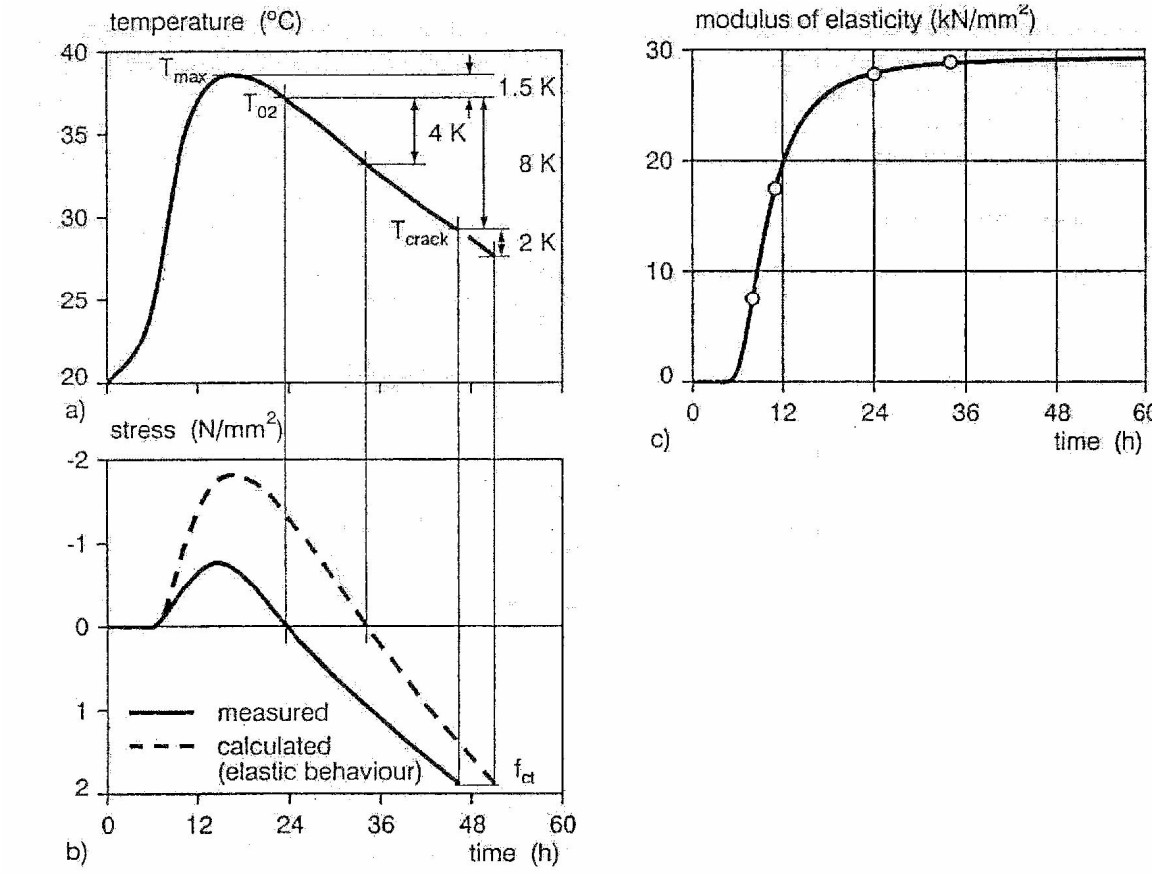


**Figure 2-16:** (A) Temperature development of restrained concrete specimen (B) Stress development of restrained specimen (C) Development of elastic modulus of concrete (Thielen and Hintzen 1994)

During hydration, cement reacts with water and heat is generated. The amount of heat generated is a function of the amount and type of cement, water-to-cementitious materials ratio, fresh concrete temperature, etc. (Schindler and Folliard 2005). The concrete will eventually harden and begin to cool until it reaches thermal equilibrium with its surrounding conditions. As a result of this temperature change, thermal stresses develop within restrained concrete. The magnitude of thermal stresses further depends

on the creep-adjusted elastic modulus, the coefficient of thermal expansion, and amount of restraint as defined in Equation 2-4 (Bamforth and Price 1995).

$$\Delta\sigma_{Thermal} = \Delta T \cdot \alpha(t) \cdot E_{cr}(t) \cdot K_r \qquad \textit{Equation 2-4}$$

where,

$\Delta\sigma_{Thermal}$ = change in concrete stress due to temperature change (psi),

$\Delta T$ = change in concrete temperature (°F),

$\alpha(t)$ = coefficient of thermal expansion of the concrete at time t (in/in/°F),

$E_{cr}(t)$ = creep-adjusted modulus of elasticity at time t (psi), and

$K_r$ = restraint factor.

A discussion of the coefficient of thermal expansion, restraint factor, and creep-adjusted modulus of elasticity can be found in Sections 2.4.1.1, 2.5.1, and 2.5.2, respectively.

#### 2.5.1.1 Coefficient of Thermal Expansion

The coefficient of thermal expansion (CTE) is the key parameter that converts temperature change in the concrete into strain. As indicated in Equation 2-5, the magnitude of strain developed is directly proportional to the temperature change and the CTE.

$$\Delta\varepsilon_{Thermal} = \Delta T \cdot \alpha(t) \qquad \textit{Equation 2-5}$$

where,

$\Delta\varepsilon_{Thermal}$ = change in concrete strain due to temperature change (in/in),

$\Delta T$ = change in temperature (°F), and

$\alpha(t)$ = coefficient of thermal expansion of the concrete at time t (in/in/°F).

The CTE varies as a function of the individual constituents of the concrete (Emanuel and Hulsey 1977). Variables such as aggregate type, water-to-cementitious materials ratio, and age affect the CTE of concrete. The variations of CTE of concrete due to the use of different aggregates can be seen in Figure 2-17. The CTE of concrete is directly related to the CTE of the aggregate used in the mixture proportions (Metha and Monteiro 2006). As the CTE of the aggregate is increased, the CTE of the concrete is increased.

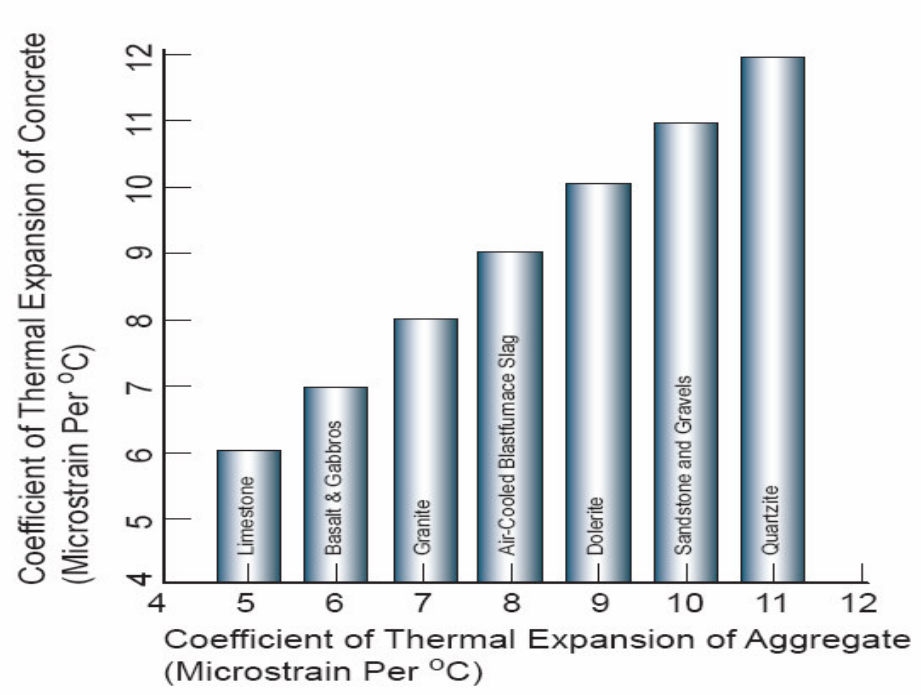


**Figure 2-17:** Influence of aggregate CTE on CTE of hardened concrete (Mehta and Monteiro 2006)

The influence of aggregate type on CTE of hardened concrete is easy to evaluate since it is directly related to the CTE of the aggregate used in the mixture proportions. However, the effects of water-to-cementitious materials ratio and age are more difficult to quantify. As shown in Figure 2-18, the evolution of the CTE of concrete with respect to time changes as the concrete age increases.

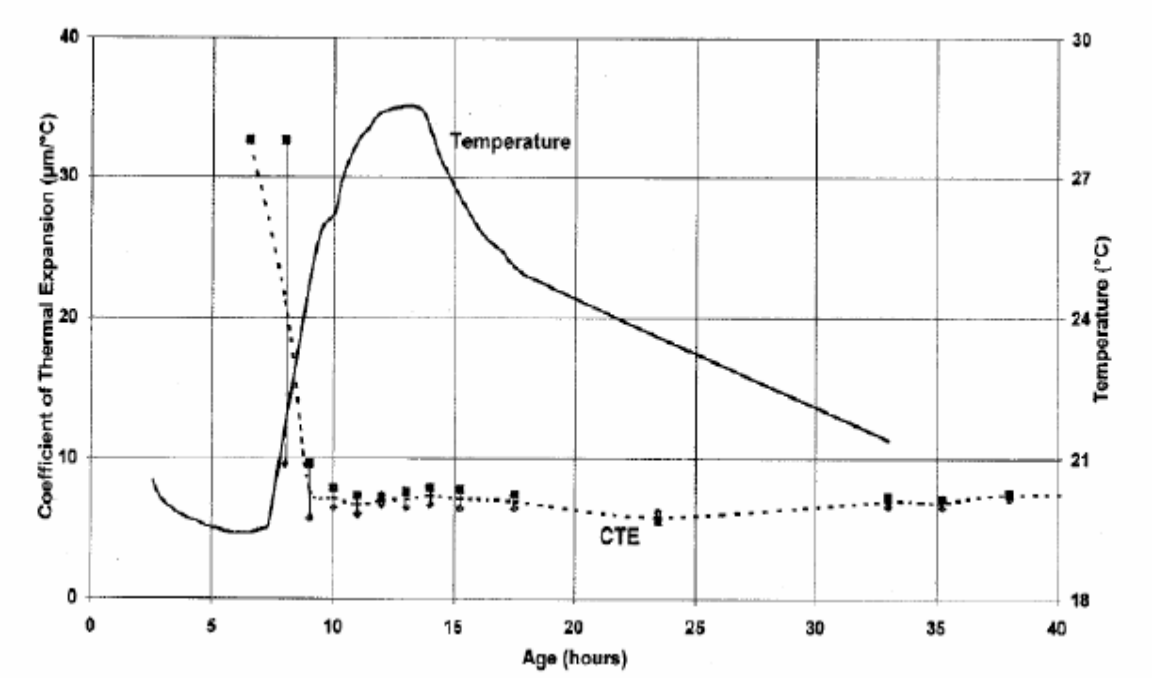


**Figure 2-18:** Evolution of the CTE in hardening concrete (Kada et al. 2002)

The decrease of CTE within the first few hours just after hydration is related to the amount of water that the concrete possesses at an early age. Water has a higher CTE (20 x $10^{-6}$ in/in/°F) as compared to the other constituents in the concrete (5 to14 x $10^{-6}$ in/in/°F); therefore, young concrete has a much higher CTE (Bjontegaard 1999). As pointed out by ACI Committee 517 (1980), the CTE of fresh concrete is several times higher than the CTE of hardened concrete.

After the concrete has set, Kada et al. (2002) found that the CTE remained constant. However, Bjøntegaard (1999) discovered that the CTE increased after setting, as shown in Figure 2-19. Bjøntegaard (1999) states that the CTE development increases by 40% from setting until stable values are reached.

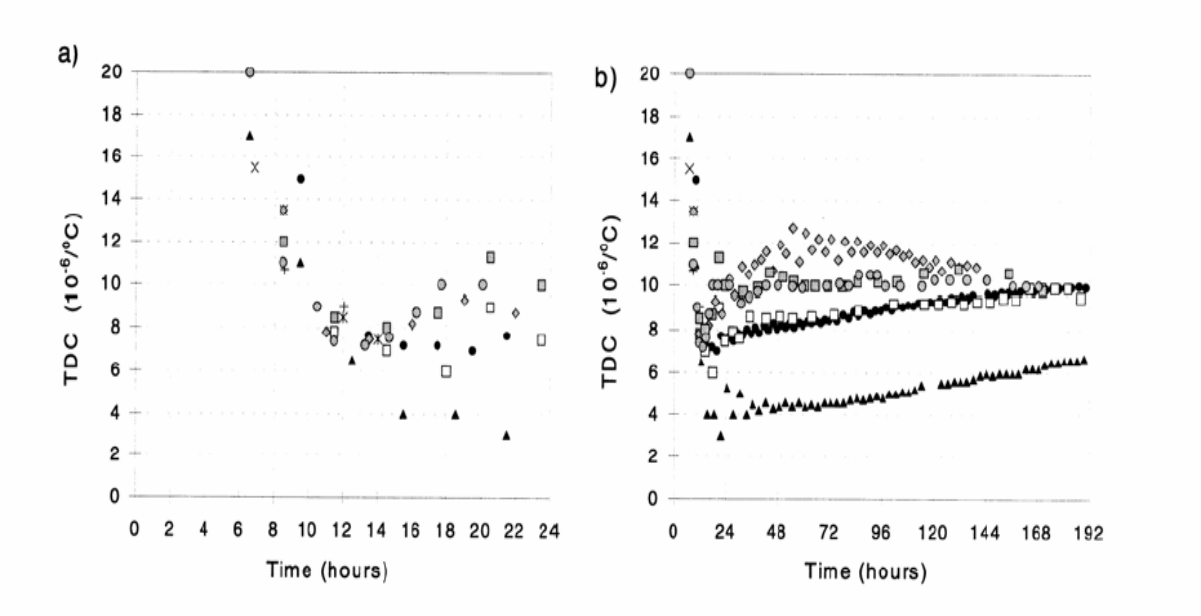


**Figure 2-19:** Thermal dilation coefficients (TDC) of hardening concrete (Bjøntegaard 1999)

### 2.5.2 EARLY-AGE SHRINKAGE

Concrete shrinkage is due to the migration or loss of water. Holt 2001 states "As water is lost to evaporation (drying shrinkage) or internal reactions (autogenous shrinkage), tensile stresses are generated." As a result of a slow elastic modulus development, large strains may only create small stresses at early-ages. However, these stresses at early-ages are more critical because the concrete has not developed much strength. Even if the resulting stresses are small, microscopic cracks may still form. If early cracks are

internal and microscopic, long-term shrinkage may cause the cracks to widen and spread. A discussion of drying shrinkage, autogenous shrinkage, and chemical shrinkage can be found in Sections 2.4.2.1, 2.4.2.2, and 2.4.2.3, respectively.

#### 2.5.2.1 Drying Shrinkage

Drying shrinkage is the moisture loss from within the hardened concrete which decreases the volume with time (ACI 209R 1997). The rate of water loss from unsealed concrete surfaces is highly dependent upon environmental conditions. Conditions such as wind, relative humidity, and temperature affect the rate of evaporation. Unlike heat dissipation of mass concrete elements, moisture loss from the core of mass concrete occurs extremely slowly. The slow migration of moisture from within concrete elements is highly dependent upon the length it has to travel; therefore, thinner members tend to dry faster than larger members. The resulting trend linking drying shrinkage and volume-to-surface ratio is shown in Figure 2-20.

Although drying shrinkage is a slow process compared to heat dissipation of large concrete members, it must be considered in design. ACI 207.2R (1997) states that the restraint of drying shrinkage is completely internal, and will result in tensile stresses developing on the surface. However, effective curing methods and changes in aggregate size and type can be used to control drying shrinkage (ACI 207.2R 1997).

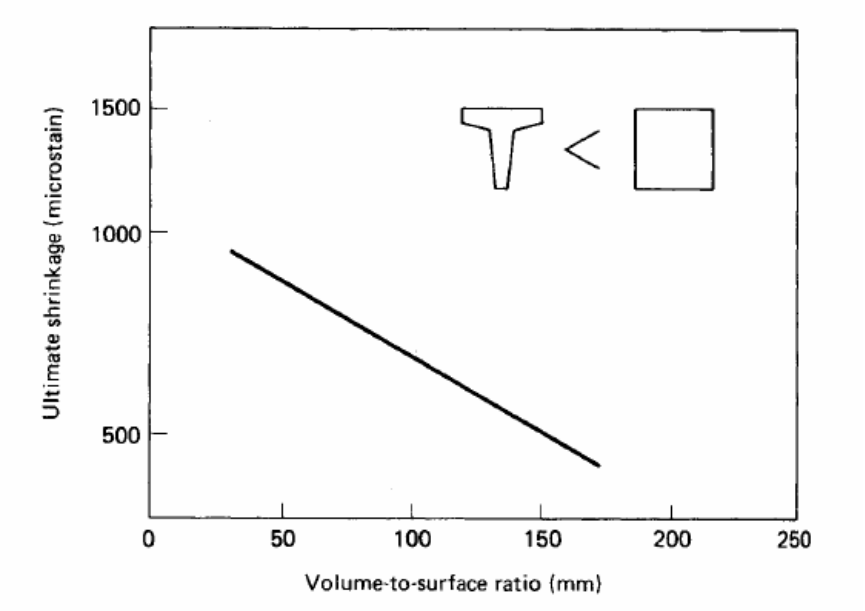


**Figure 2-20:** Effect of volume-to-surface ratio on the drying shrinkage of concrete (Mindness and Young 1981)

#### 2.5.2.2 Autogenous Shrinkage

When efficient curing methods are used to reduce drying shrinkage and measures are taken to prevent the development of thermal stresses, concrete can still experience significant volume change. This volume change is associated with autogenous shrinkage. Autogenous shrinkage is the external volume change of concrete with no moisture transfer to the surrounding environment which occurs under isothermal conditions (Bentur 2003). It is a result of chemical shrinkage which is associated with the hydration of cement particles (Holt 2001). Chemical shrinkage is an internal volume change where as autogenous shrinkage is an external volume change.

Autogenous shrinkage was documented for the first time in the 1930s by Lynam (1934). At that time, autogenous shrinkage was thought to only occur at very low water-to-cement ratios that were beyond the practical range of concrete. But with the advancement of concrete, low water-to-cement ratios are a very common occurrence in today's structural design. Even though many strength and durability aspects are now improved, the risk of autogenous shrinkage is greater and needs to be studied. Figure 2-21 illustrates the effect of water-to-cement ratio on autogenous shrinkage.

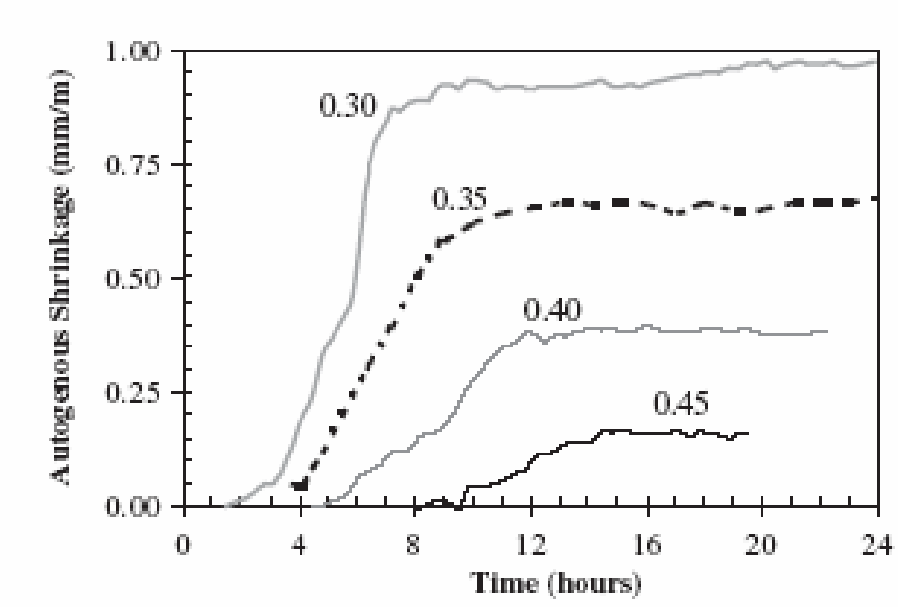


**Figure 2-21:** Effect of water-to-cement ratio on autogenous shrinkage (Holt and Leivo 2004)

Although autogenous shrinkage has been known for many years, only recently have studies resulted in models to estimate the autogenous shrinkage. In 1999, Hedlund and

Westman published an empirical formula for the estimation of autogenous shrinkage (Equation 2-6 and Equation 2-7).

$$\varepsilon_{co}(t) = \varepsilon_{co\infty} \cdot \beta_{so}(t) \qquad \textit{Equation 2-6}$$

where,

t = age of concrete (days),

$\varepsilon_{co\infty}$ = final value of autogenous shrinkage, and

$\varepsilon_{co}(t)$ = autogenous shrinkage at time t.

$$\beta_{so}(t) = 1.14(-\left[\frac{t_{so}}{t - t_{start}}\right]^{0.3}) \qquad \textit{Equation 2-7}$$

where,

$\beta_{so}(t)$ = time distribution of autogenous shrinkage,

$t_{so}$ = time parameter (days), and

$t_{start}$ = starting time (days).

The starting time for shrinkage measurements varies between 9 and 24 hours (Hedlund and Westman 1999). This is when the concrete is stiff enough to take a measurement which is established by judgment. The time parameter, $t_{so}$, is a constant for all high performance concrete (HPC) and is typically 5 days. The final value of autogenous shrinkage, $\varepsilon_{co\infty,}$ can be calculated from the following equation (Hedlund and Westman 1999):

$$\varepsilon_{so\infty} = (-0.6 + 1.2 \cdot \frac{w}{b}) \cdot 10^{-3} \qquad \textit{Equation 2-8}$$

where,

$w$ = weight of the water (lbs) and

$b$ = weight of the binder (lbs).

The European Standard (Eurocode 2001) was the first to include a method for the prediction of long-term autogenous shrinkage strains (Holt 2001). Their model to predict the autogenous shrinkage, in Equation 2-9 and Equation 2-10 is very similar to the model of Hedlund and Westman.

$$\varepsilon_{cs} = \beta_{cc}(t) \cdot \varepsilon_{cs,\infty} \qquad \textit{Equation 2-9}$$

where,

$\varepsilon_{cs}$ = autogenous shrinkage strain (microstrain),

$\varepsilon_{cs,\infty} = 2.5(f_{c'} - 10) \times 10^{-3}$, and

$f_{c'}$ = characteristic compressive strength of concrete at 28 days (MPa).

$$\beta_{cc}(t) = \exp\left\{ s\left[ 1 - \left( \frac{28}{t/t_1} \right)^{1/2} \right] \right\} \qquad \textit{Equation 2-10}$$

where,

$\beta_{cc}(t)$ = time distribution of autogenous shrinkage,

s = coefficient depending on the type of cement,

t = age of concrete (days), and

$t_1$ = 1 day.

The values of s in Equation 2-10 are 0.20 for rapid-hardening high-strength cement, 0.25 for normal and rapid-hardening cements, and 0.38 for slowly hardening cements.

According to Holt (2001), variations in autogenous shrinkage over the cross section or depth of the concrete member do not occur. This is due to the low porosity of high-strength concrete where the internal water will be distributed once the material has hardened and thermal equilibrium has been reached. Unlike autogenous shrinkage, drying shrinkage is dependent upon the moisture gradient across the concrete element which is caused by uneven evaporation due to large volume-to-surface ratios.

#### 2.5.2.3 Chemical Shrinkage

As discussed in the previous section, autogenous shrinkage is a result of chemical shrinkage during the first few hours after hydration has started. Chemical shrinkage, commonly referred to as le Chatlier shrinkage, is the internal volume reduction associated with the reaction of cement and water (Holt 2001). It is caused by the volume changes that occur as a result of Bogue compounds reacting with water as seen in Figure 2-22.

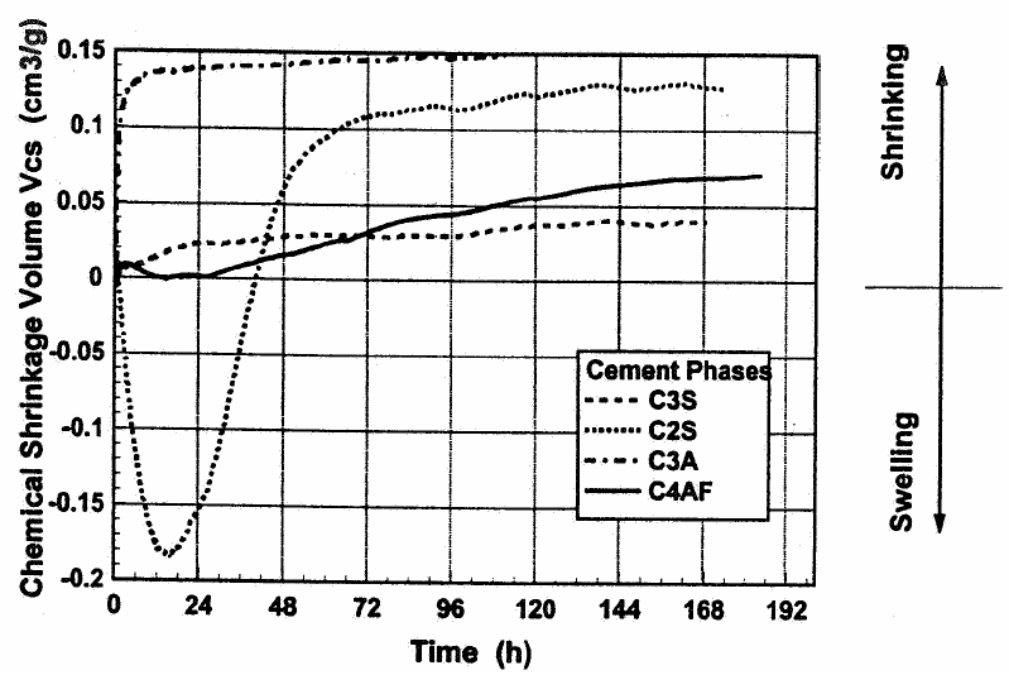


**Figure 2-22:** Influence of cement composition on chemical shrinkage (Paulini 1996)

Since chemical shrinkage is based on the volume change of the hydration products, molecular weights can be used in the calculation of chemical shrinkage. Paulini (1996) used Equation 2-11 to estimate the total volume change attributed to chemical shrinkage by the percentage of each Bogue compound.

$$V_{CS-Total} = 0.0532[C_3S] + 0.0400[C_2S] + 0.1113[C_4AF] + 0.1785[C_3A] \qquad \textit{Equation 2-11}$$

where,

$V_{CS\text{-}Total}$ = total volume of chemical shrinkage.

This equation indicates that cement chemistry will affect the autogenous shrinkage due to the varying chemical shrinkage at early ages (Holt 2001). As an example, if the $C_3A$ content is high in a particular cement, then the shrinkage will be greater than a low $C_3A$ content cement.

Many other variables affect the rate of chemical shrinkage; however, they do not affect the overall magnitude (Holt 2004). The rate of chemical shrinkage is dependent upon concrete mixture proportions and cement composition such as fineness. The fineness of the cement and the water-to-cement ratio affect the rate of the reaction rather than the overall magnitude of shrinkage. Other variables such as cement type, admixture type and dosage, and addition of pozzolans have been found to affect the rate of chemical shrinkage (Sellevold et al. 1994). Higher reaction rates of cement will lead to larger chemical shrinkage magnitudes, which will lead to greater autogenous shrinkage (Holt 2004). Conditions that lead to large autogenous shrinkage magnitudes may produce greater total shrinkage, which increases the cracking risk of mass concrete structures.

## 2.6 DEVELOPMENT OF EARLY-AGE STRESSES

Early-age stresses originate from volume change as a result of thermal, drying, autogenous, and chemical shrinkage coupled with restraint conditions that prevent or alter the movement of concrete. These stresses develop due to strains that are induced by early-age volume change as the concrete grows in stiffness. Over time, stresses may exceed the tensile strength of the concrete which will result in cracking.

### 2.6.1 RESTRAINT CONDITIONS

Restraint conditions of the concrete element are of utmost importance when determining stresses induced by early-age volume change. As demonstrated in Equation 2-4, the restraint factor ($K_r$) is commonly used to quantify the level of restraint provided by internal and external conditions (ACI 207.2R 1997). The restraint factor is within the range of 0% to 100% depending on the surrounding conditions with 0% being free movement and 100% being fully restrained.

Restraint stresses can be divided into two major categories, internal and external. Internal restraint is caused by temperature gradients that form as a result of uneven cooling within the concrete member. During cooling, the surface of the concrete cools more rapidly than the interior of the element which creates thermal gradients (ACI 207.2R 1997).

External restraint is caused by the conditions surrounding or supporting the concrete element that prevents free movement. External restraints could include, but are not limited to, soil, adjacent structures, and foundations (ACI 207.2R 1997). The degree of restraint is primarily dependent upon the relative dimensions, strength, and modulus of elasticity of the concrete specimen (ACI 207.2R 1997).

The reduction of the overall restraint of the concrete member can significantly decrease the cracking tendency. Figure 2-23 demonstrates the temperature, stress, and strength development of a concrete element that is fully restrained (100%) from movement. As shown, reducing the restraint factor diminishes the risk of cracking due to the reduction in stresses.

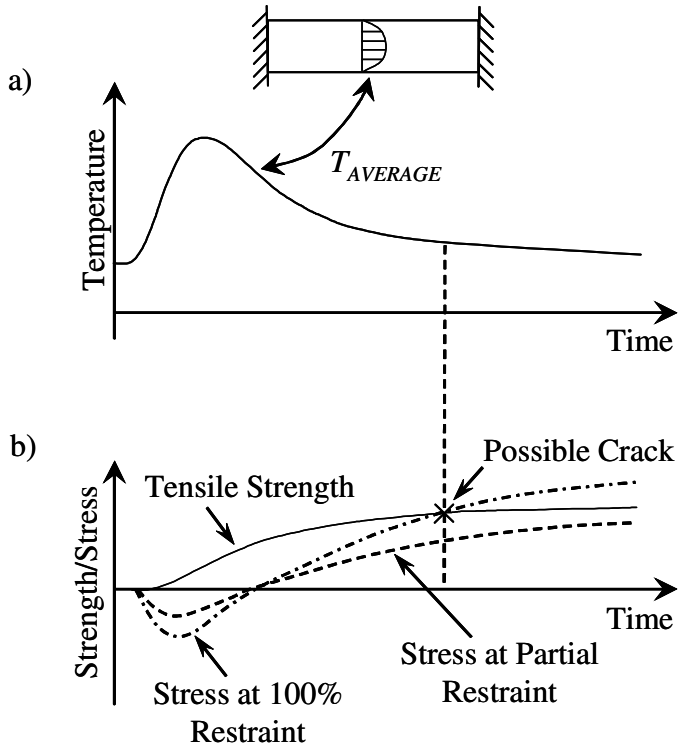


**Figure 2-23:** Evolution of temperature development and thermal stresses for different restraint conditions (Nilsson 2003)

### 2.6.2 EARLY-AGE CREEP BEHAVIOR

Early-age concrete undergoes deformations due to volume change as discussed previously. Restraint of these deformations creates stresses in the concrete. Creep and associated relaxation occur due to the viscoelastic response of early-age concrete; therefore, these properties must be considered when assessing the cracking risk of concrete during the first few days after placement.

Creep is the increase in strain with respect to time under a constant load. If a linear-elastic material is subjected to a constant load, then it will respond instantaneously with a

deformation that remains constant. However, if the load is removed, then the material will return to its original shape. Concrete, on the other hand, is not a linear-elastic material especially at early-ages; therefore, understanding early-age nonlinear creep behavior is very important when calculating restraint stresses in early-age concrete (Westman 1999).

Concrete creep can be divided into two major categories; recoverable and irrecoverable deformation (Westman 1999). Recoverable deformation is recovered fully after unloading due to the elastic nature of the concrete. Irrecoverable deformation causes the concrete paste to behave plastically; therefore not recovering deformation after the load is removed. Figure 2-24 illustrates the general behavior of hardening concrete with loading and unloading taking place. Elastic deformation can be recovered instantaneously after the load is removed. The delayed elastic recovery, commonly referred to as creep recovery, is the portion of creep-induced deformation that will be recovered over time. The net effect after loading and unloading has taken place, is the irrecoverable deformation (Emborg 1989).

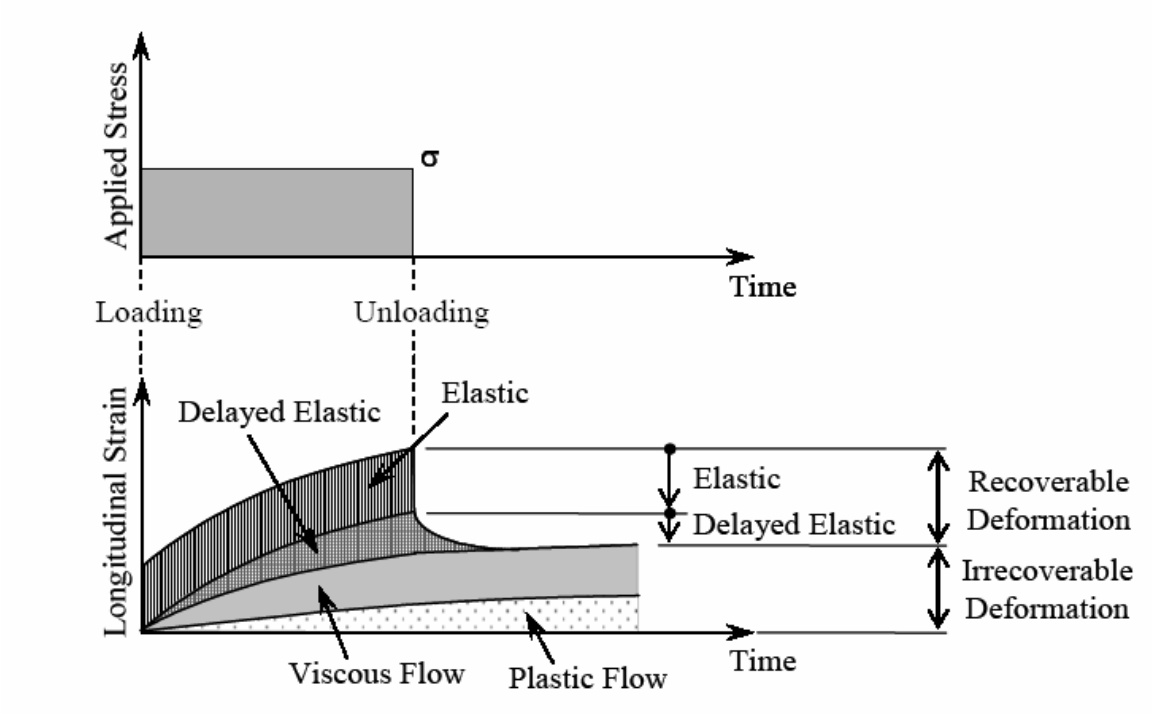


**Figure 2-24:** Generalized creep behavior of hardening concrete (Emborg 1989)

Factors that influence creep can be divided into two major categories: internal and external. The internal factors are cement type, mixture proportions, water-to-cement ratio, etc. (Emborg 1989). External factors include the type and intensity of loading, duration of loading, age at loading, moisture content, and the change in relative humidity and temperature of the ambient conditions.

Creep in early-age concrete members is very complex. Due to the low strength of young concrete, the nonlinear portion of the stress-strain relation is reached at much lower stress levels than in concrete at later ages. As a result, many complex models have been proposed to describe the time varying nature of creep (Westman 1999, Bazant and

Chern 1985, Emborg 1989). These models were developed using prior models for long-term creep estimates (Larson 2003).

## 2.7 METHODS FOR DETERMINING EARLY-AGE STRESSES

The mechanisms that cause internal volume changes in early-age concrete are very complex. The stresses that are generated cannot be determined by measuring deformations alone (Breitenbucher 1990). As a result, accurate measurement of restraint-induced stresses is very difficult. Many laboratory tests have been developed to measure the restraint stresses and quantify the cracking tendency of concrete. Test such as the concrete ring test, restrained prism test, and temperature-stress testing machine (TST) are methods of determining the cracking tendency of various concrete mixtures; however, this thesis only involves the use of the rigid cracking frame as a testing method. See Whigham (2005) and Mangold (1998) for further discussion of other testing methods.

### 2.7.1 RIGID CRACKING FRAME (RCF)

The rigid cracking frame, illustrated in Figure 2-25, is comprised of two mild steel crossheads and two Invar side bars. In order for the concrete to be restrained, the crossheads are constructed using dovetails on each end. These connections are tapered to reduce the stresses in the crosshead. The dovetail is lined with teeth that grip the concrete. To further prevent slippage of the concrete, cross head braces are bolted to the top and bottom of the crosshead; these restrain expansion as the concrete goes into tension.

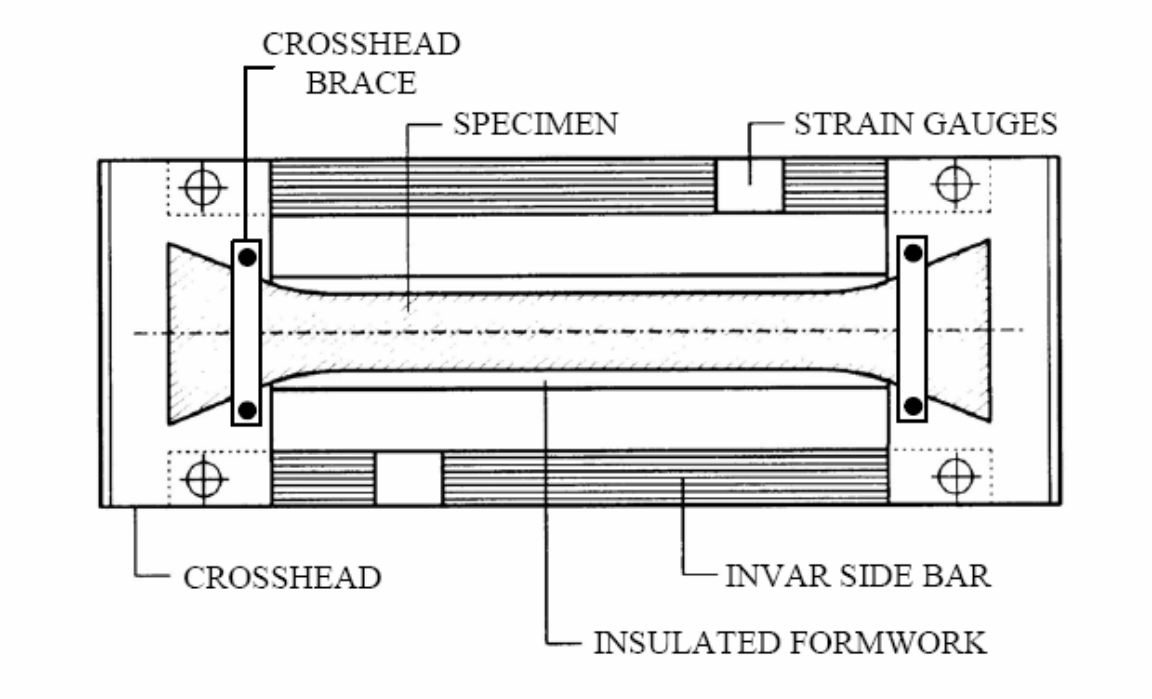


**Figure 2-25:** Diagram of the Rigid Cracking Frame (Springenschmid et al. 1994)

Invar side bars are used to minimize the effect of temperature change on the length and stress of the concrete member. The Invar bars have a coefficient of thermal expansion (α), of 1 x $10^{-6}$/°C, which is significantly less than that of ordinary mild steel, 12 x $10^{-6}$/°C (Whigham 2005). The forces developed within the bars causes an elastic deformation, which is recorded by the strain gauges.

Insulated formwork is used to prevent moisture loss and to allow proper heating and cooling in the concrete specimen. The formwork is designed to insulate the test specimen, producing a heat of hydration approximately equal to a 50-cm-thick specimen (Breitenbucher 1989). The formwork also provides support for the fresh concrete, which allows measurements to be taken as soon as the concrete has been placed. The formwork can be connected to an external heating and cooling water circulator. Copper tubing is

built within the formwork, which allows temperature control without contamination of the test specimen; therefore, measurement of thermal stresses can be determined for an arbitrary temperature profile (Mangold 1998).

Due to the small elastic deformations of the steel bars, the degree of restraint of the cracking frame is reduced. The degree of restraint is 100% for fresh concrete, and can be as low as 80% for hardened concrete (Mangold 1998). Since the rigid cracking frame does not have the ability to change the amount of restraint, Mangold (1994) has developed a model to compute the stress response at various degrees of restraint. The rigid cracking frame can be modeled as an elastic spring, shown in Figure 2-26, which is attached to the concrete (Mangold 1994). The rigid cracking frame can be modeled as a spring because the concrete will crack in tension long before the steel will reach yielding stresses.

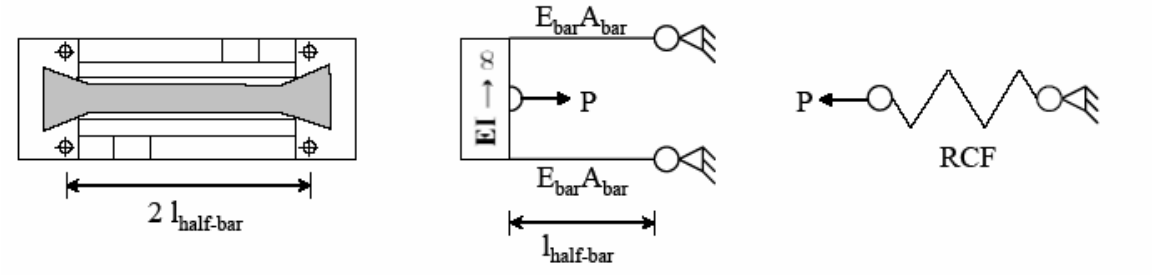


**Figure 2-26:** Spring model of the Rigid Cracking Frame (Mangold 1994)

The degree of restraint that the concrete experiences in the rigid cracking frame is time-dependent. As previously stated, the degree of restraint changes from 100% to 80% as the concrete hardens. The degree of restraint varies proportionally with the

development of the modulus of elasticity of the concrete specimen as shown in Equation 2-12 (Mangold 1998). In this equation, the rigid cracking frame is considered to be fixed at the midlength.

$$R_f = 1 - \frac{A_c E_c(t)}{A_s E_s} \qquad \textit{Equation 2-12}$$

where,

$R_f$ = restraint factor (dimensionless)

$A_c$ = cross-sectional area of concrete specimen ($in^2$),

$E_c(t)$ = time-dependent modulus of elasticity of the concrete (ksi),

$A_s$ = cross-sectional area of steel side bars ($in^2$), and

$E_s$ = modulus of elasticity of Invar side bars (ksi).

### 2.7.2 Concrete Behavior in the Rigid Cracking Frame

In order to fully quantify the stresses developed in early-age concrete, the restrained behavior must be completely studied. Figure 2-27 illustrates the five stages that Breitenbücher (1990) used to discuss the behavior of a restrained concrete specimen in the rigid cracking frame. Stage I occurs directly after placement of the concrete during which the fresh concrete temperature remains constant. Stresses do not form since the concrete has not set and thus has near-zero stiffness. Stage II begins with the start of hydration and is marked by the initial set of the concrete. During this stage, heat is developed from hydration, but stresses do not occur due to the plastic nature of early-age

concrete. Stage III begins upon final set of the concrete. The mechanical properties of the concrete begin to develop due to the rapid progress of hydration rise. Compressive stresses within the concrete specimen originate from the development of the elastic modulus coupled with the rapid temperature rise. During Stage IV, the concrete temperature begins to fall. The compressive stresses are reduced at a rapid pace as the temperature decreases. The rapid reduction in compressive stresses is a result of relaxation of the young concrete as well as the increased elastic modulus (Breitenbücher 1990). As the concrete compressive stresses decrease, the specimen reverts back to a stress free state. The temperature at which the concrete returns to zero stress is referred to as the zero stress temperature ($T_{zs}$). During Stage V, the heat due to hydration begins to subside. Tensile stresses begin to form as the elastic modulus increases and the relaxation decreases. Tensile stresses continue to rise until the stresses exceed the tensile capacity of the concrete. Once the tensile capacity has been reached, the concrete will crack. The temperature at which the concrete cracks is referred to as the cracking temperature ($T_{cr}$).

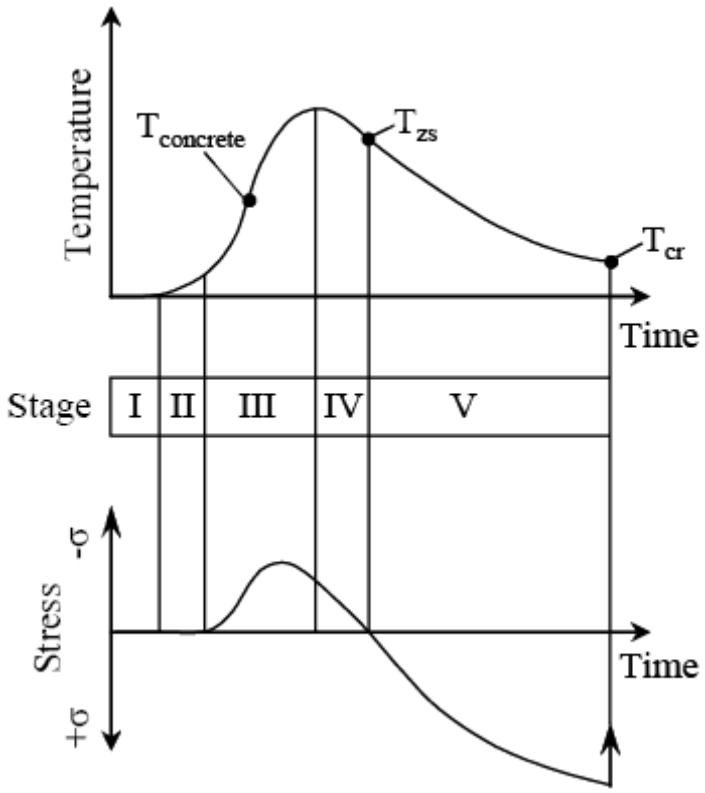


**Figure 2-27:** Behavior of concrete specimen in the Rigid Cracking Frame (Breitenbücher 1990)

## 2.8 CONCLUDING REMARKS

Cracking in concrete due to early-age volume change is a complex phenomenon and is caused by many variables. Effects such as thermal, drying, and autogenous shrinkage coupled with restraint conditions create stresses that can exceed the tensile strength of the concrete. In order to fully understand the mechanisms driving early-age cracking, each variable must be studied. Quantification of these variables can be an extremely hard task particularly at early-ages, therefore making prediction of cracking tendencies very difficult.

# CHAPTER 3

# LABORATORY TESTING PROGRAM AND MATERIALS

In order to accomplish the objective set forth in Section 1.2 of Chapter 1, an experimental laboratory testing program was undertaken. The laboratory testing program was designed to evaluate the effects of placement temperature, ambient temperature, cement type, supplementary cementing materials, air entrainment, and water-to-cementitious materials ratio on the cracking tendency of concrete mixtures. The laboratory test setup developed by Whigham (2005) was implemented with modifications.

## 3.1 EXPERIMENTAL TESTING PROGRAM

The experimental testing program was designed to investigate the restraint stresses due to early-age volume change. In order to study the mechanisms controlling early-age restraint stresses, the following equipment was used: two rigid cracking frames, a free shrinkage frame, match-curing box, and a semi-adiabatic caliorimeter. Each concrete mixture was placed in the rigid cracking frames and subjected to isothermal conditions and a match-curing temperature profile in order to separate thermal and autogenous shrinkage effects. The free shrinkage frame was subjected to the match-curing temperature profile in order to measure volume change under restraint-free conditions. The match-curing box was subjected to the same temperature profile so that the

mechanical properties of the concrete in the rigid cracking frame and the free shrinkage frame could be determined.

Figure 3-1 shows a schematic of the experimental testing program. The rigid cracking frame "A", free shrinkage frame, and match-curing box are used to study the combined affects of autogenous and thermal shrinkage on the development of restraint stresses. The rigid cracking frame, free shrinkage frame, and match curing box are connected to a computer and circulator which drive the concrete to the temperature history shown. The rigid cracking frame simulates the stress development of a restrained concrete member. The free shrinkage frame was used to measure the deformations that cause stress development in the rigid cracking frame. The match-curing box was used to condition the molded concrete cylinder specimen so that the mechanical properties could be determined.

The rigid cracking frame "B" was held under isothermal conditions for the duration of the test in order to study the development of autogenous shrinkage stresses. Since the research conducted in this thesis is part of a bigger ongoing research project, the result obtained from the isothermal rigid cracking frame will be used to develop a model for estimation of autogenous shrinkage.

A list of the additional tests performed on the fresh and hardened concrete is provided. The semi-adiabatic calorimeter was used to obtain hydration parameters to calculate the temperature history for match-curing the concrete specimens.

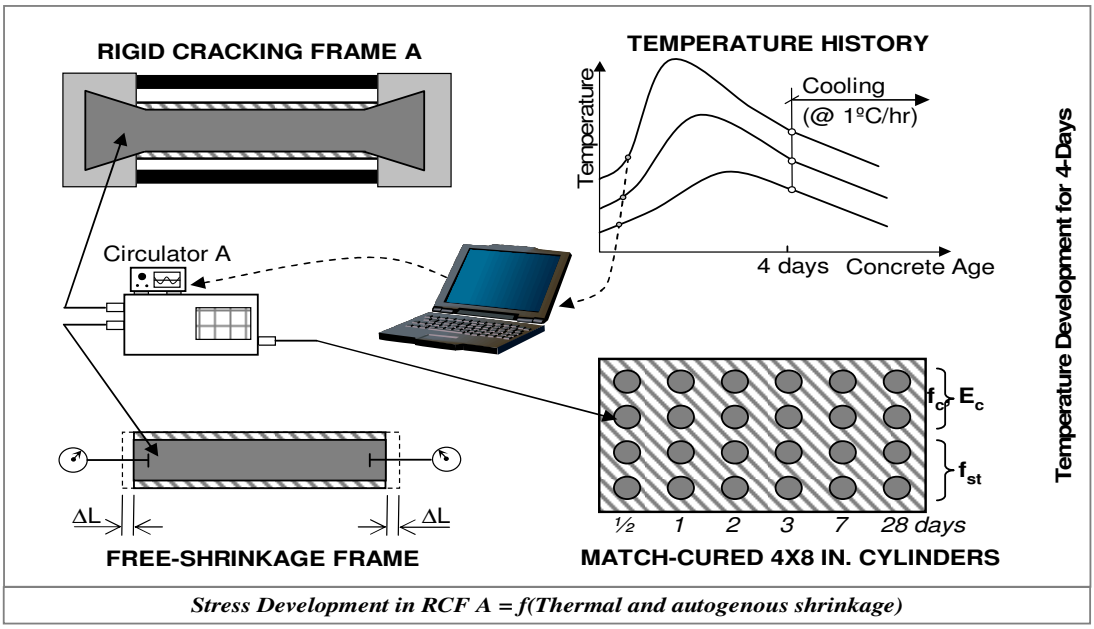


*Stress Development in RCF A = f(Thermal and autogenous shrinkage)*

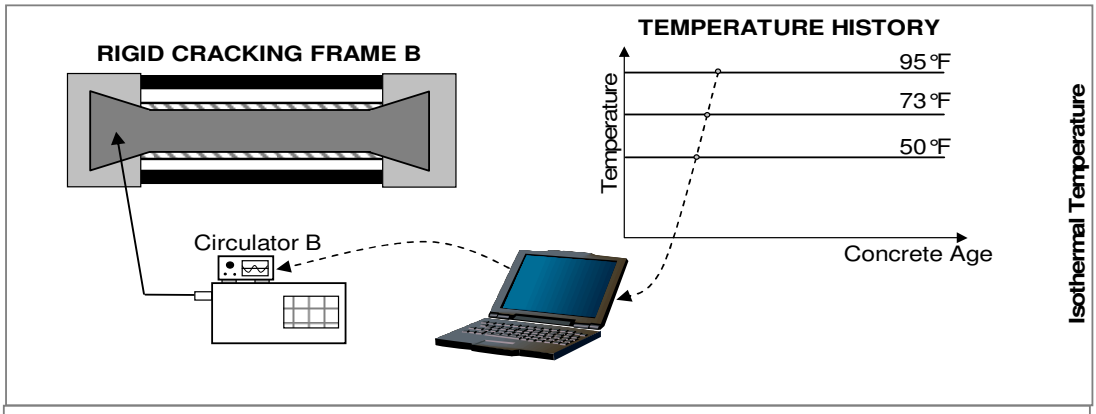


*Stress Development in RCF B = f(Autogenous shrinkage)*

ADDITIONAL TESTS

- Semi-Adiabatic Calorimetry
- Conventional drying shrinkage
  - Start drying at 7-days
- $f_c$ at 7, and 28-day (moist cured)
- Fresh concrete properties
  - Slump, Air
- Setting

**Figure 3-1:** Schematic of experimental testing program

### 3.1.1 SEMI-ADIABATIC CALIORIMETRY

The semi-adiabatic hydration drum (Quadrel iQdrum 300) was used to record the heat signature of each concrete mixture. The semi-adiabatic hydration drum is shown in Figure 3-2. The data recovered from the hydration drum were then used to calculate the parameters that define the progress of hydration each specific mixture (Schindler and Folliard 2005). These hydration parameters, found in Appendix D, were then used to model the temperature evolution in a typical mass concrete member as described in the next section.

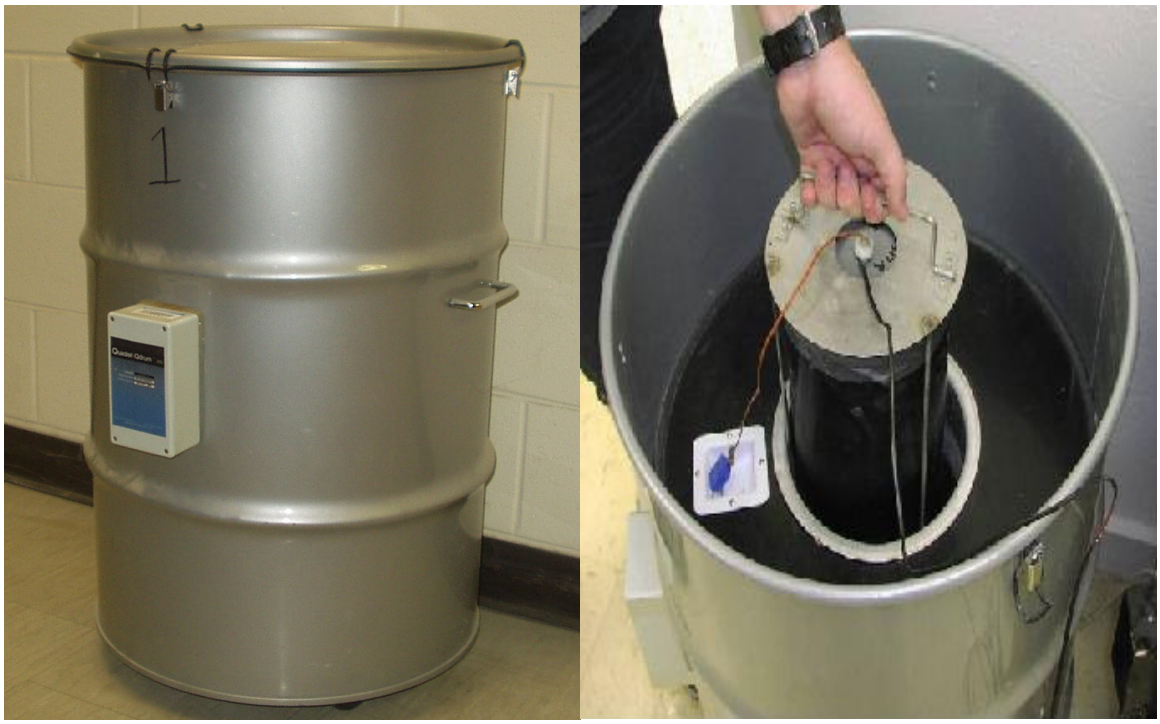


**Figure 3-2:** Semi-adiabatic hydration drum (Quadrel iQdrum 300)

### 3.1.2 CRACKING FRAME TEMPERATURE DEVELOPMENT PROGRAM

The next step for each mixture was to generate a temperature history that could be expected if that mixture was placed in a typical mass concrete structural element. A cracking frame temperature development program, developed by The University of Texas at Austin, was used to generate a temperature profile by modeling a 1.0 meter thick wall as shown in Figure 3-3. The ambient temperature surrounding the concrete specimen was constrained to be constant. The temperature history generated by the computer program represents the center point temperature of the wall core as it changes over time.

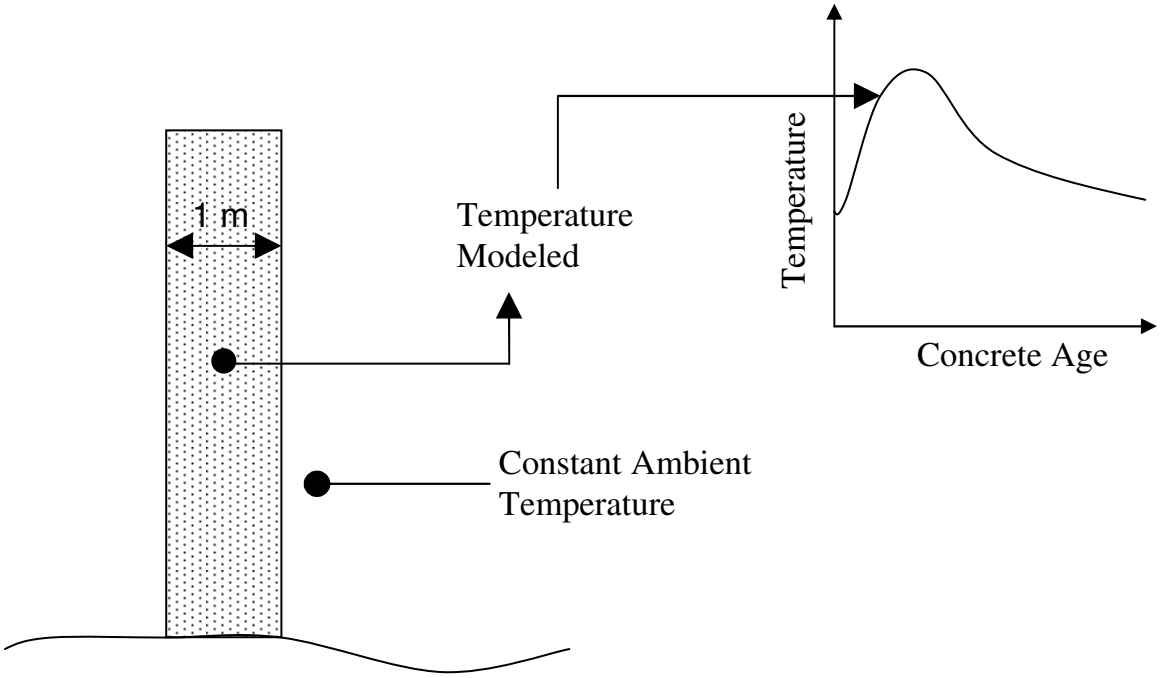


**Figure 3-3:** Schematic of temperature history modeling

The mixture proportions, aggregate type, placement temperature, ambient temperature, specimen size, and hydration parameters are input variables that the program uses to develop a temperature profile. The fresh concrete placement

temperatures were selected to be 50°F, 73°F, and 95°F. The ambient temperatures were chosen to be 50°F, 73°F, and 95°F. These temperatures were selected so that the effects of lowering the placement temperature in hot weather conditions and seasonal temperature changes could be studied. The resulting temperature profile is exported into MS Excel® and converted into a text document. The computer program used to control the match curing test uses the text document as input when driving the concrete to the desired temperature profile. Typical temperature profiles from the cracking frame temperature development program can be seen in Figure 3-4.

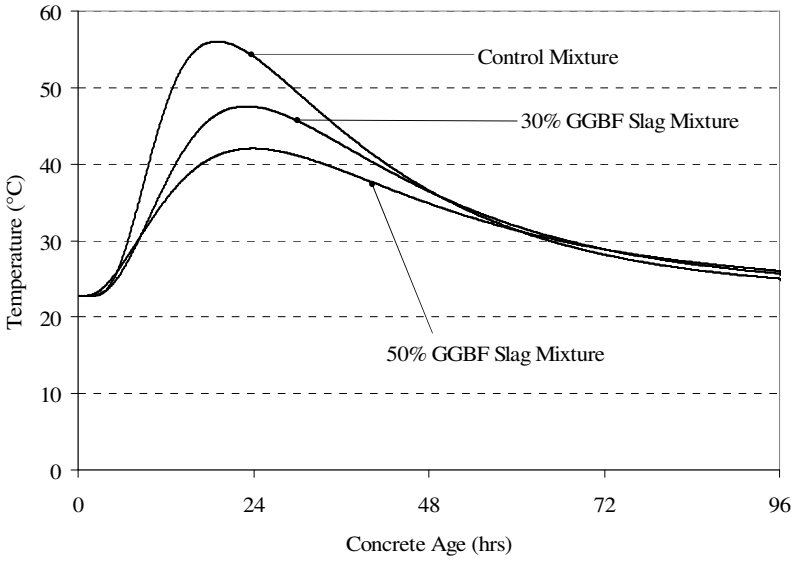


**Figure 3-4:** Temperature profiles from cracking frame temperature development program

### 3.1.3 RIGID CRACKING FRAME

In Section 2.7.1 an introduction to the rigid cracking frame test setup is provided. The experimental testing program uses two rigid cracking frames (see Figure 3-5) as discussed in Whigham (2005) with some exceptions. The first cracking frame is subjected to a match-curing temperature profile (see Figure 3-4) to simulate a 1.0 meter thick specimen. Reasons for changes are as follows:

- To produce temperatures representative of mass concrete members
- To minimize thermal differences from crosshead to middle of the concrete specimen. In the previous study, the test was started without water in the cross-head and this produced large temperature differences throughout the concrete specimen.
- To reduce dependence upon fresh concrete temperature. The circulator now adjusts temperature immediately after placement.
- To evaluate the effects of seasonal changes such as cold and hot fresh concrete placement temperatures.

The second cracking frame is subjected to isothermal conditions so that the effect of autogenous shrinkage can be isolated and studied. The isothermal cracking frame test was conducted under three temperature conditions: 50°F, 73°F, and 95°F. These temperatures were selected to match the fresh concrete placement temperatures for the cracking frame subjected to varying temperature profiles.

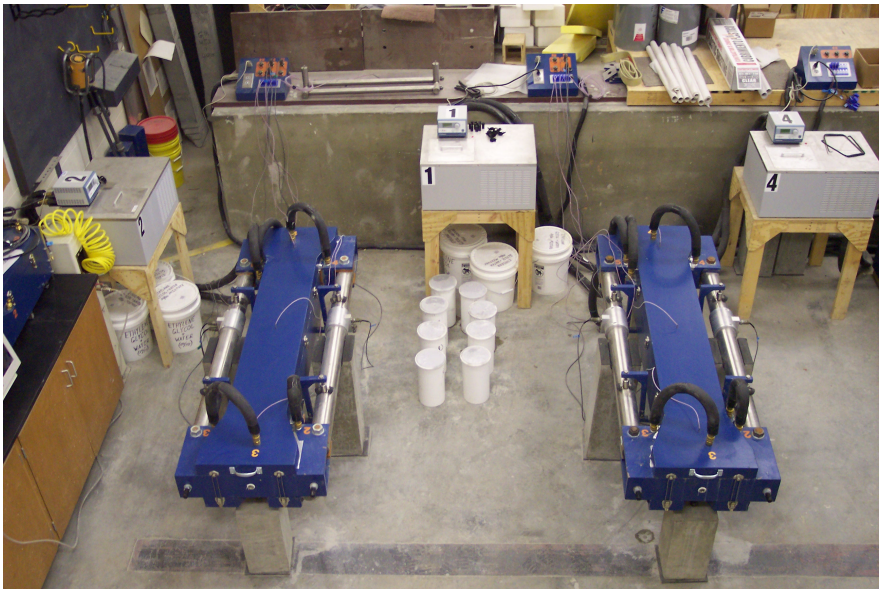


**Figure 3-5:** Rigid cracking frames

Once a previous test is complete, the specimen and any remaining debris are removed from the rigid cracking frame. The inside of the formwork is lined with a layer of plastic sheeting that is taped to the formwork. This layer is used to protect and prevent the concrete from adhering to the formwork. Silicon is used to smooth the area between the crossheads and formwork to prevent stress concentrations.

After the concrete is mixed, the fresh concrete is placed into the rigid cracking frame formwork with two lifts. Each lift is vibrated to ensure proper consolidation. The concrete is smoothed using a wooden trowel. A layer of plastic is secured to the formwork over the concrete to prevent moisture loss. All plastic edges are sealed together with adhesive aluminum foil tape. The thermally insulated lid is then secured to the formwork. Two temperature probes are embedded into the concrete via holes through the lid. The strain gauge wires are securely fastened to the Invar rods. Quick disconnect

hoses are fastened to the formwork and circulator so that concrete in the rigid cracking frame can be temperature controlled.

Under the testing procedure described by Whigham (2005), both cracking frames were allowed to hydrate naturally for four days. After 96 hours, both frames were cooled at 1°C/hr until the concrete was cracked.

Using the current testing procedure, as shown in Figure 3-1, the isothermal frame was allowed to run for 144 hours at a constant temperature. The match-curing cracking frame followed the prescribed temperature profile for 96 hours and then cooled at 1°C/hr thereafter. These times were selected so that the test could be conducted every week. The practice of cooling the concrete at 1°C/hr after 96 hours also matches the approach used by Springenschmid and Breitenbücher (1998).

### 3.1.4 FREE SHRINKAGE FRAME

The free shrinkage frame is an addition to the testing program since the work of Whigham (2005). The specimen in this frame is match-cured using the same temperature profile as the concrete in the match-curing cracking frame. The free shrinkage frame is used to measure the deformation under zero-restraint conditions.

#### 3.1.4.1 Free Shrinkage Frame Design

The free shrinkage frame consists of a thermally insulated box, four steel plates, and a supporting steel frame as shown in Figures 3-6 and 3-7. The box serves as the formwork for the freshly placed concrete as well as the system to match cure the concrete to the temperature profile used for the cracking frame. The dimensions of the concrete

specimen are 150 mm x 150 mm x 600 mm; however, the effective gauge length of the test specimen is 500 mm as indicated in Figure 3-6. There are two stainless steel plates at each end of the formwork. The outer plate is connected via bolts to the formwork. The inner plate is connected to the outer plate with bolts that allow for retraction once the concrete has reached initial set.

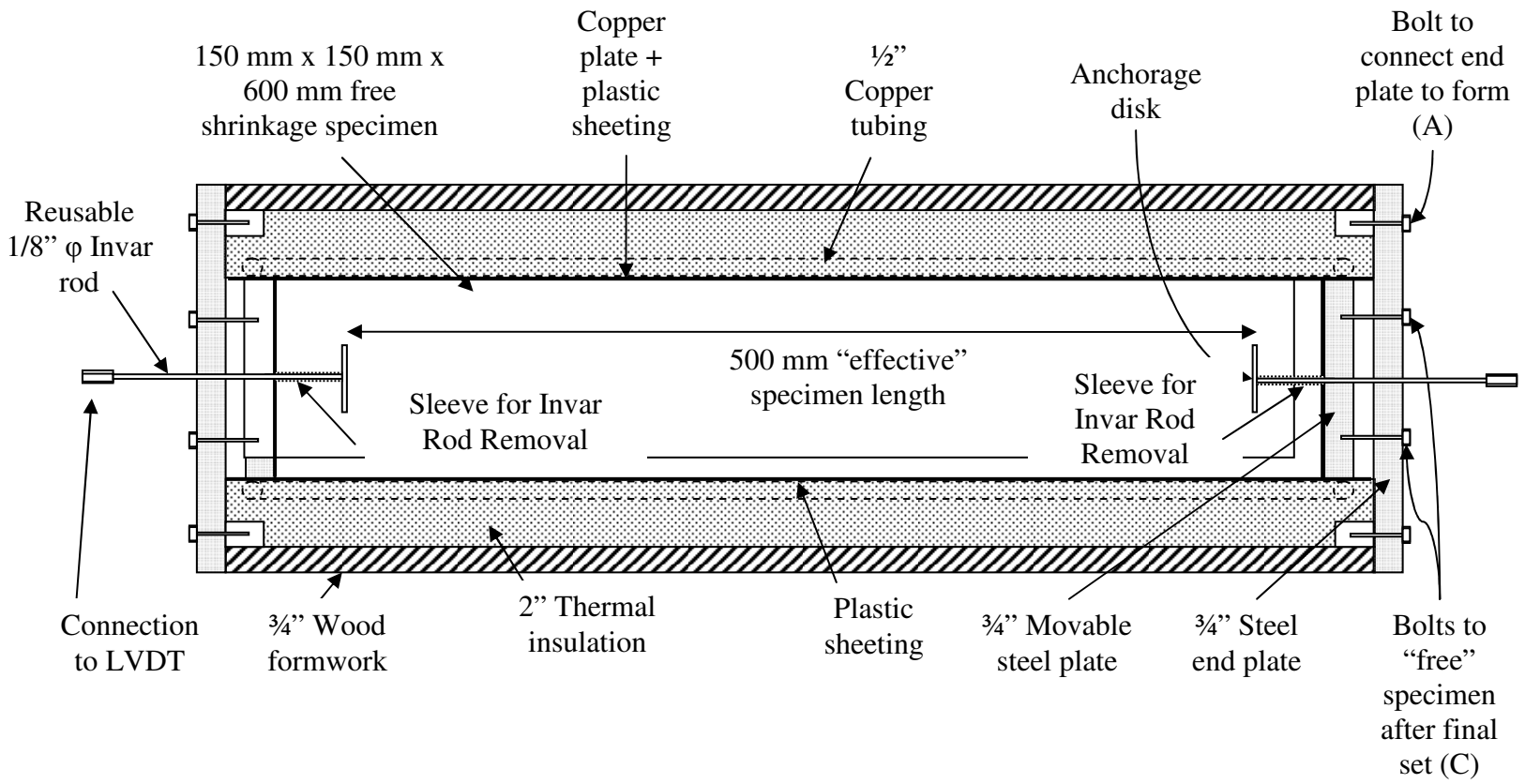


**Figure 3-6:** Free shrinkage frame detail in plan view

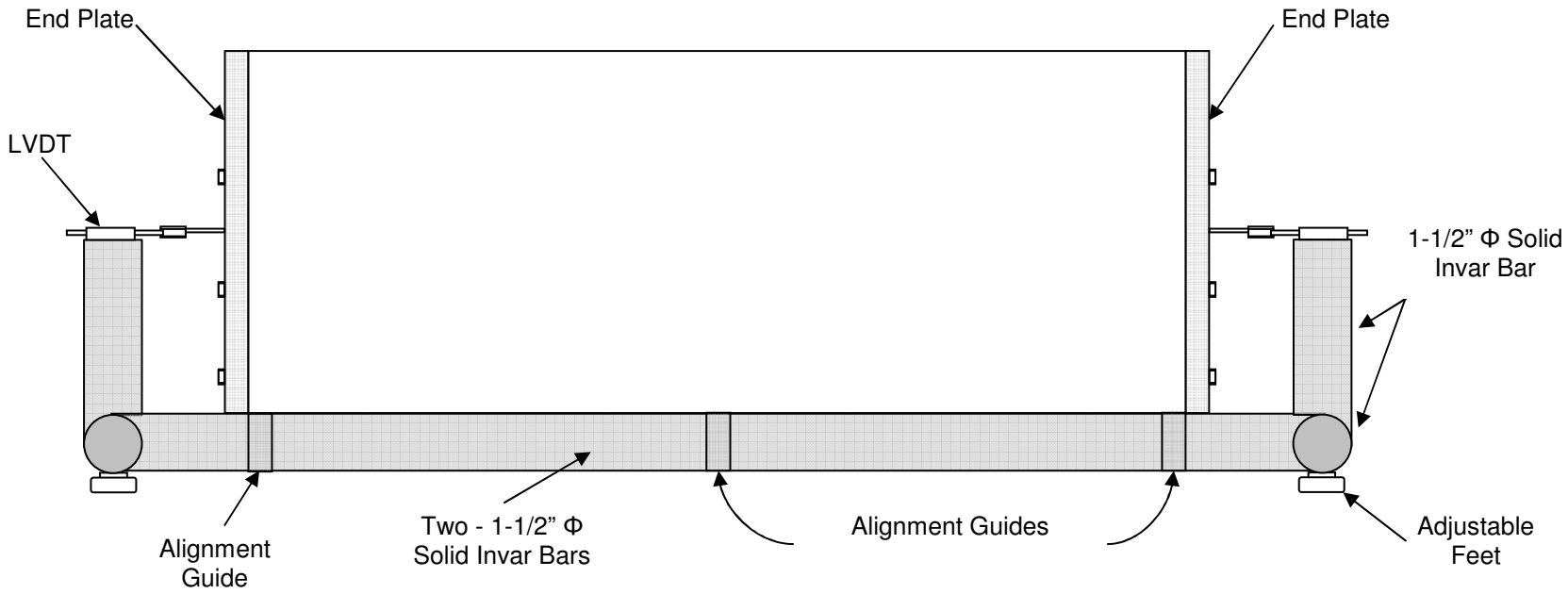


**Figure 3-7:** Elevation view of free shrinkage frame

As shown in Figure 3-6, a 1/8-in diameter Invar rod is placed through the inner and outer plates on each side which hold it into position. The rod is connected to an anchorage disk within the concrete and to the LVDT. The LVDT is securely fastened to the supporting frame using standard mounting holes and small bolts. A small plastic sleeve is placed around each Invar bar to allow easy recovery after testing is complete.

In Figure 3-7, the supporting steel frame is shown. The frame consists of Invar steel bars to reduce the effect that ambient temperature changes may have on the recorded length change. The reduction in movement allows for accurate measurements to be taken without large errors due to ambient temperature changes. Further details of free shrinkage frame are available in Appendix A.

#### 3.1.4.2 Free Shrinkage Frame Preparation

Once a previous test is complete, the specimen and any remaining debris are removed. Then, the inner plates are returned to their original starting position. The inside of the formwork is lined with an outer layer of plastic sheeting that is taped to the formwork. This layer is used to protect and prevent the concrete from adhering to the formwork. A lubricant such as WD40® is sprayed onto the outer layer of plastic sheeting. An inner layer of plastic sheeting is placed inside the outer layer, as shown in Figure 3-8. Thus, the lubricant is between the two layers of plastic sheeting. The inner layer of plastic is not taped to the formwork which would alter the movement of the concrete specimen, and is folded over the concrete after placement. Therefore, the concrete prism is completely sealed by the inner layer of plastic, yet able to move freely inside the formwork.

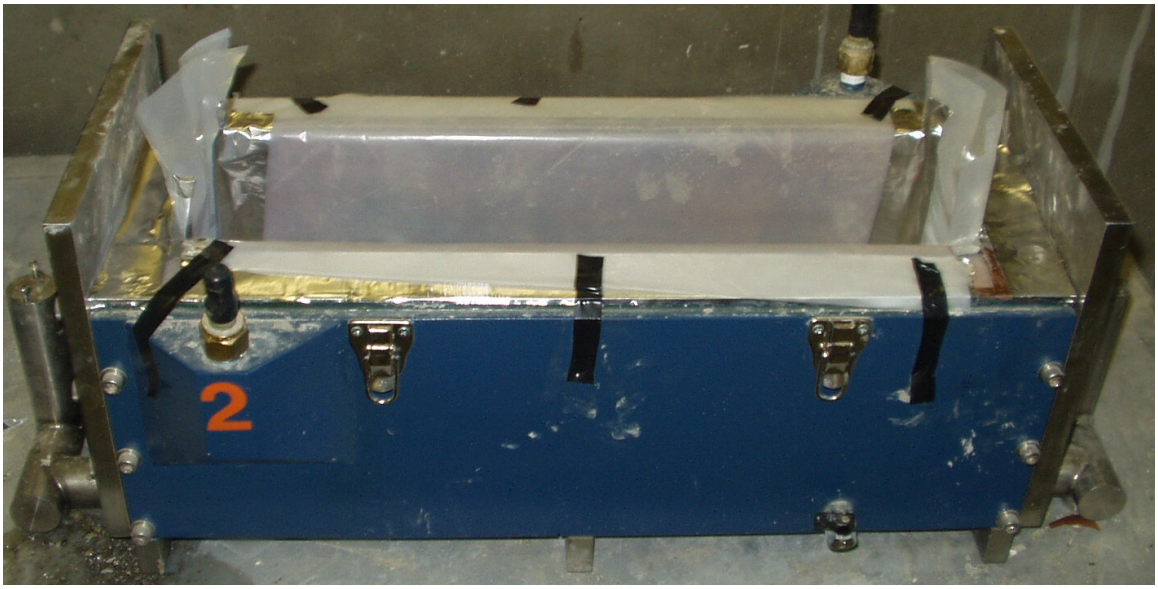


**Figure 3-8:** Free shrinkage frame lined with two layers of plastic

### 3.1.4.3 Free Shrinkage Frame Test Method

The fresh concrete is placed into the free shrinkage frame formwork in two lifts. Each lift is vibrated to ensure proper consolidation. The concrete surface is smoothed using a wooden trowel. The inner layer of plastic sheeting is folded over the top of the fresh concrete and a layer of plastic is secured to the formwork over the concrete to prevent moisture loss. All plastic edges are sealed together with adhesive aluminum foil tape. The thermally insulated lid is then secured to the formwork. Two temperature probes are embedded into the concrete via holes through the lid. The LVDTs are securely fastened to the Invar rods and the supporting steel frame. Quick disconnect hoses are fastened to the formwork and circulator so that concrete in the free shrinkage frame can be temperature controlled. The free shrinkage frame ready for testing is shown in Figure 3-

9. After the concrete has reached initial set, the inner plate is backed away to allow measurement of expansion and contraction of the prism.

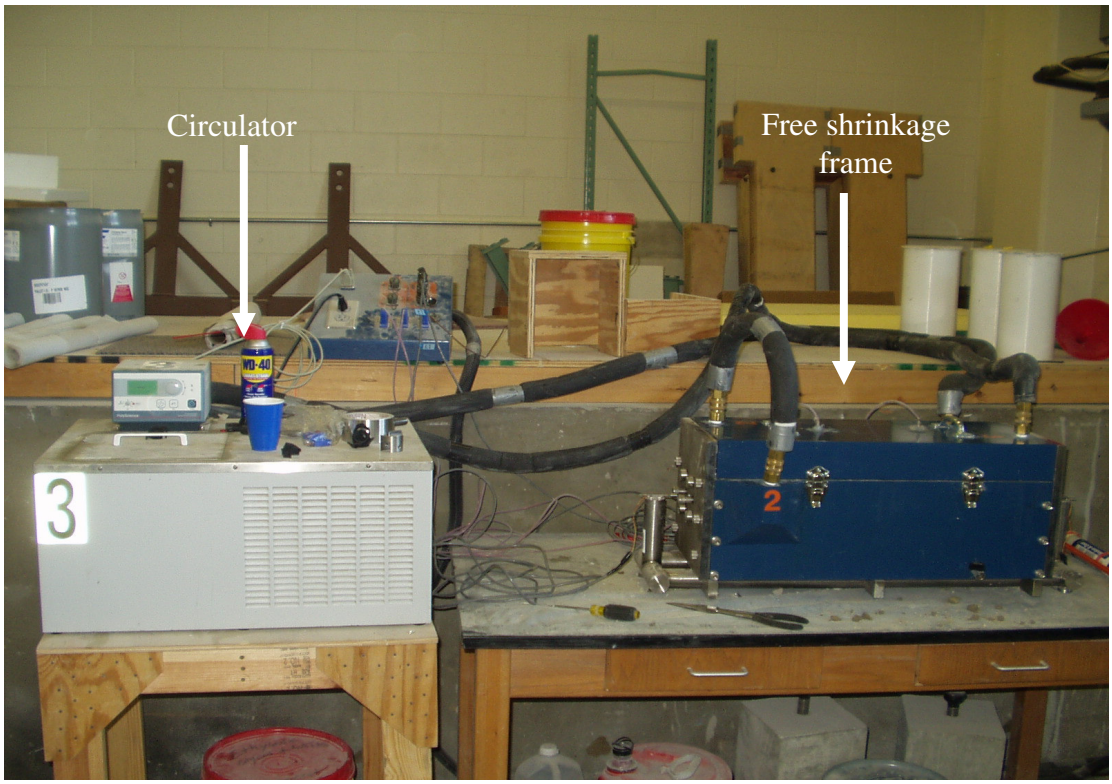


**Figure 3-9:** Free shrinkage frame ready for testing

### 3.1.5 CYLINDER MATCH-CURING SYSTEM

A match-curing system was required to condition the temperature of all molded cylinders and the setting test specimen. The cylinders in the match-curing system were subjected to the same temperature profile as the free shrinkage frame and the match-cured cracking frame. The match-curing system consists of two Igloo® coolers, which can be seen in Figure 3-10. The larger cooler has a 120-quart capacity while the smaller has a 25-quart

capacity. The larger cooler was sized to hold 24 - 4”x 8” cylinders for testing of mechanical properties. The smaller cooler houses one 7 ½”x 6” can for the setting test.

**Figure 3-10:** Match-curing system

The match-curing system is an open system, which is different from that described by Whigham (2005); therefore, the elevations of each cooler with respect to the circulator had to be adjusted so that the water level would remain constant throughout. The two coolers are in series with one another; therefore, a 2-in diameter hose was used to connect the coolers. The circulator pumps temperature-controlled water into the larger cooler. The water is circulated from the larger cooler into the smaller cooler via the connection hose. The water is then pumped from the smaller cooler back to the circulator to complete the circuit.

### 3.1.6 DATA ACQUISITION

As a result of all the changes made to the testing program of Whigham (2005), the match-curing computer program was updated. The modifications are as follows:

- Inclusion of free shrinkage frame
- Initiation of match-curing just after placement of concrete
- Inclusion of isothermal rigid cracking frame

The data acquisition system is similar to the system developed by Whigham (2005), except for the free shrinkage frame. The datalogger program was updated to include the new addition. Two concrete temperature probes, two LVDTs, and one air temperature probe from the free shrinkage frame were utilized in addition to the testing setup outlined by Whigham (2005).

## 3.2 CONCRETE MIXTURES EVALUATED

The laboratory testing program was designed to evaluate the effects of placement temperature, ambient temperature, cement type, cementitious materials, air entrainment, and water-to-cementitious materials ratio on the cracking tendency of concrete mixtures. Table 3-1 outlines the laboratory testing program used to test these variables. Table 3-2 outlines the mixture proportions of each concrete mixture. The following notation is used:

- CTRL – Control Mixture
- 30C – 30% Class C Fly Ash
- 20C – 20% Class C Fly Ash

- 30SG – 30% GGBF Slag
- 50SG – 50% GGBF Slag
- 25C6SF – 25% Class C Fly Ash and 6% Silica Fume
- 25F6SF – 25% Class F Fly Ash and 6% Silica Fume
- 20F30SG – 20% Class F Fly Ash and 30% GGBF Slag
- WC32 – Water-to-Cement Ratio = 0.32
- WC38 – Water-to-Cement Ratio = 0.38
- WC48 – Water-to-Cement Ratio = 0.48
- WC53 – Water-to-Cement Ratio = 0.53
- TYPE3 – Type III Cement
- AEA – Air Entrainment

In order to systematically evaluate the effects of concrete constituents and temperature on the cracking sensitivity of a mixture, a control mixture was established for comparison purposes. The control mixture, identified by CTRL, consists of a standard Type I cement, water-to-cement ratio of 0.42, with No. 57 siliceous river gravel, placed at 73°F, and with the 1.0 meter thick wall element exposed to ambient temperature conditions of 73°F. The control mixture is representative of mixtures typically used in Texas mass concrete elements.

**Table 3-1A:** Laboratory Testing Program

| Mix ID | Batch ID Number | Effect of: | Fresh Concrete Temp ($T_{ci}$) | Ambient Temp ($T_{air}$) | Cement | | W/C | Fly Ash | | | | | Slag | | Chemical Admixtures | | |
|---|---|---|---|---|---|---|---|---|---|---|---|---|---|---|---|---|---|
| | | | | | C1 | C2 | | FA1 | | FA2 | FA3 | | SG1 | | WR1 | WR2 | A1 |
| | | | | | Type I - Capitol | Type III - Cemex | | Rockdale - 20% | Rockdale - 30% | Deely Spr. - 30% | Comanche - 20% | Comanche - 30% | Gr. 120 Holcim 30% | Gr. 120 Holcim 50% | HRWR | MB-200N | AEA |
| CTRL | A | **Control Mix:** Type I Cement + Gravel | 73ºF | 73ºF | X | | 0.42 | | | | | | | | | X | |
| | B | Tci + Tair | 50ºF | 50ºF | X | | 0.42 | | | | | | | | | X | |
| | C | Tci + Tair | 95ºF | 95ºF | X | | 0.42 | | | | | | | | | X | |
| | D | Tci + Tair | 73ºF | 95ºF | X | | 0.42 | | | | | | | | | X | |
| | E | Tci + Tair | 50ºF | 95ºF | X | | 0.42 | | | | | | | | | X | |
| 30C | | 30% Class C Fly ash (FA3) | 73ºC | 73ºF | X | | 0.42 | | | | | X | | | | X | |
| 20C | | 20% Class C Fly ash (FA3) | 73ºC | 73ºF | X | | 0.42 | | | | X | | | | | X | |
| 30SG | A | Tci + Tair + 30% Gr. 120 Slag | 73ºF | 73ºF | X | | 0.42 | | | | | | X | | | X | |
| | B | Tci + Tair + 30% Gr. 120 Slag | 50ºF | 50ºF | X | | 0.42 | | | | | | X | | | X | |
| | C | Tci + Tair + 30% Gr. 120 Slag | 95ºF | 95ºF | X | | 0.42 | | | | | | X | | | X | |
| | D | Tci + Tair + 30% Gr. 120 Slag | 73ºF | 95ºF | X | | 0.42 | | | | | | X | | | X | |
| | E | Tci + Tair + 30% Gr. 120 Slag | 50ºF | 95ºF | X | | 0.42 | | | | | | X | | | X | |
| 50SG | A | Tci + Tair + 50% Gr. 120 Slag | 73ºF | 73ºF | X | | 0.42 | | | | | | | X | | X | |
| | B | Tci + Tair + 50% Gr. 120 Slag | 50ºF | 50ºF | X | | 0.42 | | | | | | | X | | X | |
| | C | Tci + Tair + 50% Gr. 120 Slag | 95ºF | 95ºF | X | | 0.42 | | | | | | | X | | X | |
| | D | Tci + Tair + 50% Gr. 120 Slag | 73ºF | 95ºF | X | | 0.42 | | | | | | | X | | X | |
| | E | Tci + Tair + 50% Gr. 120 Slag | 50ºF | 95ºF | X | | 0.42 | | | | | | | X | | X | |

**Table 3-1B:** Laboratory Testing Program

| Mix ID | Batch ID Number | Effect of: | Fresh Concrete Temp ($T_{ci}$) | Ambient Temp ($T_{air}$) | Cement | | W/C | Fly Ash | | | | | Slag | | Chemical Admixtures | | |
|---|---|---|---|---|---|---|---|---|---|---|---|---|---|---|---|---|---|
| | | | | | C1 | C2 | | FA1 | | FA2 | FA3 | | SG1 | | WR1 | WR2 | A1 |
| | | | | | Type I - Capitol | Type III - Cemex | | Rockdale - 20% | Rockdale - 30% | Deely Spr. - 30% | Comanche - 20% | Comanche - 30% | Gr. 120 Holcim 30% | Gr. 120 Holcim 50% | HRWR | MB-200N | AEA |
| 25C6SF | | Ternary: 25% Class C (FA2) + 6% SF | 73ºF | 73ºF | X | | 0.42 | | | X | | | | | | X | |
| 25F6SF | | Ternary: 25% Class F (FA1) + 6% SF | 73ºF | 73ºF | X | | 0.42 | | X | | | | | | | X | |
| 20F30SG | | Tci+Tair+20% Class F (FA1) +30% Slag | 73ºF | 73ºF | X | | 0.42 | X | | | | | X | | | X | |
| WC32 | | w/c = 0.32 | 73ºF | 73ºF | X | | 0.32 | | | | | | | | X | X | |
| WC38 | A | Tci + Tair + w/c = 0.38 | 73ºF | 73ºF | X | | 0.38 | | | | | | | | X | X | |
| | B | Tci + Tair + w/c = 0.38 | 50ºF | 50ºF | X | | 0.38 | | | | | | | | X | X | |
| | C | Tci + Tair + w/c = 0.38 | 95ºF | 95ºF | X | | 0.38 | | | | | | | | X | X | |
| | D | Tci + Tair + w/c = 0.38 | 73ºF | 95ºF | X | | 0.38 | | | | | | | | X | X | |
| | E | Tci + Tair + w/c = 0.38 | 50ºF | 95ºF | X | | 0.38 | | | | | | | | X | X | |
| WC48 | | w/c = 0.48 | 73ºF | 73ºF | X | | 0.48 | | | | | | | | | | |
| WC53 | | w/c = 0.53 | 73ºF | 73ºF | X | | 0.53 | | | | | | | | | | |
| TYPE3 | A | Type III Cement | 73ºF | 73ºF | | X | 0.42 | | | | | | | | | X | |
| | B | Type III Cement + Tci + Tair | 50ºF | 50ºF | | X | 0.42 | X | | | | | X | | | X | |
| | C | Type III Cement + Tci + Tair | 95ºF | 95ºF | | X | 0.42 | X | | | | | X | | | X | |
| | D | Type III Cement + Tci + Tair | 73ºF | 95ºF | | X | 0.42 | X | | | | | X | | | X | |
| | E | Type III Cement + Tci + Tair | 50ºF | 95ºF | | X | 0.42 | X | | | | | X | | | X | |
| AEA | | AEA | 73ºF | 73ºF | X | | 0.42 | | | | | | | | | X | X |

**Table 3-2A:** Concrete Mixture Proportions

| Mix ID | Water (pcy) | Type I cement (pcy) | Type III cement (pcy) | Class F Fly Ash (pcy)* | Class C Fly Ash (pcy)** | Class C Fly Ash (pcy)*** | Silica Fume (pcy) | GGBF Slag (pcy) | Coarse Aggregate (pcy) | Fine Aggregate (pcy) | HRWR (oz./cwt) | MB-200N (oz./cwt) | AEA (oz./cwt) | Target Air (%) | w/cm |
|---|---|---|---|---|---|---|---|---|---|---|---|---|---|---|---|
| CTRL | 237 | 564 | -- | -- | -- | -- | -- | -- | 1927 | 1285 | -- | 4 | -- | 2 | 0.42 |
| 30C | 237 | 395 | -- | -- | -- | 169 | -- | -- | 1927 | 1285 | -- | 4 | -- | 2 | 0.42 |
| 20C | 237 | 451 | -- | -- | -- | 113 | -- | -- | 1927 | 1265 | -- | 4 | -- | 2 | 0.42 |
| 30SG | 237 | 395 | -- | -- | -- | -- | -- | 169 | 1927 | 1270 | -- | 4 | -- | 2 | 0.42 |
| 50SG | 238 | 282 | -- | -- | -- | -- | -- | 282 | 1927 | 1263 | -- | 4 | -- | 2 | 0.42 |
| 25C6SF | 239 | 389 | -- | -- | 141 | -- | 34 | -- | 1927 | 1227 | -- | 4 | -- | 2 | 0.42 |
| 25F6SF | 240 | 389 | -- | 141 | -- | -- | 34 | -- | 1927 | 1227 | -- | 4 | -- | 2 | 0.42 |

* Rockdale
** Deely Spruce
*** Comanche

**Table 3-2B:** Concrete mixture Proportions

| Mix ID | Water (pcy) | Type I cement (pcy) | Type III cement (pcy) | Class F Fly Ash (pcy)* | Class C Fly Ash (pcy)** | Class C Fly Ash (pcy)*** | Silica Fume (pcy) | GGBF Slag (pcy) | Coarse Aggregate (pcy) | Fine Aggregate (pcy) | HRWR (oz./cwt) | MB-200N (oz./cwt) | AEA (oz./cwt) | Target Air (%) | w/cm |
|---|---|---|---|---|---|---|---|---|---|---|---|---|---|---|---|
| 20F30SG | 241 | 282 | -- | 113 | -- | -- | -- | 169 | 1927 | 1285 | -- | 4 | -- | 2 | 0.42 |
| WC32 | 211 | 658 | -- | -- | -- | -- | -- | -- | 1915 | 1271 | 14 | -- | -- | 2 | 0.32 |
| WC38 | 232 | 611 | -- | -- | -- | -- | -- | -- | 1910 | 1266 | 10 | -- | -- | 2 | 0.38 |
| WC48 | 248 | 517 | -- | -- | -- | -- | -- | -- | 1935 | 1290 | -- | -- | -- | 2 | 0.48 |
| WC53 | 249 | 470 | -- | -- | -- | -- | -- | -- | 1952 | 1306 | -- | -- | -- | 2 | 0.53 |
| TYPE3 | 237 | -- | 564 | -- | -- | -- | -- | -- | 1927 | 1280 | -- | 4 | -- | 2 | 0.42 |
| AEA | 237 | 564 | -- | -- | -- | -- | -- | -- | 1927 | 1276 | -- | 4 | 5 | 6 | 0.42 |

* Rockdale
** Deely Spruce
*** Comanche

As shown in Table 3-1, five of the mixtures were placed at different temperature conditions. The effect of placement temperature and ambient temperature conditions were varied to study the effects of seasonal changes and reduction of placement temperature under summer conditions. These changes are denoted by the Batch ID. The following notation will be used to present and discuss the variations in temperature.

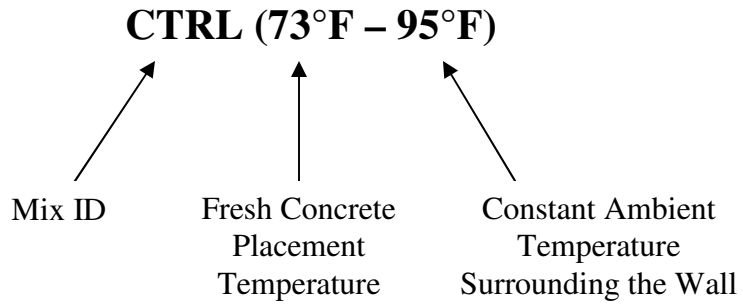


### 3.3 EXPERIMENTAL PROCEDURES

The experimental procedure outlined in Whigham (2005) was closely followed. All concrete mixing in this project was performed in a climate-controlled concrete laboratory. The raw materials used in the production of the concrete batches were also stored in the laboratory. Portland cement was stored in standard 94-lb sacks while the supplementary cementing materials were stored in sealed 5-gallon buckets or sealed 55-gallon drums. The coarse and fine aggregates were stored in sealed 55-gallon drums. The aggregates were replenished from large stockpiles stored outdoors at the Auburn University facilities division in Auburn, Alabama.

### 3.3.1 BATCHING

Moisture corrections were conducted using a small digital scale and a hot plate. After the moisture content of the aggregates was determined, the materials were placed in 5-gallon buckets with lids to prevent any moisture loss.

To produce concrete with a cold or hot placement temperature, the raw materials were placed in an environmental chamber for at least 48 hours prior to mixing. To produce concrete with placement temperatures of 50°F or 95°F, the environmental chamber was set to 35°F or 115°F respectively. To produce concrete at room temperature (73°F), the raw materials were placed in the concrete laboratory for at least 24 hours prior to mixing.

### 3.3.2 MIXING PROCEDURE

Just prior to each batch, the concrete mixer was "buttered" using cement, sand, and water to produce a mortar to coat the inside of the mixer. Once this mortar was removed, the raw materials were added. Approximately one third of the aggregates were then placed in the mixer, alternating rock and sand to ensure proper mixing. Then, one third of the cement and water was added. The materials were allowed to mix thoroughly before the next one third of the materials was added. This process was continued until all materials were added to the concrete mixer. Once all materials were placed in the mixer, the concrete was allowed to mix for five minutes to ensure thorough mixing of all constituents.

### 3.3.3 FRESH CONCRETE TESTING

After completion of mixing, the following fresh concrete properties were tested:

- Slump according to ASTM C 143 (2003),
- Unit weight according to ASTM C 138 (2001),
- Air content according to ASTM C 231 (2004),
- Fresh concrete temperature according to ASTM C 1064 (2004), and
- Setting times according to ASTM C 403 (1999).

### 3.3.4 HARDENED CONCRETE TESTING

Hardened concrete properties were evaluated using the following test methods:

- Compressive strength according to ASTM C 39 (2003),
- Static modulus of elasticity according to ASTM C 469 (2002),
- Splitting tensile strength according to ASTM C 496 (2004),
- Drying shrinkage according to ASTM C 157 (2004), and
- Permeability according to ASTM C 1202 (1997).

## 3.4 MATERIALS

To determine the effect of cement type and supplementary cementing materials on the cracking sensitivity of concrete mixes, several different raw materials were examined. The following sections provide a detailed discussion of the cement type, supplementary cementing materials, aggregates, and chemical admixtures used to produce the concrete mixtures as outlined in Section 3.2.

### 3.4.1 CEMENT TYPE

In order to assess the effects of cement type on the cracking sensitivity of a concrete mixture, two different types of cement were used:

- Type I portland cement – manufactured by Capitol in San Antonio, Texas, and
- Type III portland cement – manufactured by CEMEX in Demopolis, Alabama

The Type I cement was shipped from Texas to Auburn University specifically for this study. Both cement types were sampled and sent to an independent commercial laboratory for a chemical analysis. The results of the chemical analysis are shown in Table 3-3.

**Table 3-3:** Chemical properties of the cement types

| Parameter | Portland Cement | | |
|---|---|---|---|
| | **Type I *** | **Type I **** | **Type III** |
| Silicon dioxide, $SiO_2$ (%) | 20.66 | 21.25 | 20.20 |
| Aluminum oxide, $Al_2O_3$ (%) | 5.46 | 5.31 | 5.01 |
| Iron oxide, $Fe_2O_3$ (%) | 2.01 | 1.87 | 3.74 |
| Calcium oxide, CaO (%) | 64.06 | 63.61 | 62.50 |
| Magnesium oxide, MgO (%) | 1.19 | 1.30 | 1.04 |
| Alkalies ($Na_2O + 0.658K_2O$) (%) | 0.52 | 0.51 | 0.31 |
| Sulfur trioxide, $SO_3$ (%) | 3.34 | 3.56 | 4.62 |
| Loss on ignition, LOI (%) | 1.97 | 1.87 | 1.87 |
| Insoluble Residue (%) | -- | -- | -- |
| Tricalcium silicate, $C_3S$ (%) | 54.72 | 48.94 | 48.76 |
| Dicalcium silicate, $C_2S$ (%) | 17.95 | 24.00 | 21.14 |
| Tricalcium aluminate, $C_3A$ (%) | 11.07 | 10.91 | 6.95 |
| Tetracalcium aluminoferrite, $C_4AF$ (%) | 6.12 | 5.69 | 11.37 |
| Blaine ($m^2/kg$) | 350 | 350 | 560 |

*First shipment

**Second shipment

### 3.4.2 SUPPLEMENTARY CEMENTING MATERIALS

In order to evaluate the effects of supplementary cementing materials (SCMs) on the cracking sensitivity of a concrete mixture, six different types of SCMs were used:

- Class C fly ash – distributed by Boral Materials in Comanche, Texas,
- Class C fly ash – distributed by Boral Materials in Deely Spruce, Texas,
- Class F fly ash – distributed by Boral Materials in Rockdale, Texas,
- Silica Fume Force 10000 – distributed by WR Grace, and

- Grade 120 GGBF Slag – distributed by Holcim in New Orleans, Louisiana

All supplementary cementing materials were sampled and sent to an independent commercial laboratory for a chemical analysis. The results of the chemical analysis are shown in Table 3-4.

**Table 3-4:** Chemical properties of supplementary cementing materials

| Parameter | Class C FA | | Class F FA | Silica Fume | GGBF Slag |
|---|---|---|---|---|---|
| | Comanchee | Deely Spruce | Rockdale | WR Grace | Holcim |
| Silicon dioxide, $SiO_2$ (%) | 33.74 | 38.01 | 51.52 | 93.64 | 38.75 |
| Aluminum oxide, $Al_2O_3$ (%) | 18.37 | 19.69 | 24.56 | 0.28 | 9.01 |
| Iron oxide, $Fe_2O_3$ (%) | 5.26 | 6.21 | 4.20 | 0.09 | 0.45 |
| Calcium oxide, CaO (%) | 28.46 | 23.03 | 13.27 | 0.57 | 35.92 |
| Magnesium oxide, MgO (%) | 5.37 | 4.70 | 2.29 | 0.6 | 13.24 |
| Alkalies ($Na_2O + 0.658K_2O$) (%) | 1.88 | 2.16 | 0.87 | 0.71 | 0.47 |
| Sulfur trioxide, $SO_3$ (%) | 2.27 | 1.55 | 0.50 | 0.21 | 1.69 |
| Loss on ignition, LOI (%) | 0.43 | 0.57 | 0.41 | 3.22 | -0.48 |

### 3.4.3 COARSE AGGREGATE

In order to maintain consistency in the evaluation of the cracking tendency of various concrete mixtures at Auburn University and The University of Texas at Austin, a siliceous river gravel from Victoria, Texas was used by both schools. This aggregate was trucked to Auburn in two 10-ton loads. The aggregate was sampled and tested to determine the gradation, bulk specific gravity, and absorption capacity. The No. 57 river

gravel was found to be in accordance with ASTM C 33 (2003). The gradation can be found in Figure 3-11. The bulk specific gravity and absorption capacity can be found in Table 3-5.

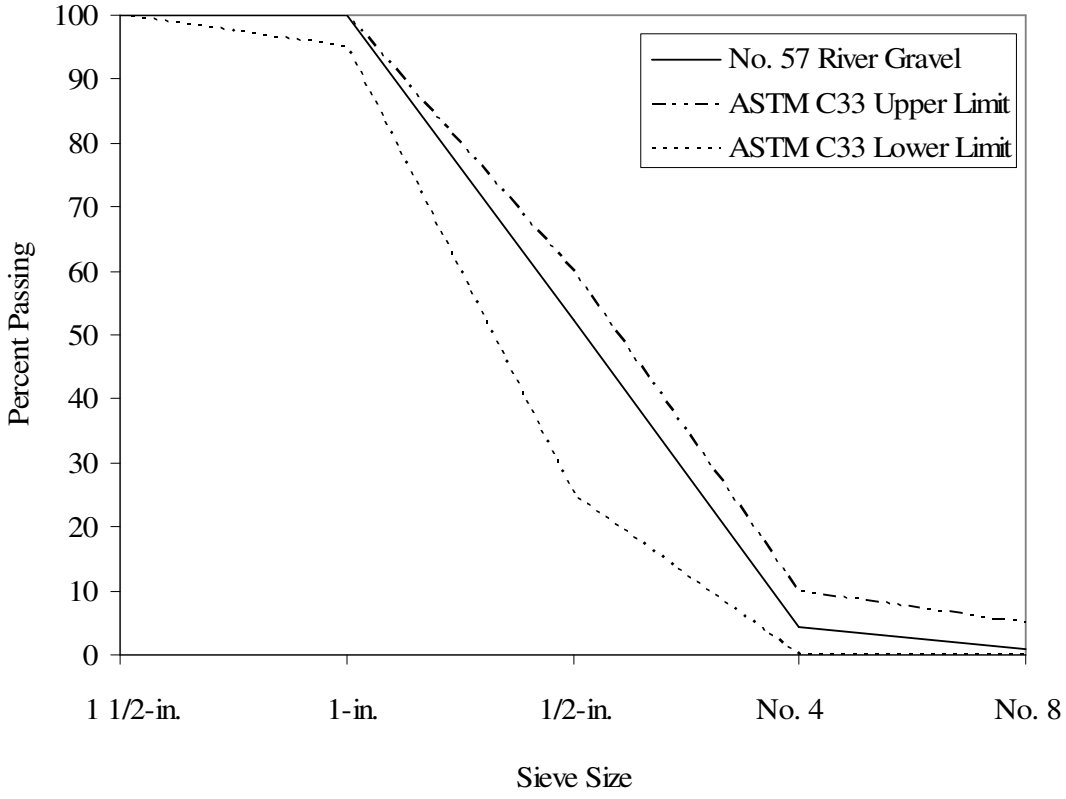


**Figure 3-11:** No. 57 siliceous river gravel gradation

**Table 3-5:** Aggregate specific gravity and absorption capacity

| Material | Bulk Specific Gravity (SSD) | Absorption Capacity (%) |
|---|---|---|
| Siliceous River Gravel | 2.568 | 0.82 |
| Siliceous River Sand | 2.650 | 0.66 |

### 3.4.4 FINE AGGREGATE

The fine aggregate used throughout this project was a siliceous river sand from Victoria, Texas. The fine aggregate was sampled, and the gradation, bulk specific gravity, and absorption capacity were determined. The fine aggregate was found to satisfy the gradation requirements of ASTM C33 (2003). The gradation of the fine aggregate can be found in Figure 3-12. The bulk specific gravity and absorption capacity are shown in Table 3-5.

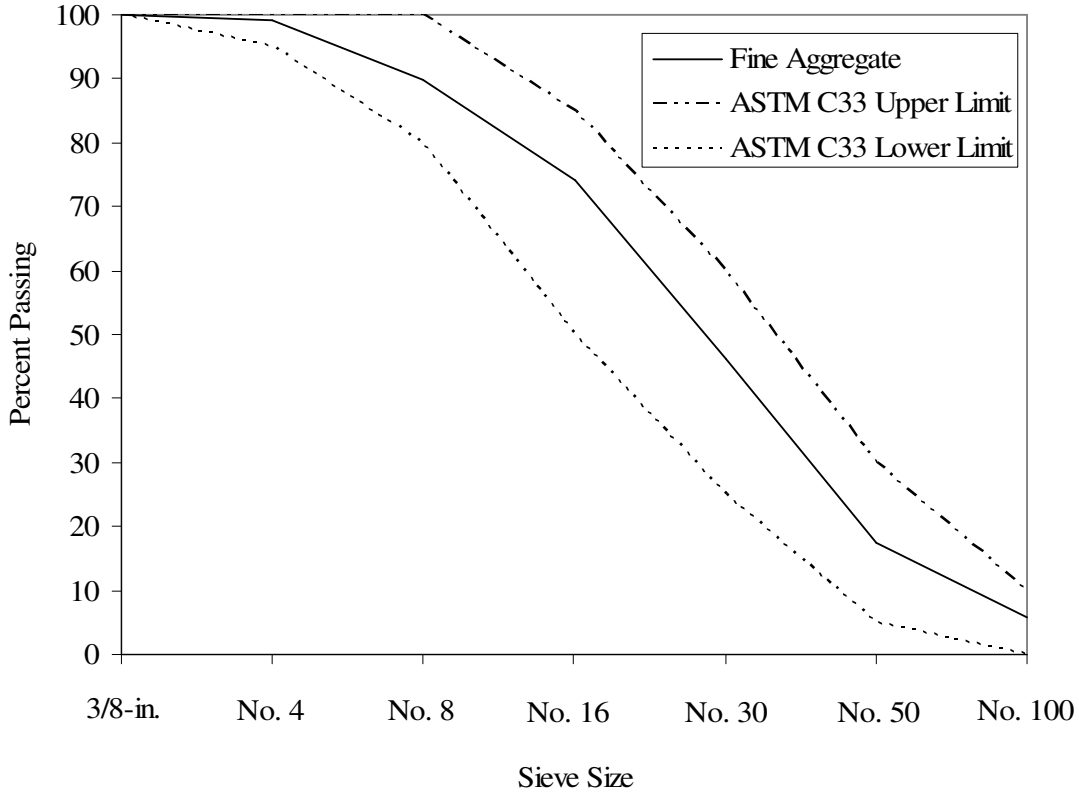


**Figure 3-12:** Fine aggregate gradation

### 3.4.5 Chemical Admixtures

The chemical admixtures used throughout this project were obtained from BASF Admixtures, Inc. The admixture mixture proportions can be found in Table 3-2. The following chemical admixtures were each used in at least one of the concrete mixtures:

- Glenium 3000 NS – High range water reducer,
- Pozzolith 200 N – Mid-range water reducer, and
- AE90 – Air entraining admixture

# CHAPTER 4

# PRESENTATION OF RESULTS

The results obtained from the laboratory testing program outlined in Chapter 3 are presented in this chapter. The fresh and hardened concrete properties of each mixture are presented. The remainder of the chapter focuses on the results obtained from the two rigid cracking frames and the free shrinkage frame. Discussion of these results can be found in Chapter 5. The notation used throughout this chapter is consistent with the notation described in Section 3.2 of Chapter 3.

## 4.1 FRESH CONCRETE PROPERTIES

As discussed in Chapter 3, several tests were performed on the fresh concrete before placement and cylinder production. These tests included slump, unit weight, air content, temperature, and setting. All tests were conducted according to their respective ASTM standard.

In order to produce the desired amount of concrete for testing, two different batches were used. The batch sizes are 5.50 $ft^3$ and 2.50 $ft^3$. Since the fresh concrete properties did not differ very much between the two batches and were found to be within acceptable limits, the average value of each property is shown in Table 4-1. See Appendix B for actual test values of each batch.

It is noteworthy that the fresh concrete temperature of each batch varied from the targeted fresh concrete temperature. However, since water was circulated within the formwork and crosshead, the fresh concrete temperature was quickly altered to reach its target. An evaluation of the concrete temperature test data reveals that each mixture reached ±1°C of its target temperature within 4 hours.

## 4.2 HARDENED CONCRETE PROPERTIES

As previously discussed in Chapter 3, the hardened concrete properties were tested at multiple intervals based on their respective placement temperature. The 7-day and 28-day splitting tensile strength, compressive strength, and modulus of elasticity results are given in Table 4-2. The early-age developments of these properties are presented in Section 4.2.2 for each mixture.

**Table 4-1A:** Fresh concrete properties

| Mixture | Fresh Temp (°F) | Slump (in.) | Air (%) | Unit Weight ($lb/ft^3$) | Initial Set (hrs) | Final Set (hrs) |
|---|---|---|---|---|---|---|
| CTRL (73°F - 73°F) | 75 | 1/2 | 3.0 | 148.2 | 4.0 | 5.4 |
| CTRL (50°F - 50°F) | 41 | 2 | 3.2 | 148.2 | 8.3 | 11.1 |
| CTRL (95°F - 95°F) | 104 | 1/2 | 2.7 | 150.2 | 3.1 | 3.9 |
| CTRL (73°F - 95°F) | 75 | 1 | 3.0 | 149.3 | 4.3 | 5.8 |
| CTRL (50°F - 95°F) | 38 | 2 1/2 | 3.0 | 147.8 | 5.1 | 6.5 |
| 30C (73°F - 73°F) | 73 | 5 | 2.1 | 149.3 | 9.0 | 11.5 |
| 20C (73°F - 73°F) | 73 | 5 | 2.2 | 148.0 | 8.0 | 9.6 |
| 30SG (73°F - 73°F) | 74 | 1/2 | 2.3 | 149.0 | 6.0 | 7.7 |
| 30SG (50°F - 50°F) | 40 | 5 | 2.4 | 147.9 | 9.3 | 12.4 |
| 30SG (95°F - 95°F) | 101 | 1/2 | 2.5 | 148.4 | 3.8 | 5.4 |
| 30SG (73°F - 95°F) | 72 | 1/2 | 2.3 | 148.7 | 5.7 | 7.6 |
| 30SG (50°F - 95°F) | 41 | 3 1/2 | 2.5 | 148.3 | 7.5 | 10.5 |
| 50SG (73°F - 73°F) | 71 | 1/2 | 2.1 | 148.4 | 7.2 | 8.9 |
| 50SG (50°F - 50°F) | 40 | 3 | 2.2 | 149.3 | 9.0 | 12.5 |
| 50SG (95°F - 95°F) | 104 | 0 | 2.1 | 149.0 | 3.6 | 5.2 |
| 50SG (73°F - 95°F) | 75 | 1/2 | 2.1 | 148.8 | 6.0 | 7.4 |
| 50SG (50°F - 95°F) | 44 | 5 1/2 | 2.0 | 148.2 | 8.8 | 11.4 |

**Table 4-1B:** Fresh concrete properties

| Mixture | Fresh Temp (°F) | Slump (in.) | Air (%) | Unit Weight ($lb/ft^3$) | Initial Set (hrs) | Final Set (hrs) |
|---|---|---|---|---|---|---|
| 25C6SF (73°F - 73°F) | 73 | 1 1/2 | 2.5 | 148.3 | 9.7 | 14.3 |
| 25F6SF (73°F - 73°F) | 73 | 1 1/2 | 2.5 | 147.5 | 8.0 | 9.6 |
| 20F30SG (73°F - 73°F) | 73 | 4 1/2 | 2.2 | 148.9 | 14.8 | 18.3 |
| WC32 (73°F - 73°F) | 75 | 4 | 2.6 | 150.7 | 3.7 | 6.4 |
| WC38 (73°F - 73°F) | 74 | 4 | 3.0 | 149.4 | 3.7 | 5.0 |
| WC38 (50°F - 50°F) | 43 | 9 | 3.0 | 148.7 | 7.3 | 10.8 |
| WC38 (95°F - 95°F) | 94 | 2 | 2.4 | 150.3 | 3.1 | 4.0 |
| WC38 (73°F - 95°F) | 75 | 5 1/2 | 2.9 | 148.2 | 3.6 | 5.0 |
| WC38 (50°F - 95°F) | 37 | 8 1/2 | 2.4 | 150.0 | 5.0 | 7.4 |
| WC48 (73°F - 73°F) | 74 | 1 /12 | 2.5 | 148.2 | 4.0 | 5.5 |
| WC53 (73°F - 73°F) | 75 | 1 1/2 | 2.7 | 147.3 | 4.3 | 5.8 |
| TYPE3 (73°F - 73°F) | 73 | 1/2 | 2.1 | 150.3 | 4.0 | 5.4 |
| TYPE3 (50°F - 50°F) | 39 | 3 | 2.3 | 148.8 | 6.2 | 9.3 |
| TYPE3 (95°F - 95°F) | 95 | 1/2 | 2.3 | 147.0 | 4.2 | 5.3 |
| TYPE3 (73°F - 95°F) | 73 | 1/2 | 2.1 | 150.0 | 4.2 | 5.3 |
| TYPE3 (50°F - 95°F) | 39 | 3 | 2.3 | 148.8 | 6.8 | 9.6 |
| AEA (73°F - 73°F) | 71 | 1 1/2 | 6.5 | 144.4 | 6.6 | 8.1 |

**Table 4-2A:** 7-day and 28-day mechanical properties

| Mixture | Splitting Tensile Strength (psi) | | Compressive Strength (psi) | | Modulus of Elasticity (ksi) | |
|---|---|---|---|---|---|---|
| | 7-day | 28-day | 7-day | 28-day | 7-day | 28-day |
| CTRL (73°F - 73°F) | 600 | 660 | 5180 | 5680 | 5700 | 5750 |
| CTRL (50°F - 50°F) | 690 | 755 | 6090 | 7040 | 6550 | 6250 |
| CTRL (95°F - 95°F) | 540 | 600 | 4860 | 5160 | 5950 | 6050 |
| CTRL (73°F - 95°F) | 640 | 645 | 5730 | 5890 | 6350 | 6350 |
| CTRL (50°F - 95°F) | 555 | 595 | 4790 | 5460 | 5400 | 6000 |
| 30C (73°F - 73°F) | 545 | 560 | 5670 | 5790 | 5750 | 6000 |
| 20C (73°F - 73°F) | 590 | 630 | 5460 | 5700 | 5950 | 6050 |
| 30SG (73°F - 73°F) | 635 | 705 | 5250 | 5650 | 6050 | 6100 |
| 30SG (50°F - 50°F) | 645 | 655 | 5850 | 6320 | 6300 | 6500 |
| 30SG (95°F - 95°F) | 530 | 565 | 4960 | 5190 | 5650 | 6150 |
| 30SG (73°F - 95°F) | 645 | 680 | 5300 | 5510 | 6100 | 6200 |
| 30SG (50°F - 95°F) | 670 | 665 | 5680 | 5710 | 6150 | 6200 |
| 50SG (73°F - 73°F) | 590 | 665 | 4650 | 5350 | 5550 | 6500 |
| 50SG (50°F - 50°F) | 715 | 720 | 5730 | 6400 | 6050 | 6400 |
| 50SG (95°F - 95°F) | 550 | 605 | 5000 | 5610 | 5750 | 6350 |
| 50SG (73°F - 95°F) | 575 | 635 | 4890 | 5650 | 6000 | 6150 |
| 50SG (50°F - 95°F) | 585 | 620 | 4010 | 4410 | 6050 | 6100 |

**Table 4-2B:** 7-day and 28-day mechanical properties

| Mixture | Splitting Tensile Strength (psi) | | Compressive Strength (psi) | | Modulus of Elasticity (ksi) | |
|---|---|---|---|---|---|---|
| | 7-day | 28-day | 7-day | 28-day | 7-day | 28-day |
| 25C6SF (73°F - 73°F) | 500 | 555 | 4430 | 5870 | 5450 | 6150 |
| 25F6SF (73°F - 73°F) | 565 | 595 | 4810 | 5150 | 5400 | 5450 |
| 20F30SG (73°F - 73°F) | 575 | 635 | 5540 | 6060 | 6000 | 6250 |
| WC32 (73°F - 73°F) | 695 | 770 | 7350 | 7770 | 6700 | 6650 |
| WC38 (73°F - 73°F) | 645 | 690 | 5810 | 6120 | 5600 | 6000 |
| WC38 (50°F - 50°F) | 710 | 740 | 6480 | 7520 | 6200 | 6500 |
| WC38 (95°F - 95°F) | 535 | 565 | 5710 | 5910 | 5900 | 6250 |
| WC38 (73°F - 95°F) | 670 | 720 | 5480 | 6240 | 5700 | 6100 |
| WC38 (50°F - 95°F) | 570 | 625 | 7780 | 8190 | 6450 | 6450 |
| WC48 (73°F - 73°F) | 565 | 630 | 4190 | 5000 | 5150 | 5750 |
| WC53 (73°F - 73°F) | 490 | 600 | 3940 | 4720 | 5550 | 5800 |
| TYPE3 (73°F - 73°F) | 530 | 580 | 5630 | 5900 | 6500 | 6500 |
| TYPE3 (50°F - 50°F) | 675 | 720 | 6720 | 7330 | 5850 | 6250 |
| TYPE3 (95°F - 95°F) | 545 | 555 | 5120 | 5140 | 5400 | 5500 |
| TYPE3 (73°F - 95°F) | 600 | 635 | 5800 | 5620 | 5900 | 5950 |
| TYPE3 (50°F - 95°F) | 645 | 675 | 5890 | 6590 | 6150 | 6200 |
| AEA (73°F - 73°F) | 400 | 465 | 3640 | 4260 | 5150 | 5250 |

### 4.2.1 DRYING SHRINKAGE

The drying shrinkage results were obtained using ASTM C 157. The specimens were prepared with the same concrete batch as the rigid cracking frames but were allowed to hydrate naturally under room conditions instead of being match-cured. The specimens were placed in a moist-curing room and demolded twenty-four hours later. The specimens are placed in a lime-saturated bath for seven days including the period in the molds in accordance with ASTM C 157. After curing, the specimens are placed in a temperature and humidity-controlled room and readings are taken up to 64 weeks.

Since the rigid cracking frames and the free shrinkage frame are sealed, drying shrinkage is eliminated from causing restraint stresses; however, drying shrinkage deformations must be considered when determining the total restraint stresses that may occur in a structure exposed to ambient conditions. Conditions such as temperature can affect the magnitude of total shrinkage due to drying. As discussed in Chapter 2, placement temperatures can be controlled to mitigate early-age stresses; however, if the concrete is allowed to hydrate naturally like the shrinkage specimens, then the drying shrinkage magnitude will be approximately the same as a mixture that was not cooled.

The effect of placement temperature on drying shrinkage is shown in Figure 4-1. The fresh concrete placement temperature did not affect the magnitude of drying shrinkage. All mixtures produced approximately the same magnitude of drying shrinkage at 56 days.

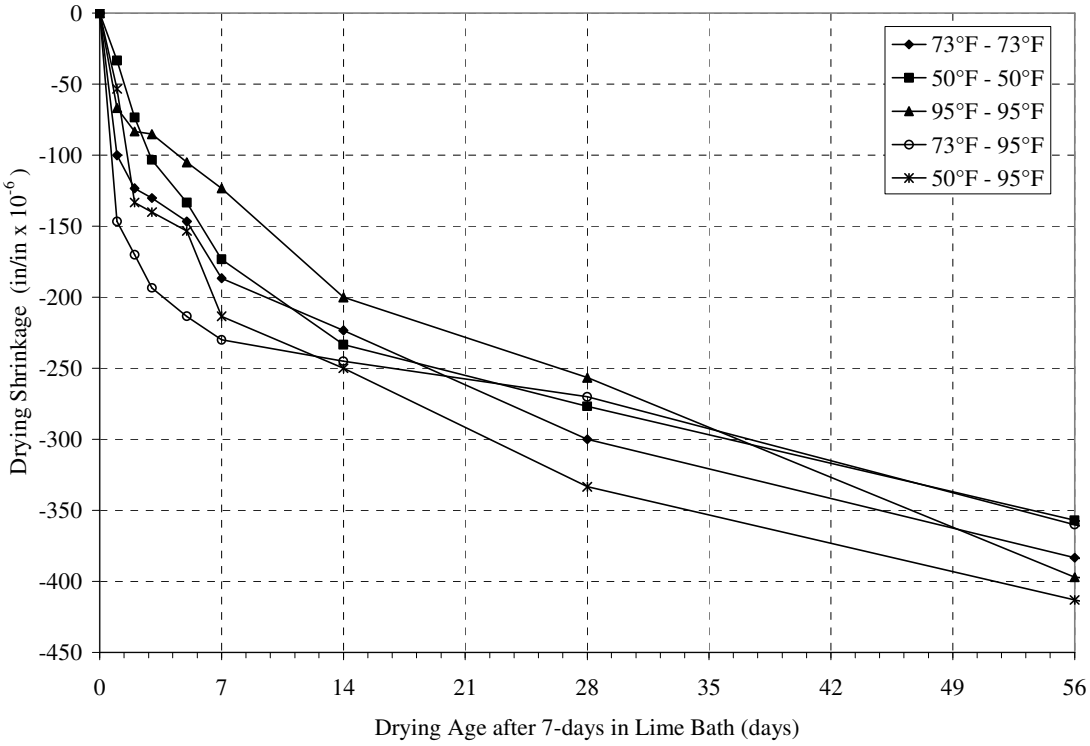


**Figure 4-1:** Effect of placement temperature of control mixture on drying shrinkage

The use of supplementary cementing materials is another method used to mitigate early-age restraint stresses in mass concrete. Unlike varying the placement temperature, SCMs reduce the magnitude of drying shrinkage due to the reduction in porosity. Figure 4-2 illustrates the reduction in drying shrinkage when SCMs are applied as mitigation measure for the control of early-age restraint stresses.

The use of SCMs had a substantial affect on the magnitude of drying shrinkage. The Class C fly ash reduced the overall shrinkage much more than the GGBF slag. The increase in replacement percentages of each SCM reduced drying shrinkage in the prisms.

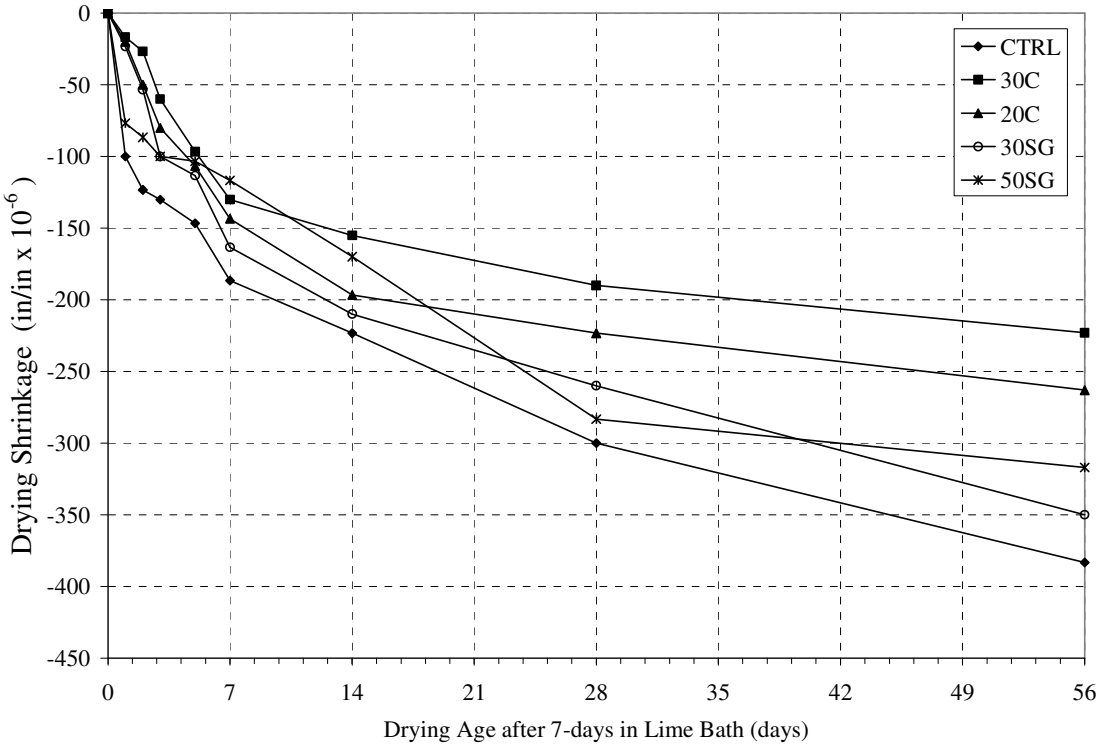


**Figure 4-2:** Effect of SCMs on drying shrinkage for 73°F – 73°F batches

All drying shrinkage measurements were taken for 64 weeks; however, early-age is considered in this study to be 7 days or less. Therefore, 56 days gives sufficient data to assess the effect of drying shrinkage on early-age cracking.

### 4.2.2 EARLY-AGE MECHANICAL PROPERTIES

Early-age mechanical properties are important when studying the cracking tendency of concrete mixtures. The compressive strength of the concrete at early-ages has little importance; however, the tensile strength and modulus of elasticity are vital components to understanding the cracking tendency of various mixtures.

As discussed in Chapter 2, as the stiffness of the concrete grows, small temperature changes create large tensile stresses if restrained. Once stresses exceed the tensile capacity of the concrete, cracking may occur. This section will present the early-age mechanical behavior of the concrete mixtures outlined in Chapter 3.

#### 4.2.2.1 Control Mixture

As previously discussed in Chapter 2, the curing temperature of the concrete will have an effect on the rate of development of early-age mechanical properties. The mechanical properties test results of the control mixture shown in Figure 4-3 illustrate the effect of temperature. The 7-day compressive and tensile strength of the 95°F-95°F mixture is reduced compared to the other temperature conditions; however, decreasing the placement temperature to 73°F increased all mechanical properties after 24 hours.

#### 4.2.2.2 Fly Ash Mixture

Supplementary cementing materials such as fly ash increase the compressive strength at 7 days slightly; however, the early-age properties can be affected due to retardation from the fly ash. Figure 4-4 illustrates the effect of fly ash on the development of mechanical properties at early-ages. As the replacement percentages are increased, the modulus of elasticity is reduced at all ages but all fly ash mixtures had a stiffness greater than the control mixture. The fly ash mixtures have a reduced tensile strength at all ages while the compressive strength is substantially lower prior to 3 days.

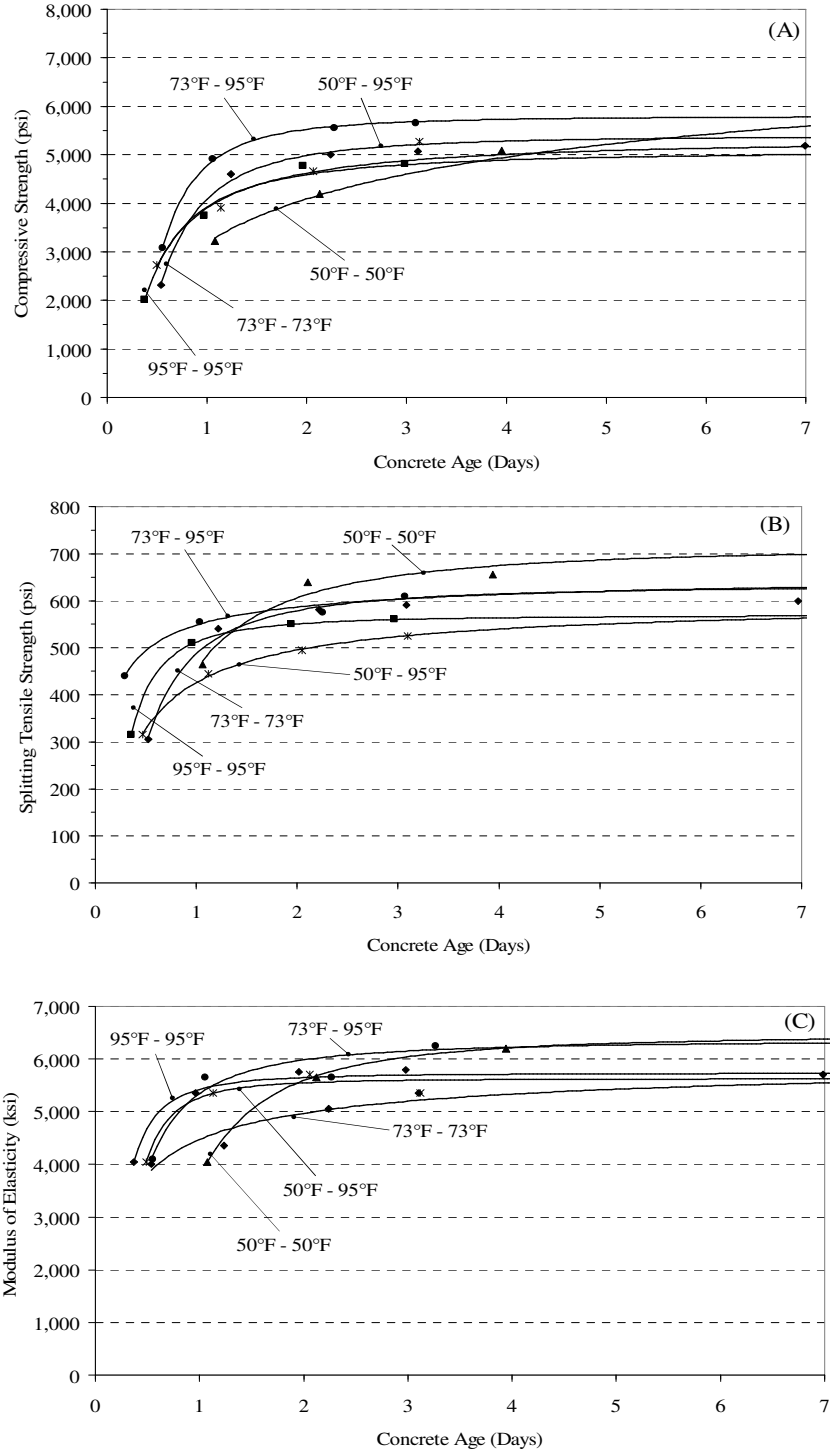


**Figure 4-3:** Development of early-age mechanical properties of the control mixture (Mix ID = CTRL) (A) Compressive strength, (B) tensile strength, and (C) modulus of elasticity

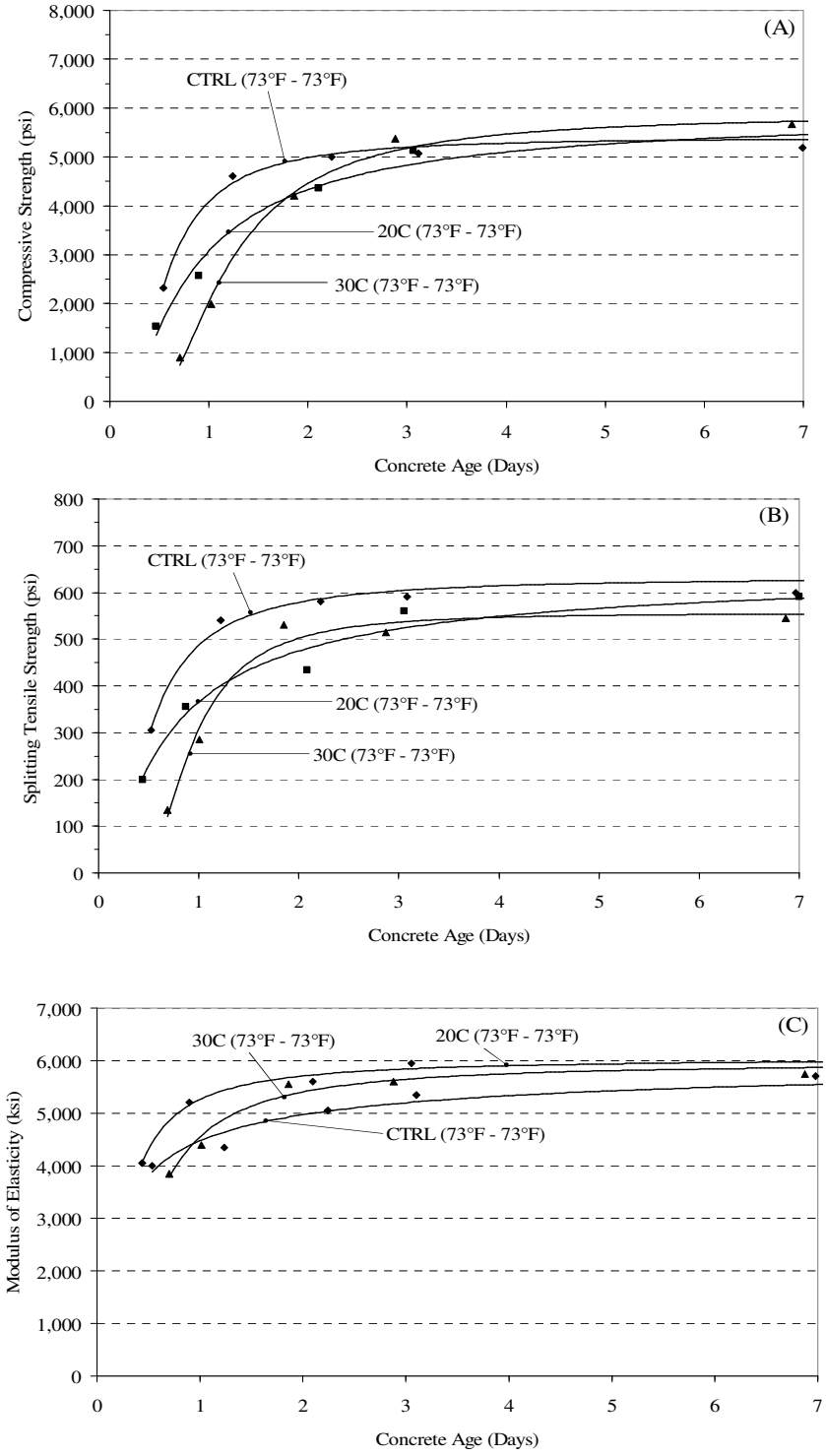


**Figure 4-4:** Development of early-age mechanical properties (Mix ID = CTRL, 20C, and 30C) (A) Compressive strength, (B) tensile strength, and (C) modulus of elasticity

#### 4.2.2.3 30% GGBF Slag

As discussed in Chapter 2, GGBF slag has a very high activation energy which causes it to be very temperature sensitive. As a result, the early-age mechanical properties are affected the same way much like the setting properties. Low curing conditions, i.e. 50°F-50°F, cause the slag mixtures to hydrate slowly; therefore, mechanical properties develop at a slow pace as shown in Figure 4-5. The 95°F-95°F mixture had reduced compressive strength, tensile strength, and stiffness at 7 days. However, the reduction in placement temperature creates higher strengths and stiffness after 2 days.

#### 4.2.2.4 50% GGBF Slag

As discussed in the previous section, slag mixtures are very temperature dependent. Just like the 30% GGBF slag mixtures, the 50% GGBF slag mixtures' mechanical properties will vary with the curing temperature; however, the 50% slag mixtures will be more affected by the curing temperature as shown in Figure 4-6. Prior to 3 days the rate of strength development is reduced. The temperature sensitivity of the 50% slag mixtures is extremely noticeable in the 50°F-50°F mixture. This mixture underwent the lowest temperature development, which reduced the rate of development of mechanical properties prior to 5 days.

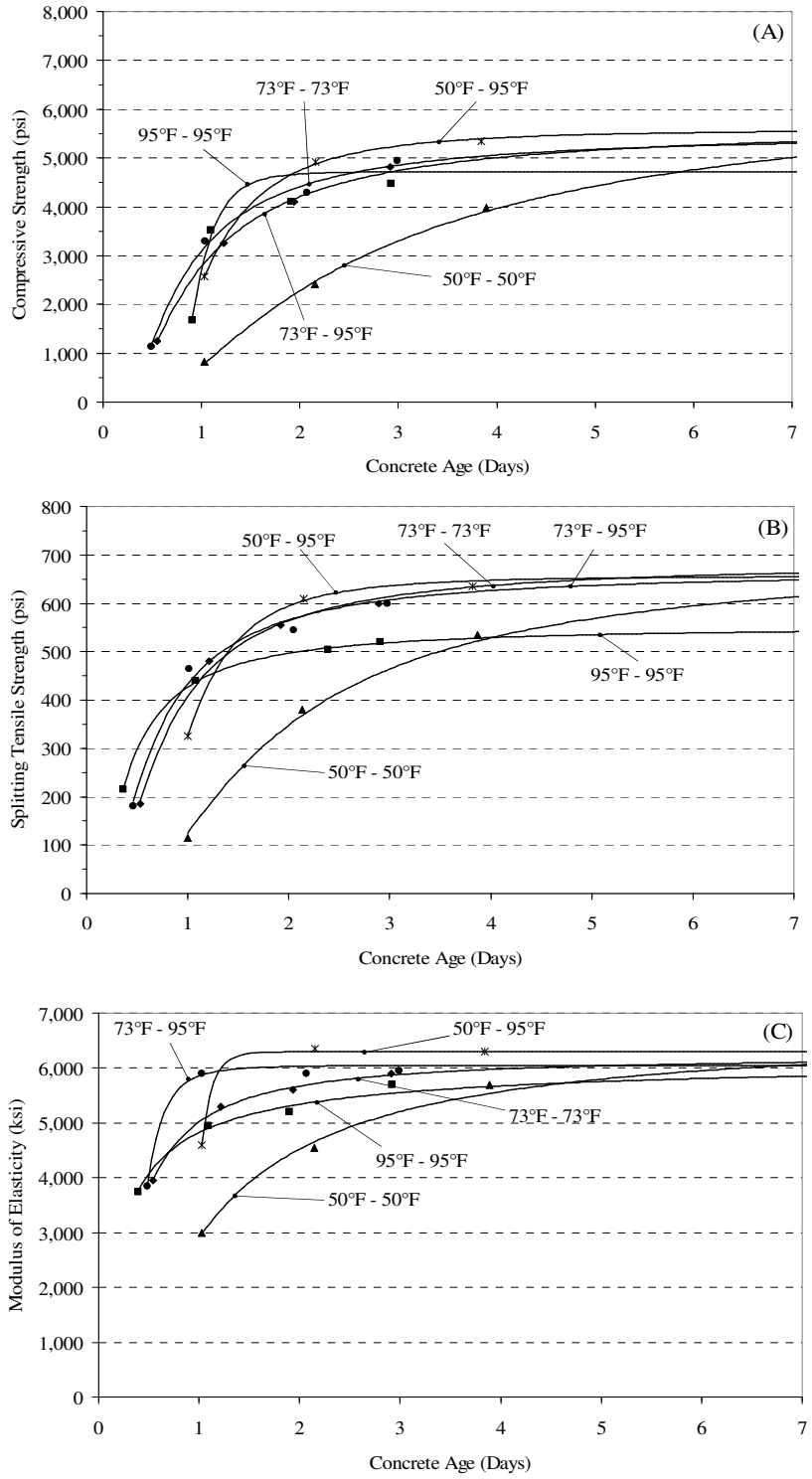


**Figure 4-5:** Development of early-age mechanical properties (Mix ID = 30SG)

(A) Compressive strength, (B) tensile strength, and (C) modulus of elasticity

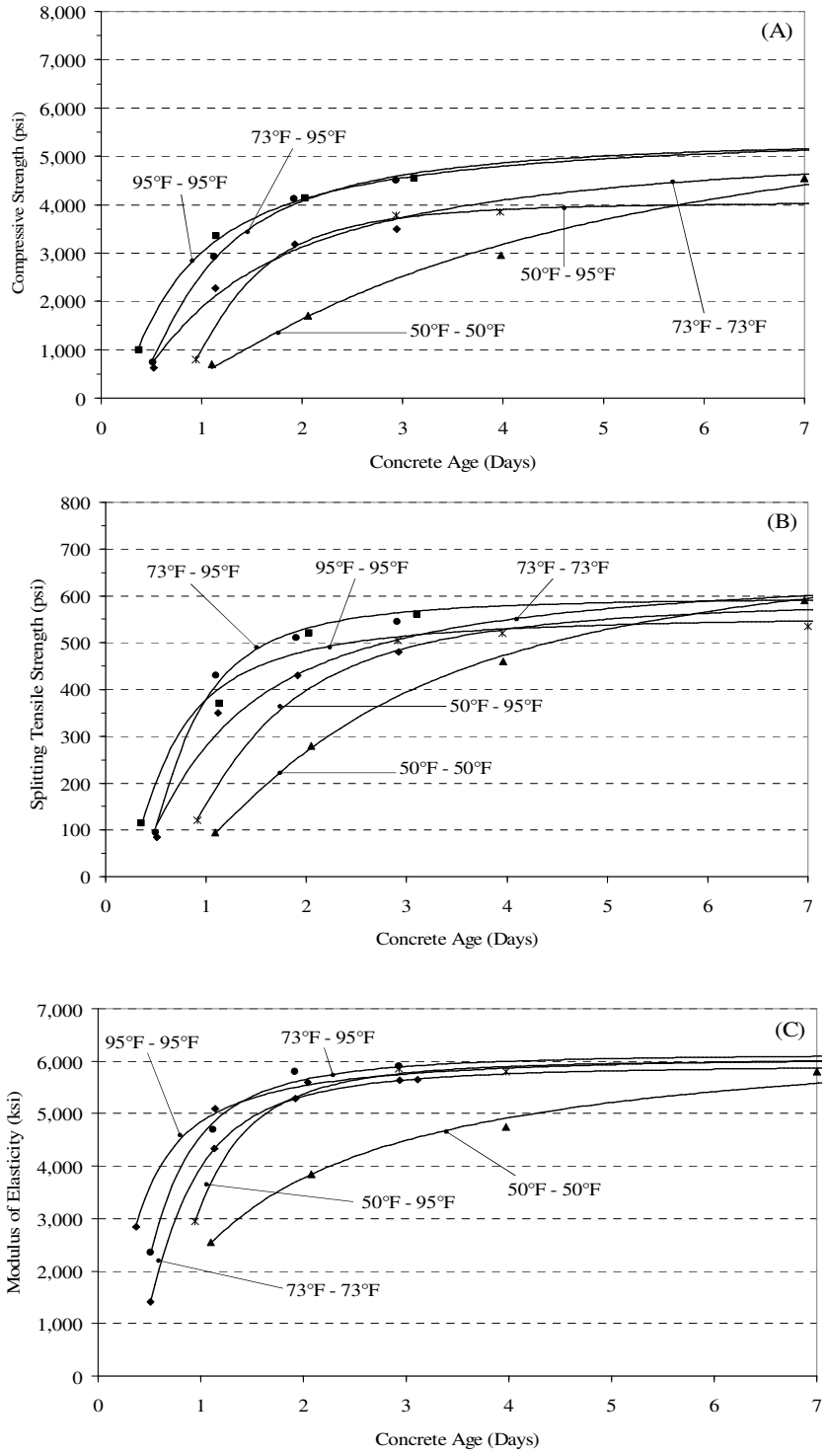


**Figure 4-6:** Development of early-age mechanical properties (Mix ID = 50SG)

(A) Compressive strength, (B) tensile strength, and (C) modulus of elasticity

#### 4.2.2.5 Ternary Blend Mixtures

Ternary blend concrete mixtures contain two types of supplementary cementing materials. As discussed previously, SCMs reduce the overall amount of heat generated in a mass concrete member. Low heat generation leads to slow development of mechanical properties. As shown in Figure 4-7, the rate of development of both tensile and compressive strengths are reduced when ternary blend mixtures are used. After 2 days, the modulus of elasticity of all ternary mixtures exceeded that of the control mixture.

#### 4.2.2.6 Low Water-to-Cement Ratio

As discussed in Chapter 2, low water-to-cement ratio mixtures produce considerably more heat than a normal to high water-to-cement ratio mixture. As a result, the hot placement temperature, i.e. 95°F-95°F, reduces the tensile strength after 24 hours, which can be attributed to weaker bonds in the interfacial transition zone due to rapid temperature development (Mehta and Monteiro 2006). However, the reduction of the placement temperature increased the tensile strength after 24 hours as shown in Figure 4-8. The modulus of elasticity for all the mixtures was similar at all ages excluding the 73°F-73°F mixture.

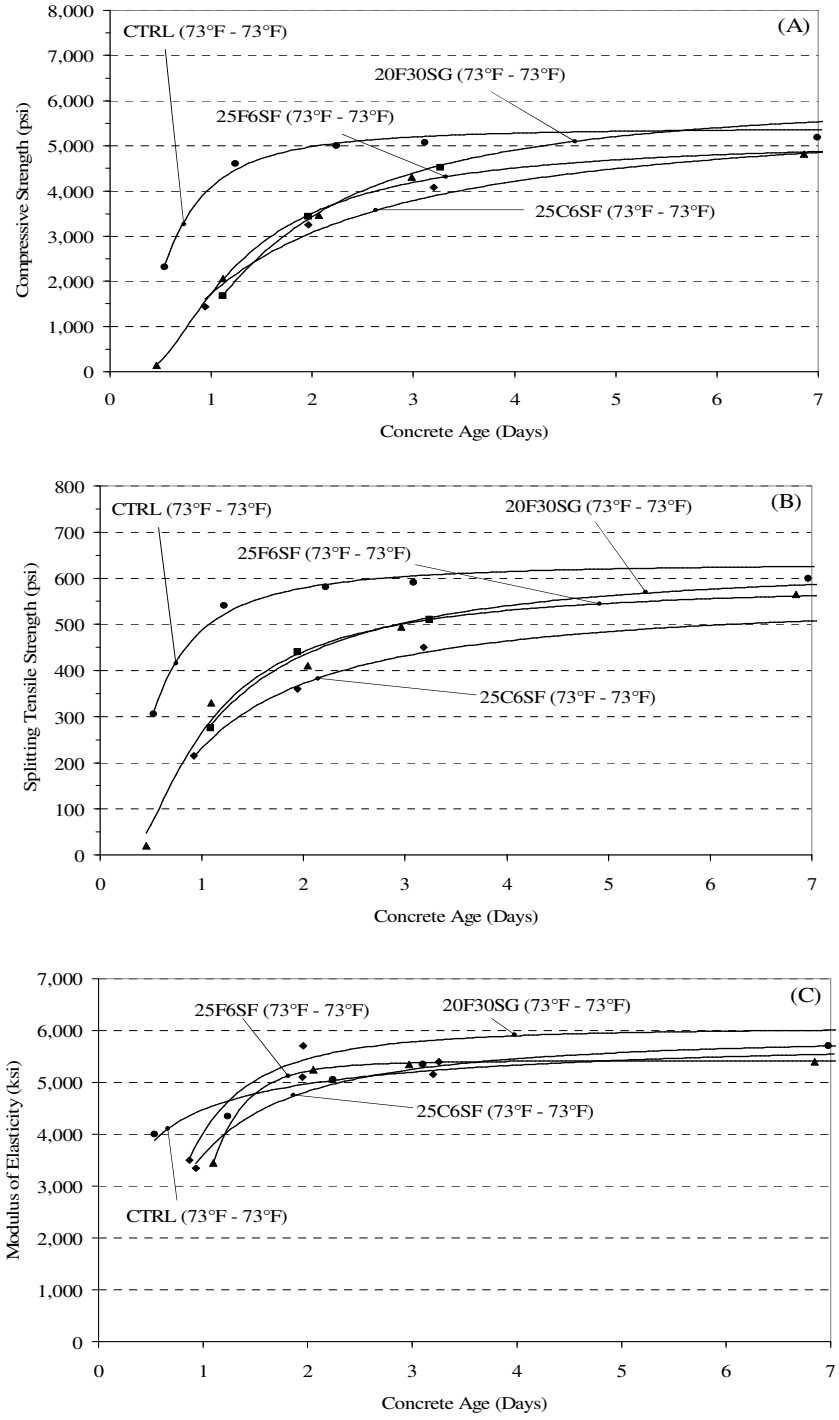


**Figure 4-7:** Development of early-age mechanical properties for ternary blend mixtures (Mix ID = CTRL, 20C30SG, 30C6SF, and 30F6SF) (A) Compressive Strength, (B) tensile strength, and (C) modulus of elasticity

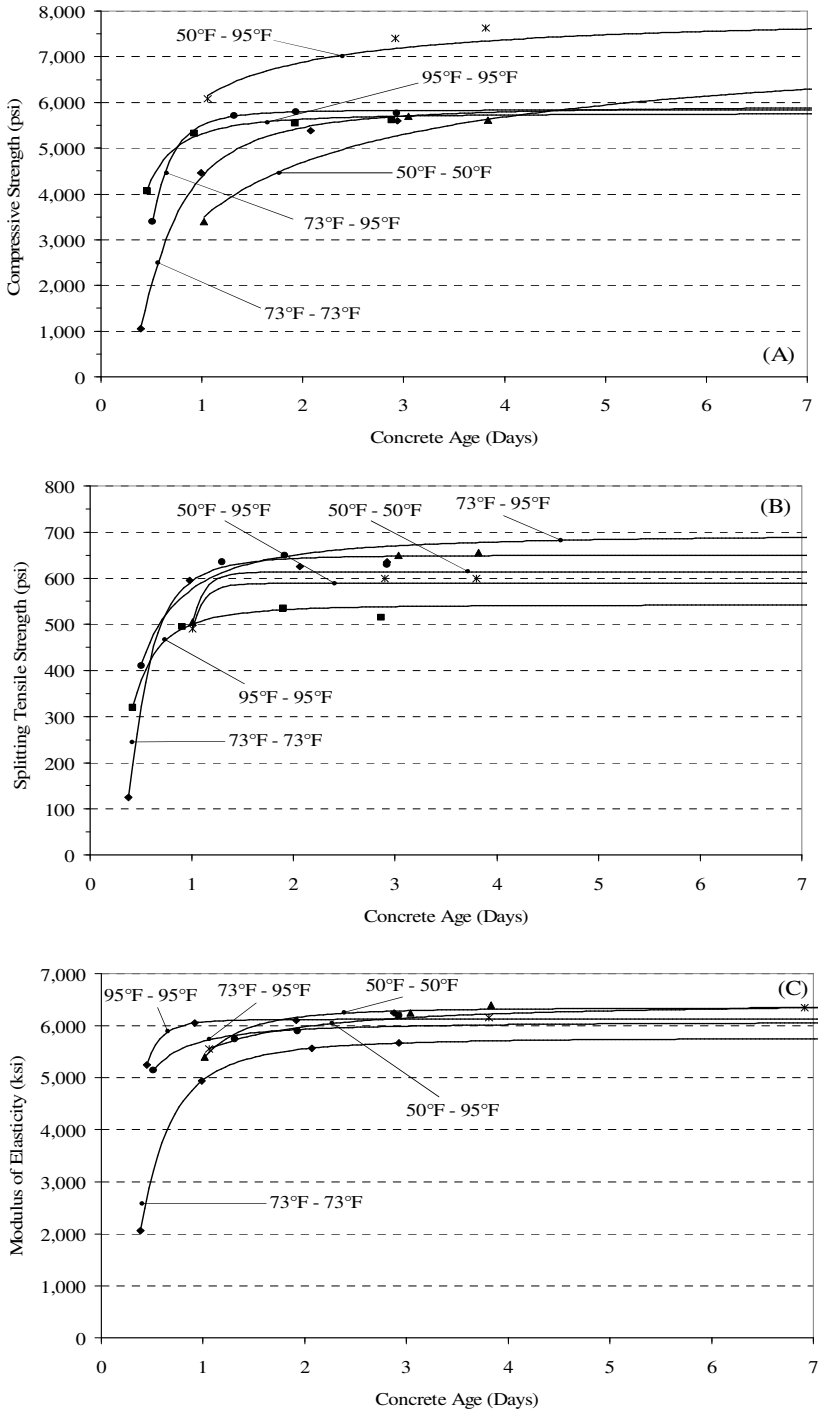


**Figure 4-8:** Development of early-age mechanical properties for low water-to-cement ratio mixture (Mix ID = WC38) (A) Compressive strength, (B) tensile strength, and (C) modulus of elasticity

#### 4.2.2.7 Type III Cement

Type III cement mixtures generate more heat during hydration as compared to a Type I cement due to the increase in fineness. Rapid heat generation is an indication of rapid hydration which increases the rate at which mechanical properties develop. Due to the increase in heat generation, early-age mechanical properties are higher; however, long-term strengths may be reduced. As a result, the 95°F-95°F mixture had a reduced compressive strength and stiffness at 7 days. Lowering of the placement temperature increased the mechanical properties after 2 days.

#### 4.2.2.8 Air Entrainment

The addition of 1% air generally reduces the compressive strength by approximately 5% (Kosmatka et al. 2002). This is because of the increased porosity of the hydrated cement paste. As a result the mechanical properties at early and later ages are reduced when air is added to the control mixture. The effect of air entrainment on the development of mechanical properties is shown in Figure 4-10. The compressive and tensile strength of the air-entrained mixture are much lower than the control mixture at all ages; however, the modulus of elasticity for the air-entrained mixture is only slightly reduced at 7 days.

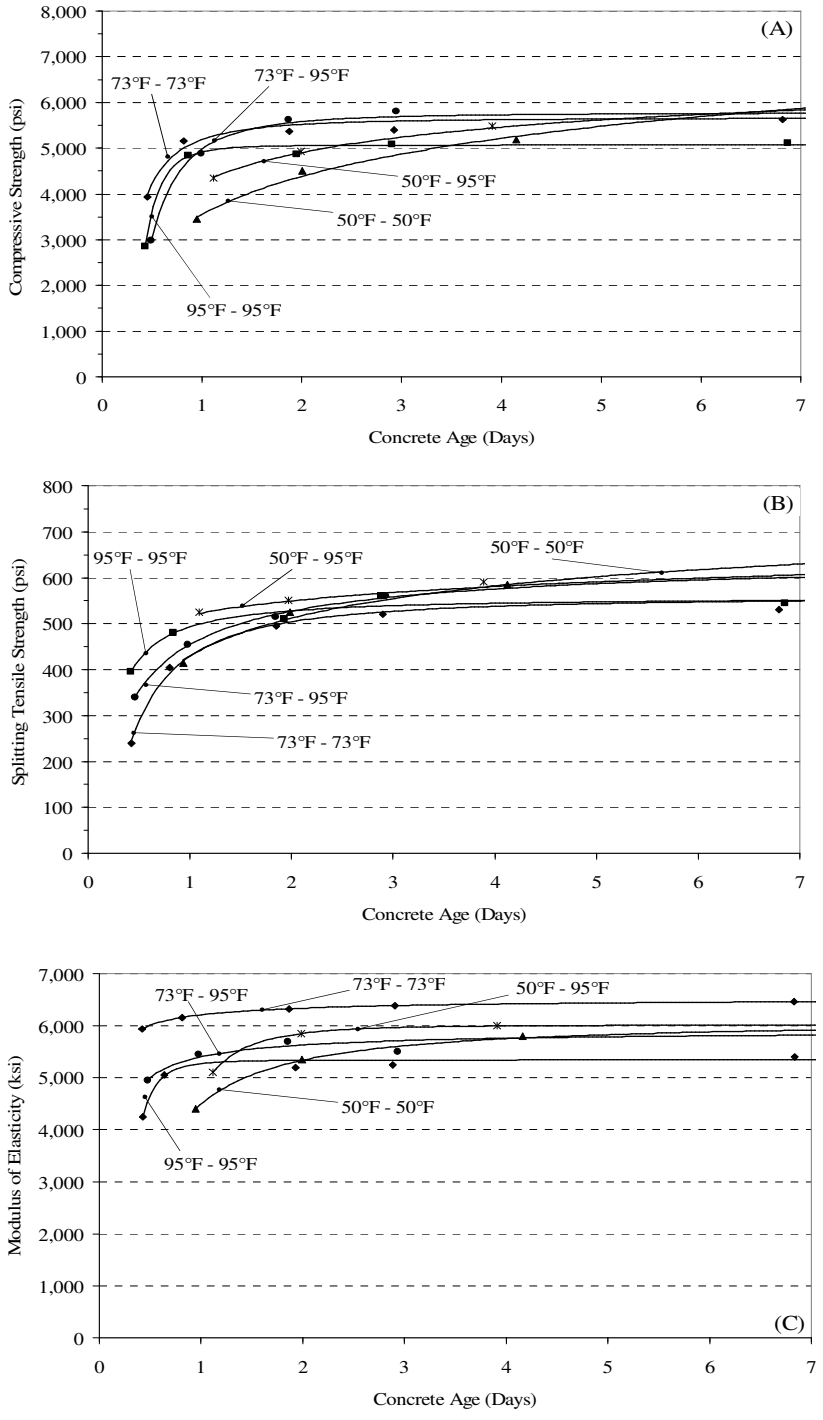


**Figure 4-9:** Development of early-age mechanical properties for the Type III mixture (Mix ID = TYPE3) (A) Compressive strength, (B) tensile strength, and (C) modulus of elasticity

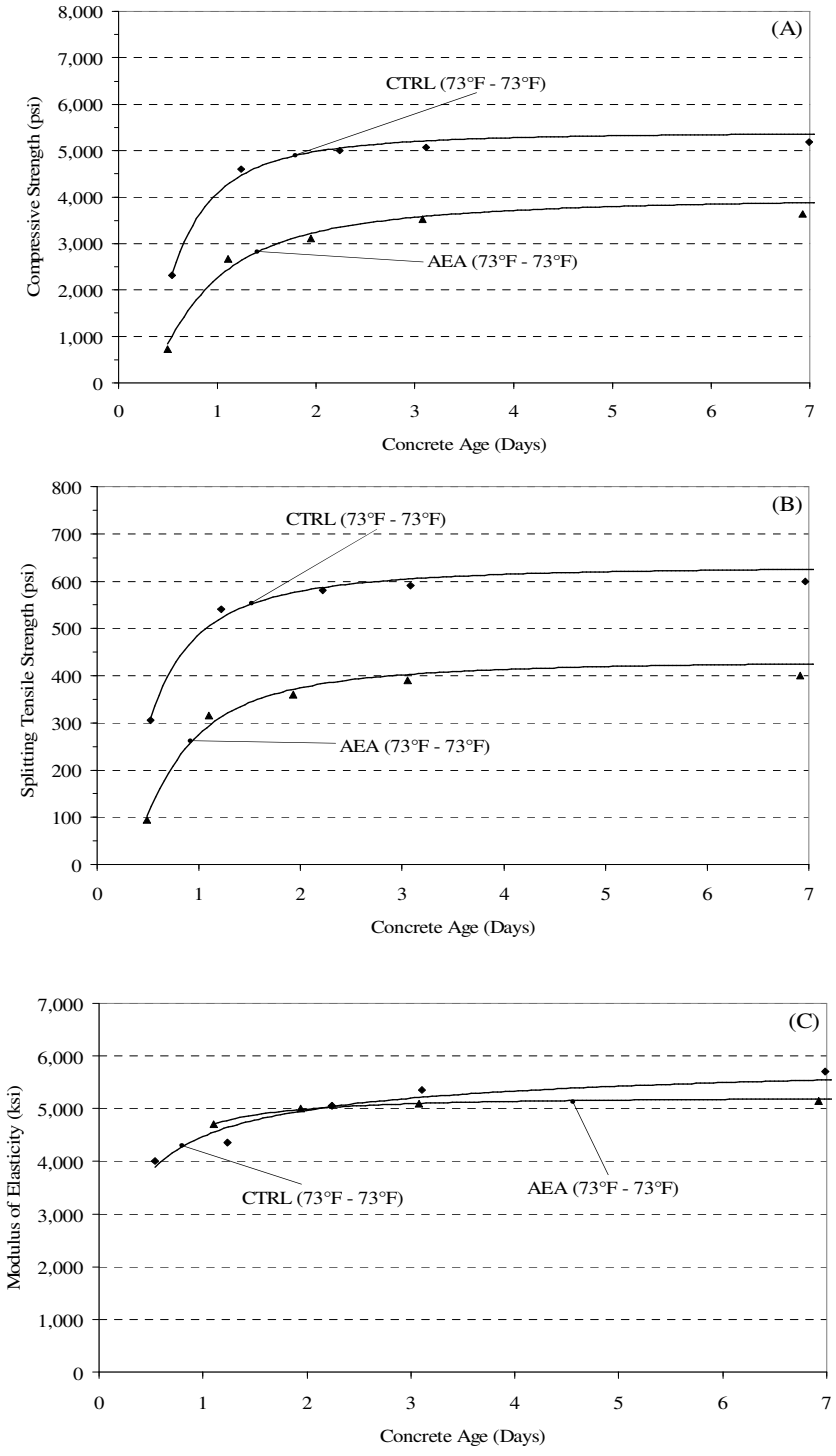


**Figure 4-10:** Development of early-age mechanical properties for the AEA mixture (Mix ID = AEA) (A) Compressive strength, (B) tensile strength, and (C) modulus of elasticity

#### 4.2.2.9 Effect of Water-to-Cement Ratio

As the water-to-cement ratio is increased, the heat generated during hydration is decreased as shown in Figure 4-20. The low water-to-cement ratio mixtures gain strength and stiffness at a faster rate than higher water-to-cement ratio mixtures as shown in Figure 4-11. As the water-to-cement ratio is lowered, the overall strength gain is higher.

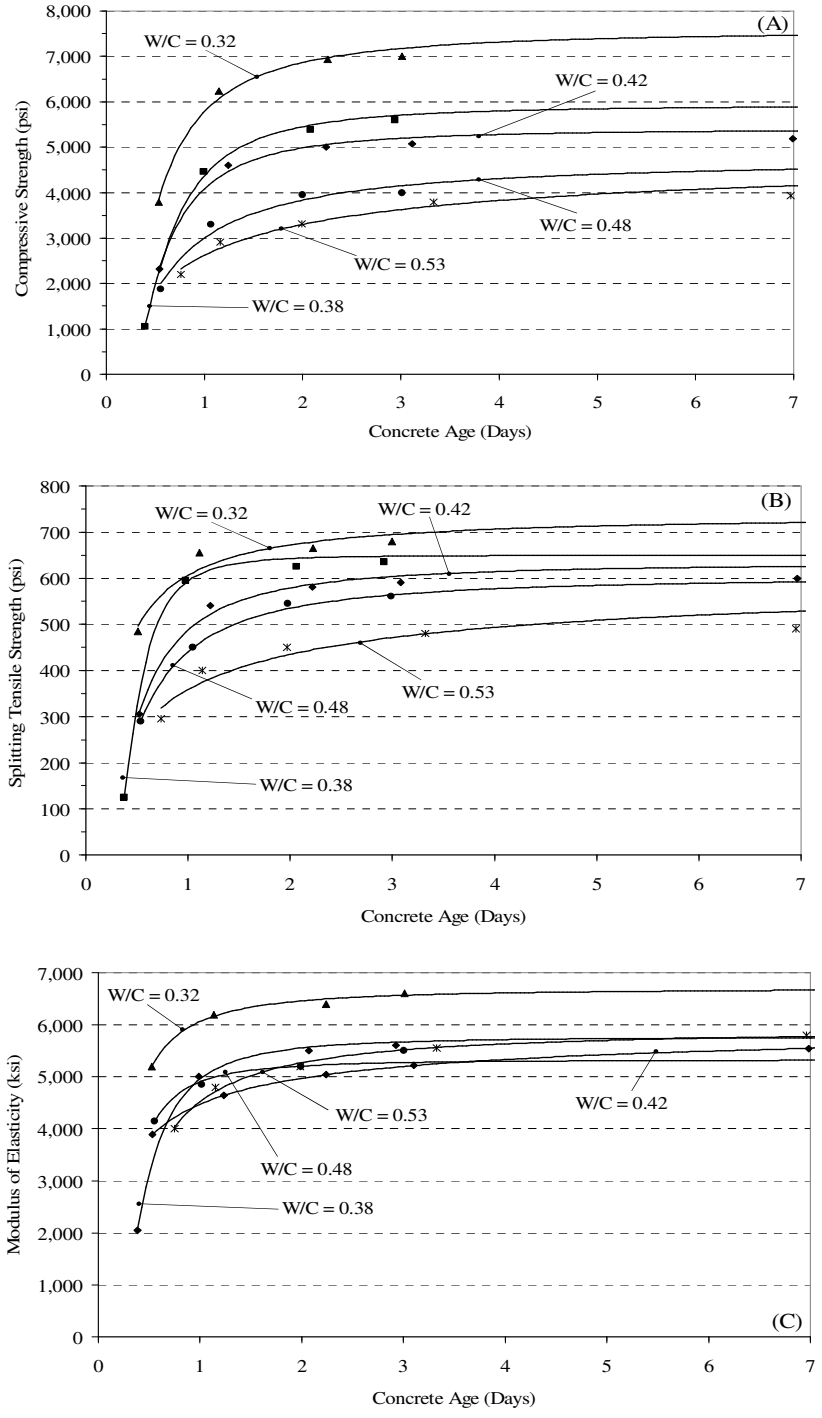


**Figure 4-11:** Development of early-age mechanical properties for the varied water-to-cement ratio mixtures (Mix ID = WC32, WC38, CTRL, WC48, and WC53) (A) Compressive strength, (B) tensile strength, and (C) modulus of elasticity

## 4.3 MATCH-CURED RIGID CRACKING FRAME

In the following section the results of the match-cured rigid cracking frame tests and free shrinkage frame tests outlined in Chapter 3 are presented. The free shrinkage frame results are presented in Section 4.3.10. Some pertinent match-cured rigid cracking frame results are summarized in Table 4-3. The parameters listed in each column of Table 4-3 are defined as follows:

(1) $T_{C0}$ = fresh concrete placement temperature (°F),

(2) $\sigma_{C\text{-}max}$ = maximum compressive stress (psi),

(3) $t_{\sigma c\text{-}max}$ = concrete age when the maximum compressive stress ($\sigma_{C\text{-}max}$) is reached (hours),

(4) $T_{C\text{-}max}$ = maximum in-place concrete temperature (°F),

(5) $t_{TC\text{-}max}$ = concrete age when the maximum temperature($T_{C\text{-}max}$) is reached (hours),

(6) $T_{zs}$ = concrete temperature at which the compressive stresses are reduced to zero, referred to as the zero-stress temperature, (°F),

(7) $t_{zs}$ = concrete age when the zero-stress temperature ($T_{zs}$) occurs (hours),

(8) $\sigma_{cr}$ = maximum tensile stress at cracking (psi),

(9) $T_{cr}$ = concrete temperature at cracking (°F),

(10) $t_{cr}$ = concrete age at cracking (hours), and

(11) $\Delta T_{cr}$ = temperature difference required to produce cracking (°F)

**Table 4-3A:** Summary of match-cured rigid cracking frame results

| Mixture | | (1) $T_{C0}$ (°F) | (2) $\sigma_{c\text{-}max}$ (psi) | (3) $t_{\sigma c\text{-}max}$ (hrs) | (4) $T_{c\text{-}max}$ (°F) | (5) $t_{Tc\text{-}max}$ (hrs) | **(6) $T_{zs}$ (°F)** | (7) $t_{zs}$ (hrs) | (8) $\sigma_{cr}$ (psi) | **(9) $T_{cr}$ (°F)** | (10) $t_{cr}$ (hrs) | **(11) $\Delta T_{cr}$ (°F)** |
|---|---|---|---|---|---|---|---|---|---|---|---|---|
| CTRL | (73°F - 73°F) | 75 | -357 | 18.0 | 132 | 19.2 | **112** | 36.3 | 301 | **88** | 60.2 | **23** |
| CTRL | (50°F - 50°F) | 39 | -150 | 25.1 | 97 | 27.3 | **90** | 38.0 | 356 | **63** | 72.3 | **27** |
| CTRL | (95°F - 95°F) | 92 | -446 | 15.8 | 163 | 16.1 | **134** | 33.0 | 259 | **111** | 54.1 | **23** |
| CTRL | (73°F - 95°F) | 70 | -437 | 17.1 | 150 | 19.3 | **124** | 40.6 | 322 | **95** | 98.4 | **29** |
| CTRL | (50°F - 95°F) | 48 | -377 | 22.0 | 141 | 23.8 | **119** | 47.2 | 337 | **92** | 100.1 | **27** |
| 30C | (73°F - 73°F) | 71 | -186 | 27.9 | 110 | 31.9 | **103** | 45.7 | 322 | **81** | 88.7 | **22** |
| 20C | (73°F - 73°F) | 74 | -220 | 21.8 | 119 | 23.7 | **109** | 36.2 | 292 | **86** | 63.8 | **23** |
| 30SG | (73°F - 73°F) | 75 | -216 | 21.2 | 117 | 22.9 | **106** | 38.8 | 324 | **81** | 82.3 | **24** |
| 30SG | (50°F - 50°F) | 50 | -95 | 34.4 | 79 | 35.7 | **73** | 54.4 | 319 | **44** | 104.4 | **29** |
| 30SG | (95°F - 95°F) | 90 | -330 | 14.3 | 152 | 15.8 | **133** | 31.9 | 301 | **110** | 57.0 | **23** |
| 30SG | (73°F - 95°F) | 72 | -376 | 20.2 | 139 | 22.3 | **119** | 45.8 | 309 | **98** | 97.2 | **21** |
| 30SG | (50°F - 95°F) | 52 | -374 | 26.9 | 132 | 29.7 | **113** | 57.4 | 325 | **90** | 101.7 | **23** |
| 50SG | (73°F - 73°F) | 71 | -134 | 22.3 | 110 | 24.2 | **101** | 38.6 | 344 | **79** | 96.4 | **22** |
| 50SG | (50°F - 50°F) | 46 | -67 | 34.1 | 71 | 36.6 | **65** | 61.3 | 250 | **43** | 104.0 | **22** |
| 50SG | (95°F - 95°F) | 90 | -243 | 15.2 | 142 | 16.8 | **130** | 31.7 | 298 | **109** | 58.8 | **21** |
| 50SG | (73°F - 95°F) | 82 | -269 | 22.4 | 130 | 24.6 | **117** | 47.8 | 295 | **96** | 98.3 | **21** |
| 50SG | (50°F - 95°F) | 54 | -254 | 29.6 | 124 | 32.6 | **110** | 63.8 | 285 | **88** | 103.6 | **22** |

**Table 4-3B:** Summary of match-cured rigid cracking frame results

| Mixture | | (1) $T_{C0}$ (°F) | (2) $\sigma_{c\text{-}max}$ (psi) | (3) $t_{\sigma c\text{-}max}$ (hrs) | (4) $T_{c\text{-}max}$ (°F) | (5) $t_{Tc\text{-}max}$ (hrs) | **(6) $T_{zs}$ (°F)** | (7) $t_{zs}$ (hrs) | (8) $\sigma_{cr}$ (psi) | **(9) $T_{cr}$ (°F)** | (10) $t_{cr}$ (hrs) | **(11) $\Delta T_{cr}$ (°F)** |
|---|---|---|---|---|---|---|---|---|---|---|---|---|
| 25C6SF | (73°F - 73°F) | 70 | -152 | 25.3 | 113 | 27.5 | **107** | 39.1 | 313 | **83** | 75.4 | **24** |
| 25F6SF | (73°F - 73°F) | 72 | -195 | 23.0 | 112 | 25.2 | **101** | 40.0 | 333 | **75** | 96.9 | **26** |
| 20F30SG | (73°F - 73°F) | 68 | -147 | 27.8 | 103 | 30.3 | **95** | 48.6 | 271 | **72** | 99.2 | **23** |
| WC32 | (73°F - 73°F) | 75 | -391 | 16.3 | 138 | 17.3 | **116** | 31.8 | 321 | **93** | 50.3 | **23** |
| WC38 | (73°F - 73°F) | 74 | -360 | 17.0 | 135 | 17.9 | **114** | 33.7 | 366 | **82** | 69.3 | **32** |
| WC38 | (50°F - 50°F) | 53 | -165 | 23.5 | 100 | 26.3 | **92** | 36.3 | 375 | **63** | 70.0 | **29** |
| WC38 | (95°F - 95°F) | 86 | -550 | 15.3 | 165 | 15.3 | **133** | 32.8 | 284 | **110** | 53.2 | **23** |
| WC38 | (73°F - 95°F) | 74 | -507 | 16.2 | 152 | 17.3 | **122** | 40.4 | 357 | **88** | 101.7 | **34** |
| WC38 | (50°F - 95°F) | 47 | -452 | 20.8 | 143 | 22.0 | **118** | 48.8 | 387 | **89** | 101.6 | **29** |
| WC48 | (73°F - 73°F) | 71 | -250 | 17.8 | 125 | 18.6 | **109** | 34.3 | 327 | **82** | 71.6 | **27** |
| WC53 | (73°F - 73°F) | 73 | -188 | 17.8 | 120 | 18.7 | **108** | 33.8 | 306 | **80** | 77.9 | **28** |
| TYPE3 | (73°F - 73°F) | 73 | -430 | 14.7 | 135 | 17.4 | **114** | 33.4 | 338 | **91** | 55.2 | **23** |
| TYPE3 | (50°F - 50°F) | 50 | -202 | 22.8 | 100 | 25.4 | **91** | 36.8 | 426 | **62** | 71.8 | **29** |
| TYPE3 | (95°F - 95°F) | 88 | -344 | 15.2 | 164 | 15.3 | **145** | 26.0 | 272 | **124** | 39.2 | **21** |
| TYPE3 | (73°F - 95°F) | 73 | -479 | 15.5 | 151 | 17.2 | **126** | 38.0 | 334 | **100** | 97.8 | **26** |
| TYPE3 | (50°F - 95°F) | 49 | -442 | 20.1 | 141 | 22.1 | **120** | 44.5 | 357 | **94** | 98.8 | **26** |
| AEA | (73°F - 73°F) | 70 | -231 | 18.8 | 127 | 19.8 | **112** | 33.3 | 270 | **88** | 56.5 | **24** |

### 4.3.1 CONTROL MIXTURE

The temperature profile and stress development for the control mixture can be seen in Figures 4-12A and 4-12B. The control mixture is used as a standard mixture to evaluate how the variables affect the cracking tendency of concrete. By varying the placement and ambient temperature, the effects of temperature with respect to stress development and cracking can be studied.

### 4.3.2 FLY ASH MIXTURE

The effect of fly ash as a replacement for cement was evaluated. These mixtures were only simulated at 73°F as the placement temperature and ambient condition. The temperature profile and stress development for the fly ash mixtures can be found in Figure 4-13.

The replacement percentages were chosen to be 30% and 20% because they reflect a typical mix design used by the Texas Department of Transportation. It is clear that as the Class C fly ash dosage is increased, the maximum temperature reached decreases.

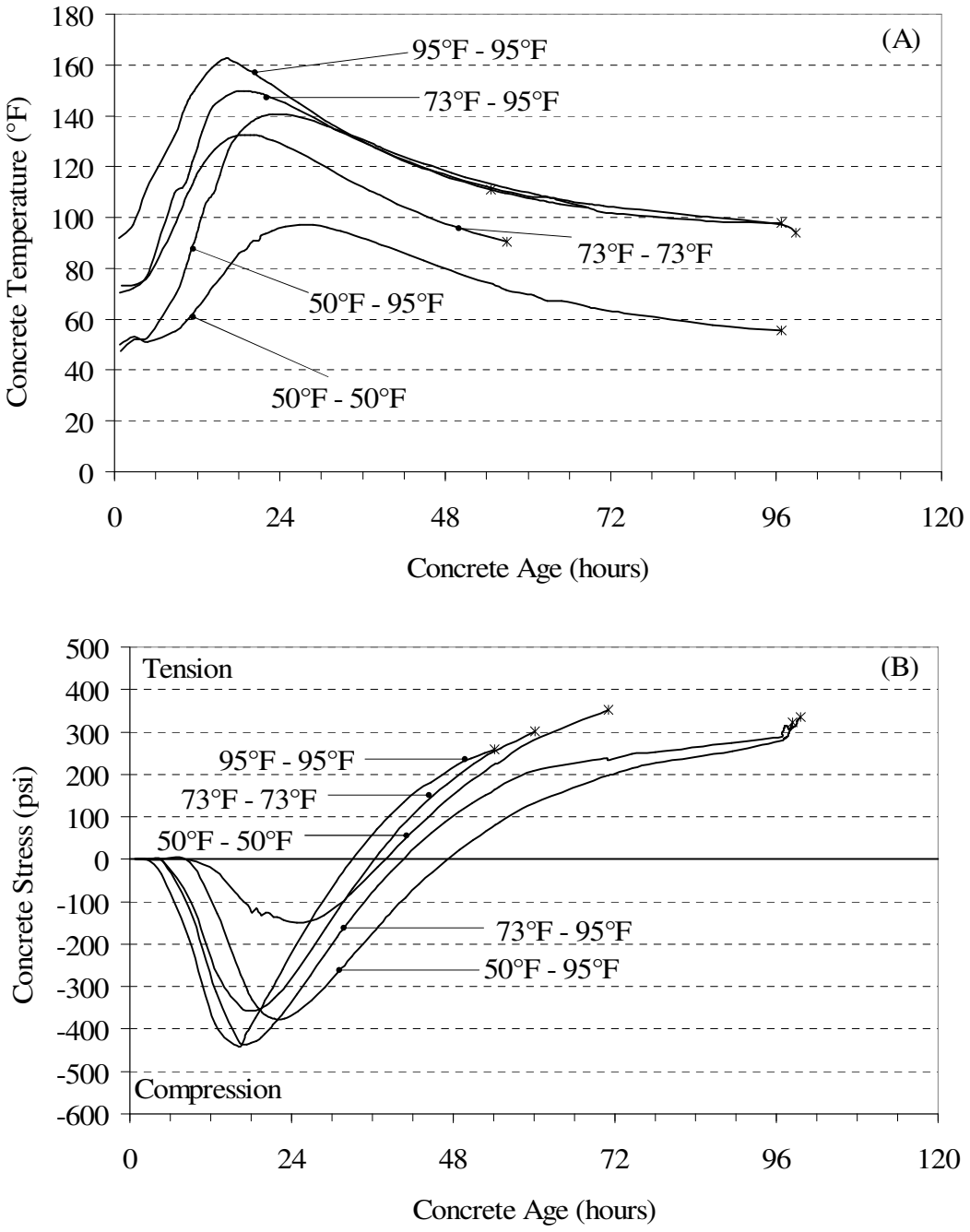


**Figure 4-12:** Test results for the control mixture (Mix ID = CTRL) (A) Temperature development and (B) stress Development

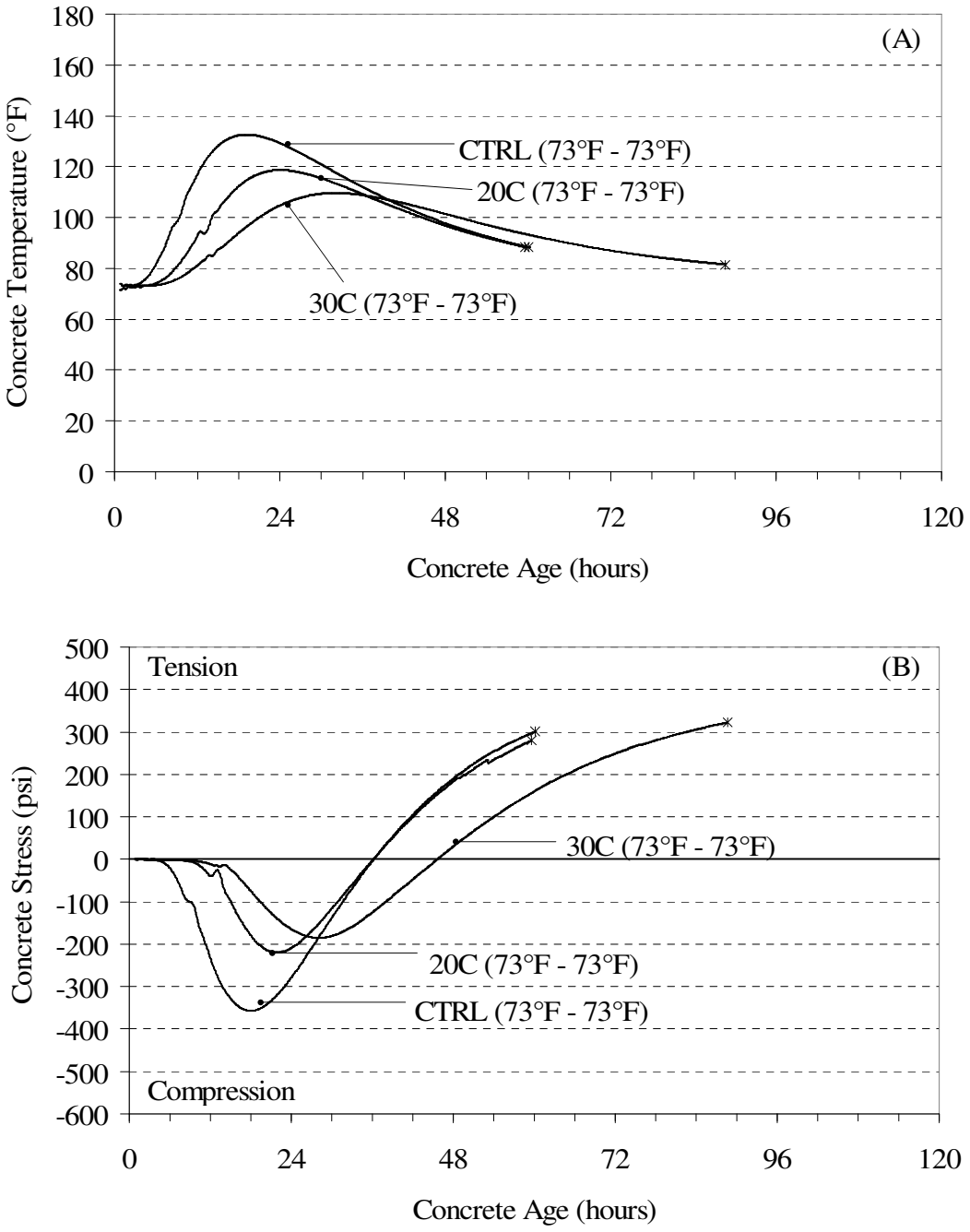


**Figure 4-13:** Test results for Class C fly ash mixtures (30C and 20C) (A) Temperature development and (B) stress development

### 4.3.3 30% GGBF SLAG MIXTURES

The temperature and stress development for the 30% GGBF slag mixture can be found in Figure 4-14. The slag used is a Grade 120, which should increase the strength at later ages as compared to cement-only systems.

GGBF slag has a relatively high activation energy, as a result, the slag is very temperature sensitive. Cold temperatures, i.e. 50°F-50°F, cause the slag mixture to become dormant. Slow development of the modulus of elasticity reduces the restrained stresses that the concrete may experience. At the 95°F-95°F condition, the slag mixture experienced a reduction in tensile strength which caused cracking earlier.

### 4.3.4 50% GGBF SLAG MIXTURES

The GGBF slag chosen for the 50% slag mixtures is the same as the 30% slag mixtures found in Section 4.3.3. Just like the 30% slag mixtures, the 50% slag mixtures are greatly affected by temperature; however, the 50% slag mixtures react more severely due to the higher percentage of slag. The temperature development and stress development for the 50% GGBF slag mixtures are shown in Figure 4-15.

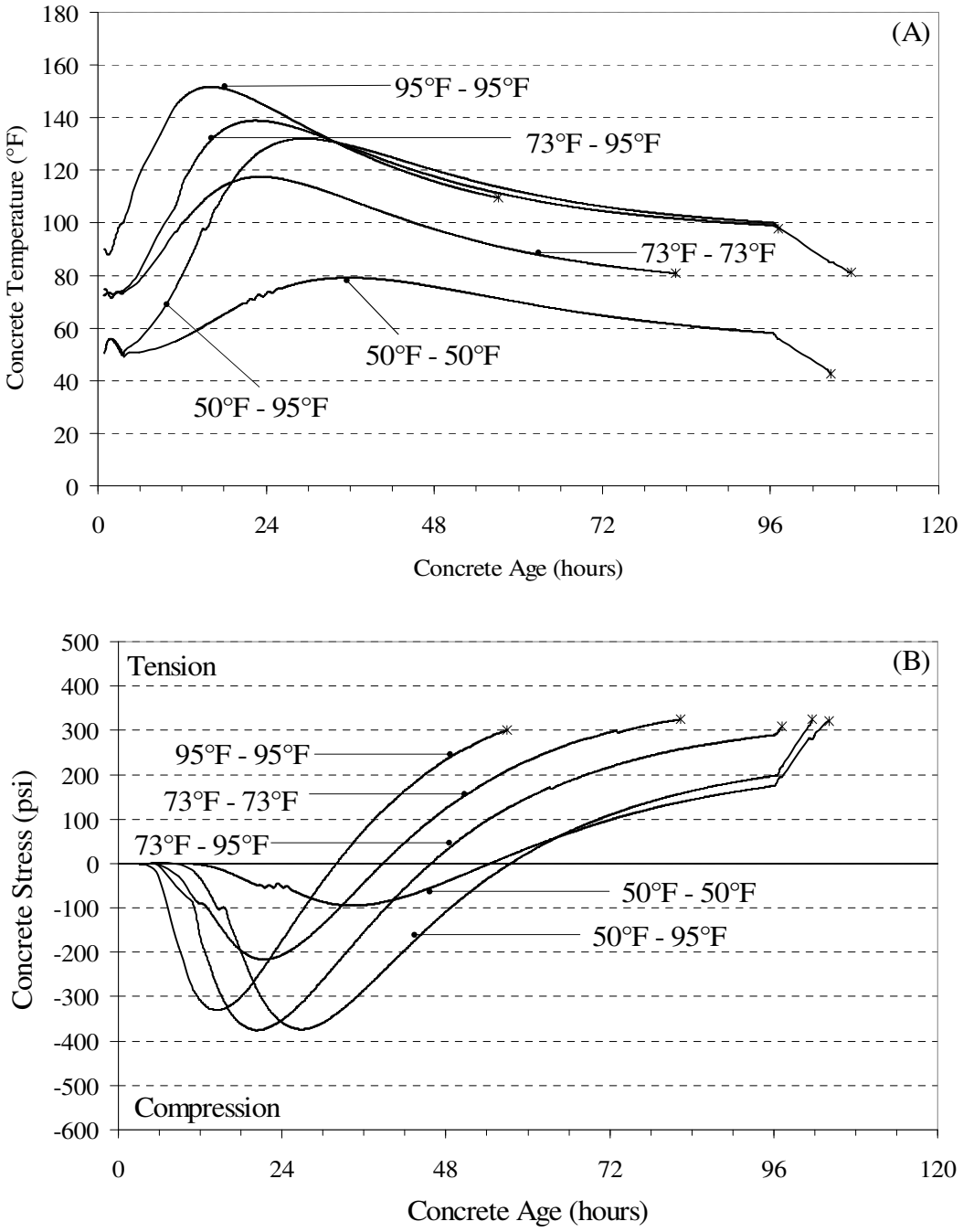


**Figure 4-14:** Test results for the 30% slag mixture (Mix ID = 30SG) (A) Temperature development and (B) stress development

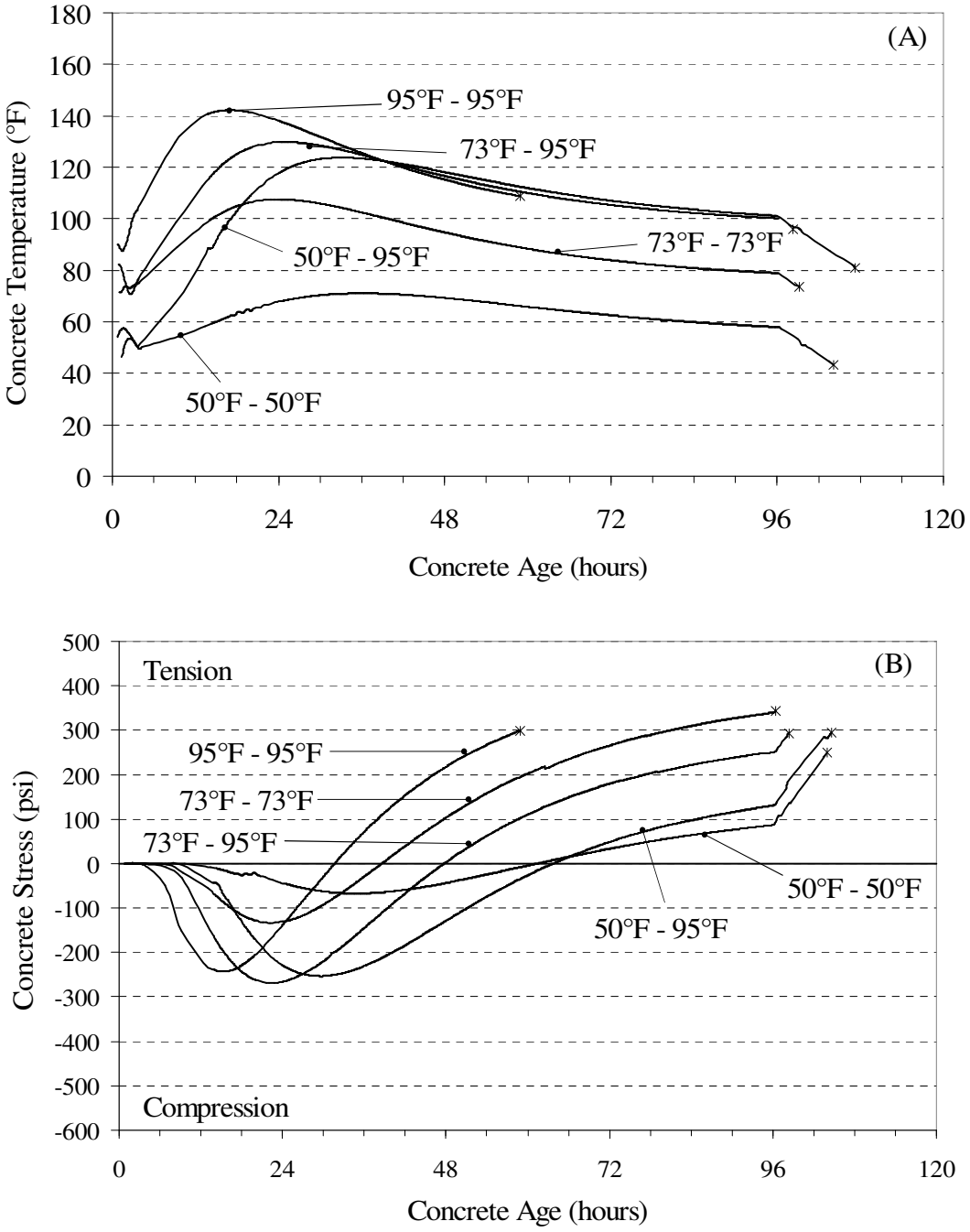


**Figure 4-15:** Test results for 50% slag mixture (Mix ID = 50SG) (A) Temperature development and (B) stress development

### 4.3.5 TERNARY BLEND MIXTURES

Ternary blend mixtures include 20% class C fly ash plus 30% GGBF slag (20C30SG), 30% class C fly ash plus 6% silica fume (30C6SF), and 30% class F fly ash and 6% silica fume (30F6SF). These ternary blend mixtures are typical high performance mixtures used in the concrete construction industry in Texas.

Ternary blend mixtures can reduce the heat generated in a large concrete member through the use of fly ash and GGBF slag; however, these SCMs have been known to retard setting and reduce the rate of early-age strength gain. To counteract the slow development of strength, silica fume may be added. The effect of using ternary blend concrete mixtures can be evaluated in Figure 4-16.

### 4.3.6 LOW WATER-TO-CEMENT RATIO MIXTURES

This section will present the effect of temperature change on the cracking tendency of a low water-to-cement ratio mixture (WC38). The effect of change in water-to-cement ratios as it pertains to early-age cracking will be presented in Section 4.3.9.

Low water-to-cement ratio mixtures provide substantial strength at early ages; however, the modulus of elasticity also grows at a rapid pace. The rapid gain in stiffness coupled with the increase in heat generation due to low water-to-cement ratios will produce higher compressive stresses at early-ages. These stresses are recovered very rapidly as the concrete member begins to cool. Rapid stress gain will in turn cause cracking at early-ages; however, the placement temperature can be varied to prevent rapid heat generation. The temperature development and stress development of the low water-to-cement ratio mixture can be found in Figure 4-17.

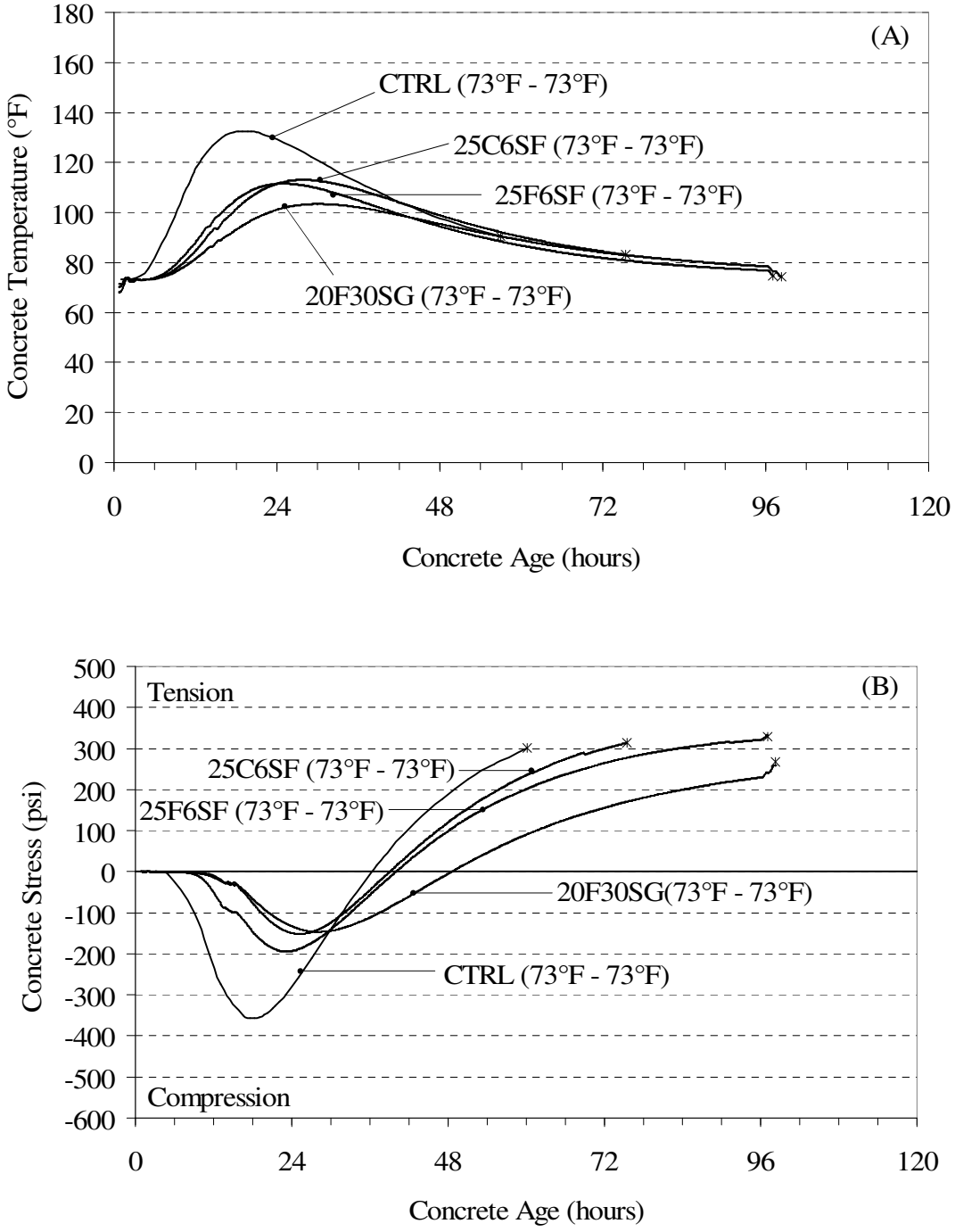


**Figure 4-16:** Test results for ternary blend mixtures (Mix ID = CTRL, 20C30SG, 30C6SF, and 30F6SF) (A) Temperature development and (B) stress development

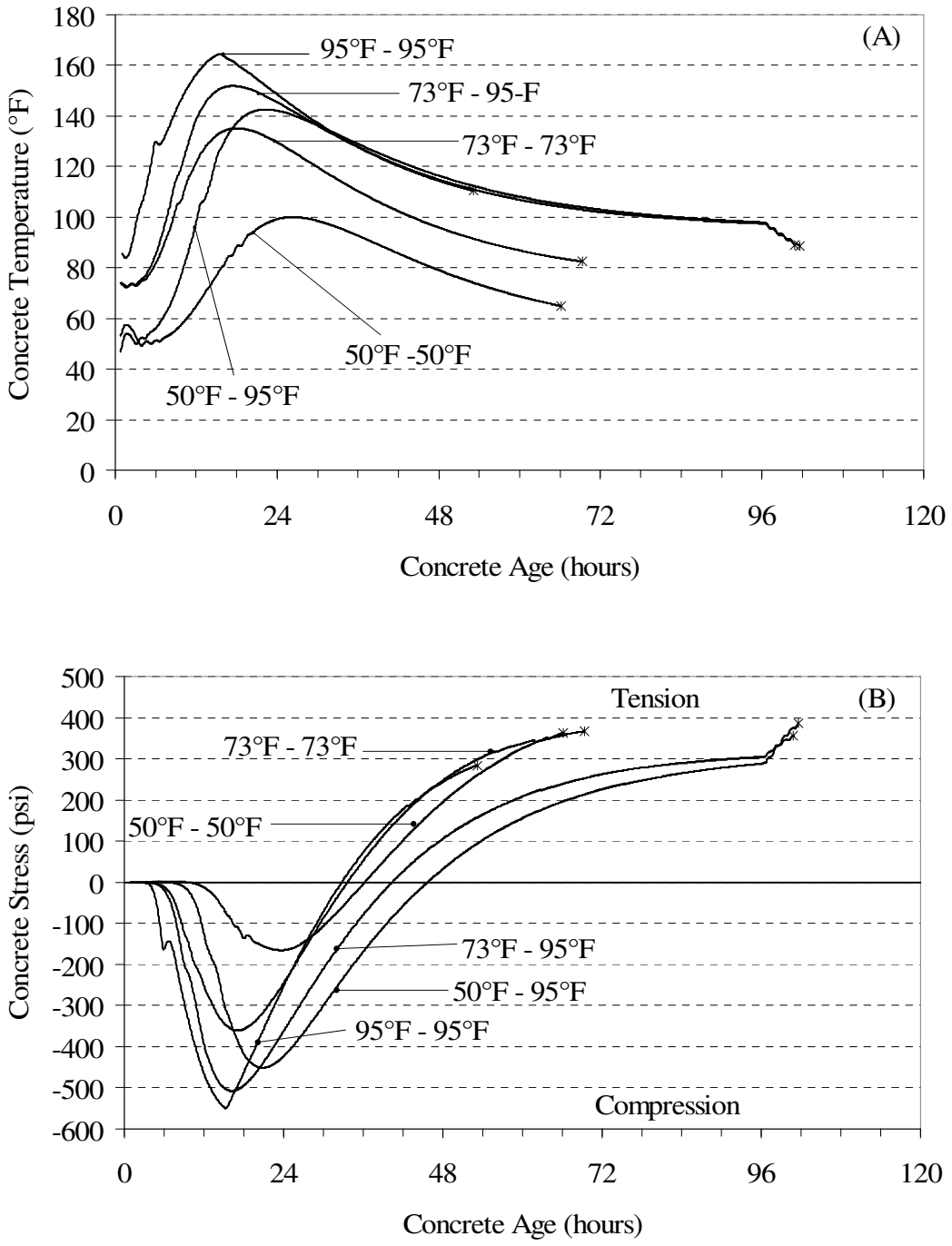


**Figure 4-17:** Test results for w/c = 0.38 mixtures (Mix ID = WC38) (A) Temperature development and (B) stress development

### 4.3.7 TYPE III CEMENT MIXTURES

Type III cement generates considerably more heat than Type I cement; however, due to the fineness of the cement, the mechanical properties grow at a more rapid pace. The rapid heat generation coupled with growing stiffness creates large compressive stresses as shown in Figure 4-18. These stresses are recovered quickly as the concrete begins to cool which leads to cracking. Lower placement temperatures can be used to prolong the time of cracking, which reduces the cracking tendency of the concrete mixtures.

### 4.3.8 AIR ENTRAINMENT MIXTURE

Air entrainment is used extensively to ensure proper mitigation of freeze/thaw deterioration; however, it reduces the early-age and long-term strength of concrete. As a result of the reduction in tensile strength, the concrete cracks earlier than the control mixture even though air-entrainment slightly reduces the heat generated in a large member. The temperature development and stress development of the air-entrained mixture can be found in Figure 4-19.

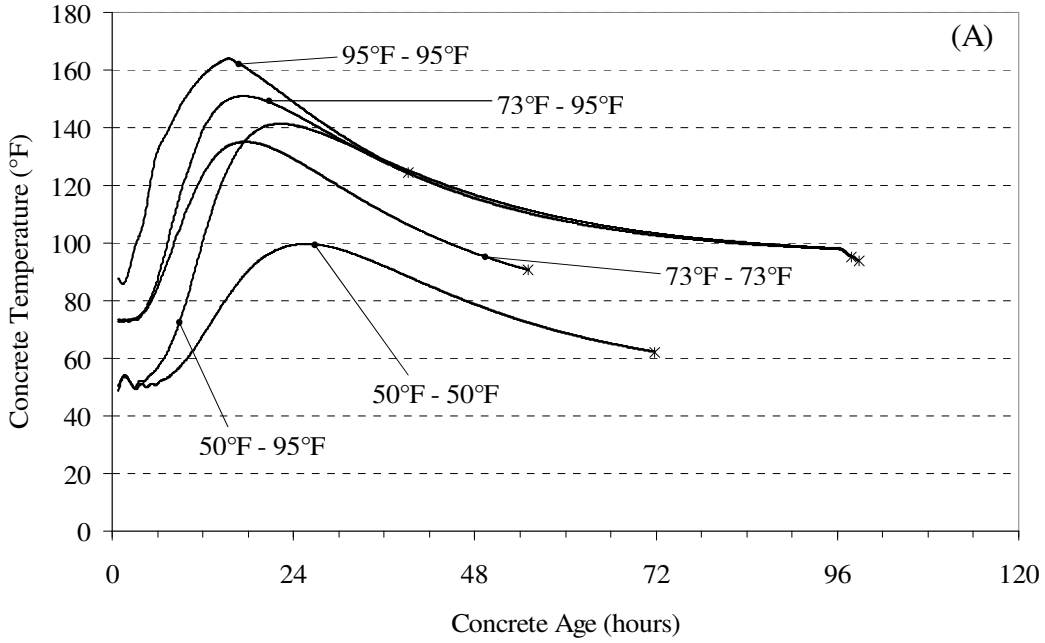


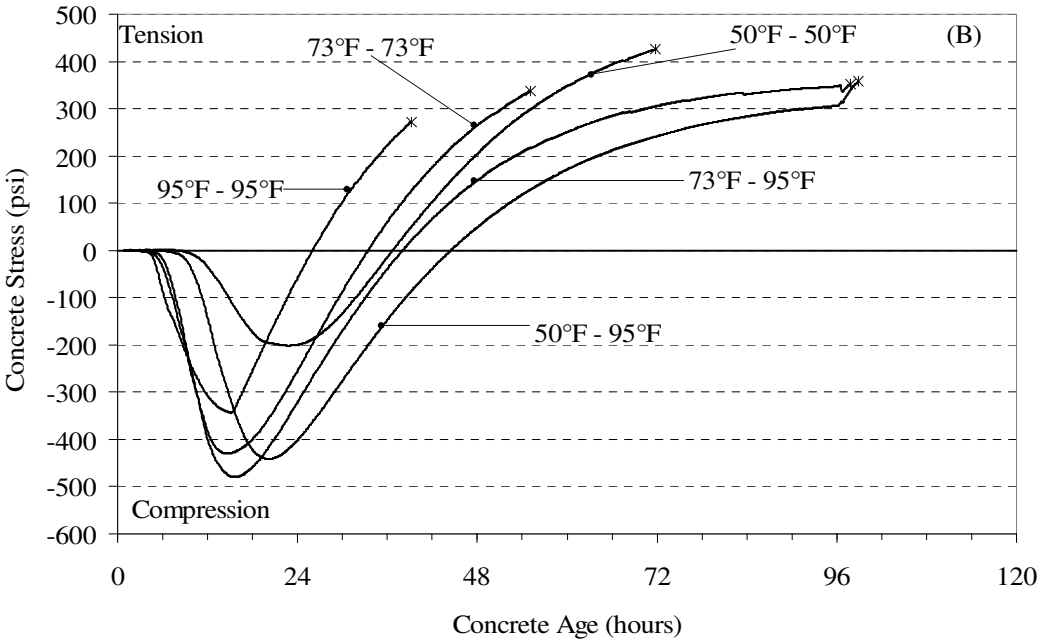


**Figure 4-18:** Test results for the Type III mixtures (Mix ID = TYPE3) (A) Temperature development and (B) stress development

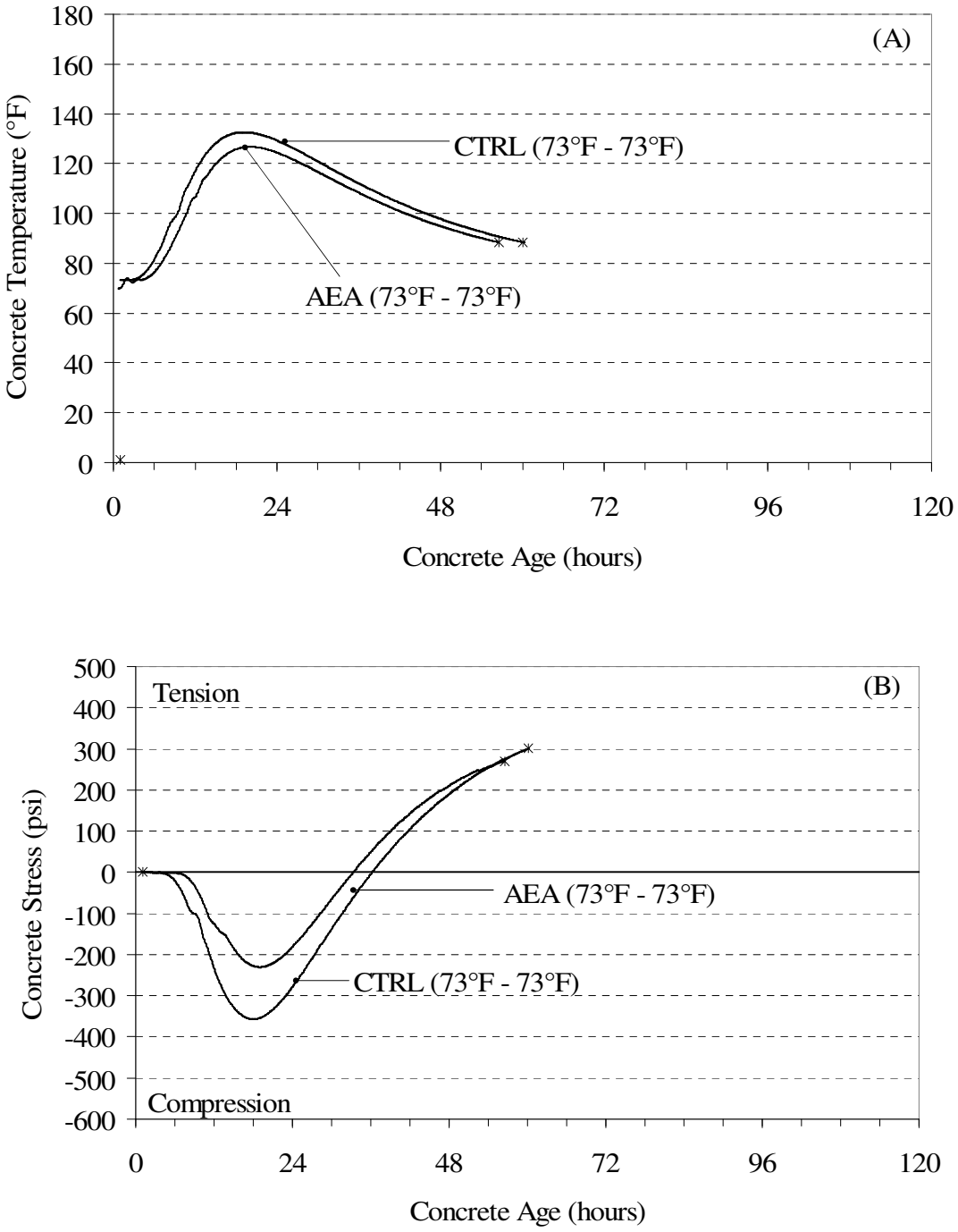


**Figure 4-19:** Test results for the air entrained mixture (Mix ID = CTRL and AEA) (A) Temperature development and (B) stress development

### 4.3.9 EFFECT OF WATER-TO-CEMENT RATIO

As discussed in Section 4.3.6, low water-to-cement ratios (w/c) generate large amounts of heat and exhibit rapid strength gain. The behavior of high water-to-cement ratios is completely opposite. As the water-to-cement ratio is increased, the temperature development is lowered and the development of mechanical properties is slowed and reduced. As a result, the higher water-to-cement ratio mixtures tend to have a lower cracking tendency than lower water-to-cement ratio mixtures as shown in Figure 4-20. The w/c = 0.38 mixture does not follow this trend; it cracked later than the control mixture.

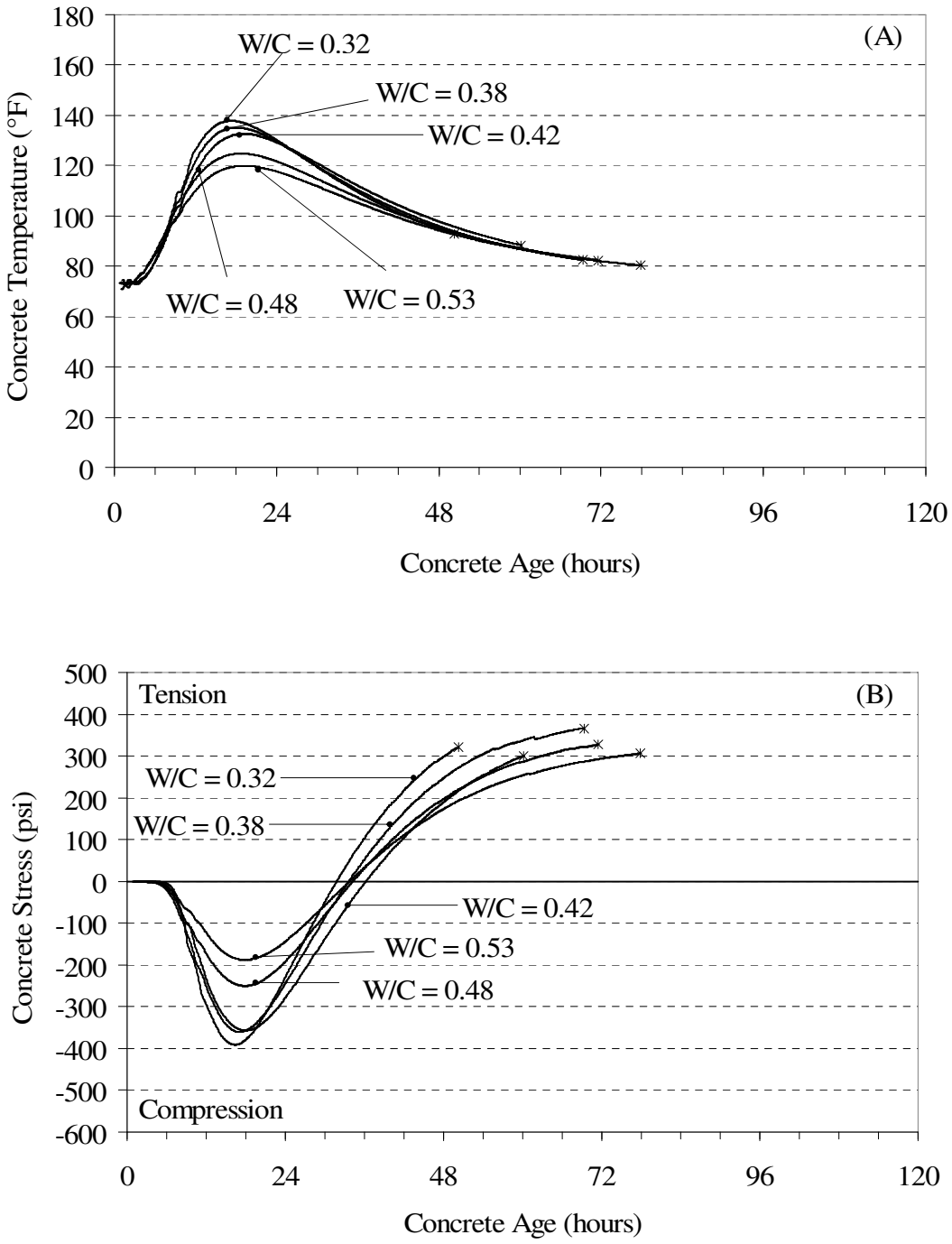


**Figure 4-20:** Test results from the varied water-to-cement ratio mixtures (Mix ID = WC32, WC38, CTRL, WC48, and WC53) (A) Temperature development and (B) stress development

### 4.3.10 FREE SHRINKAGE FRAME

The free shrinkage frame is designed to measure the free shrinkage of a concrete specimen. The specimen is match-cured to the same temperature profile as the match-cured rigid cracking frame as discussed in Chapter 3. This section presents the test results collected from the free shrinkage frame.

During the duration of this project it was determined that the spring-loaded LVDT did not properly measure the expansion and contraction of the concrete specimen. The spring-loaded LVDT resisted some of the free expansion of the concrete specimen and the use of a non-spring loaded LVDT resolved this problem. As a result, the LVDT was changed to one without a spring; therefore, some results obtained by the free shrinkage frame will not be presented in this section due to inaccurate measurements.

As shown in Figure 4-21, the maximum strain of the control mixture was resisted by the spring-loaded LVDT. The spring-loaded LVDT resisted the expansion of the concrete which caused the maximum deformation to flatten out instead of following the strains that should correspond to the temperature profile. The general shape of the plot should resemble that of the non-spring loaded LVDT; however, the magnitude of these plots should not be the same due to differences in the temperature profiles.

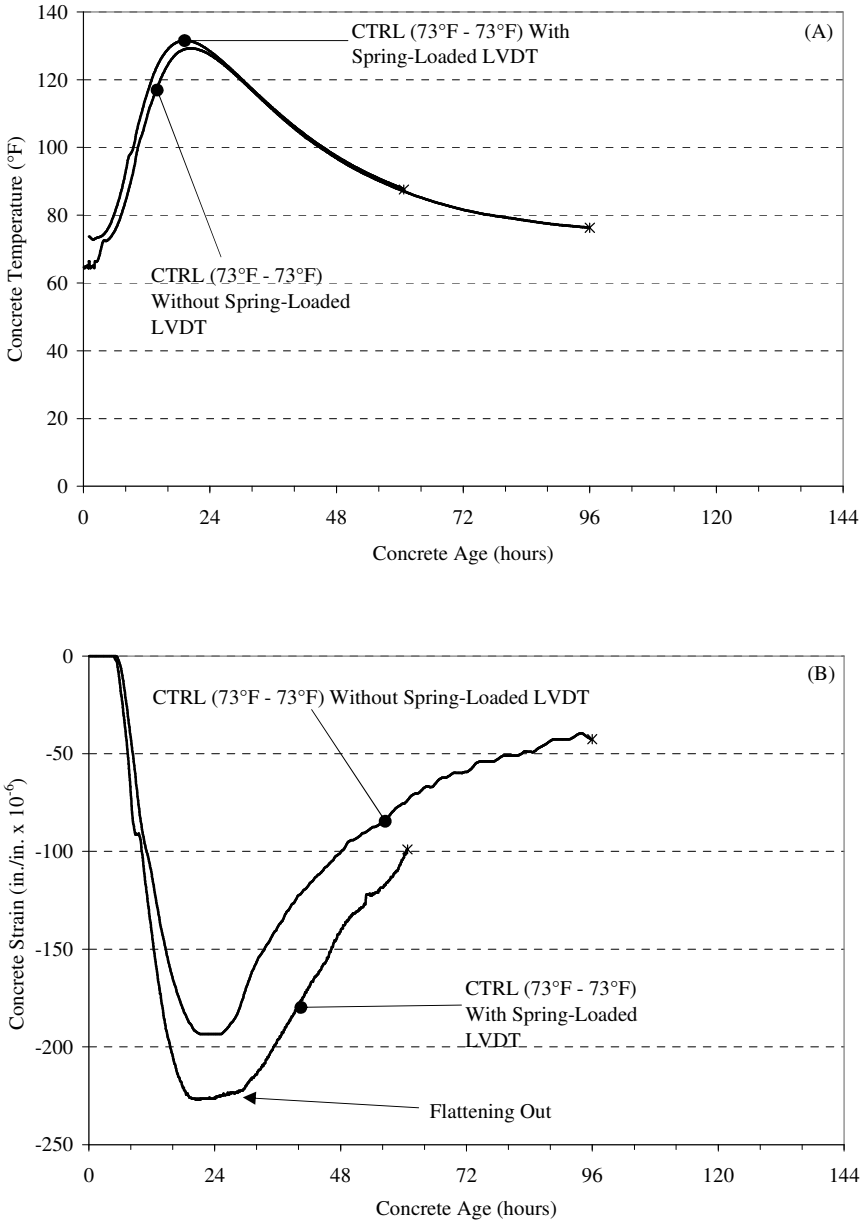


**Figure 4-21:** Free shrinkage frame results with different LVDT types (A) Temperature development and (B) concrete Strain

#### 4.3.10.1 Fly Ash

The effect of fly ash as a replacement for cement was evaluated. These mixtures were simulated at 73°F as the placement temperature with the 1.0 meter wall surrounded by 73°F. As discussed previously, increasing amounts of fly ash as a replacement for cement reduces the heat generated during hydration. The reduction in heat minimizes the deformation of the concrete prism as shown in Figure 4-22.

#### 4.3.10.2 Ternary Blend Mixtures

As discussed in Section 4.3.5, the use of supplementary cementing materials can be used to reduce the heat of hydration of a concrete mixture. As a result, the magnitude of strain experienced by the concrete prism is reduced with the increase in replacement percentages as shown in Figure 4-23.

#### 4.3.10.3 Type III Cement

Type III cement generates considerably more heat than the Type I cement. Due to the fineness of the cement, the mechanical properties grow at a more rapid pace. The rapid heat generation coupled with growing stiffness creates large contractions as shown in Figure 4-24.

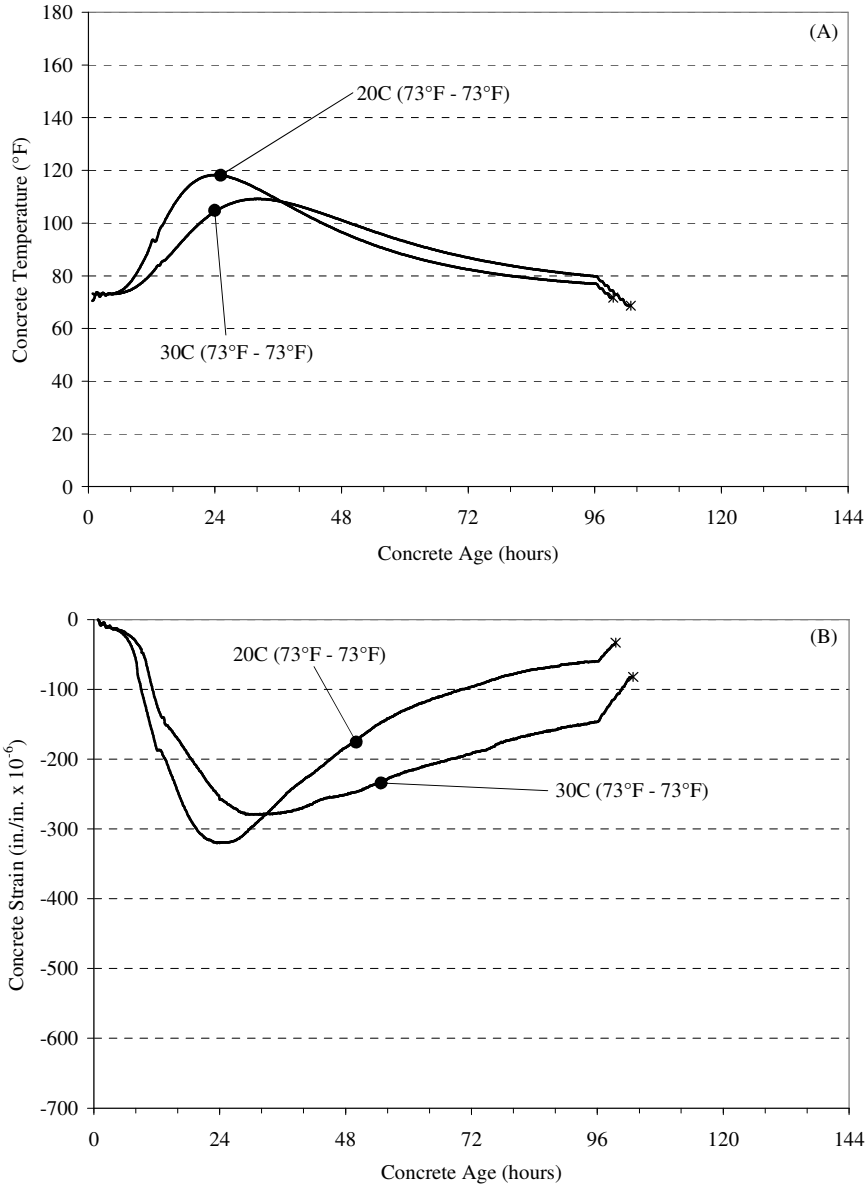


**Figure 4-22:** Test results from the Class C fly ash mixtures (Mix ID = 20C and 30C) (A) Temperature development and (B) free concrete strain

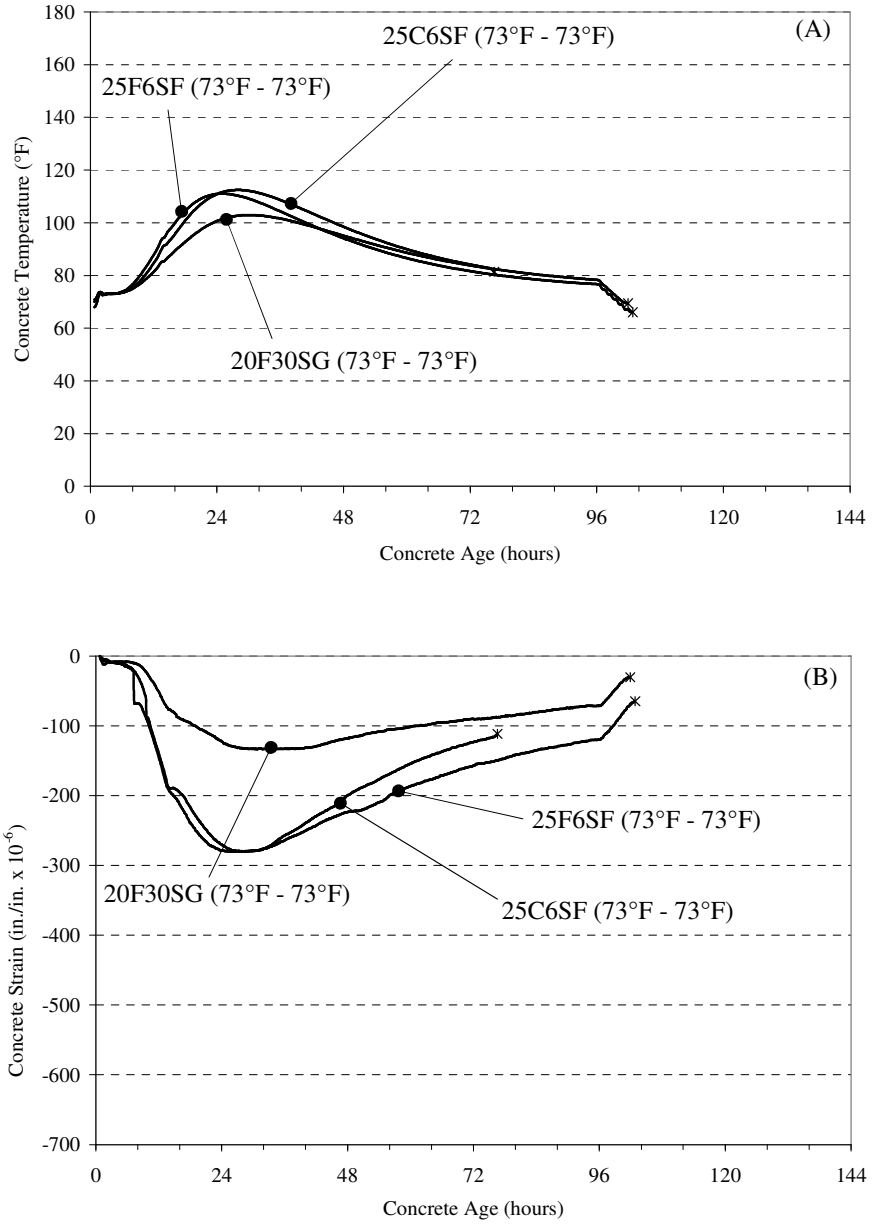


**Figure 4-23:** Test results from the ternary blend mixtures (Mix ID = 20C30SG, 30C6SF, and 30F6SF) (A) Temperature development and (B) free concrete strain

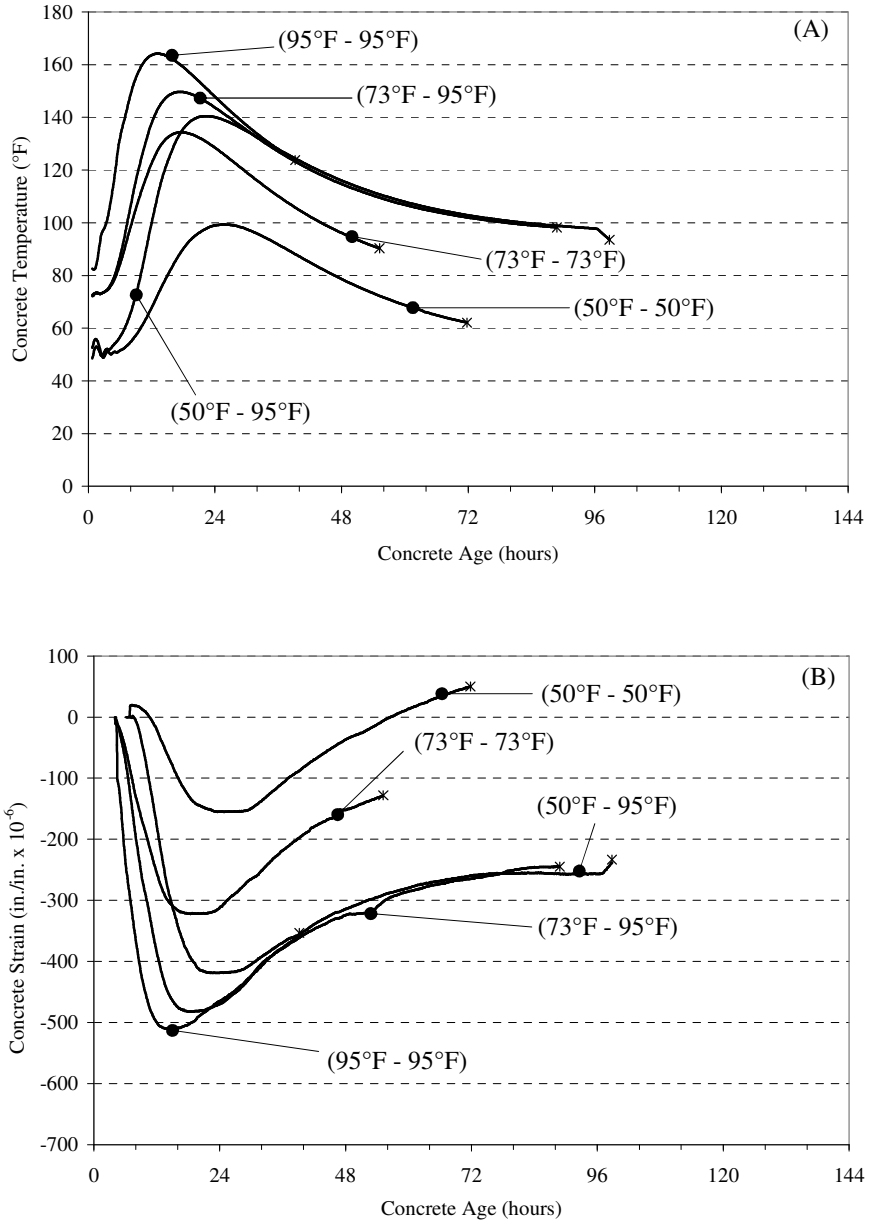


**Figure 4-24:** Test results from the Type III cement mixtures (Mix ID = TYPE3) (A) Temperature development and (B) free concrete strain

## 4.4 ISOTHERMAL RIGID CRACKING FRAME

The isothermal rigid cracking frame is used to measure the stress development due to only autogenous shrinkage. The isothermal rigid cracking frame tests were conducted at three temperatures determined by the target placement temperature of the concrete. These temperatures are 50°F, 73°F, and 95°F. This section presents the results obtained from the isothermal rigid cracking frame. Discussion of the results presented in Section 4.4 will be provided in Chapter 5.

This section presents the effect of temperature, cement type, SCMs, air entrainment, and water-to-cement ratio on stress development of the isothermal rigid cracking frame. All results of the isothermal rigid cracking frame can be found in Appendix C.

### 4.4.1 EFFECT OF CONCRETE PLACEMENT TEMPERATURE

As discussed in Chapter 3, three temperatures were chosen to conduct the isothermal rigid cracking frame test in order to determine the effect of temperature on autogenous shrinkage. These temperatures reflect seasonal temperatures that may occur during concrete placement. As shown in Figure 4-25, the seasonal temperatures are designated by the first temperature for each mixture. Although five mixtures of the control were made using three test temperatures, the overall magnitude of stress development was very close from one mixture to another.

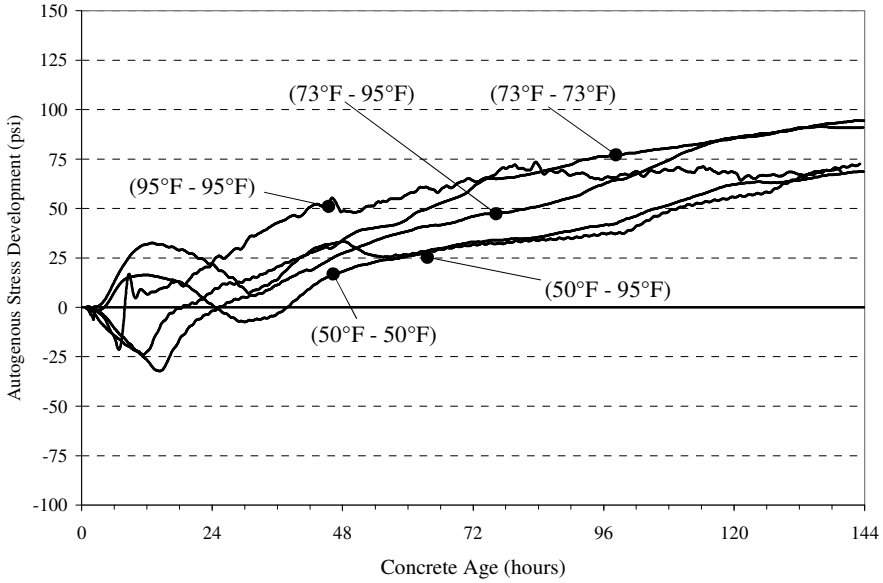


**Figure 4-25:** Autogenous shrinkage results for the control mixture (Mix ID = CTRL) using the isothermal rigid cracking frame with multiple placement temperatures

### 4.4.2 CEMENT TYPE

Two cement types were chosen to evaluate the stress development under isothermal conditions. The Type I cement, which has a lower Blaine value than the Type III cement, produced less stress at 144 hours as shown in Figure 4-26.

The magnitude of autogenous shrinkage stresses is dependent upon the rate of chemical shrinkage as discussed in Chapter 2. Chemical shrinkage is determined by the volume of Bogue compounds. The Type I cement had a larger percentage of $C_3A$ while the Type III cement had a larger volume of $C_4AF$. As a result, the differences in autogenous shrinkage magnitudes are caused by variability in the testing method.

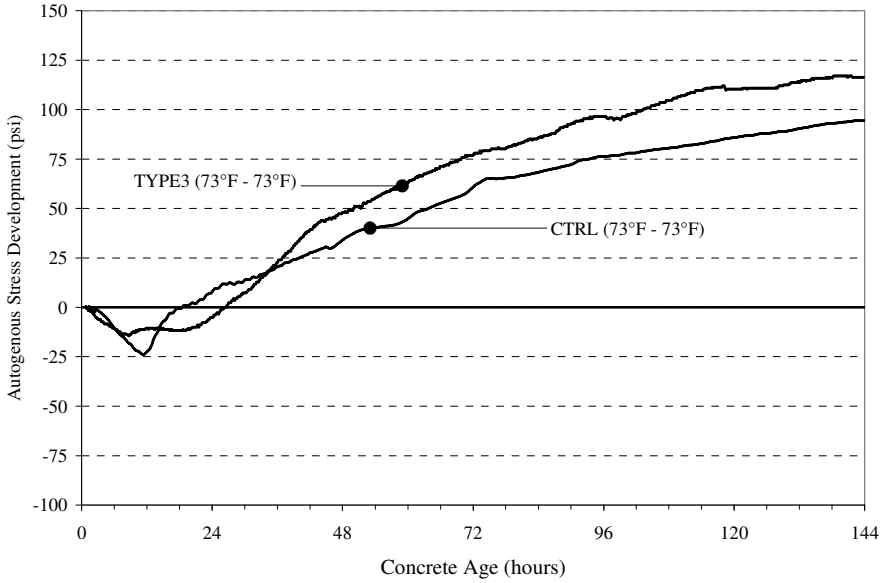


**Figure 4-26:** Autogenous shrinkage results for the control mixture and type III mixture (Mix ID = CTRL and TYPE3) using the isothermal rigid cracking frame at 73°F

### 4.4.3 SUPPLEMENTARY CEMENTING MATERIALS

As discussed in Sections 4.3.2, 4.3.3, and 4.3.4, SCMs improve the early-age cracking resistance of concrete by mitigating temperature development. SCMs also reduce the autogenous stress in the rigid cracking frame as shown in Figures 4-27 and 4-28 because they reduce the rate of hydration which in turn reduces the rate of internal relative humidity drop.

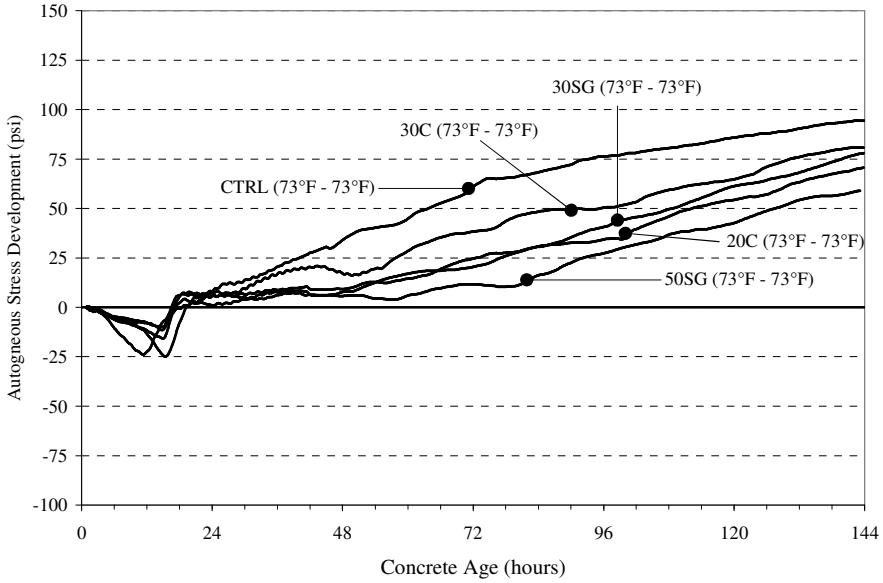


**Figure 4-27:** Autogenous shrinkage results for the control and SCM mixtures (Mix ID = CTRL, 30C, 20C, 30SG, and 50SG) using the isothermal rigid cracking frame at 73°F

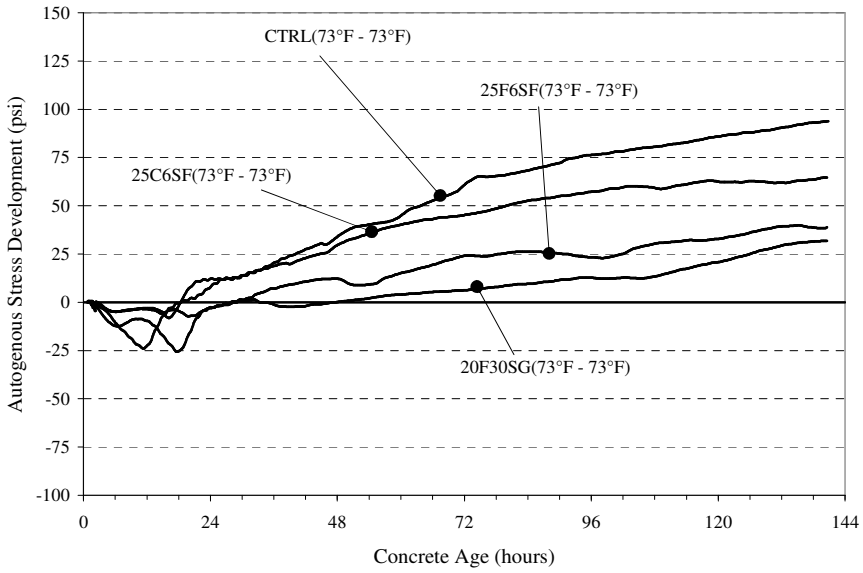


**Figure 4-28:** Autogenous shrinkage results for the ternary blend mixtures (Mix ID = CTRL, 25C6SF, 25F6SF, and 20F30SG) using the isothermal rigid cracking frame at 73°F

### 4.4.4 AIR ENTRAINMENT

The air-entrained mixture has significantly more air than the control mixture. As a result, the water inside the concrete can easily move throughout the cross section. The movement of water during hydration creates a uniform distribution of internal relative humidity, which reduces the stress development due to autogenous shrinkage shown in Figure 4-28. Hammer and Fossa (2006) found that air entrainment alters the pore water pressure which subsequently decreases autogenous shrinkage. These findings coincide with the data presented in Figure 4-28.

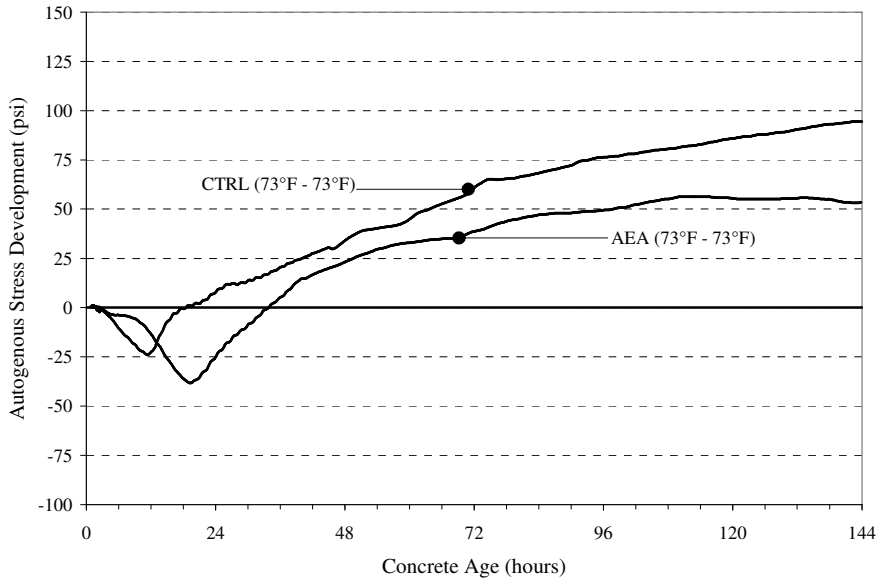


**Figure 4-28:** Autogenous shrinkage results for the control and air entrained mixture (Mix ID = CTRL and AEA) using the isothermal rigid cracking frame at 73°F

### 4.4.5 WATER-TO-CEMENT RATIO

As the water-to-cement ratio is decreased, the water available for hydration is decreased. This reduction in water more rapidly reduces the internal relative humidity which leads to increased autogenous stresses, as shown in Figure 4-29. The stress development using high water-to-cement ratio mixtures is almost a third of the lowest water-to-cement ratio mixture.

The stress development due to autogenous shrinkage seems to be approximately the same for the high water-to-cement ratio mixtures, i.e. w/c = 0.48 and 0.53. This is due to the higher amount of water available during hydration which does not reduce the internal relative humidity as fast as a low water-to-cement ratio mixture.

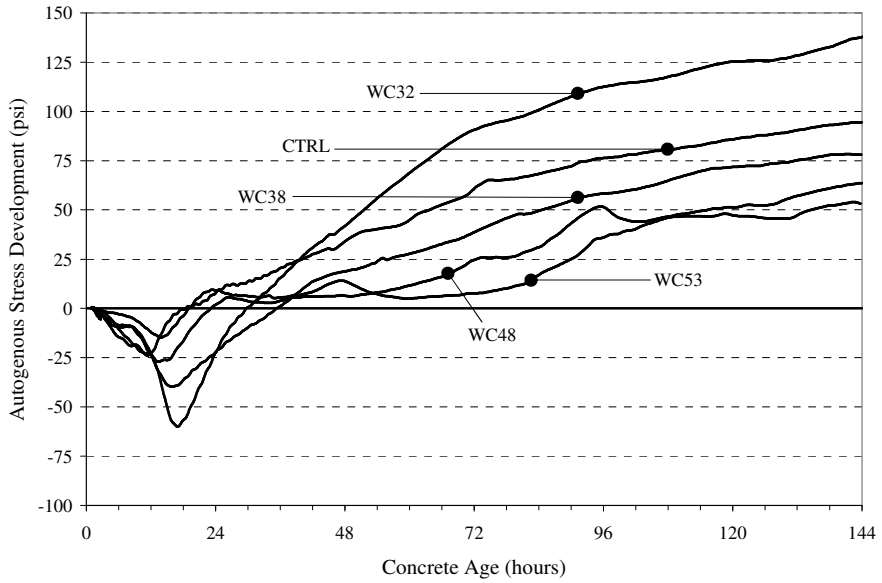


**Figure 4-29:** Autogenous shrinkage results for varied water-to-cement ratios (Mix ID = CTRL, WC32, WC38, WC48, and WC53) using the isothermal rigid cracking frame at 73°F

# CHAPTER 5

# DISCUSSION OF RESULTS

The results presented in Chapter 4 are discussed in this chapter. The effects of placement temperature, seasonal temperature changes, cement type, cementitious materials, air entrainment, and water-to-cementitious materials ratio on the cracking tendency of concrete mixtures are thoroughly discussed. The notation used throughout this chapter is consistent with the notation described in Section 3.2 of Chapter 3.

## 5.1 EFFECT OF PLACEMENT TEMPERATURE

The effect of placement temperature on the cracking tendency of concrete can only be evaluated from the behavior of the following mixtures: CTRL, 30SG, 50SG, WC38, and TYPE3. These five mixtures were placed at 50°F, 73°F, and 95°F and simulated using an ambient temperature of 95°F on the outside of the 1.0 meter thick wall. This condition allows one to evaluate the effect of curing concrete to achieve placement temperatures of 50°F, 73°F, and 95°F during warm summer months. The mechanical properties, temperature development, and stress development of these mixtures can be found in Sections 4.2 and 4.3.

### 5.1.1 CRACKING SENSITIVITY

The fresh placement temperature of a concrete mixture affects the rate of hydration. As the placement temperature increases, the rate of temperature rise increases as shown in Figures 4-12, 4-14, 4-15, 4-17, and 4-18. According to Springenschmid and Breitenbücher (1998), high temperature placements, i.e. 86°F, increase the rate of temperature development due to the acceleration of hydration.

In addition, the rate of development of the modulus of elasticity rises with the increase in placement temperature as shown in Figures 4-3, 4-5, 4-6, 4-8, and 4-9. The 30SG and TYPE3 mixtures do not follow this pattern. In these mixtures, the stiffness of the 95°F placement temperature mixture was lower than the 73°F and 50°F placement temperature conditions.

Temperature and stiffness increases create large compressive stresses in the concrete specimen. These stresses are overcome as the temperature subsides and the concrete specimen goes into tension. Once the tensile stresses exceed the tensile strength of the concrete, then cracking occurs.

#### 5.1.1.1 Portland Cement Only Mixtures

As expected, the fresh concrete placement temperature had a substantial impact on the cracking tendency of the portland cement only mixtures. Lowering of the placement temperature reduced the cracking temperature of all the portland cement only mixtures as shown in Figure 5-1. When compared to the 95°F placement temperature, the cracking temperatures of the WC38 and TYPE3 mixtures were reduced by approximately 22°F by

lowering the placement temperature to 73°F. The cracking temperature of the CTRL mixture was reduced by approximately 16°F.

According to Breitenbücher and Mangold (1994), high cement contents and high early-age strength cements increase temperature development, which leads to relatively high cracking tendencies. However, the WC38 mixture placed at 50°F and 73°F did not follow this trend due to the increase in tensile strength as compared to the CTRL mixture.

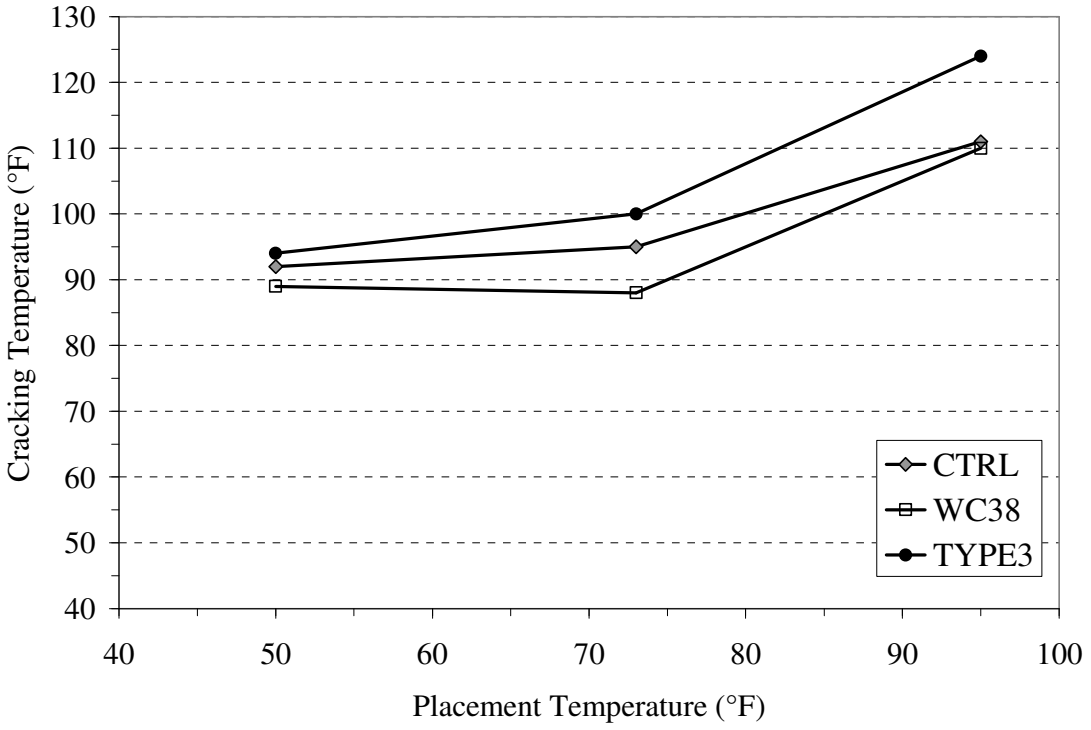


**Figure 5-1:** Effect of placement temperature on portland cement only systems

From Figures 4-3B, 4-8B, and 4-9B it may be concluded that lowering the placement temperature increases the splitting tensile strength after 2 days. However, the CTRL mixture does not follow this trend. The CTRL mixture placed at 50°F had a reduced

tensile strength prior to 7 days while the mixture placed at 73°F increased the tensile strength after at all ages. The reduction in fresh concrete placement temperature increases the tensile strength due to the reduction in temperature development. As a result, the stress-to-strength ratio is reduced prior to artificial cooling, i.e. 96 hours, with the exception of the TYPE3 mixture.

As shown in Figure 5-2, the 95°F concrete placement temperature for each mixture cracked prior to 96 hours. With the exception of the TYPE3 mixture placed at 73°F, the lower placement temperatures had additional tensile strength capacity. As a result, the remaining mixtures required artificial cooling in order to produce cracking. The TYPE3 mixture placed at 73°F had a slightly higher zero stress temperature and stiffness which caused cracking immediately after cooling began.

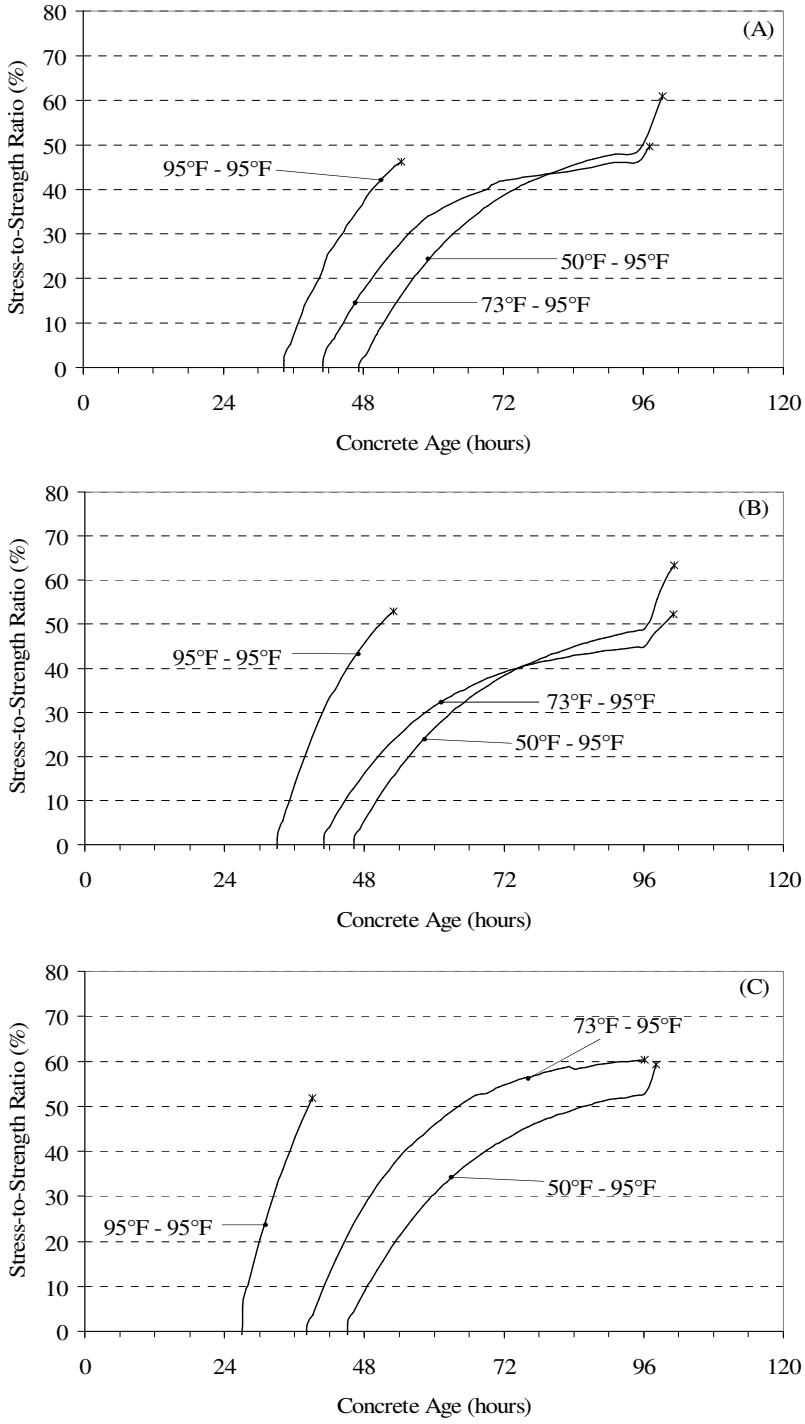


**Figure 5-2:** Effect of placement temperature on the stress-to-strength ratio of the (A) CTRL mixture, (B) WC38 mixture, and (C) TYPE3 mixture

#### 5.1.1.2 GGBF Slag Mixtures

The development of mechanical properties of the GGBF slag mixtures can be evaluated in Figures 4-5 and 4-6. The rate of strength development is affected by the change in placement temperature; however, the modulus of elasticity is only slightly affected after 5 days. As a result, the replacement of cement with GGBF slag provided slightly lower cracking temperatures at a placement of 50°F and 95°F as shown in Figure 5-3. At the 73°F placement temperature, the GGBF slag mixtures were about the same as the control mixture. The data in Figure 5-3 corresponds to the findings of Springenschmid and Breitenbücher (1998), who state the reduction of cracking temperature of a GGBF slag mixture depends on the development of the modulus of elasticity and tensile strength in the first few days.

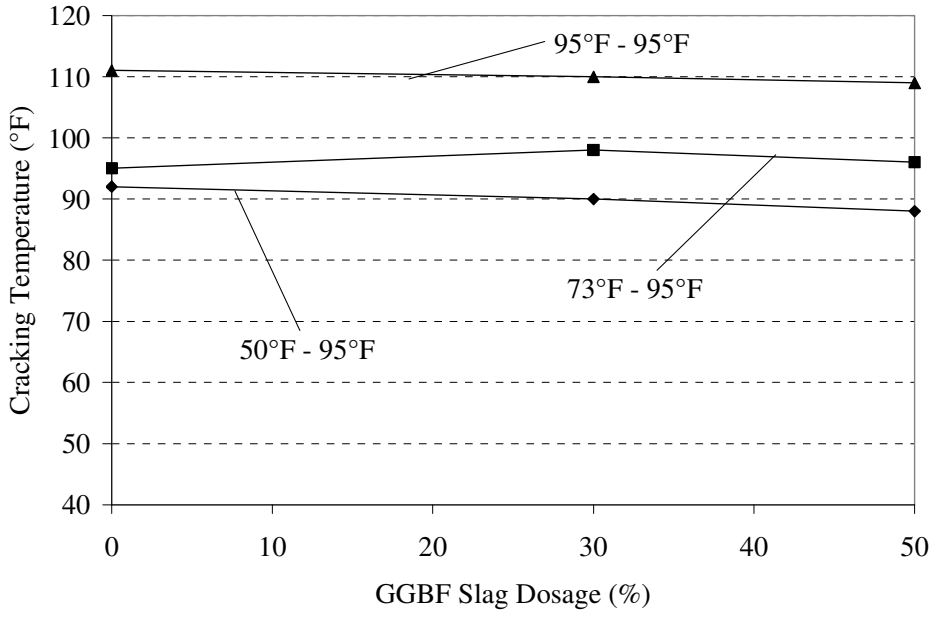


**Figure 5-3:** Effect of GGBF slag dosage on cracking temperature under various placement temperatures

Although the use of GGBF slag did not affect the cracking tendency, the reduction of cracking temperature corresponds to the trends of the portland cement only mixtures discussed in Section 5.1.1.1. The reduction of placement temperature reduces the cracking temperature of the GGBF slag mixtures as shown in Figure 5-4. When compared to the 95°F placement temperature, the cracking temperatures of the 30SG and 50SG mixtures were reduced by approximately 12°F by lowering the placement temperature to 73°F. The reduction of the placement temperature to 50°F yields an 20°F reduction in cracking temperature.

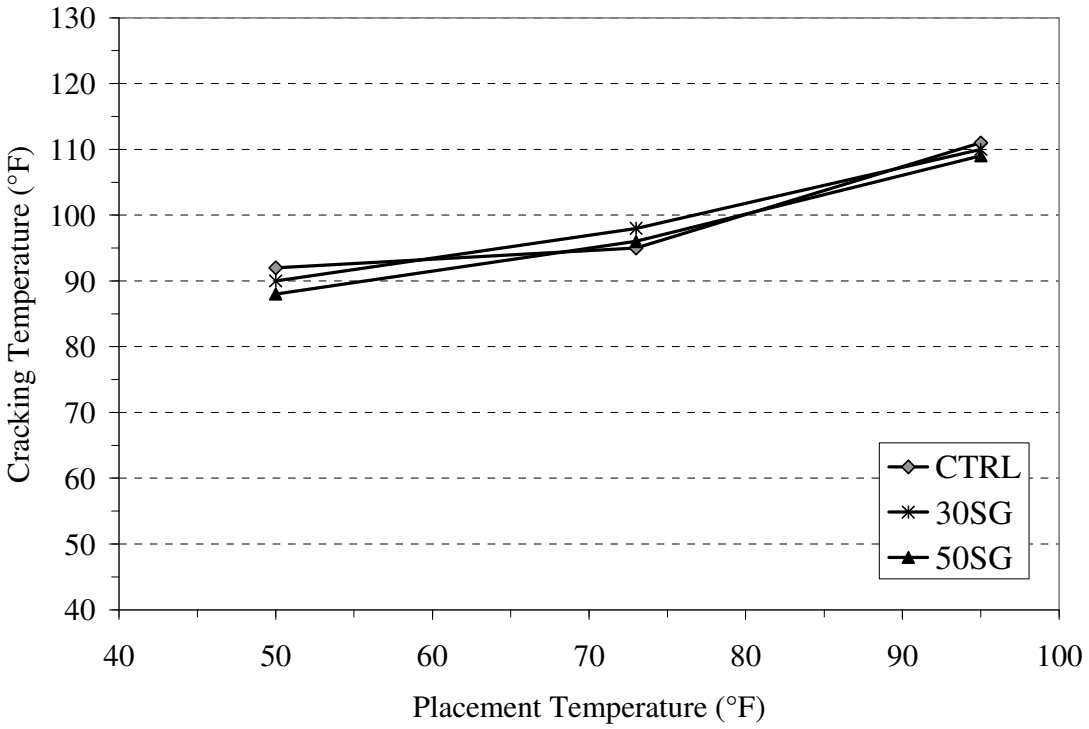


**Figure 5-4:** Effect of placement temperature on GGBF slag mixtures

The use of GGBF slag as a replacement for cement reduces the magnitude of temperature development in a concrete specimen as discussed in Section 2.1.3. The reduction of heat generation minimizes the temperature change that the concrete experiences before reaching equilibrium with the ambient conditions. The decrease in placement temperature further reduces the maximum temperature rise. As a result, the zero stress temperature is reduced, creating fewer tensile stresses relative to the tensile strength prior to 96 hours in the GGBF slag at 50°F and 73°F placement temperatures as shown in Figure 5-5. This data matches the findings of Breitenbücher and Mangold (1994), who state that slag cements lead to relatively low temperature rises during hydration and to small tensile stresses.

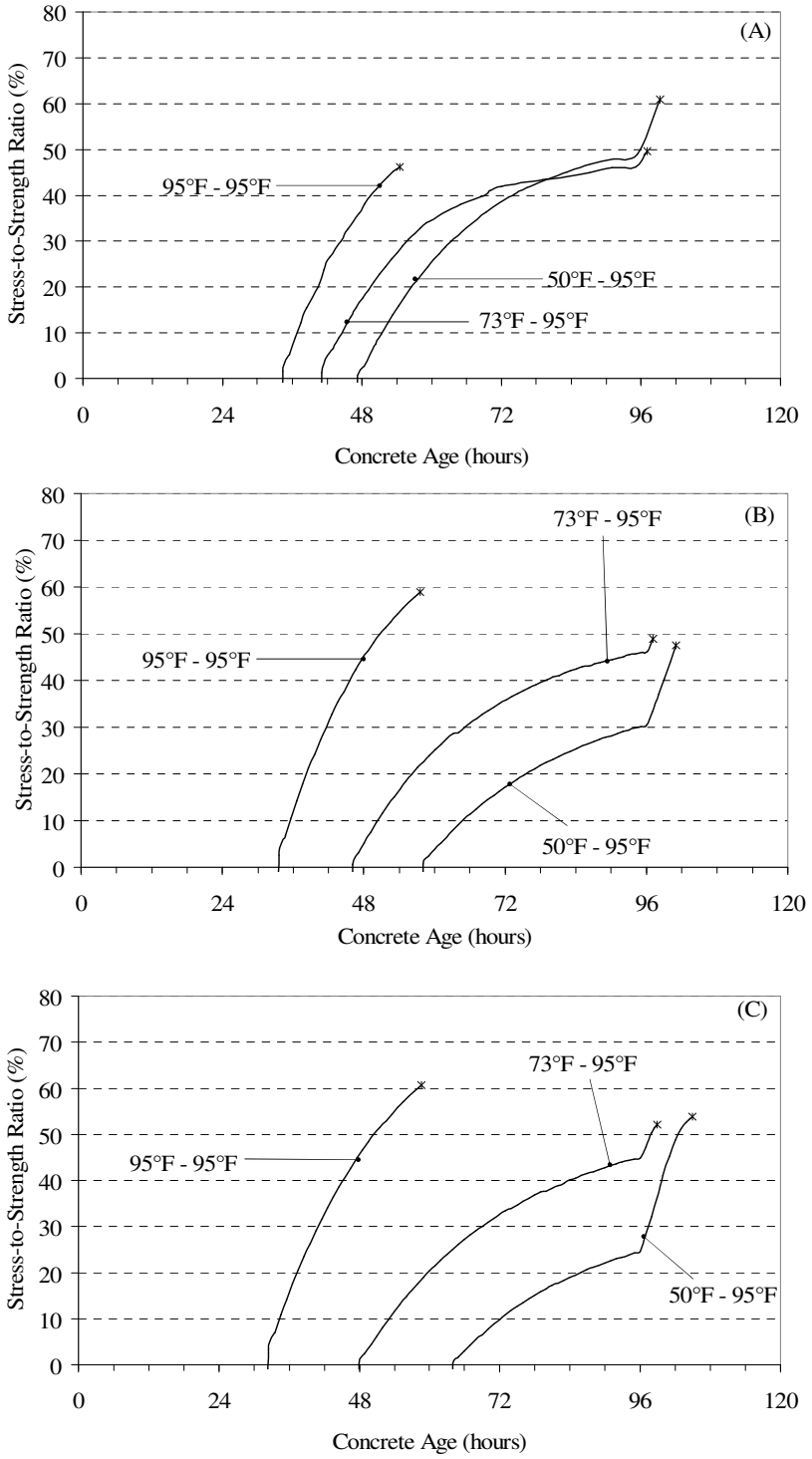


**Figure 5-5:** Effect of placement temperature on the stress-to-strength ratio of the (A) CTRL mixture, (B) 30SG mixture, and (C) 50SG mixture

### 5.1.2 AUTOGENOUS SHRINKAGE

Unlike the restrained stresses in the match-cured rigid cracking frame, the magnitude of the autogenous shrinkage stresses is not dependent upon temperature. Bjøntegaard (1999) states higher curing temperatures do not necessarily lead to higher autogenous deformations. The effect of temperature increases on the magnitude of autogenous shrinkage stresses is unsystematic and varies with cement type (Lura et al. 2001). As shown in Figures 5-6, 5-7, and 5-8, the difference in restrained stresses due to autogenous shrinkage effects is less than 25 psi at 144 hours for all portland cement only systems. The differences in stress development between the three placement temperatures within the three concrete mixtures can be attributed to variability in the testing method.

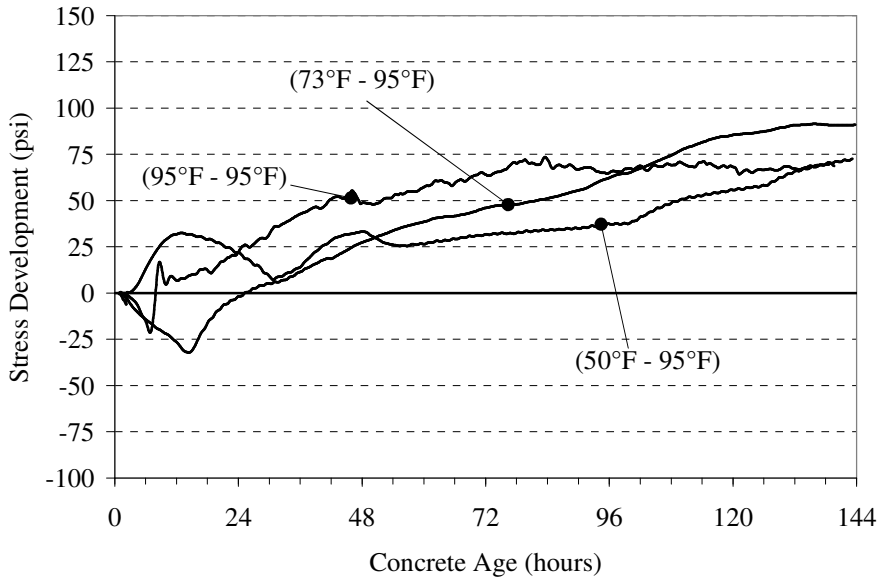


**Figure 5-6:** Effect of placement temperature on stress development under isothermal conditions of the CTRL mixture

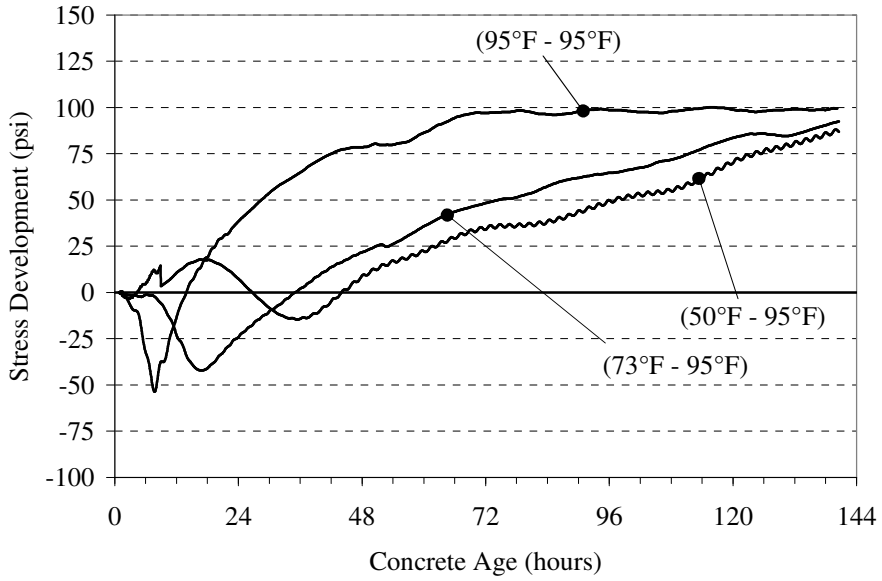


**Figure 5-7:** Effect of placement temperature on stress development under isothermal conditions of the WC38 mixture

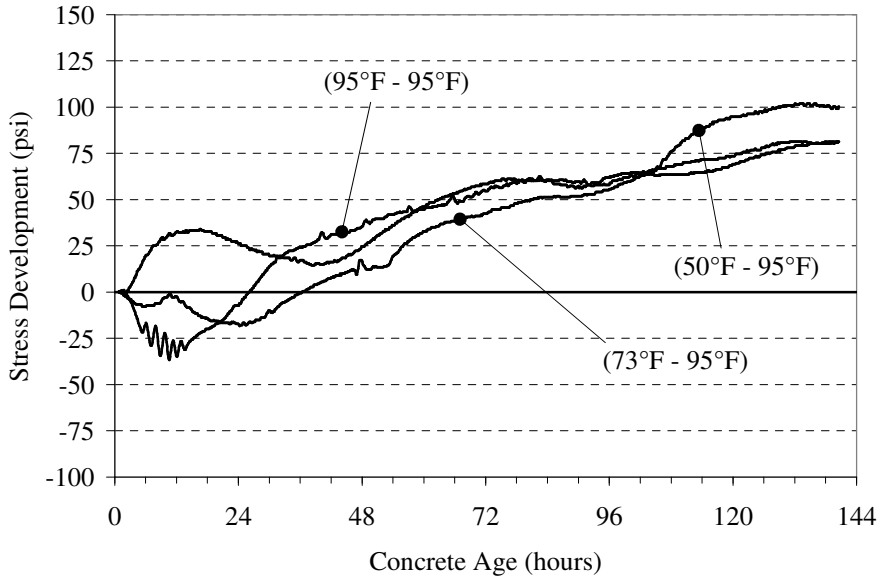


**Figure 5-8:** Effect of placement temperature on stress development under isothermal conditions of the TYPE3 mixture

As found for the portland cement only mixtures, variations of the placement temperature do not affect the magnitude of autogenous shrinkage stresses of the GGBF slag mixtures as shown in Figures 5-9 and 5-10. However, the magnitude of autogenous shrinkage was reduced when GGBF slag was used as a replacement for cement. The effect of supplementary cementing materials as they pertain to autogenous shrinkage will be discussed further in Section 5.4.

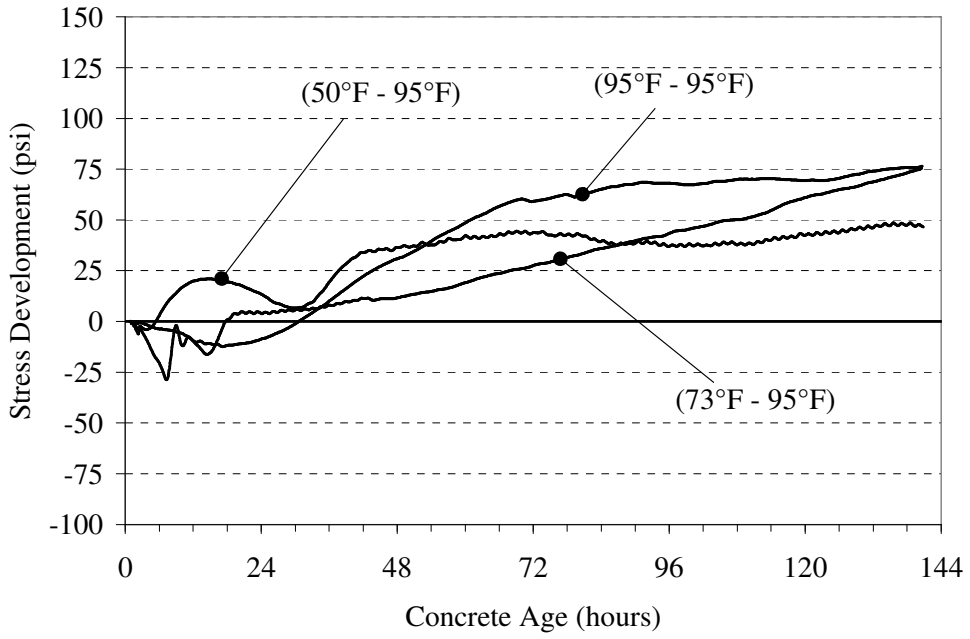


**Figure 5-9:** Effect of placement temperature on stress development under isothermal conditions of the 30SG mixture

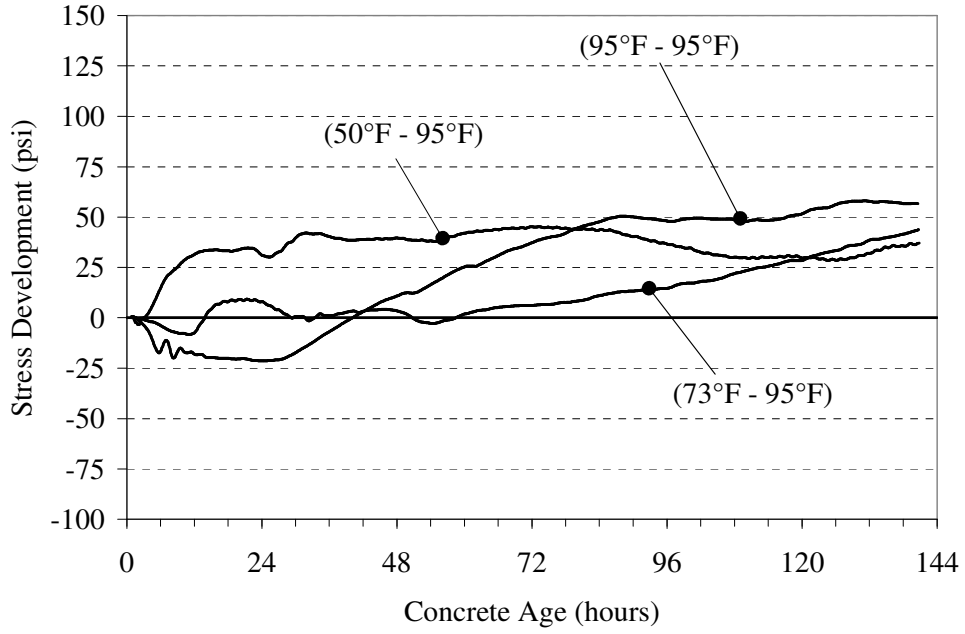


**Figure 5-10:** Effect of placement temperature on stress development under isothermal conditions of the 50SG mixture

## 5.2 EFFECTS OF SEASONAL TEMPERATURE CONDITIONS

The effect of ambient temperature on the cracking tendency of concrete is evaluated using the following mixtures: CTRL, 30SG, 50SG, WC38, and TYPE3. These five mixtures were placed at 50°F, 73°F, and 95°F and simulated using an ambient temperature of 50°F, 73°F, and 95°F surrounding the 1.0 meter thick wall specimen. These temperatures were chosen to represent typical seasonal conditions such as winter, spring/fall, and summer. The mechanical properties, temperature development, and stress development of these mixtures can be found in Sections 4.2 and 4.3.

### 5.2.1 CRACKING SENSITIVITY

The seasonal temperature condition surrounding a concrete element affects the rate of hydration. As mentioned previously, elevated temperatures amplify the rate of temperature rise as shown in Figures 4-12, 4-14, 4-15, 4-17, and 4-18.

In addition, the rate of development of the modulus of elasticity rises with the increase in seasonal temperature conditions as shown in Figures 4-3, 4-5, 4-6, 4-8, and 4-9. The 30SG and TYPE3 mixtures do not follow this pattern. In the 30SG and TYPE3 mixtures, the stiffness of the 95°F-95°F seasonal temperature condition was lower than the 73°F-73°F.

#### 5.2.1.1 Portland Cement Only Systems

As the seasonal temperature reduced, the cracking temperatures decreased as shown in Figure 5-11. Unlike the effects of placement temperature shown in Figure 5-1, there is a more pronounced trend as the cracking temperature continues downward from the 73°F to the 50°F condition. When compared to the 95°F – 95°F condition, the cracking temperatures of all the cement only mixtures were reduced by approximately 20°F to 30°F by the changes in seasonal temperature conditions to 73°F. Under seasonal temperature conditions of 50°F, the cracking temperature was reduced by 45°F to 65°F in all portland cement only mixtures. The seasonal temperature conditions thus had a substantial impact on the cracking tendency of the cement only mixtures.

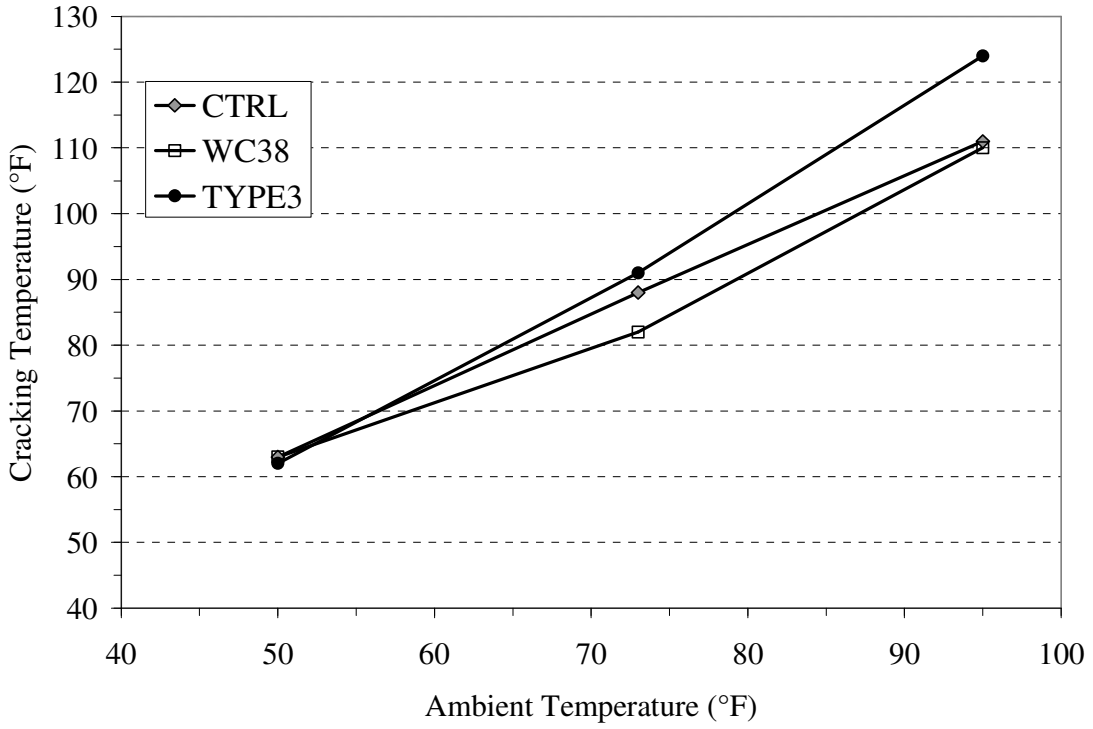


**Figure 5-11:** Effect of seasonal temperature conditions on portland cement only systems

Although the cracking temperature was reduced, the seasonal temperature changes had only small impacts on the slopes of the stress-to-strength ratio plots as shown in Figure 5-12. With the exception of the TYPE3 mixture, the similar values of stiffness reduced the development of compressive stresses, which caused the concrete specimen to go into tension at approximately the same time as the hot seasonal temperature condition.

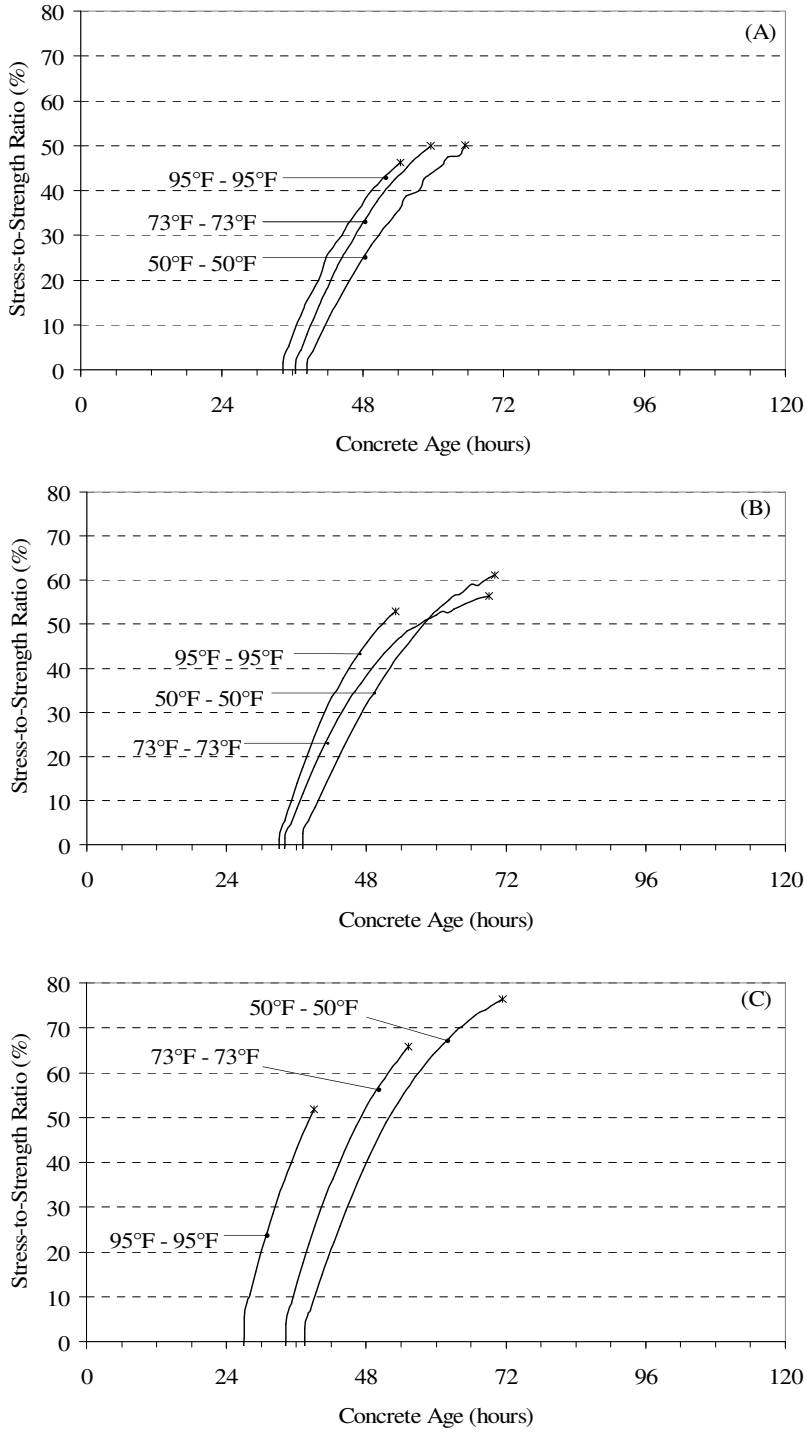


**Figure 5-12:** Effect of seasonal temperature conditions on the stress-to-strength ratio of the (A) CTRL mixture, (B) WC38 mixture, and (C) TYPE3 mixture

#### 5.2.1.2 GGBF Slag Mixtures

Seasonal temperature conditions had a substantial impact on the cracking tendency of the GGBF slag mixtures. Unlike the effects of placement temperature, the reduction in cracking temperature is much more pronounced for seasonal temperature effects as the dosage of GGBF slag is increased as shown in Figure 5-13. However, under hot seasonal temperature conditions, the use of GGBF slag did not reduce the cracking temperature. Due to the temperature sensitivity of the GGBF slag, the hot seasonal temperature condition gained stiffness much faster than the other seasonal conditions, which caused the concrete specimen to go into tension earlier.

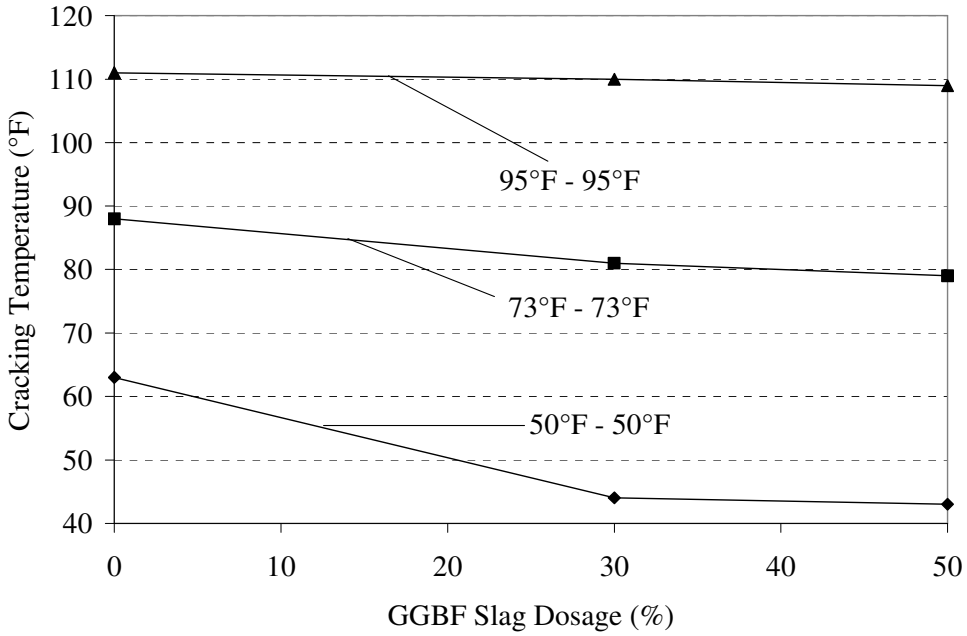


**Figure 5-13:** Effect of GGBF slag dosage on cracking temperature under various seasonal temperature conditions

Similar to the portland cement only mixtures, seasonal temperature conditions reduced the cracking tendency of the GGBF slag mixtures as shown in Figure 5-14. However, the reduction of cracking temperature for the GGBF slag mixtures is much greater at cold seasonal temperature conditions. Unlike the portland cement only mixtures, the cracking temperature of the GGBF slag and CTRL mixtures were approximately the same under hot seasonal temperature conditions, which is due to the high temperature sensitivity of the GGBF slag mixtures.

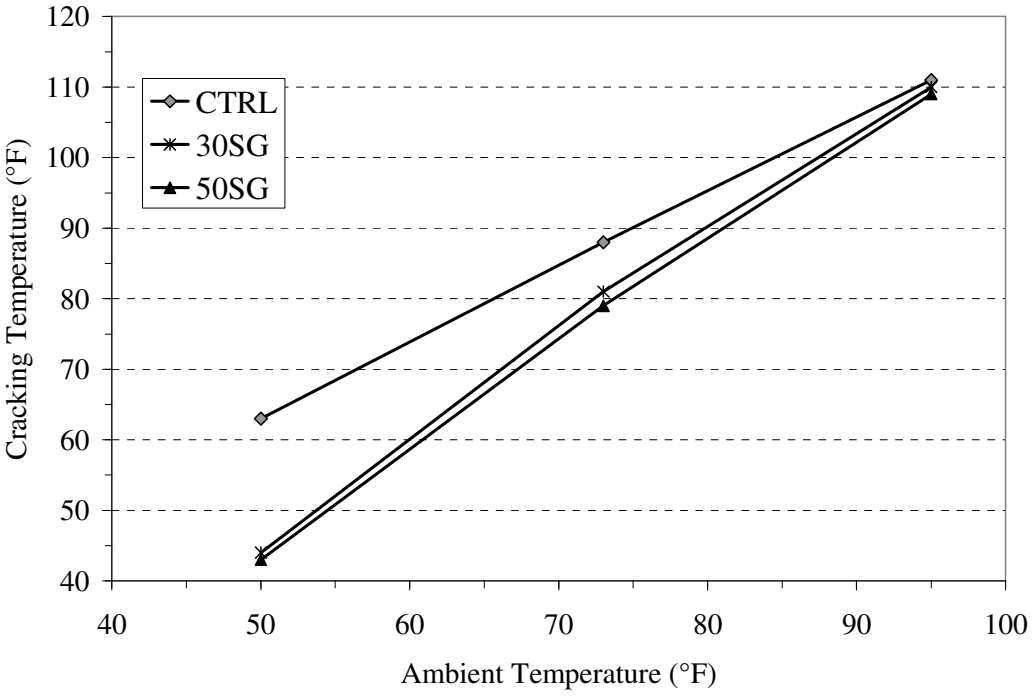


**Figure 5-14:** Effect of seasonal temperature conditions on GGBF slag mixtures

As discussed previously, the lower seasonal temperature conditions reduce the maximum temperature rise. As a result, the zero stress temperature is shifted down creating fewer tensile stresses relative to the tensile strength prior to 96 hours in the GGBF slag cold seasonal temperature conditions as shown in Figure 5-15. It is clear from Figure 5-15 that the use of GGBF slag mixtures greatly improves the cracking tendency under the 50°F and 73°F seasonal conditions.

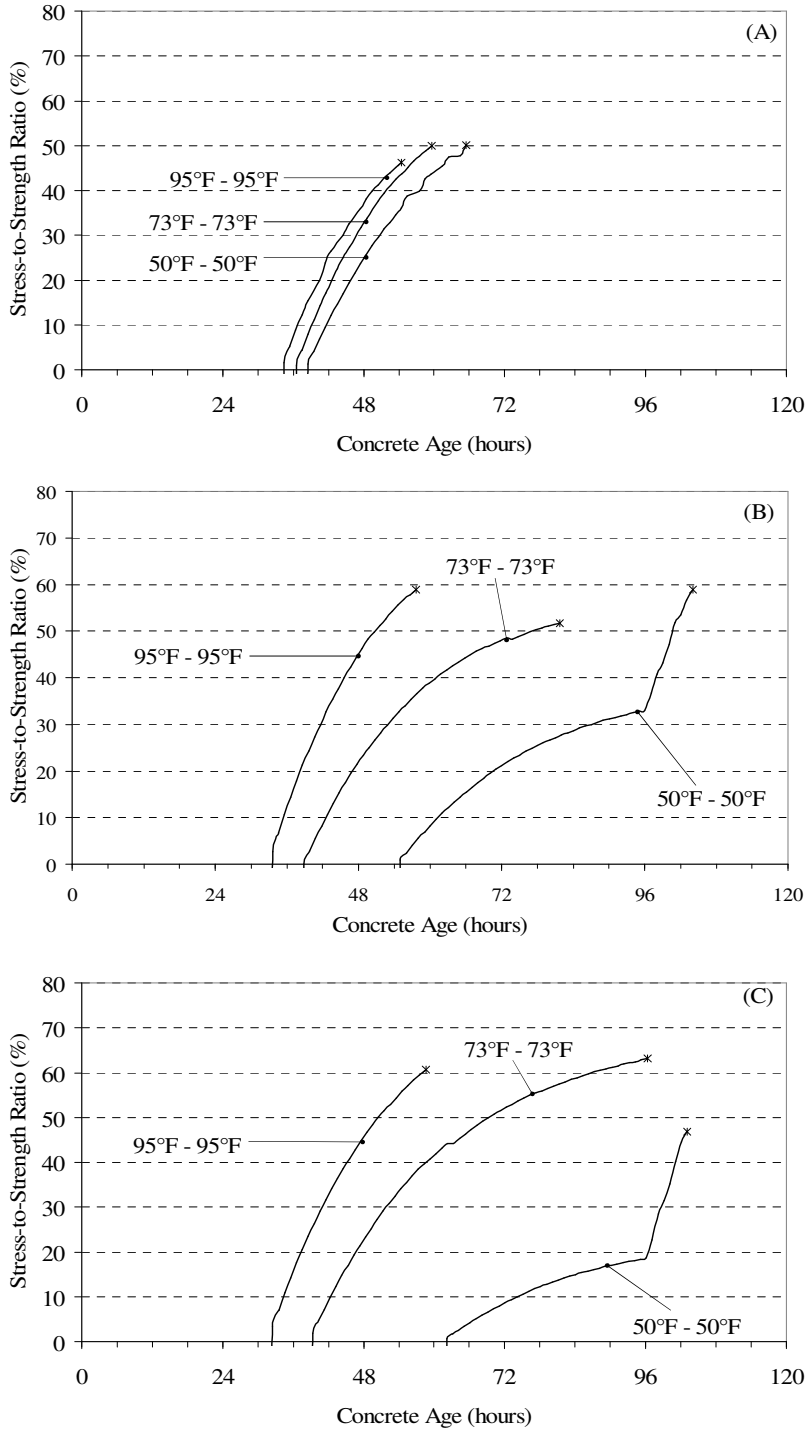


**Figure 5-15:** Effect of seasonal temperature conditions on the stress-to-strength ratio of the (A) CTRL mixture, (B) 30SG mixture, and (C) 50SG mixture

### 5.2.2 AUTOGENOUS SHRINKAGE

Due to the nature of the experimental laboratory testing program, the isothermal temperature conditions are selected based on the fresh concrete placement temperature. As a result, the trends discussed in Section 5.1.2 are applicable to this section. The reduction in seasonal temperature conditions did not greatly affect the magnitude of autogenous shrinkage stresses for the cement only mixtures as shown in Figures 5-16, 5-17, and 5-18.

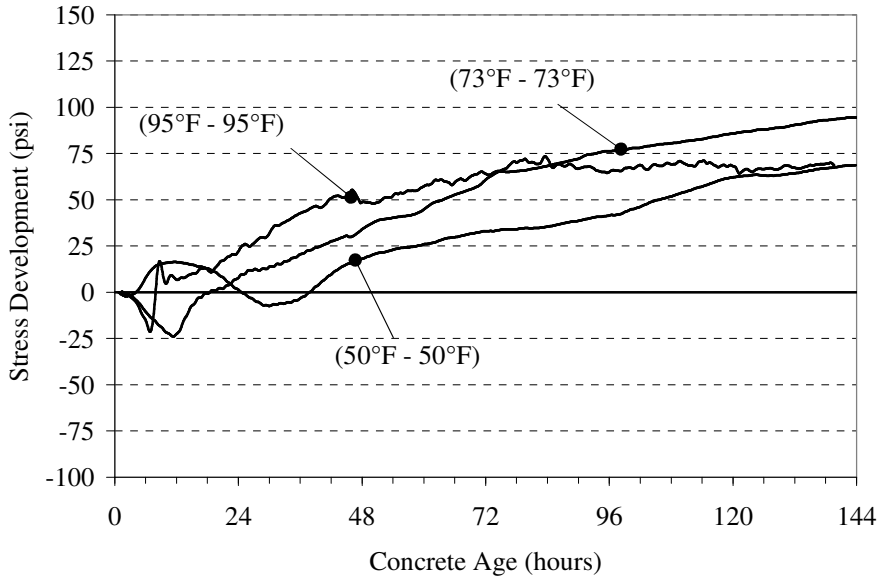


**Figure 5-16:** Effect of seasonal temperature conditions on stress development under isothermal conditions of the CTRL mixture

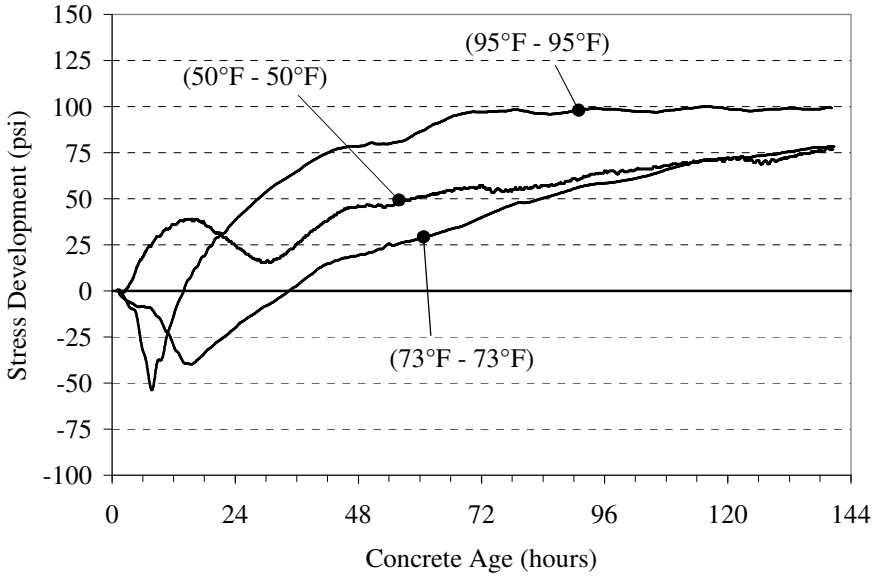


**Figure 5-17:** Effect of seasonal temperature conditions on stress development under isothermal conditions of the WC38 mixture

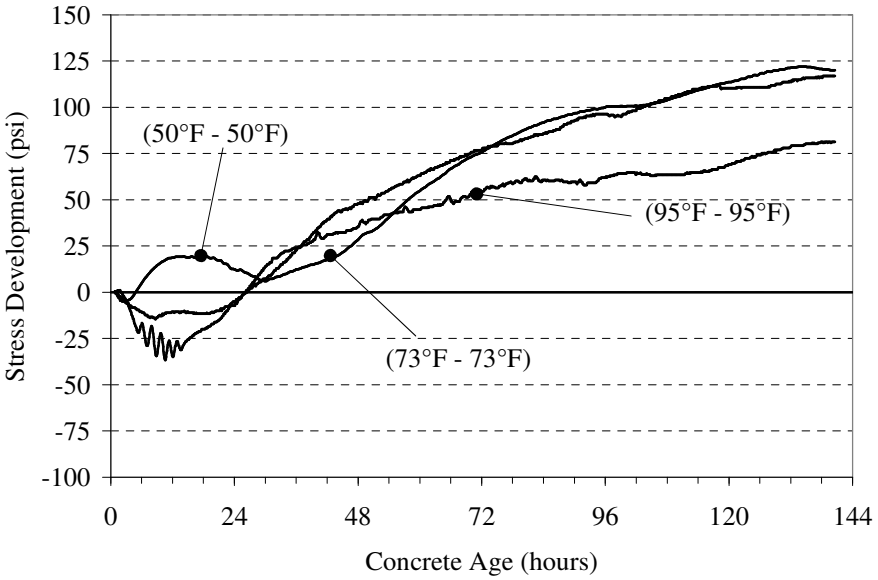


**Figure 5-18:** Effect of seasonal temperature conditions on stress development under isothermal conditions of the TYPE3 mixture

As mentioned previously, the magnitude of autogenous shrinkage stresses is not affected by variations in seasonal temperature conditions. However, the replacement of cement with GGBF slag reduces the magnitude of stresses as shown in Figures 5-16, 5-19, and 5-20. Further discussion of the effect of supplementary cementing materials is provided in Section 5.4.

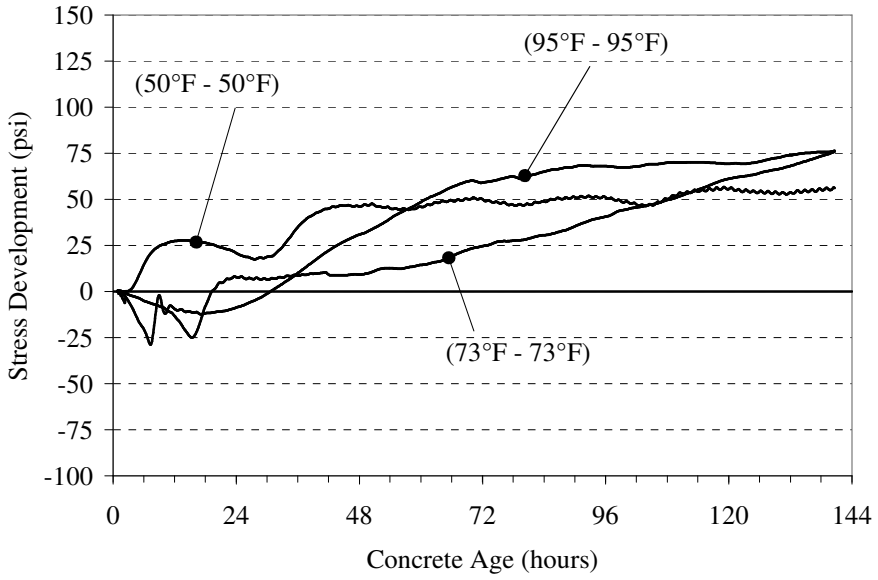


**Figure 5-19:** Effect of seasonal temperature conditions on stress development under isothermal conditions of the 30SG mixture

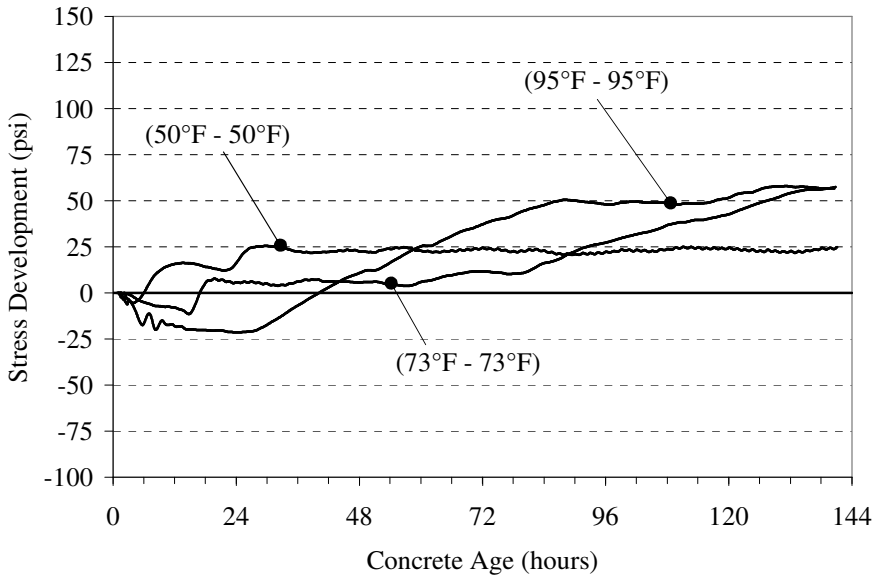


**Figure 5-20:** Effect of seasonal temperature conditions on stress development under isothermal conditions of the 50SG mixture

## 5.3 EFFECT OF CEMENT TYPE

The effect of cement type on the cracking tendency of concrete is evaluated using the following mixtures: CTRL and TYPE3. These mixtures were placed at 50°F, 73°F, and 95°F and simulated using an ambient temperature of 50°F, 73°F, and 95°F surrounding the outside of the 1.0 meter thick wall. The mechanical properties, temperature development, and stress development of these mixtures can be found in Sections 4.2 and 4.3.

### 5.3.1 CRACKING SENSITIVITY

As mentioned previously in Section 5.1.1, high cement contents and high early-age strength cements increase temperature development which leads to relatively high cracking tendencies (Breitenbücher and Mangold 1994). Increases in temperature are a result of high tricalcium aluminate ($C_3A$) contents and increased fineness of high early-age strength cements. $C_3A$ produces more heat when it reacts with water as compared to the remaining three Bogue compounds as shown in Table 2-1. The Type III cement chosen for this project had a lower $C_3A$ content than the Type I cement as shown in Table 3-3. As a result, maximum temperatures achieved by the TYPE 3 mixtures differed only slightly from that of the CTRL mixture as shown in Figures 4-12 and 4-18. The small difference in temperature can be attributed to the increase in fineness of the Type III cement.

Due to the small temperature differences and relatively similar mechanical properties, the TYPE3 mixture did not reduce the cracking temperature as shown in Figure 5-21. The CTRL mixture was found to be more effective in reducing the cracking temperature at the 73°F – 95°F and 95°F – 95°F conditions, which corresponds to the findings of Breitenbücher and Mangold (1994) and Springenschmid and Breitenbücher (1998).

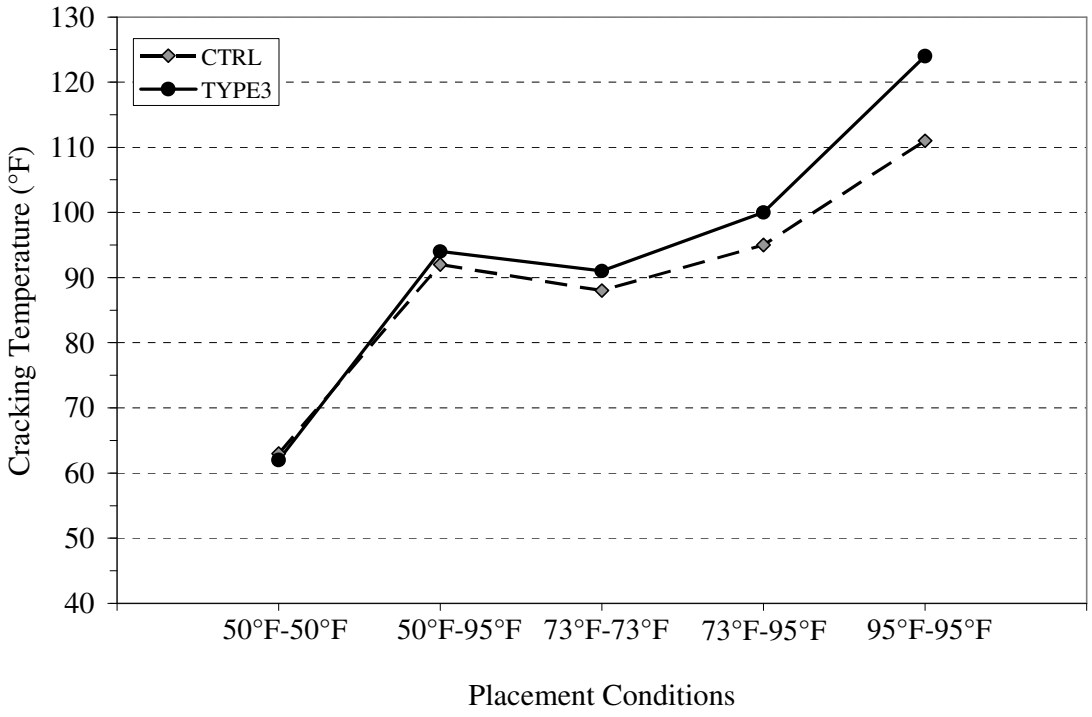


**Figure 5-21:** Effect of cement type on cracking temperature

Due to the reduction of tensile strength in the TYPE3 mixtures excluding the 50°F – 95°F condition, the time of cracking is slightly lower than the CTRL mixtures for all temperature conditions. At the 95°F – 95°F condition, the TYPE3 mixture cracked considerably earlier than the CTRL mixture as shown in Figure 5-22. Due to the increased rate of hydration associated with a higher fineness, the TYPE3 mixture at 95°F – 95°F did not develop sufficient compressive stresses before the temperature of the specimen began to fall. With fewer compressive stresses, the TYPE3 mixture experienced tensile stresses approximately 7 hours before the CTRL mixture.

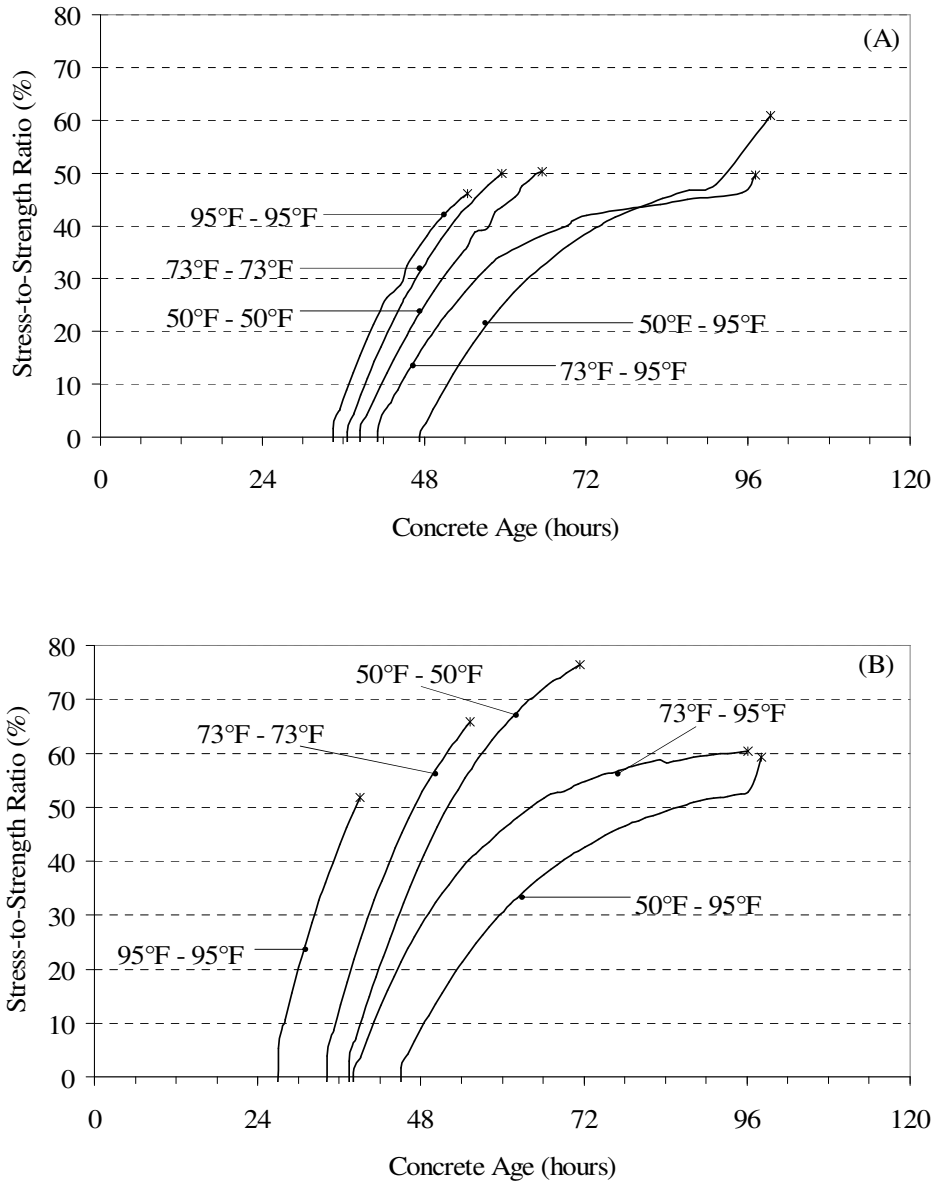


**Figure 5-22:** Effect of cement type on the stress-to-strength ratio of the (A) CTRL mixture and (B) TYPE3 mixture

### 5.3.2 AUTOGENOUS SHRINKAGE

Tazawa and Miyazawa (1997) state the magnitude of autogenous shrinkage stresses increases with increasing amounts of $C_3A$ and $C_4AF$ content. According to Holt (2001), autogenous shrinkage is caused by chemical shrinkage which is a function of the volume of Bogue compounds. However, this phenomenon is not clearly indicated by the data shown in Figure 5-23 and 5-24. The Type I cement had a larger percentage of $C_3A$ while the percentage of $C_4AF$ was lower than the Type III cement. Nevertheless, variations in autogenous shrinkage stresses due to temperature variations are unsystematic as previously mentioned.

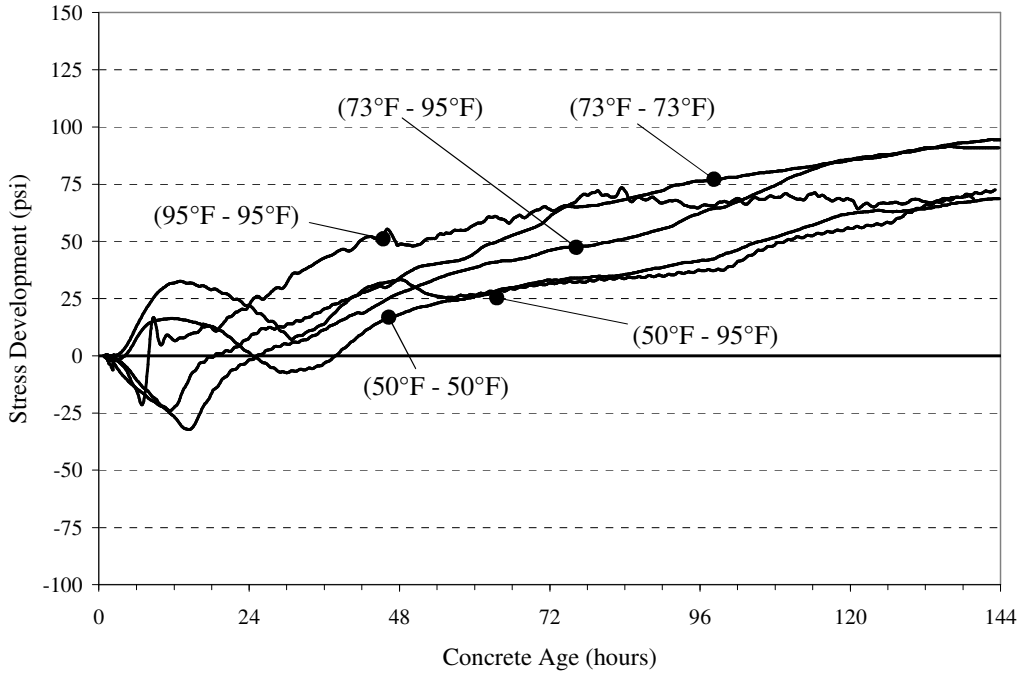


**Figure 5-23:** Effect of cement type on stress development under isothermal conditions of the CTRL mixture

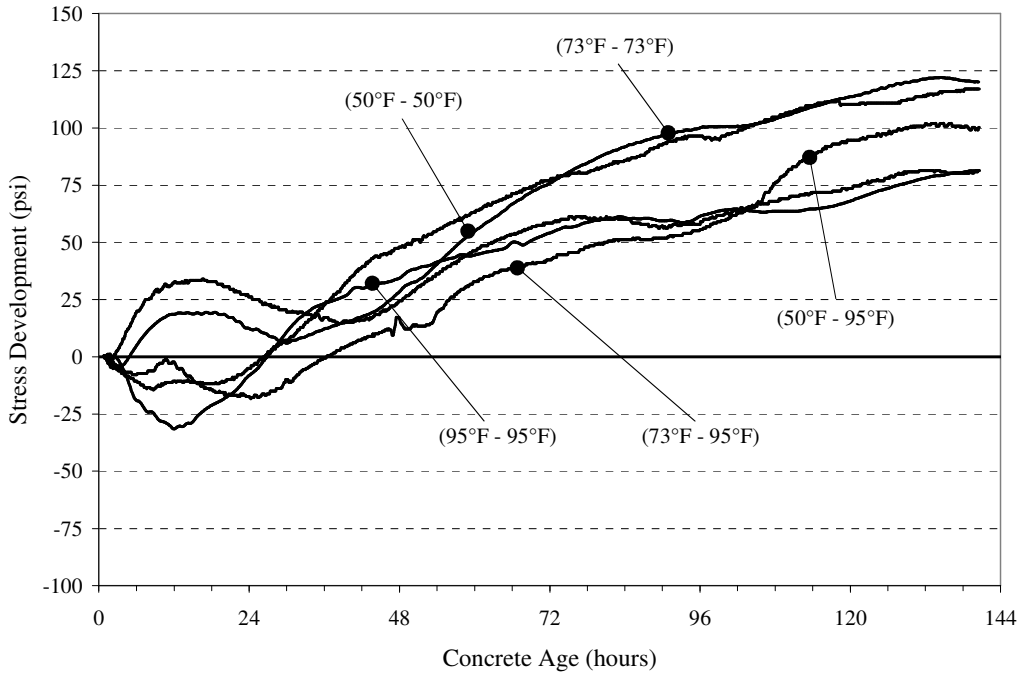


**Figure 5-24:** Effect of cement type on stress development under isothermal conditions of the TYPE3 mixture

## 5.4 EFFECT OF SUPPLEMENTARY CEMENTING MATERIALS

The effect of supplementary cementing materials on the cracking tendency of concrete is evaluated using the following mixtures: CTRL, 30SG, 50SG, 20C, and 30C. These five mixtures were placed at 73°F and simulated using an ambient temperature surrounding the 1.0 meter thick wall of 73°F. The mechanical properties, temperature development, and stress development of these mixtures can be found in Sections 4.2 and 4.3.

### 5.4.1 CRACKING SENSITIVITY

Springenschmid and Breitenbücher (1998) stated that it is current practice to reduce the cement content as much as possible in order to reduce heat development. Supplementary cementing materials (SCMs) can be used to reduce the heat generation associated with hydration as discussed in Section 2.1.3.

If the quantity of cement is reduced, then the heat generated during hydration will be reduced as shown in Figure 5-25.Under the 73°F-73°F temperature conditions, the maximum temperature reached by the control mixture is 132°F, by the 30% GGBF slag mixture is 117°F, by the 50% GGBF slag mixture is 110°F, by the 30% Class C fly ash mixture is 110°F, and by the 20% is 119°F. These substantial reductions are caused by the reduction of cement in a concrete mixture.

Restrained stress development is shown in Figure 5-26. The 30% and 50% GGBF slag and 30% Class C fly ash mixtures were very effective in mitigating cracking. The use of these three mixtures increased the time of cracking by more than 30 percent; however, the 20% Class C fly ash mixture was not effective in reducing the cracking tendency of the concrete. Although the 30% GGBF slag, 50% GGBF slag, and 30% Class C fly ash mixtures increased the time of cracking substantially, the change in temperature to cause cracking continued to be approximately the same as the control mixture as shown in Table 4-3.

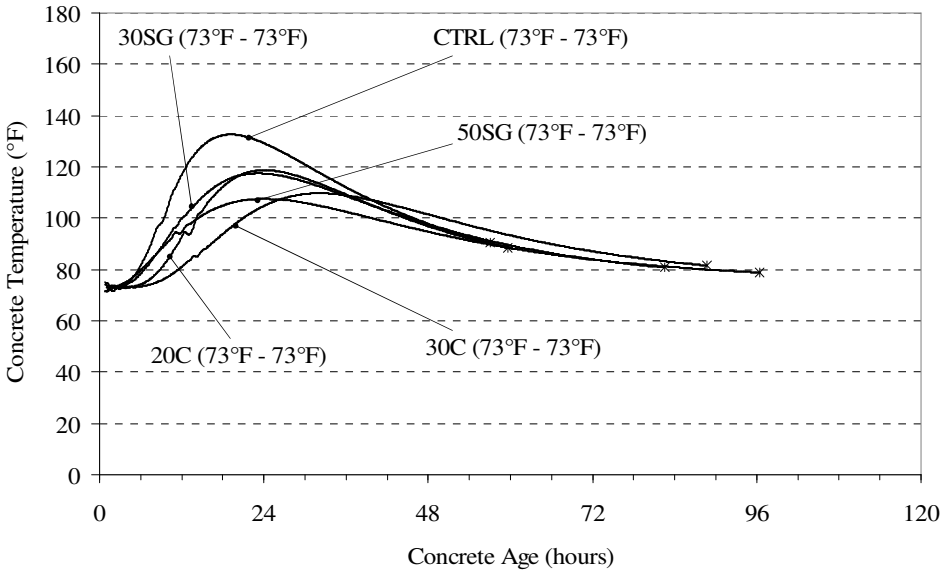


**Figure 5-25:** Effect of SCMs on temperature development at 73°F-73°F temperature conditions

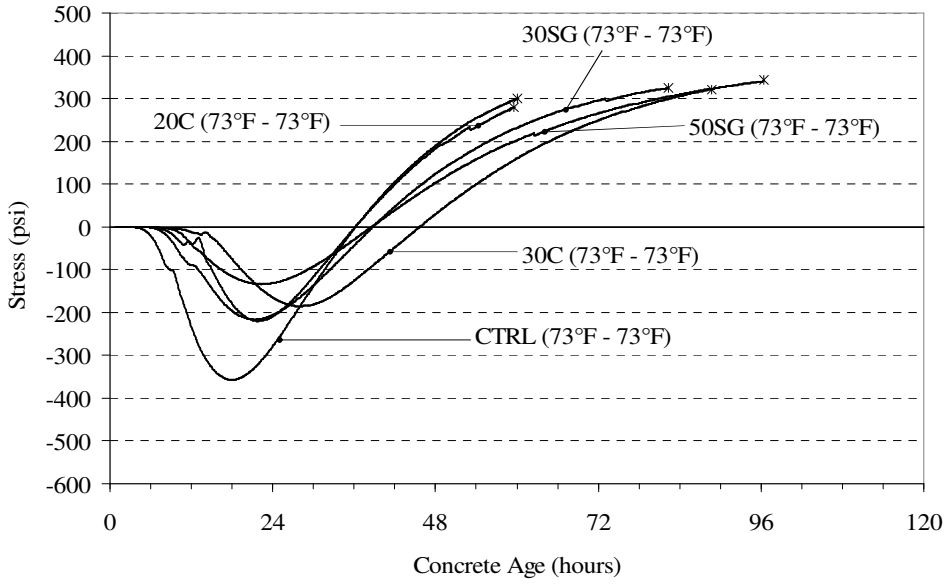


**Figure 5-26:** Effect of SCMs on stress development at 73°F-73°F temperature conditions

Under the 50°F-50°F and 95°F-95°F temperature conditions, the CTRL, 30SG, and 50SG mixtures were used to evaluate the effects of SCMs on the cracking tendencies of concrete mixtures. As shown in Figure 5-27, the GGBF slag mixtures reduced the magnitude and rate of temperature development under the 50°F-50°F conditions. As a result, the stresses of the GGBF slag mixtures were substantially lower than the CTRL mixture at the time it cracked as shown in Figure 5-28.

The GGBF slag mixtures reduced the temperature development under the 95°F-95°F temperature conditions as shown in Figure 5-29. However, the cracking times of all three mixtures were similar as shown in Figure 5-30. As a result, the GGBF slag reduces the cracking tendency when it is placed and exposed to lower temperature conditions, i.e. 50°F-50°F and 73°F-73°F, than under higher temperature conditions.

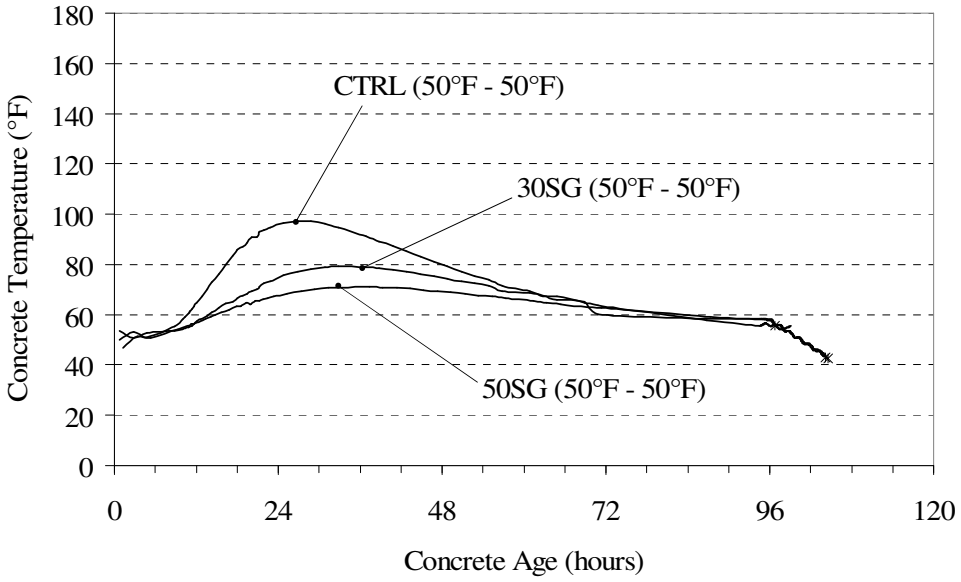


**Figure 5-27:** Effect of SCMs on temperature development at 50°F-50°F temperature conditions

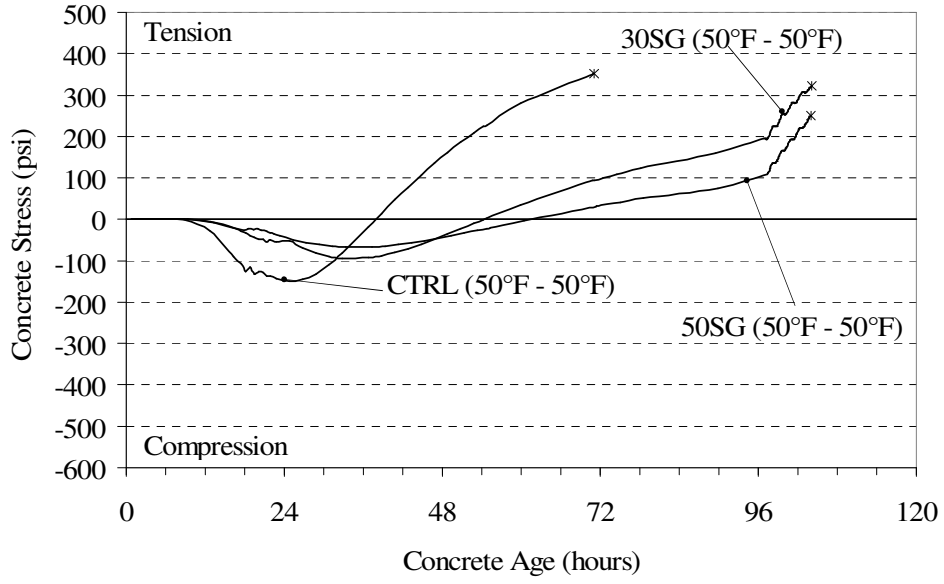


**Figure 5-28:** Effect of SCMs on stress development at 50°F-50°F temperature conditions

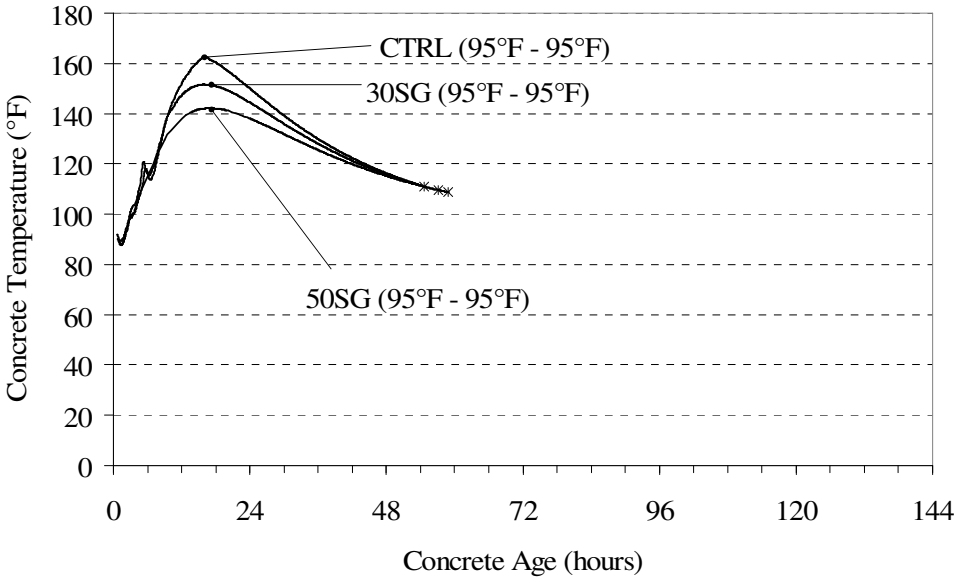


**Figure 5-29:** Effect of SCMs on temperature development at 95°F-95°F temperature conditions

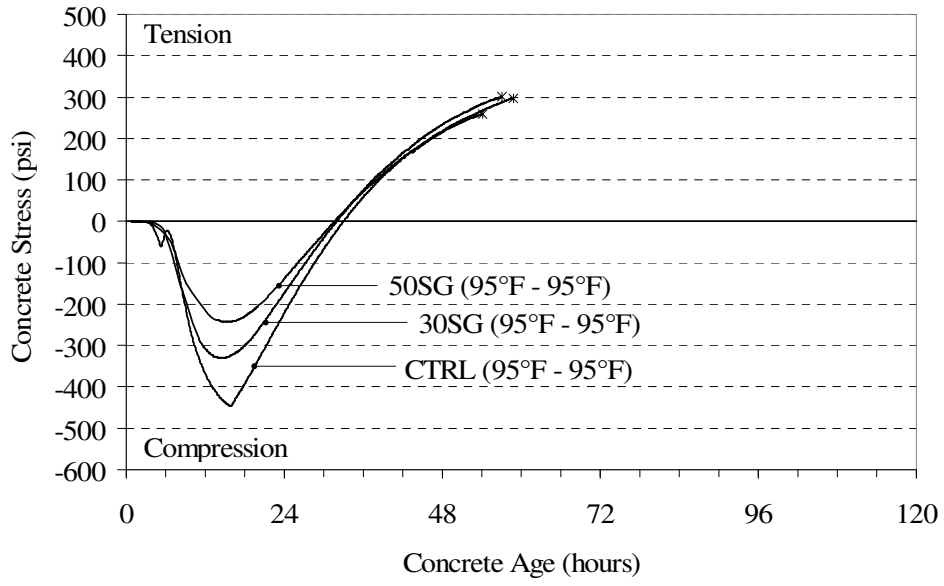


**Figure 5-30:** Effect of SCMs on stress development at 95°F-95°F temperature conditions

Due to the reduced development of heat, lower temperature changes are required in order for the concrete specimen to reach equilibrium with the ambient conditions. This results in prolonged compressive stresses and it increases the zero stress time which decreases the zero stress temperature except for the GGBF slag mixtures at 95°F-95°F. As a result, the cracking temperature of the concrete mixtures is lowered due to replacement of cement with SCMs under 50°F-50°F and 73°F-73°F temperature conditions as shown in Figure 5-31. The 20C mixture actually only provides a minimal improvement relative to the CTRL mixture.

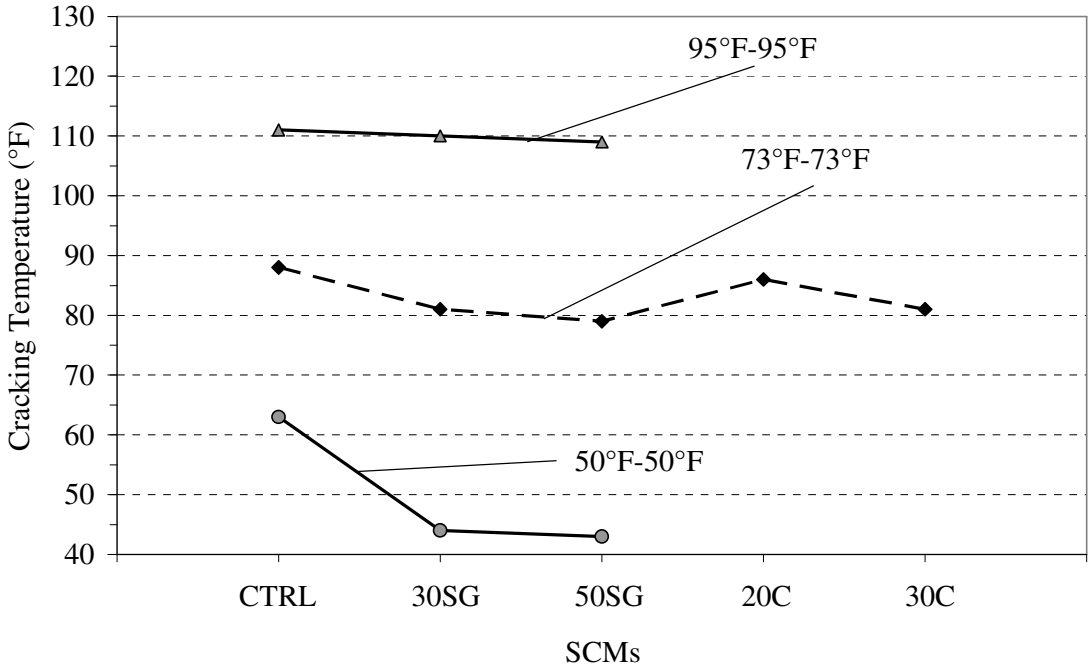


**Figure 5-31:** Effect of SCMs on cracking temperature

Springenschmid and Breitenbucher (1998) found fly ash to reduce the cracking temperature due to an increase in tensile strength of the concrete due to the pozzolanic reaction. This should improve the cracking tendency of the concrete; however, Figure 5-32 shows the replacement of cement with 20% Class C fly ash did not improve the cracking tendency.

As mentioned previously, GGBF slag lead to reduced temperature rises and reduced tensile stresses (Breitenbucher and Mangold 1994). These findings are also valid for the GGBF slag mixtures evaluated in this study. It is important to note that the stress-to-strength ratio of the GGBF slag mixtures was less at the time that the CTRL mixture cracked except for the 95°F-95°F temperature condition as shown in Figure 5-32. Therefore, GGBF slag decreased the cracking tendency of the concrete unless used under summer temperature conditions.

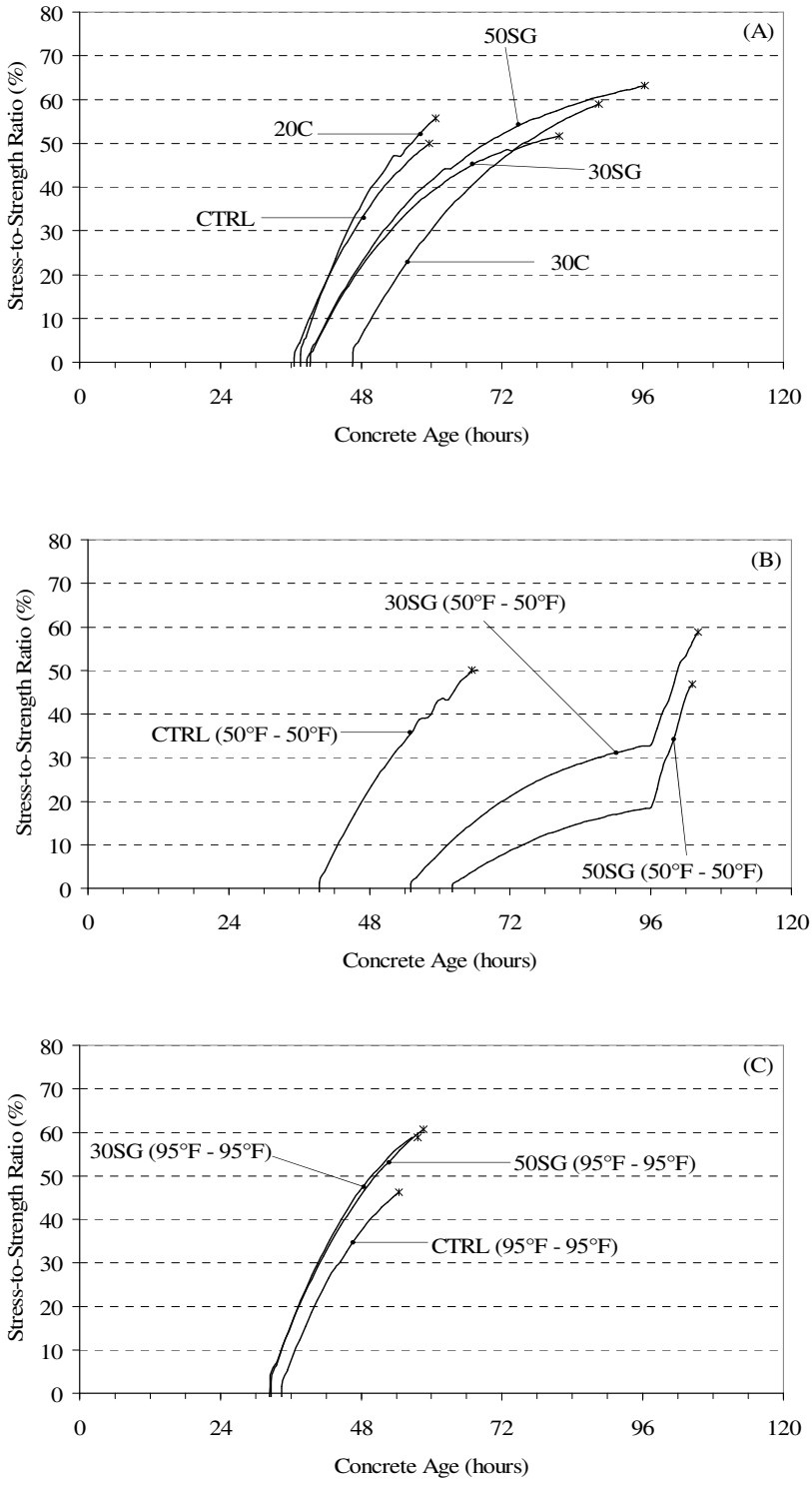


**Figure 5-32:** Effect of SCMs on the stress-to-strength ratio (A) 73°F – 73°F, (B) 50°F-50°F, and (C) 95°F-95°F

### 5.4.2 AUTOGENOUS SHRINKAGE

The use of SCMs reduces the quantity of portland cement in a concrete mixture which reduces the volume change associated with chemical shrinkage. Decreasing chemical shrinkage reduces the magnitude of autogenous shrinkage stresses as shown in Figure 5-33.

Tazawa and Miyazawa (1997) found autogenous shrinkage to increase when GGBF slag with high fineness is used. This phenomenon could be related to the denser pore structure associated with the use of GGBF slag. These smaller pores may induce higher capillary tension forces during self-desiccation which would lead to higher autogenous shrinkage stresses (Lura et al. 2001). But as Figure 5-27 clearly shows, the replacement of cement with SCMs reduces the magnitude of autogenous shrinkage stresses. The 50SG mixture is the most effective means of reducing autogenous shrinkage stresses.

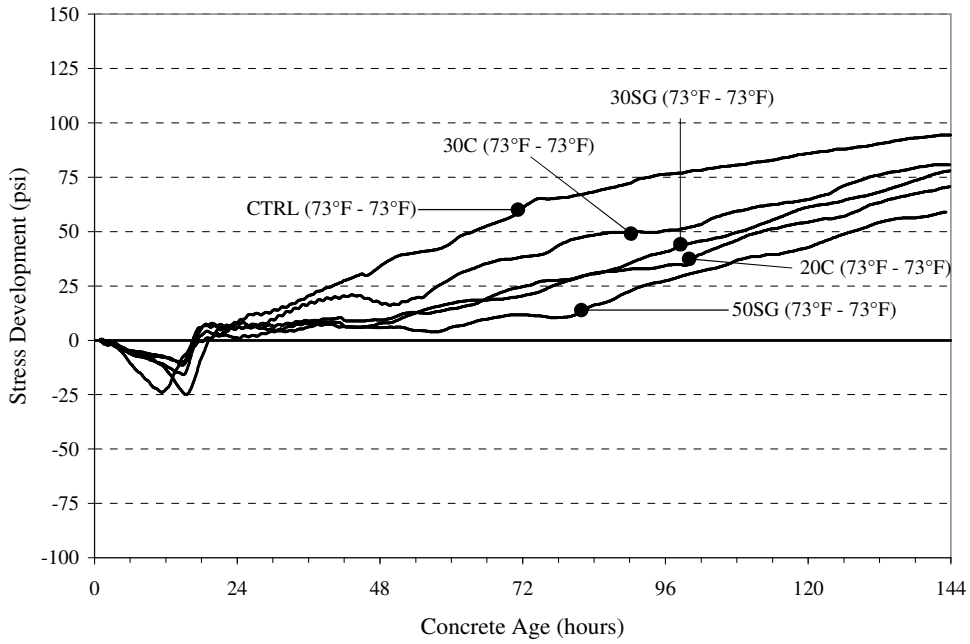


**Figure 5-33:** Effect of SCMs on stress development under 73°F isothermal conditions

## 5.5 EFFECT OF TERNARY MIXTURES

The effect of air entrainment on the cracking tendency of concrete is evaluated using the following mixtures: CTRL, 25C6SF, 25F6SF, and 20F30SG. These mixtures were placed at 73°F and simulated using an ambient temperature of 73°F surrounding the 1.0 meter thick wall. The temperature development, stress development, and mechanical properties of these mixtures can be found in Sections 4.3.5 and 4.2.2.5.

### 5.5.1 CRACKING SENSITIVITY

As discussed in Section 5.4, SCMs reduce the rate and magnitude of temperature development. As a result, the tensile strength development is reduced; however, the stiffness of the ternary mixtures is similar to the CTRL mixture after 48 hours. Due to the low generation of heat and similar stiffness, the ternary mixtures do not produce as much compressive stresses as the CTRL mixture. As a result of the low temperature development, the ternary mixtures liberate less heat before reaching equilibrium with the ambient conditions than the CTRL mixture. This difference in temperature loss increases the zero stress time of the ternary mixtures which reduces the zero stress temperature. Reduction in the zero stress temperature decreases the cracking temperature.

As shown in Figure 5-34, the ternary mixtures reduce the cracking temperature. It may be concluded that the cracking temperature may be reduced by increasing the amount of replacement of cement. It is also noted that the 25F6SF mixture reduced the cracking temperature further than the 25C6SF mixture.

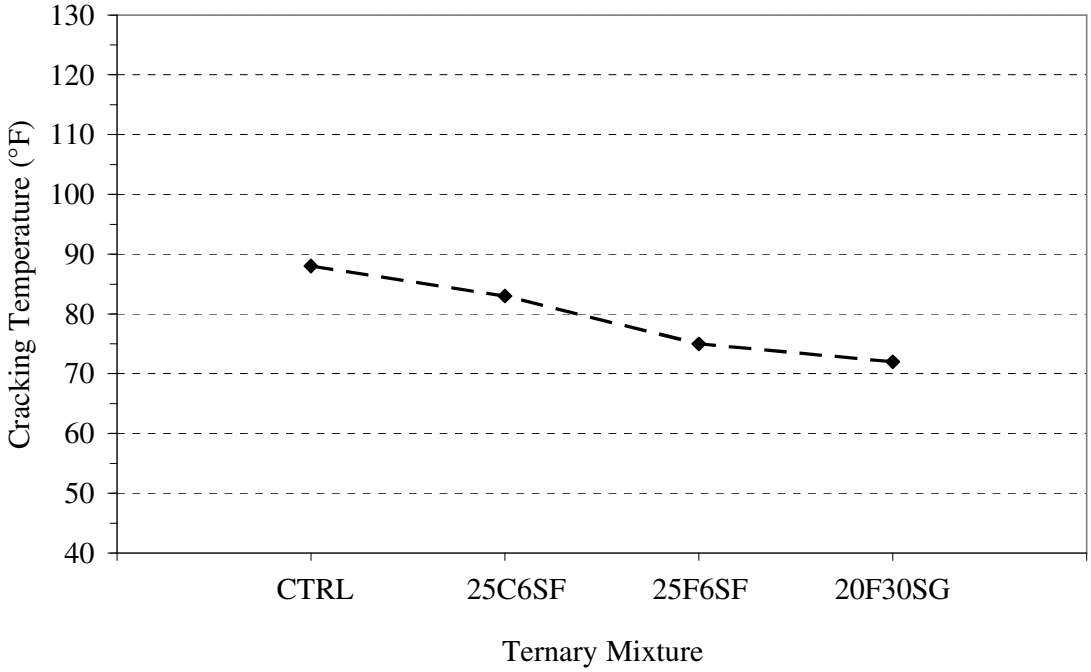


**Figure 5-34:** Effect of ternary mixtures on cracking temperature at 73°F-73°F temperature condition

As mentioned previously, ternary blend mixtures lead to reduced temperature increase. As a result, the development of tensile stresses is delayed as compared to the CTRL mixture. The reduction in tensile stresses delays the time of cracking as shown in Figure 5-35.

It is important to note that the stress-to-strength ratio of the 25F6SF and 20F30SG mixtures was less at the time that the CTRL mixture cracked. Therefore, 25F6SF and 20F30SG mixtures decreased the cracking tendency of the concrete. The development of tensile strength for all ternary mixtures is reduced due to the slow rate of heat generation.

Therefore, the stress-to-strength ratio is much higher than the CTRL mixture at the time of cracking with the exception of the 20F30SG mixture.

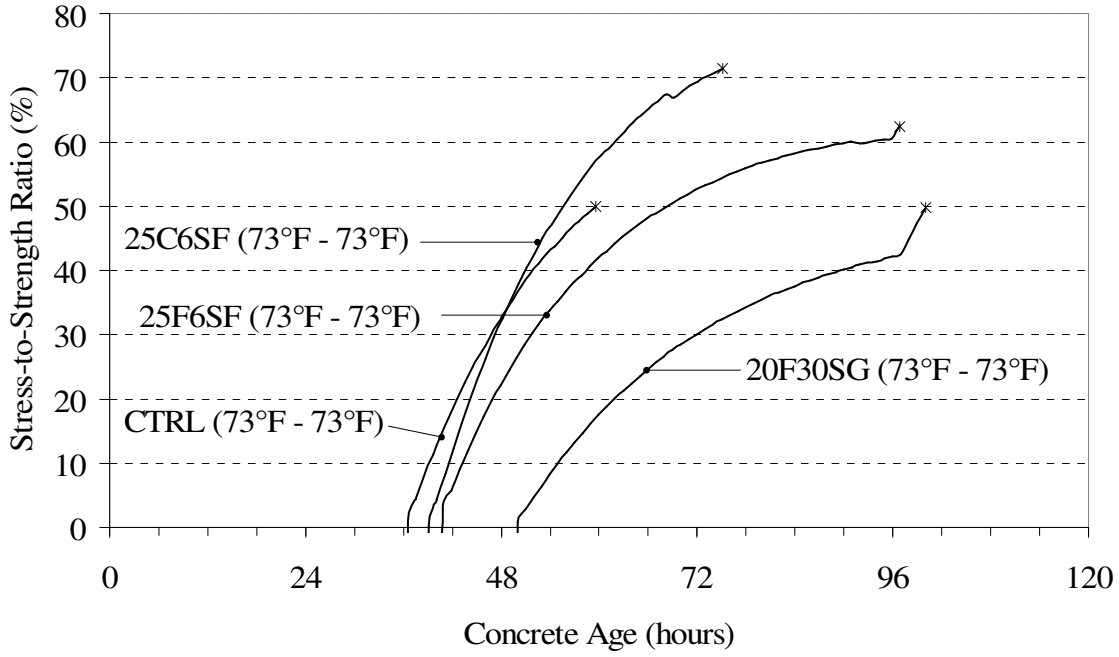


**Figure 5-35:** Effect of ternary mixtures on the stress-to-strength ratio at 73°F – 73°F temperature condition

### 5.5.2 AUTOGENOUS SHRINKAGE

As discussed in the previous section, SCMs produce denser pore structures in the hardened concrete. As a result, the magnitude of autogenous shrinkage stresses can be increased due to higher capillary tension. However, Figure 5-36 shows that SCMs reduce the magnitude of autogenous shrinkage. The 25F6SF and 20F30SG mixtures were found to be the most effective in reducing autogenous shrinkage.

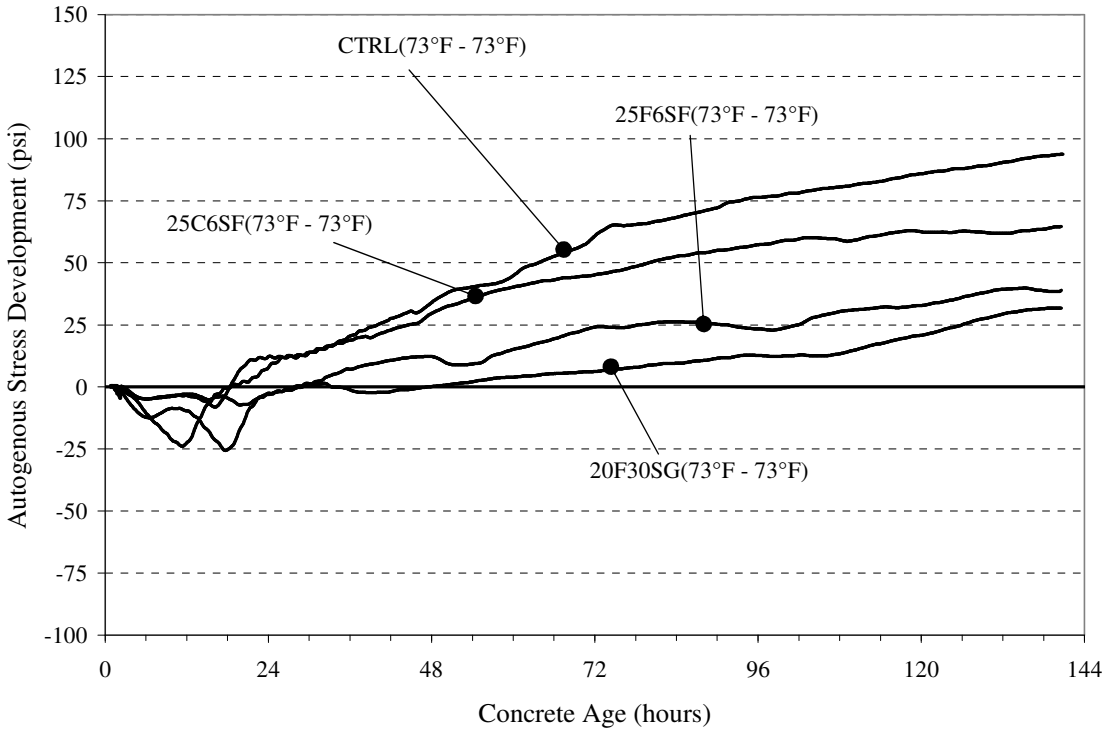


**Figure 5-36:** Effect of ternary mixtures on stress development under 73°F isothermal conditions

## 5.6 EFFECT OF AIR ENTRAINMENT

The effect of air entrainment on the cracking tendency of concrete is evaluated using the following mixtures: CTRL and AEA. These mixtures were placed at 73°F and simulated using an ambient temperature of 73°F surrounding the 1.0 meter thick wall. The temperature development, stress development, and mechanical properties of these mixtures can be found in Sections 4.3.8 and 4.2.2.8.

### 5.6.1 CRACKING SENSITIVITY

The addition of 1% air generally reduces the compressive strength by approximately 5% (Kosmatka et al. 2002). The compressive and tensile strength of the AEA mixture is much lower than the CTRL mixture at all ages; however, the modulus of elasticity for the AEA mixture is only slightly reduced at 7 days. In addition, the temperature development of the AEA mixture is slightly less than the CTRL mixture. This reduction is due to a lower specific heat which is a result of lower density. As a result, the zero stress temperature and cracking temperature of the AEA mixture is exactly the same as the CTRL mixture; however, the AEA mixture cracked prior to the CTRL mixture. Due to the lower tensile strength of the AEA mixture, the stress-to-strength ratio was much higher than the CTRL mixture as shown in Figure 5-37. The reduction in stress-to-strength ratio increases the cracking tendency of the AEA mixture.

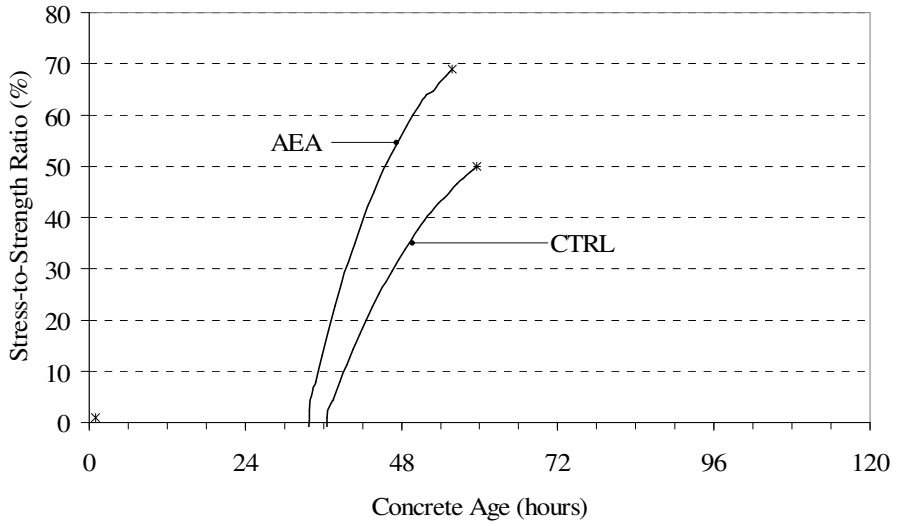


**Figure 5-37:** Effect of air entrainment on the stress-to-strength ratio at 73°F – 73°F

### 5.6.2 AUTOGENOUS SHRINKAGE

Hammer and Fossa (2006) found that air-entrainment alters the pore water pressure which subsequently decreases autogenous shrinkage. The air entrained mixture has significantly more air than the control mixture as shown in Table 4-1. The air entraining admixture also produces a smaller, well-distributed air-void system in the concrete. Improving the air-void system reduces the capillary forces which reduces autogenous shrinkage as shown in Figure 5-38.

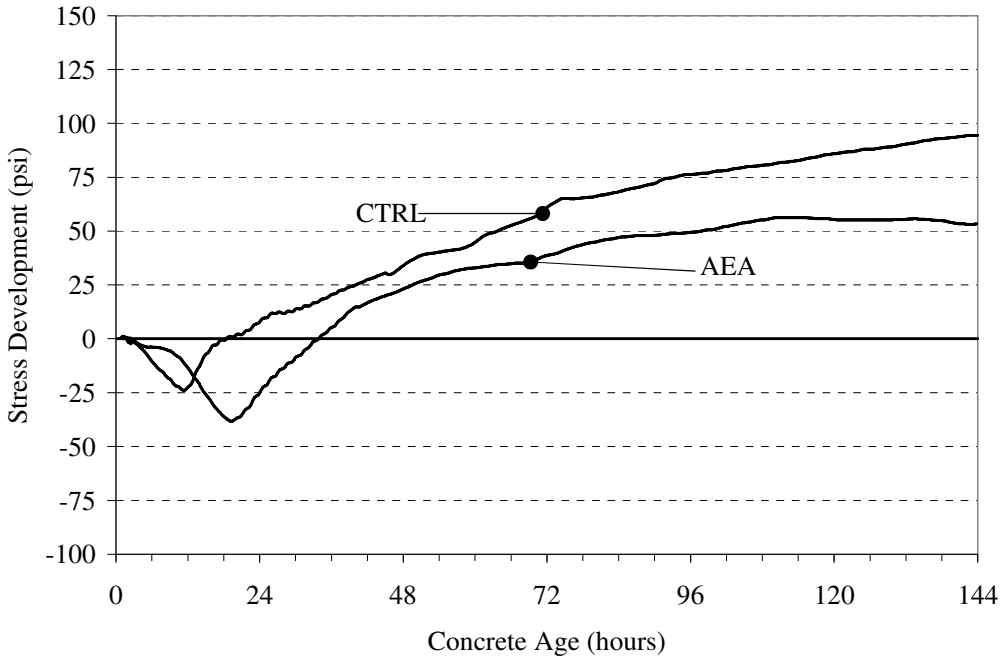


**Figure 5-38:** Effect of air entrainment on stress development under 73°F isothermal conditions

## 5.7 EFFECT OF WATER-TO-CEMENT RATIO

The effect of water-to-cement ratio (w/cm) on the cracking tendency of concrete is evaluated using the following mixtures: CTRL, WC32, WC38, WC48, and WC53. These five mixtures were placed at 73°F and simulated using an ambient temperature of 73°F surrounding the 1.0 meter thick wall. The temperature development, stress development, and mechanical properties of these mixtures can be found in Figures 4-20 and 4-11.

### 5.7.1 CRACKING SENSITIVITY

In order to produce a w/cm equal to or less than 0.42, the cement content was increased while the quantity of water was reduced. Increasing the cement content increased the temperature developments. Higher temperature developments created larger thermal changes required to equilibrate the system with the ambient conditions. As a result, the cracking temperature was generally decreased as the w/cm was increased as shown in Figure 5-39; however, the mixture with w/c = 0.38 did not follow this trend.

The cracking temperature of the WC38 mixture was slightly lower than the CTRL mixture. In general the data of this study also indicate that the cracking sensitivity is improved as the water-to-cement ratio is increased.

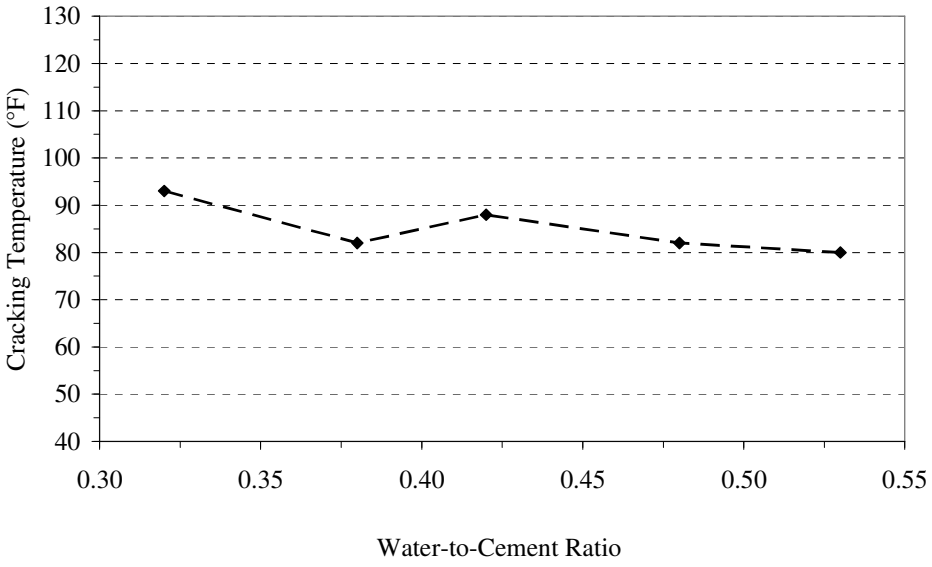


**Figure 5-39:** Effect of w/cm on cracking temperature under 73°F-73°F temperature conditions

The stress-to-strength ratio increased with the decrease of w/cm as shown in Figure 5-40. However, the slopes of the stress-to-strength ratio plots are very similar between the different w/cm. The high w/cm mixtures were more effective in reducing the cracking tendency, which corresponds to the findings of Breitenbücher and Mangold (1994).

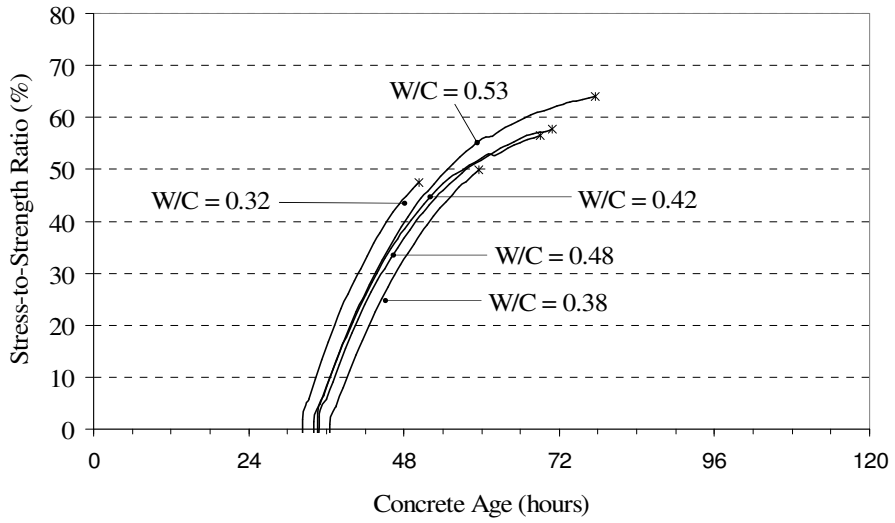


**Figure 5-40:** Effect of w/cm on the stress-to-strength ratio at 73°F – 73°F

### 5.7.2 AUTOGENOUS SHRINKAGE

As discussed by many researchers, the w/cm has a substantial affect on the magnitude of autogenous shrinkage stresses. Holt and Leivo (2004) determined that as the w/cm was reduced, autogenous shrinkage increased. Low w/cm mixtures, i.e. less than 0.40, have much lower internal relative humidity under sealed conditions (Hedlund 2000). The lack of water increases the capillary forces which increases autogenous shrinkage as shown in Figure 5-41. With the exception of the WC38 mixture, a decrease in w/cm increases the magnitude of autogenous shrinkage stresses.

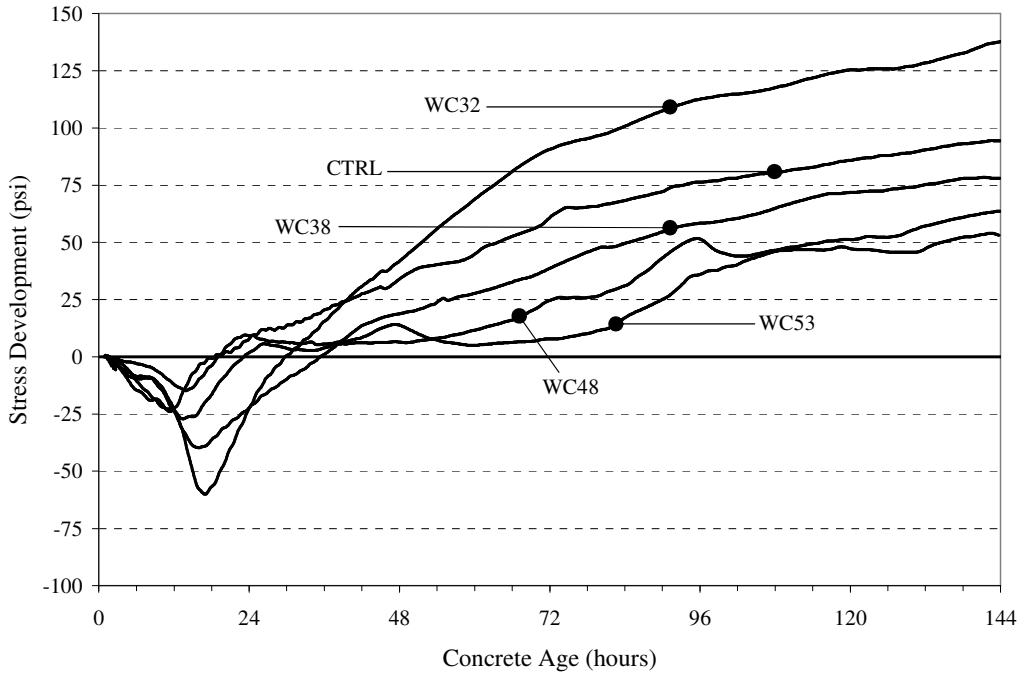


**Figure 5-41:** Effect of w/cm on stress development under 73°F isothermal conditions

## 5.8 DISCUSSION OF STRESS-TO-STRENGTH RATIOS AT FAILURE

To obtain the stress-to-strength ratio, the stress developed by the concrete in the match-cured rigid cracking frame is divided by the splitting tensile strength. At the time of cracking, one might expect the stress-to-strength ratio to be approximately 100 percent. However, due to the specimen size relative the test cylinder, rate of loading, and type of loading, the values of the stress-to-strength ratios fall between 50 to 80 percent.

The concrete specimen in the rigid cracking frame has a much higher volume than the splitting tensile test cylinder, which produces a higher probability of a flaw in the concrete. The rate of loading between the two specimens is also very important. The splitting tensile test specimen is loaded until failure which occurs in less than 5 minutes.

However, the rigid cracking frame specimen in under stress for approximately 5 days before failure. The type of testing is also very important. The concrete specimen in the rigid cracking frame is a direct tension loading. However, the splitting tensile test does not measure tensile strength directly.

## 5.9 SUMMARY

Under the current testing program, two rigid cracking frames were used to evaluate the restrained stress development of concrete specimens at early-ages. Thirty-four mixtures were evaluated under both match-cured and isothermal conditions. The effects of placement temperature, seasonal temperature conditions, cement type, supplementary cementing materials, air entrainment, and water-to-cementitious ratio on the cracking tendency of concrete mixtures were thoroughly examined.

### 5.9.1 CRACKING SENSITIVITY

The results obtained from the laboratory testing program reveal that the fresh concrete placement temperature had a substantial impact on the early-age stress development of a concrete specimen in the rigid cracking frame. Lowering of the placement temperature reduced the cracking temperature, which corresponds to the findings of Springenschmid and Breitenbücher (1998). A placement temperature of 50°F and 73°F produced a reduced stress-to-strength ratio relative to a 95°F placement temperature prior to artificial cooling in the portland cement only mixtures. Consequently, the time of cracking was increased, which indicates that cracking tendency was improved.

The GGBF slag mixtures did not effectively reduce the cracking tendency at various placement temperatures when cooled and placed under hot weather conditions. However, reducing the placement temperature of the GGBF slag mixtures substantially decreased the stress-to-strength ratio prior to cooling which corresponds to the trends of the portland cement only mixtures.

Reducing the seasonal temperature conditions had a similar effect as lowering the placement temperature; however, there is a more pronounced trend as the cracking temperature continues downward from the 73°F to the 50°F condition.

Seasonal temperature conditions have a distinct effect on GGBF slag mixtures. Milder seasonal conditions were found to decrease the cracking tendency of the concrete specimen; however, under hot seasonal temperature conditions, the GGBF slag mixtures behaved similar to the plain portland cement mixtures.

Unlike the temperature changes, changing the cement type had little influence on the cracking tendency of the concrete specimens. However, the control mixture was found to be more effective in reducing the cracking temperature at the 73°F – 95°F and 95°F – 95°F conditions which correspond to the findings of Breitenbucher and Mangold (1994) and Springenschmid and Breitenbucher (1998).

The supplementary cementing materials (SCMs) reduced the peak heat of hydration significantly. All of the SCM mixtures reduced the cracking tendency of the concrete specimen with the exception of the 20% Class C fly ash mixture under 73°F-73°F temperature conditions. The 20% Class C fly ash mixture reduced the development of heat; however, the mixture developed stiffness at a much quicker rate than the remaining SCM mixtures. As a result, the zero stress temperature of the control and 20% Class C

fly ash mixtures were very similar which produced cracking at approximately the same time negating the reduction of temperature development. GGBF slag was not effective in reducing the cracking tendency under 95°F-95°F temperature conditions; however, it substantially lowered the cracking temperature under 50°F-50°F temperature conditions.

The use of air entrainment increased the cracking tendency of the concrete specimen which contradicts the findings of Springenschmid and Breitenbucher (1998). The AEA mixture reduced the temperature development slightly; however, the AEA mixture cracked prior to the control mixtures. The increase in cracking tendency is caused by the reduction of tensile strength in the AEA mixture.

With the exception of the control mixture, the cracking tendency of concrete mixtures decreased as the water-to-cement ratio is increased. The cracking temperature decreases with increasing water-to-cement ratio.

### 5.9.2 AUTOGENOUS SHRINKAGE

The data collected for all the mixtures reveal that autogenous shrinkage is not affected by temperature within the normal range of placement temperatures. This data corresponds to the findings of Bjøntegaard (1999) and Lura et al. (2001). The differences in stress development between the various temperatures can be attributed to variability in the testing method.

Research has found that cement type, i.e. variations in the volume of Bogue compounds, can affect the magnitude of autogenous shrinkage (Tazawa and Miyazawa 1997 and Holt 2001). In this present study, the Type I cement had a larger percentage of

$C_3A$ while the percentage of $C_4AF$ was lower than the Type III cement. The autogenous shrinkage stresses for the two cement types were similar.

SCMs were found to slightly reduce autogenous shrinkage stresses with the increase in replacement percentage. The use of SCMs reduces the quantity of portland cement in a concrete mixture, which reduces the volume change associated with chemical shrinkage. Decreasing chemical shrinkage reduces the magnitude of autogenous shrinkage stresses.

Air entrainment effectively reduces the magnitude of autogeneous shrinkage. Hammer and Fossa (2006) found that air entrainment alters the pore water pressure which subsequently decreases autogenous shrinkage. Improving the air-void system with an air entraining admixture reduces the capillary forces that cause autogenous shrinkage.

Based on the variables evaluated in this study, the water-to-cement ratio is the variable that has the most significant effect on the magnitude of autogenous shrinkage stresses. As the water-to-cement ratio is decreased, autogenous shrinkage stresses increase. Low water-to-cement ratios reduce the amount of available water and as a result the internal relative humidity in a concrete specimen as hydration progresses. As a result, the lack of water amplifies the capillary tensile forces which increase autogenous shrinkage.

# CHAPTER 6

# CONCLUSIONS AND RECOMMENDATIONS

Early-age cracking in mass concrete is a severe problem that may reduce the structure's functional life. Cracking originates from stresses induced by volume change as a result of thermal, drying, autogenous, and chemical shrinkage coupled with restraint conditions that prevent movement of the concrete. Over time, stresses may exceed the tensile strength of the concrete, which will result in cracking.

The mechanisms driving early-age cracking are influenced by many complex variables, and many of these mechanisms are not clearly understood. In order to better understand the mechanisms driving early-age cracking, the primary variables that influence the cracking sensitivity of the concrete were evaluated in this study.

The experimental testing program utilized two rigid cracking frames, a free shrinkage frame, match-curing system, and a semi-adiabatic hydration drum. Each concrete mixture was placed in the rigid cracking frames. One specimen subjected to isothermal conditions while another was subjected to a match-curing temperature profile in order to distinguish thermal and autogenous shrinkage. The free shrinkage frame was subjected to the match-curing temperature profile in order to measure volume change under free restraint conditions. The match-curing system was subjected to the same temperature profile as the match-cured rigid cracking frame so that the mechanical properties and

setting times of the concrete in the rigid cracking frame and the free shrinkage frame could be determined.

Thirty-four mixtures were chosen to evaluate the effects of placement temperature, seasonal temperature conditions, and concrete constituents on the cracking tendency of concrete mixtures. The effects of placement temperature were investigated by batching concrete mixtures at three different temperatures: 50°F, 73°F, and 95°F. The effects of seasonal temperature changes were investigated by match-curing each concrete specimen to a simulated temperature profile based on its respective hydration parameters. The effects of concrete constituents were evaluated by examining different cement types, multiple water-to-cement ratios, air entrainment, and supplementary cementing materials.

## 6.1 CONCLUSIONS

The test method developed and discussed in this thesis is a realistic indicator of early-age restraint stresses. This testing program provides a means to measure the development of restraint stresses in concrete members during early-ages. Results from the experimental laboratory testing program justify the following conclusions:

### 6.1.1 CRACKING SENSITIVITY

- Lowering of the placement temperature reduces the cracking tendency of all mixtures evaluated in this study.
- When compared to a placement temperature of 95°F, placement temperatures of 50°F and 73°F produce a reduced stress-to-strength ratio prior to artificial cooling. This indicates that cooling the fresh concrete prior to placement in hot

weather conditions will reduce the amount of strength consumed by thermal effects. This will reduce the likelihood of early-age cracking in structures.

- GGBF slag mixtures did not effectively reduce the cracking tendency of concretes cooled and placed under hot weather conditions. The use of GGBF slag significantly improved the cracking tendency of the plain Type I cement mixture when it was placed under non-summer conditions.
- The GGBF slag mixtures were very efficient in delaying the time of cracking. Thirty percent replacement of Class C fly ash was found to reduce the magnitude of temperature development and prolong cracking; however, a twenty percent replacement slightly increased the cracking tendency.
- The use of ternary blend mixtures decreases the cracking tendency of the concrete. Ternary blend mixtures substantially reduce the temperature development of a mass concrete member.
- The use of air entrainment increases the cracking tendency of the concrete. The air entrainment mixture reduced the temperature development slightly; however, it also reduced the tensile capacity such that the air-entrained cracked before the control mixture.
- Variations in the water-to-cement ratio affected the rate and magnitude of heat generation. As the water-to-cement ratio was decreased, the magnitude of temperature rise increased. High temperature and stiffness developments associated with an decrease in water-to-cement ratio increased the cracking tendency tremendously.

### 6.1.2 AUTOGENOUS SHRINKAGE

- Fresh concrete placement temperature and seasonal temperature variations did not affect the magnitude of autogenous shrinkage stresses.
- SCMs were found to reduce autogenous shrinkage stresses with the increase in replacement percentage. The use of SCMs reduces the quantity of portland cement in a concrete mixture which reduces the volume change associated with chemical shrinkage. Decreasing chemical shrinkage reduces the magnitude of autogenous shrinkage stresses.
- Air entrainment slightly reduces the magnitude of autogeneous shrinkage.
- Based on the variables evaluated in this study, the water-to-cement ratio is the variable that has the most significant effect on the magnitude of autogenous shrinkage stresses. As the water-to-cement ratio was decreased, the autogenous shrinkage stresses increased.

## 6.2 RECOMMENDATIONS

In order to develop a more accurate understanding of early-age behavior of concrete, the following additional research is recommended:

- Further investigations into the effect of concrete constituents on the early-age behavior of concrete such as different cement types and brands and aggregate type.
- Implementation of relative humidity sensors to further study and quantify autogenous shrinkage.

- Determination of an accurate model for estimation of the time-dependent nature of the coefficient of thermal expansion.

Based on the experience gained through the execution of this experimental testing program outlined in Chapter 3 of this thesis, the following equipment modifications are recommended:

- The use of a non-spring loaded LVDT is required to accurately measure the free deformation of a concrete specimen at early-ages.
- Over-sized holes in the free shrinkage frame outer and inner plates may be needed to prevent inaccurate measurements due to friction.
- Use a closed circuit system for the match-curing box to ensure proper fluid levels are maintained in the circulator.

## REFERENCES


ACI 116R-12. 1997. *Cement and Concrete Terminology*. Farmington Hills, MI: American Concrete Institute.

ACI 207.1R-96. 1996. *Mass Concrete*. Farmington Hills, MI: American Concrete Institute.

ACI 207.2R. 1973. *Effect of Restraint, Volume Change, and Reinforcement on Cracking of Mass Concrete*. Farmington Hills, MI: American Concrete Institute.

ACI 207.2R. 1997. *Effect of Restraint, Volume Change, and Reinforcement on Cracking of Mass Concrete*. Farmington Hills, MI: American Concrete Institute.

ACI 209R. 1997. *Prediction of Creep, Shrinkage, and Temperature in Concrete Structures.* Farmington Hills, MI: American Concrete Institute.

ACI 232.2R. 1997. *Use of Fly Ash in Concrete.* Farmington Hills, MI: American Concrete Institute.

ACI 233.R. 1997. *Ground Granulated Blast-Furnace Slag as a Cementitious Constituent in Concrete*. Farmington Hills, MI: American Concrete Institute.

ACI 318. 2005. *Building Code Requirements for Structural Concrete and Commentary*. Farmington Hills, MI: American Concrete Institute.

ACI 517.2R-80. 1980. *Accelerated Curing of Concrete at Atmospheric Pressure*. Farmington Hills, MI: American Concrete Institute.

ASTM C 1064. 2004. Standard Test Method for Temperature of Freshly Mixed Hydraulic-Cement Concrete. American Society for Testing and Materials. West Conshohocken, PA.

ASTM C 138. 2001. Standard Test Method for Density (Unit Weight), Yield, and Air Content (Gravimetric) of Concrete. American Society for Testing and Materials. West Conshohocken, PA.

ASTM C 143. 2003. Standard Test Method for Slump of Hydraulic-Cement Concrete. American Society for Testing and Materials. West Conshohocken, PA.

ASTM C 157. 2004. Standard Test Method for Length Change of Hardened Hydraulic-Cement Mortar and Concrete. American Society for Testing and Materials. West Conshohocken, PA.

ASTM C 1581. 2004. Standard Test Method for Determining Age at Cracking and Induced Tensile Stress Characteristics of Mortar and Concrete under Restrained Shrinkage. American Society for Testing and Materials. West Conshohocken, PA.

ASTM C 192. 2002. Standard Practice for Making and Curing Concrete Test Specimens in the Laboratory. American Society for Testing and Materials. West Conshohocken, PA.

ASTM C 231. 2004. Standard Test Method for Air Content of Freshly Mixed Concrete by the Pressure Method. American Society for Testing and Materials. West Conshohocken, PA.

ASTM C 33. 2003. Standard Specification for Concrete Aggregates. American Society for Testing and Materials. West Conshohocken, PA.

ASTM C 39. 2003. Standard Test Method for Compressive Strength of Cylindrical Concrete Specimens. American Society for Testing and Materials. West Conshohocken, PA.

ASTM C 469. 2002. Standard Test Method for Static Modulus of Elasticity and Poisson's Ratio of Concrete in Compression. American Society for Testing and Materials. West Conshohocken, PA.

ASTM C 496. 2004. Standard Test Method for Splitting Tensile Strength of Cylindrical Concrete Specimens. American Society for Testing and Materials. West Conshohocken, PA.

ASTM C 670. 2003. Standard Practice for Preparing Precision and Bias Statements for Test Methods for Construction Materials. American Society for Testing and Materials. West Conshohocken, PA.

ASTM C 403. 2004. Standard Test Method for Time of Setting of Concrete Mixtures by Penetration Resistance. American Society for Testing and Materials. West Conshohocken, PA.

ASTM C 1074. 2004. Standard Practice for Estimating Concrete Strength by the Maturity Method. American Society for Testing and Materials. West Conshohocken, PA.

Bamforth, P.B. 1980. In Situ Measurement of the Effect of Partial Portland Cement Replacement Using Either Fly Ash or Ground Granulated Blast-Furnace Slag on the Performance of Mass Concrete. *Institution of Civil Engineers*, Part 2, Vol 69: 777-800. London.

Bamforth, P.B. and W.F. Price. 1995. *Concreting Deep Lifts and Large Volume Pours*. Westminster London: Construction Industry Research and Information Association. CIRIA Report 135.

Bažant, Z.P. and E. Osman. 1976. Double Power Law for Basic Creep of Concrete. *Materials and Structures* 9, no. 49: 3-11.

Bažant, Z.P. and J.C. Chern. 1985a. Log Double Power Law for Concrete Creep. *Journal of the American Concrete Institute* 82, no. 5: 665-675.

Bažant, Z.P. and J.C. Chern. 1985b. Triple Power Law for Concrete Creep. *Journal of Engineering Mechanics* 111, no. 1: 63-83.

Bažant, Z.P. and J.C. Chern. 1985c. Concrete Creep at Variable Humidity. *Materials and Structures* 18, no. 103: 1-19.

Bjøntegaard, Ø. 1999. *Thermal Dilation and Autogenous Deformation as Driving Forces to Self-Induced Stresses in High Performance Concrete*. Doctoral Thesis. Norwegian University of Science and Technology, Division of Structural Engineering.

Bogue, R.H. 1929. Calculations of the Compounds in Portland Cement. *Industrial and Engineering Chemistry 1*, no. 4: 192.

Breitenbücher, R. 1990. Investigation of Thermal Cracking with the Cracking-Frame. *Materials and Structures* 23, no. 135: 172-177.

Breitenbücher, R. and M. Mangold. 1994. Minimization of Thermal Cracking in Concrete at Early Ages. In *RILEM Proceedings 25, Thermal Cracking in Concrete at Early Ages*, ed. R. Springenschmid, 205-212. London: E & FN Spon.

Carino, N.J. and H.S. Lew. 2001. The Maturity Method: From Theory to Application. National Institute of Standards and Technology.

Emanuel, J.H. and L. Hulsey. 1977. Prediction of the Thermal Coefficient of Expansion of Concrete. *Journal of the American Concrete Institute* 74, no. 4: 149-155.

Emborg, M. 1989. *Thermal Stresses in Concrete Structures at Early Ages*. Doctoral Thesis. Luleå University of Technology, Division of Structural Engineering.

FDOT. 2002. *Structures Design Guidelines (LRFD).* Tallahassee, FL: Florida Department of Transportation.

Federal Highway Administration High Performance Concrete Website (FHWA). 2005. Located on the World Wide Web at: http://knowledge.fhwa.dot.gov/cops/hpcx.nsf/home?openform&Group=HPC%20Cast-in-Place%20Construction&tab=WIP

Fulton, F.S. 1974. The Properties of Portland Cement Containing Milled Granulated Blast-Furnace Slag. Portland Cement Institute. 4-46. Johannesburg.

Hammer, T.A., and K.T. Fossa. 2006. Influence of Entrained Air Voids on Pore Water Pressure and Volume Change of Concrete Before and During Setting. *Materials and Structures 39*: 801-808.

Hedlund, H. 2000. *Hardening Concrete: Measurement and Evaluation of Non-Elastic Deformation and Associated Restraint Stresses*. Doctoral Thesis. Luleå University of Technology, Division of Structural Engineering.

Hedlund, H. and G. Westman. 1999. Evaluation and Comparison of Sealed and Non-Sealed Shrinkage Deformation Measurements of Concrete. In JCI Proceedings, *Autogenous Shrinkage of Concrete*, 121-132. New York: Routledge.

Holt, E. and M. Leivo. 2004. Cracking Risks Associated with Early Age Shrinkage. *Cement and Concrete Composites* 26, no. 5: 521-530.

Holt, E. 2004. Contribution of Mixture Design to Chemical and Autogenous Shrinkage of Concrete at Early Ages. *Cement and Concrete Research* 35, no. 3: 464-472.

Holt, E. 2001. *Early Age Autogenous Shrinkage of Concrete*. Doctoral Thesis. The University of Washington in Seattle.

Kada, H., M. Lachemi, N. Petrov, O. Bonnequ, and P.-C. Aïtcin. 2002. Determination of the Coefficient of Thermal Expansion of High Performance Concrete from Initial Setting. *Materials and Structures* 35, no. 245: 35-41.

Kosmatka, H., B. Kerkhoff, and W.C. Panarese. 2002. Design and Control of Concrete Mixtures. 14th Edition. Skokie, Illinois. Portland Cement Association.

Krauss, P.D. and E.A. Rogalla. 1996. *Transverse Cracking in Newly Constructed Bridge Decks*. Washington D.C.: Transportation Research Board, National Research Council. NCHRP Report 380.

Lange, D. and S. Altougat. 2002. Early Thermal Changes. In *RILEM Report 25, Thermal Cracking in Concrete at Early Ages*, ed. A. Bentur, 37-38. RILEM Publications S.A.R.L.

Larson, M. 2003. *Thermal Crack Estimation in Early Age Concrete: Models and Methods for Practical Application*. Doctoral Thesis. Luleå University of Technology, Division of Structural Engineering.

Lura, P., K. van Breugel, and I. Maruyama. 2001. Effect of Curing Temperature and Type of Cement on Early-Age Shrinkage of High-Performance Concrete. *Cement and Concrete Research 31*, no. 12: 1867-1872.

Lynam, C.G. 1934. *Growth and Movement in Portland Cement Concrete*. London: Oxford University Press.

Mangold, M. 1994. *The Development of Restraint and Intrinsic Stresses in Concrete Members during Hydration*. Doctoral Thesis. Technical University of Munich.

Mangold, M. 1998. Methods for Experimental Determination of Thermal Stresses and Crack Sensitivity in the Laboratory. In *RILEM Report 15, Prevention of Thermal Cracking in Concrete at Early Ages*, ed. R. Springenschmid, 26-39. London: E & FN Spon.

Mehta, P. K. and P.J.M. Monterio. 2006. *Concrete: Microstructure, Properties, and Materials*. 3rd Edition. McGraw-Hill, Inc. New York, NY.

Mindess, S., J. Young, and D. Darwin. 2002. *Concrete*. 2nd Edition. Prentice Hall. Upper Saddle River, NJ.

Mindess, S., and J.F. Young. 1981. *Concrete*. Prentice Hall. Upper Saddle River,NJ

Nilsson, M. 2003. *Restraint Factors and Partial Coefficients for Crack Risk Analyses of Early Age Concrete Structures*. Doctoral Thesis 2003:19. Luleå University of Technology, Division of Structural Engineering.

Paulini, P. 1996. Outlines of Hydraulic Hardening – an Energetic Approach. In Workshop NTNU/SINTEF*, Early Volume Changes and Reactions in Paste-Mortar-Concrete*. Trondheim, Norway.

Sakai, E., S. Miyahara, S. Ohsawa, S. Lee, and M. Daimon. 2005. Hydration of Fly Ash Cement. *Cement and Concrete Research* 35, no. 6: 1135-1140.

Schindler, A. and K. Folliard. 2005. Heat of Hydration Models for Cementitious Materials. *Journal of American Concrete Institute 102*, no. 1: 24-33

Sellevold, E., Ø. Bjøntegaard, H. Justnes, and P.A. Dahl. 1994. High Preformance Concrete: Early Volume Change and Cracking Tendency. In *RILEM Proceedings 25, Thermal Cracking in Concrete at Early Ages*, ed. R. Springenschmid, 230-236. London: E & FN Spon.

Sioulas, B. and J.G. Sanjayan. 2000. Hydration Temperatures in Large High-Strength Concrete Columns Incorporating Slag. *Cement and Concrete Research* 30, no.11: 1791-1799.

Springenschmid, R. and R. Breitenbücher. 1998. Influence of Constituents, Mix Proportions and Temperature on Cracking Sensitivity of Concrete. In *RILEM Report 15, Prevention of Thermal Cracking in Concrete at Early Ages*, ed. R. Springenschmid, 40-50. London: E & FN Spon.

Springenschmid, R., R. Breitenbücher, and M. Mangold. 1994. Development of the Cracking Frame and the Temperature-Stress Testing Machine. In *RILEM Proceedings 25, Thermal Cracking in Concrete at Early Ages*, ed. R. Springenschmid, 137-144. London: E & FN Spon.

Tazawa, E. and S. Miyazawa. 1997. Influence of Constituents and Composition on Autogenous Shrinkage of Cementitious Materials. *Magazine of Concrete Research 49*, No. 178: 15-22.

Thielen, G. and W. Hintzen. 1994. Investigation of Concrete Behaviour Under Restraint with a Temperature-Stress Test Machine. In *RILEM Proceedings 25, Thermal Cracking in Concrete at Early Ages*, ed. R. Springenschmid, 145-152. London: E & FN Spon.

Townsend, C.L. 1965. Control of Cracking in Mass Concrete Structures. Engineering Monograph No. 34. Water Resources Technical Publication. U.S. Department of the Interior. Bureau of Reclamation. 1965.

TxDOT. 2004. *Standard Specifications for Construction and Maintenance of Highways, Streets, and Bridges*. Texas Department of Transportation. Austin, Texas. pp 500.

USBR. Concrete Manual. 8th Edition. Water Resources Technical Publication. U.S. Department of the Interior. Bureau of Reclamation. 1975.

Verbeck, G.J. and R.H. Helmuth. 1968. Structure and Physical Properties of Cement Paste. Proceedings of 5th International Symposium on Chemistry of Cement. Tokyo, Part III, p 1-32.

Wade, S. 2005. *Evaluation of the Maturity Method to Estimate Concrete Strength*. Master Thesis. Auburn University, Department of Civil Engineering.

Waller, V., L. d'Aloïa, F. Cussigh, and S. Lecrux. 2004. Using the Maturity Method in Concrete Cracking Control at Early Ages. *Cement and Concrete Composites* 26, no.5: 589-599.

Wang, Ch. And W.H. Dilger. 1994. Prediction of Temperature Distribution in Hardening Concrete. In *RILEM Proceedings 25, Thermal Cracking in Concrete at Early Ages*, ed. R. Springenschmid, 21-28. London: E & FN Spon.

Westman, G. 1999. *Concrete Creep and Thermal Stresses: New Creep Models and their Effects on Stress Development*. Doctoral Thesis. Luleå University of Technology, Division of Structural Engineering.

Whigham, J.A. 2005. *Evaluation of Restraint Stresses and Cracking in Early-Age Concrete with the Rigid Cracking Frame*. Master Thesis. Auburn University, Department of Civil Engineering.

# APPENDIX A

# FREE SHRINKAG FRAME

The objective of this appendix is to present additional design drawings to aid in the construction of the free shrinkage frame. Additional testing pictures will be provided to demonstrate the set-up and execution of the free shrinkage frame as outlined in the laboratory testing program in Chapter 3. The design drawings and pictures can be found in sections A.1 and A.2 respectively.

## A.1 FREE SHRINKAGE FRAME DRAWING DETAILS

The following figures will illustrate the construction specifications of the free shrinkage frame.

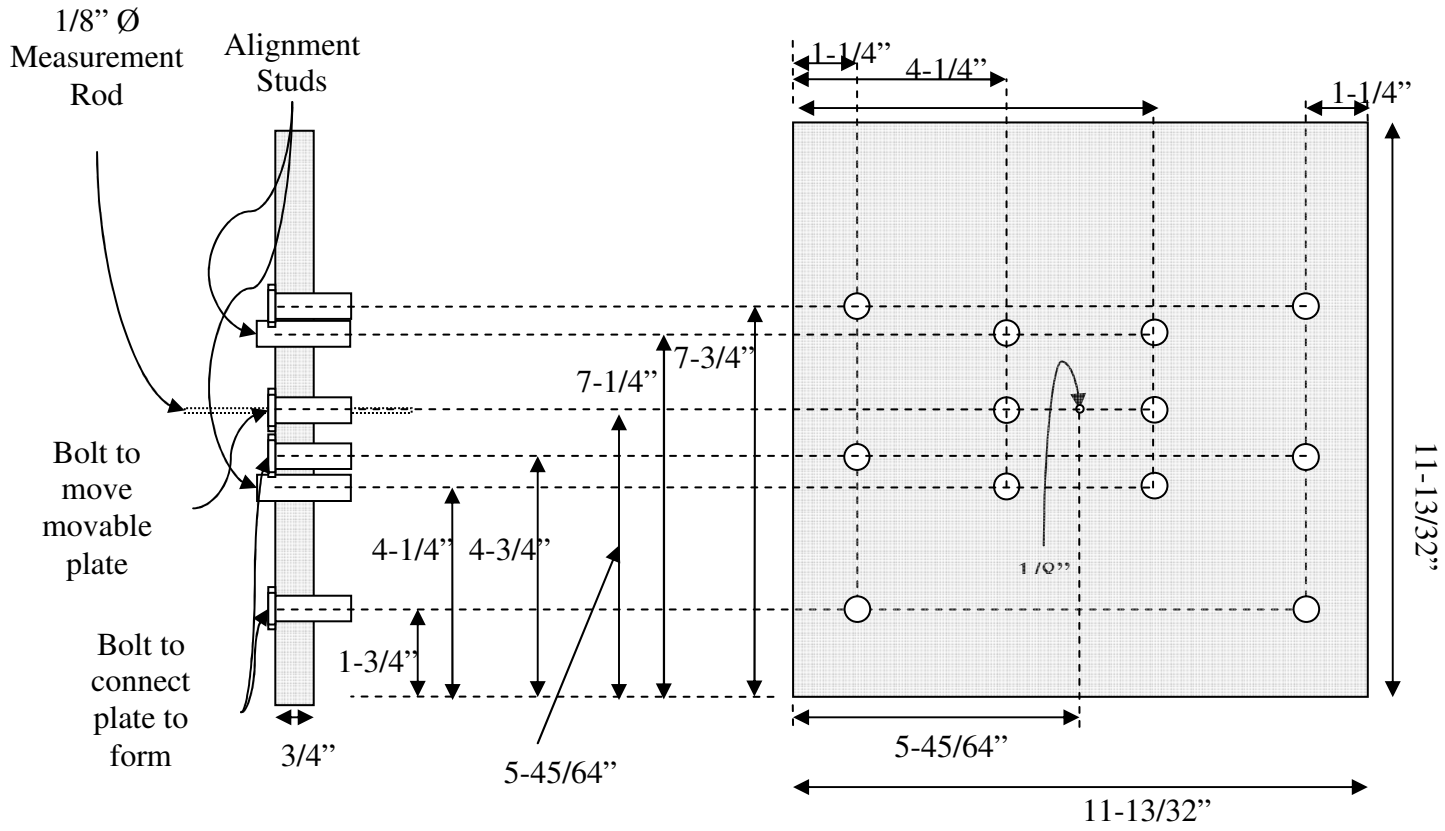


**Figure A-1:** Side and elevation view of outer plate

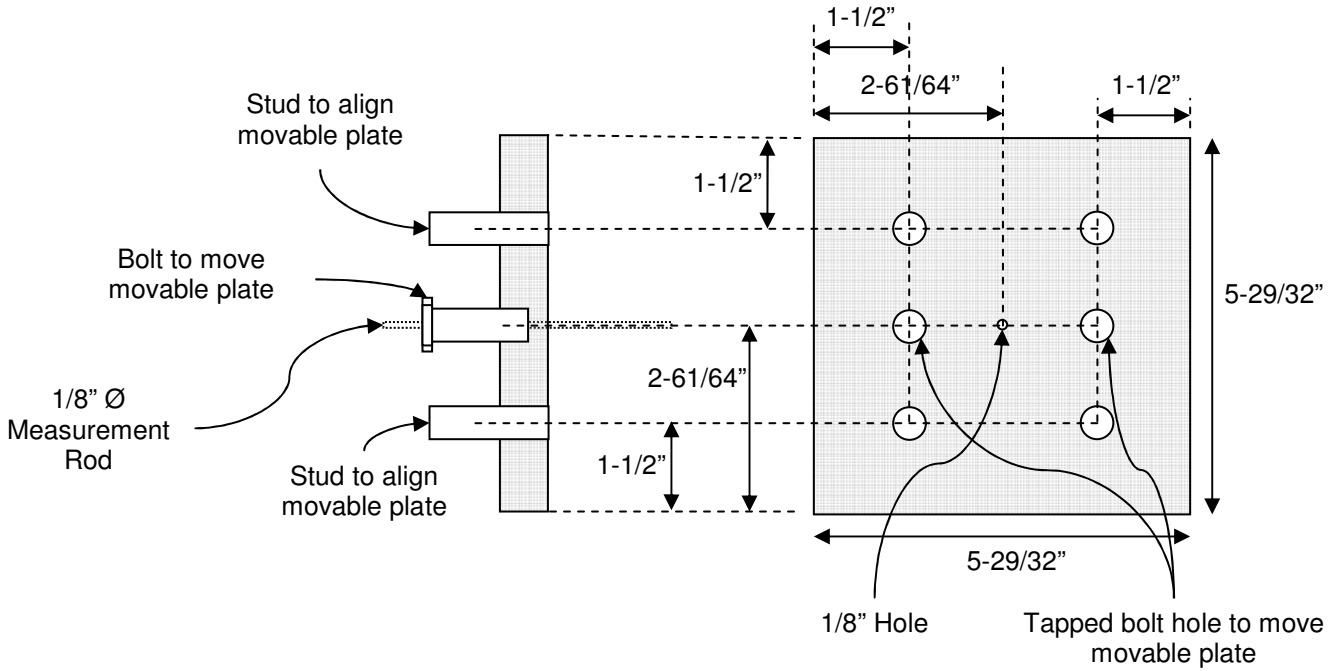


**Figure A-2:** Side and elevation view of inner plate

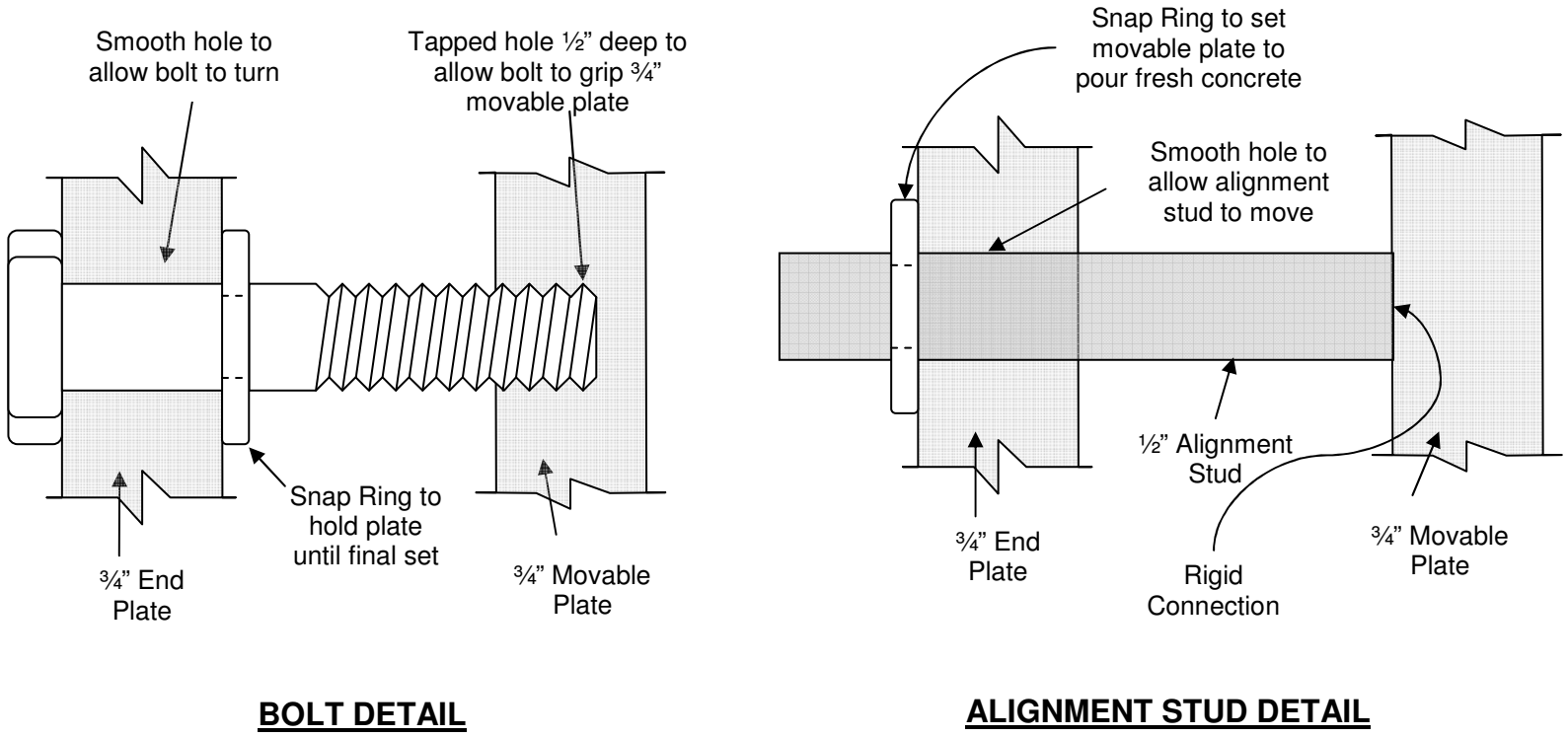


**Figure A-3:** Bolt and alignment stud detail

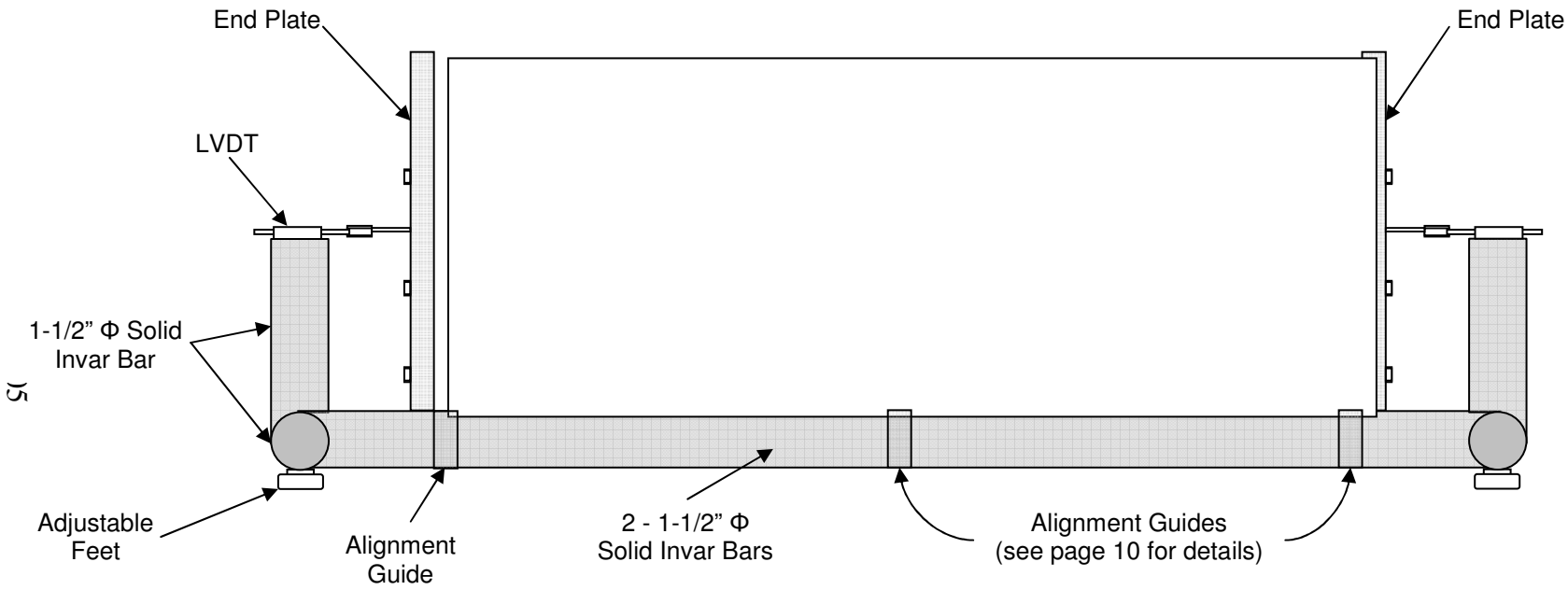


**Figure A-4:** Elevation view of free shrinkage frame

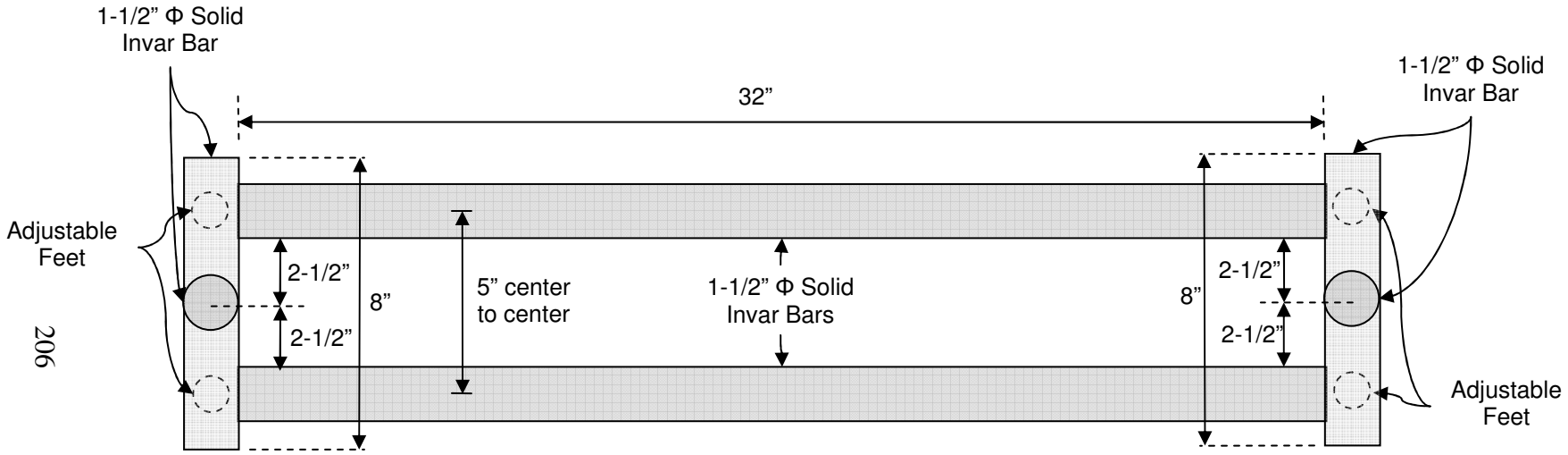


**Figure A-5:** Top view of free shrinkage frame

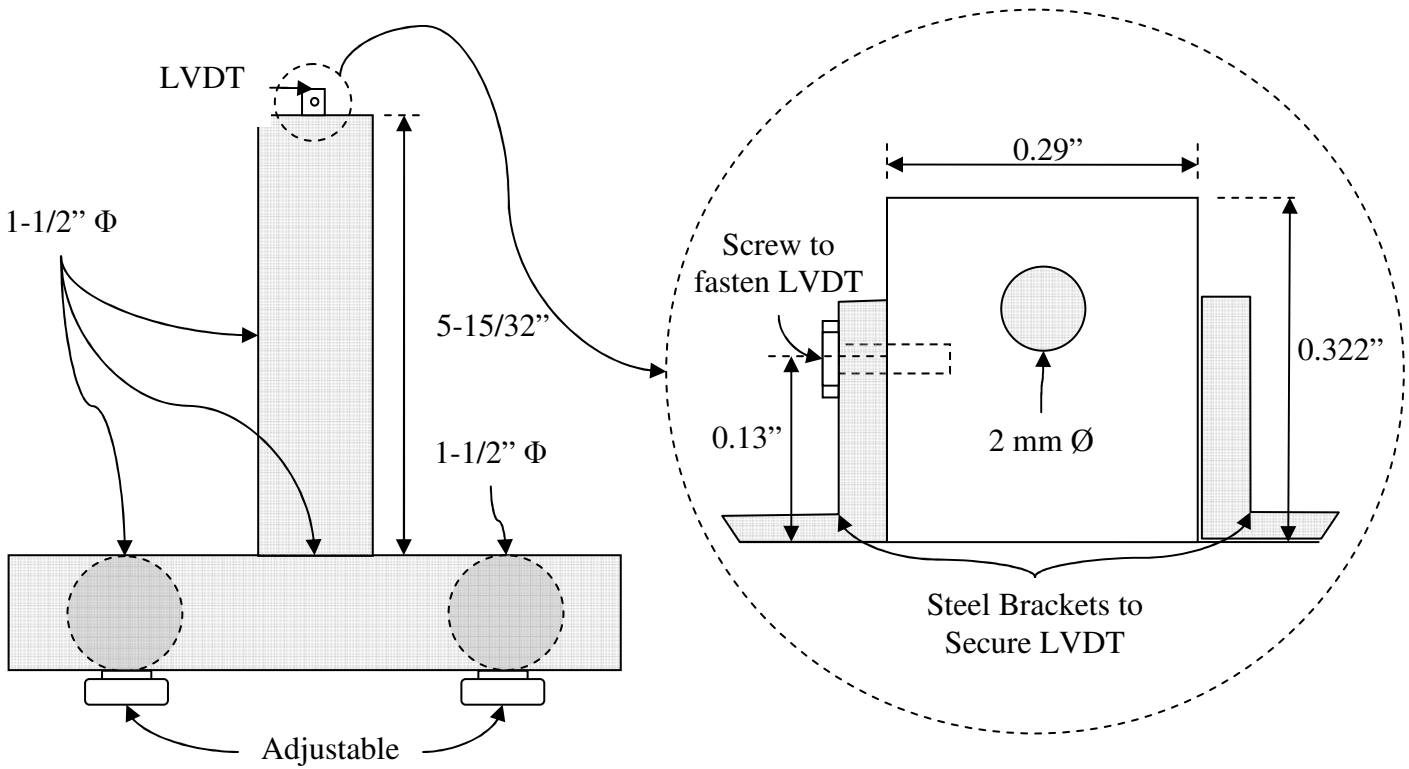


**Figure A-6:** End view of free shrinkage frame and LVDT connection detail

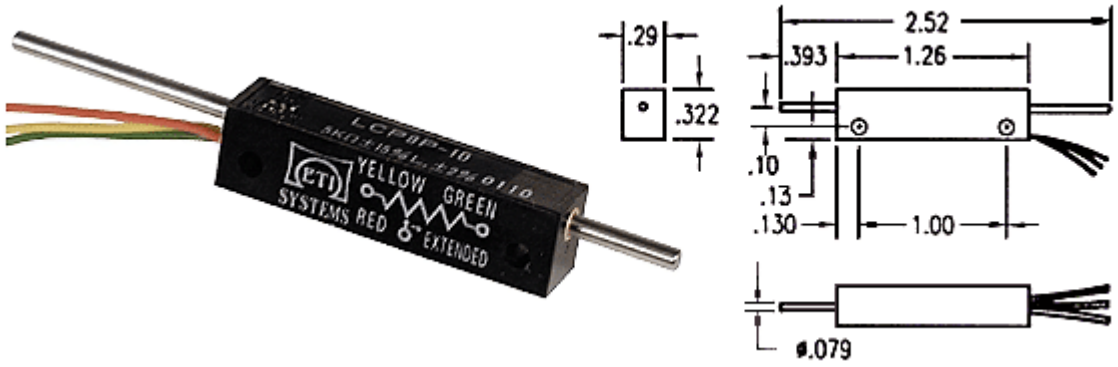


**Figure A-7:** LVDT specifications

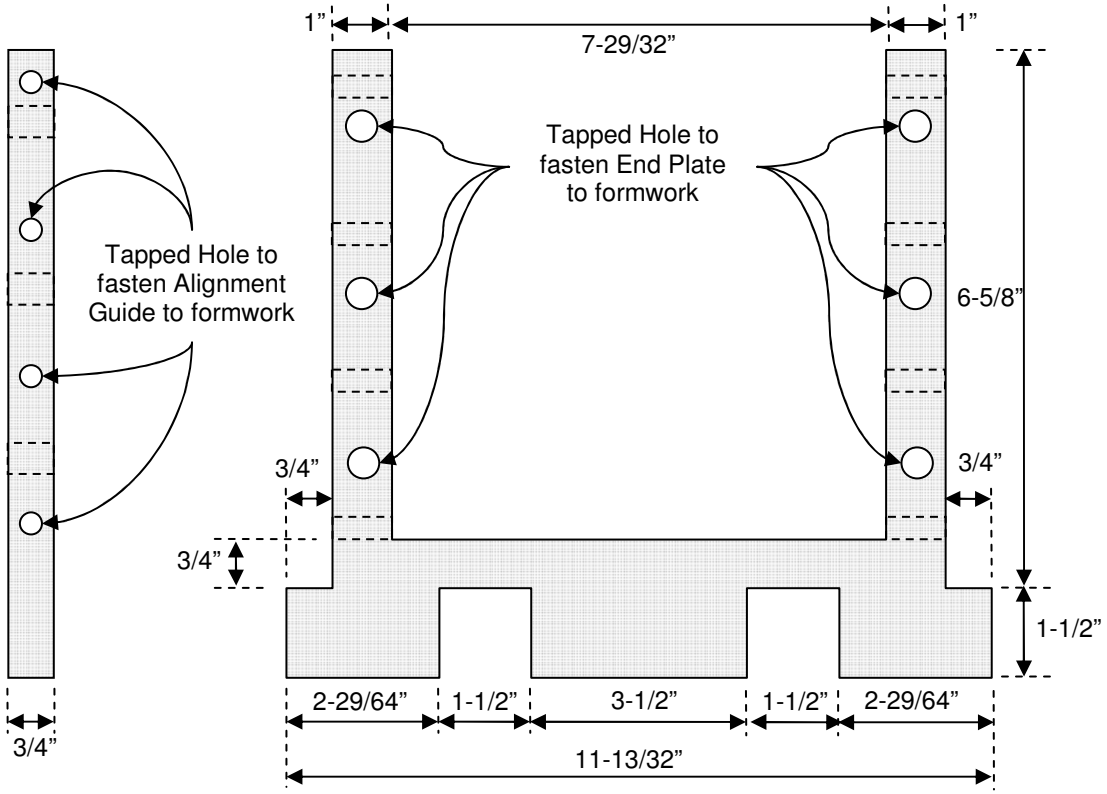


**Figure A-8:** End alignment guide

## A.2 FREE SHRINKAGE FRAME TESTING PICTURES

The following pictures will demonstrate the setup and testing procedure for the free shrinkage frame.

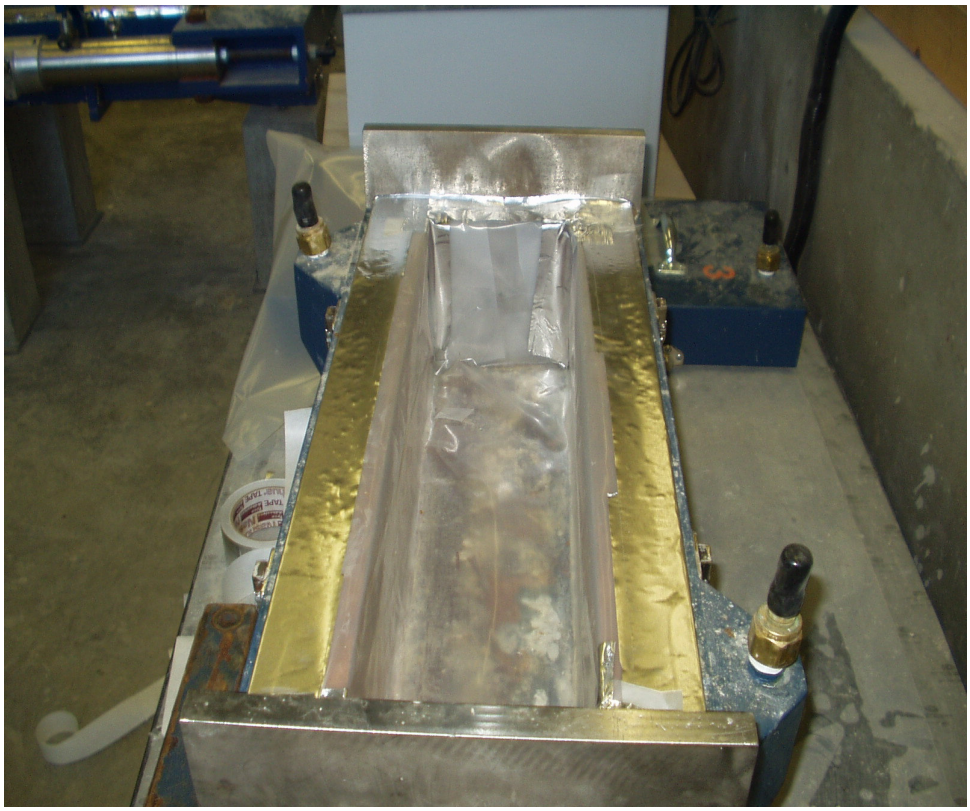

**Figure A-9:** Free shrinkage frame with first layer of plastic


**Figure A-10:** Application of WD40® to first layer of plastic


**Figure A-11:** Second layer of plastic secured by electrical tape

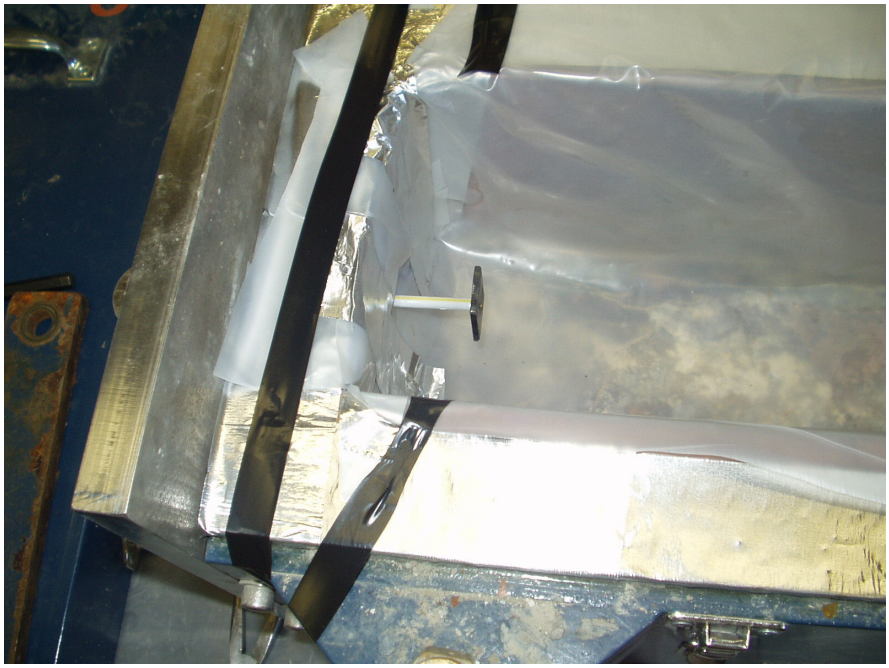

**Figure A-12:** Measurement rod with anchor plate

**Figure A-13:** Application of silicon around measurement rod

**Figure A-14:** Application of first layer of concrete

**Figure A-15:** Vibration of the first layer of concrete


**Figure A-16:** Application of second layer of concrete


**Figure A-17:** Vibration of second layer of concrete

**Figure A-18:** Finishing of the fresh concrete

**Figure A-19:** Removal of electrical tape

**Figure A-20:** Folding plastic over the fresh concrete

**Figure A-21:** Taping plastic to prevent moisture loss

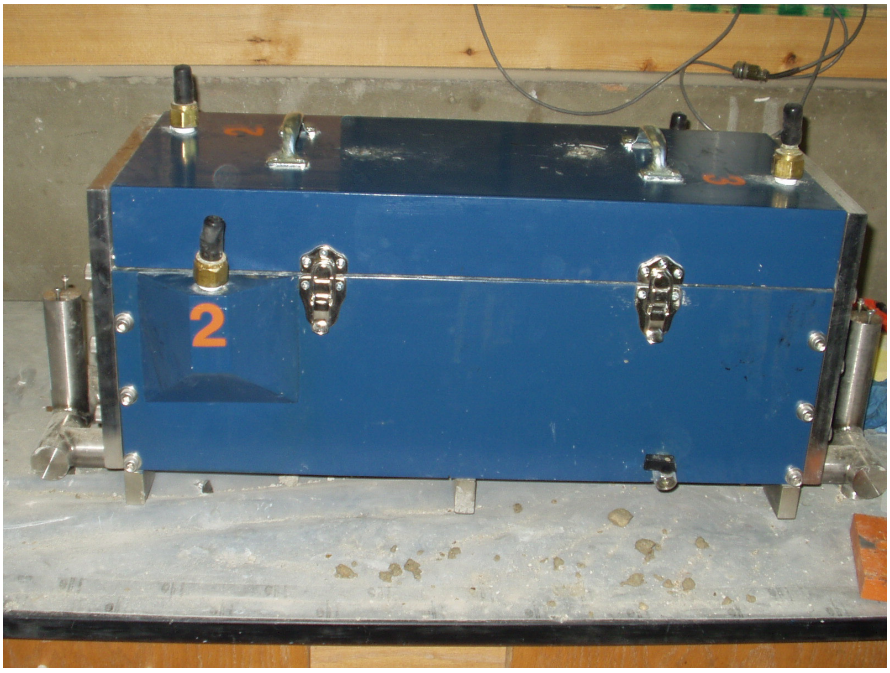


**Figure A-22:** Free shrinkage frame with lid

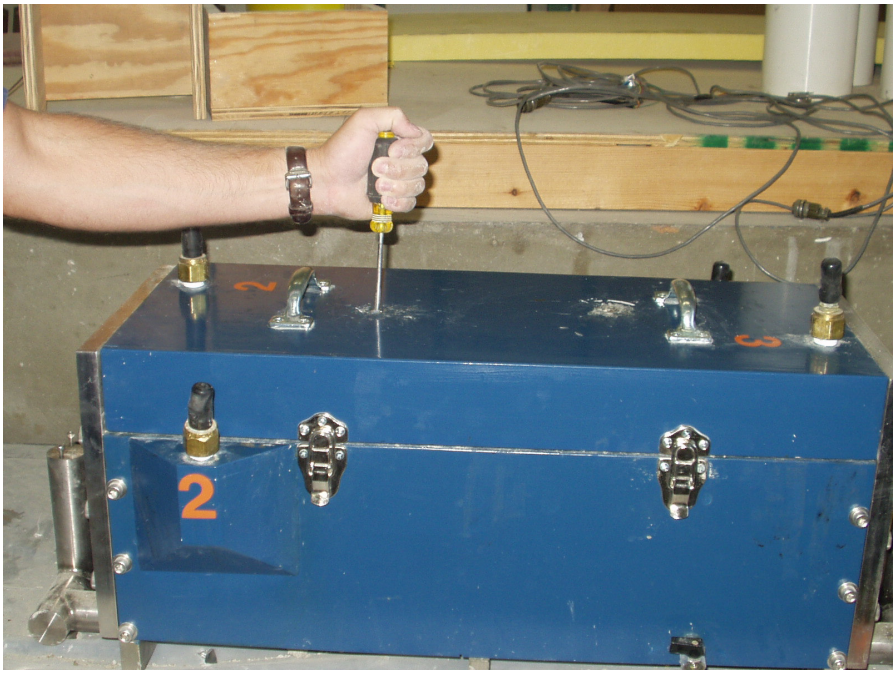


**Figure A-23:** Preparing for temperature probes

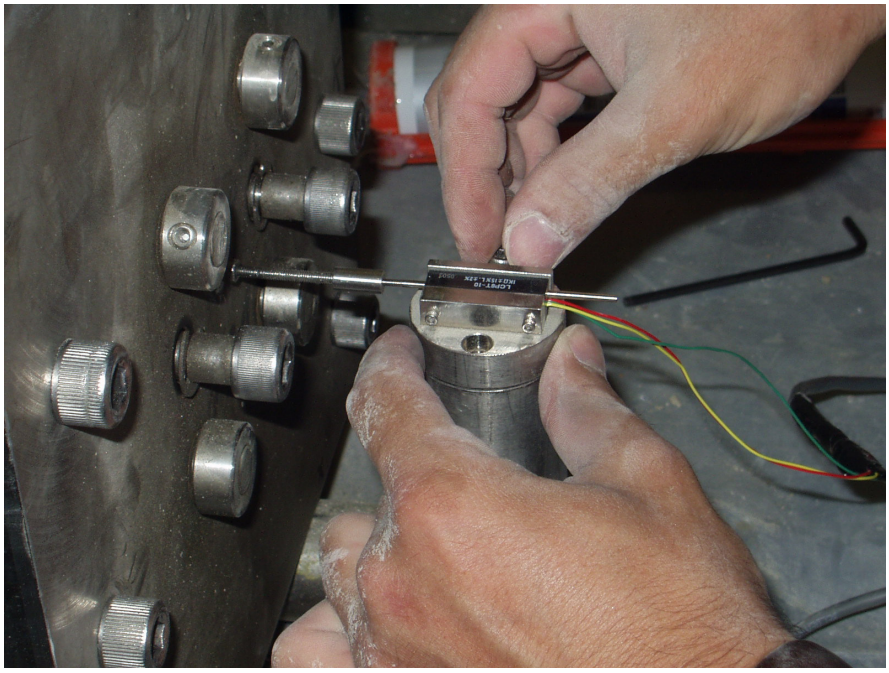

**Figure A-24:** Connecting the LVDT to the measurement rod

**Figure A-25:** Application of silicon around temperature probes


**Figure A-26:** Free shrinkage frame ready for testing

## APPENDIX B

## FRESH CONCRETE PROPERTIES

The objective of this appendix is to present the fresh concrete properties for each concrete mixture. As discussed in Chapter 3, each mixture has two batches. These batches are denoted as "A" and "B". The following table will present the temperature, slump, air content, unit weight, and setting times for the concrete mixtures.

**Table B-1A:** Fresh concrete properties

| Mixture | Batch | Temp (°F) | Slump (in.) | Air (%) | Unit Weight (lb/ft3) | Initial Set (hrs) | Final Set (hrs) |
|---|---|---|---|---|---|---|---|
| CTRL (73°F - 73°F) | A | 75 | 1/2 | 2.9 | 148.3 | 3.98 | 5.44 |
| | B | 75 | 1/2 | 3.0 | 148.0 | | |
| CTRL (50°F - 50°F) | A | 39 | 2 | 3.3 | 148.1 | 8.33 | 11.13 |
| | B | 42 | 2 | 3.0 | 148.3 | | |
| CTRL (95°F - 95°F) | A | 104 | 1/2 | 2.6 | 148.4 | 3.07 | 3.89 |
| | B | 104 | 0 | 2.7 | 150.0 | | |
| CTRL (73°F - 95°F) | A | 75 | 1 | 2.9 | 148.8 | 4.30 | 5.80 |
| | B | 75 | 0 | 3.0 | 149.5 | | |
| CTRL (50°F - 95°F) | A | 38 | 2 1/2 | 3.0 | 148.0 | 5.10 | 6.50 |
| | B | 39 | 3 1/2 | 2.9 | 147.5 | | |

**Table B-1B:** Fresh concrete properties

| Mixture | Batch | Temp (°F) | Slump (in.) | Air (%) | Unit Weight (lb/ft3) | Initial Set (hrs) | Final Set (hrs) |
|---|---|---|---|---|---|---|---|
| 30C (73°F - 73°F) | A | 73 | 5 | 2.1 | 149.1 | 8.99 | 11.51 |
| | B | 73 | 4 1/2 | 2.0 | 149.5 | | |
| 20C (73°F - 73°F) | A | 73 | 5 | 2.3 | 147.9 | 7.95 | 9.60 |
| | B | 73 | 4 1/2 | 2.0 | 148.1 | | |
| 30SG (73°F - 73°F) | A | 74 | 1/2 | 2.3 | 149.2 | 6.04 | 7.69 |
| | B | 74 | 1/2 | 2.3 | 148.7 | | |
| 30SG (50°F - 50°F) | A | 40 | 5 | 2.5 | 148.6 | 9.31 | 12.43 |
| | B | 39 | 5 1/2 | 2.3 | 147.2 | | |
| 30SG (95°F - 95°F) | A | 101 | 1/2 | 2.6 | 148.8 | 3.81 | 5.43 |
| | B | 98 | 1 | 2.3 | 148.0 | | |
| 30SG (73°F - 95°F) | A | 72 | 1/2 | 2.2 | 148.4 | 5.68 | 7.57 |
| | B | 71 | 0 | 2.3 | 148.9 | | |
| 30SG (50°F - 95°F) | A | 41 | 3 1/2 | 2.6 | 147.7 | 7.54 | 10.48 |
| | B | 40 | 3 1/2 | 2.4 | 148.8 | | |
| 50SG (73°F - 73°F) | A | 71 | 1/2 | 2.0 | 148.6 | 7.20 | 8.86 |
| | B | 71 | 1/2 | 2.1 | 148.2 | | |
| 50SG (50°F - 50°F) | A | 38 | 3 | 2.2 | 149.3 | 9.00 | 12.46 |
| | B | 41 | 3 | 2.3 | 149.3 | | |
| 50SG (95°F - 95°F) | A | 105 | 0 | 2.0 | 149.2 | 3.57 | 5.24 |
| | B | 102 | 0 | 2.2 | 148.6 | | |
| 50SG (73°F - 95°F) | A | 77 | 1/2 | 2.1 | 148.5 | 6.03 | 7.41 |
| | B | 73 | 1/2 | 2.1 | 149.0 | | |
| 50SG (50°F - 95°F) | A | 46 | 6 | 1.9 | 148.0 | 8.83 | 11.35 |
| | B | 41 | 5 | 2.1 | 148.4 | | |

**Table B-1C:** Fresh concrete properties

| Mixture | Batch | Temp (°F) | Slump (in.) | Air (%) | Unit Weight (lb/ft3) | Initial Set (hrs) | Final Set (hrs) |
|---|---|---|---|---|---|---|---|
| 25C6SF | A | 73 | 1 | 2.6 | 148.1 | 9.69 | 14.26 |
| (73°F - 73°F) | B | 73 | 2 | 2.3 | 148.6 | | |
| 25F6SF | A | 73 | 1 | 2.6 | 146.8 | 7.95 | 9.60 |
| (73°F - 73°F) | B | 73 | 1 1/2 | 2.3 | 148.1 | | |
| 20F30SG | A | 73 | 4 | 2.3 | 148.5 | 14.76 | 18.31 |
| (73°F - 73°F) | B | 73 | 4 1/2 | 2.1 | 149.2 | | |
| WC32 | A | 75 | 4 | 2.5 | 150.8 | 3.70 | 6.38 |
| (73°F - 73°F) | B | 75 | 4 | 2.7 | 150.6 | | |
| WC38 | A | 74 | 3 1/2 | 2.8 | 149.3 | 3.66 | 4.99 |
| (73°F - 73°F) | B | 75 | 4 1/2 | 3.2 | 149.4 | | |
| WC38 | A | 43 | 9 | 2.9 | 148.8 | 7.33 | 10.77 |
| (50°F - 50°F) | B | 44 | 9 | 3.1 | 148.5 | | |
| WC38 | A | 95 | 1 1/2 | 2.5 | 150.5 | 3.09 | 4.00 |
| (95°F - 95°F) | B | 92 | 2 1/2 | 2.3 | 150.0 | | |
| WC38 | A | 75 | 5 1/2 | 2.9 | 148.2 | 3.59 | 5.04 |
| (73°F - 95°F) | B | 75 | 5 | 2.9 | 148.2 | | |
| WC38 | A | 36 | 8 1/2 | 2.3 | 150.2 | 5.00 | 7.40 |
| (50°F - 95°F) | B | 38 | 8 | 2.4 | 149.7 | | |
| WC48 | A | 75 | 1 /12 | 2.6 | 148.0 | 3.95 | 5.52 |
| (73°F - 73°F) | B | 73 | 1 1/2 | 2.4 | 148.3 | | |
| WC53 | A | 75 | 1 1/2 | 2.7 | 147.4 | 4.30 | 5.80 |
| (73°F - 73°F) | B | 75 | 1 1/2 | 2.6 | 147.2 | | |

**Table B-1D:** Fresh concrete properties

| Mixture | Batch | Temp (°F) | Slump (in.) | Air (%) | Unit Weight (lb/ft3) | Initial Set (hrs) | Final Set (hrs) |
|---|---|---|---|---|---|---|---|
| TYPE3 (73°F - 73°F) | A | 73 | 0 | 2.1 | 150.5 | 3.98 | 5.44 |
| | B | 73 | 1/2 | 2.0 | 150.1 | | |
| TYPE3 (50°F - 50°F) | A | 38 | 3 | 2.3 | 148.4 | 6.17 | 9.25 |
| | B | 40 | 3 | 2.2 | 149.2 | | |
| TYPE3 (95°F - 95°F) | A | 95 | 1/2 | 2.2 | 146.4 | 4.15 | 5.29 |
| | B | 94 | 1/2 | 2.3 | 147.6 | | |
| TYPE3 (73°F - 95°F) | A | 73 | 1/2 | 2.2 | 149.2 | 4.15 | 5.29 |
| | B | 73 | 1/2 | 2.0 | 150.1 | | |
| TYPE3 (50°F - 95°F) | A | 38 | 3 | 2.3 | 148.4 | 6.76 | 9.56 |
| | B | 40 | 3 | 2.2 | 149.2 | | |
| AEA (73°F - 73°F) | A | 70 | 1 1/2 | 6.5 | 144.7 | 6.62 | 8.05 |
| | B | 71 | 1 1/2 | 6.5 | 144.1 | | |

## APPENDIX C

## ISOTHERMAL RIGID CRACKING FRAME

The objective of this appendix is to present the results from the isothermal rigid cracking frame. As discussed in Chapter 3, the tests were performed at three temperatures: 50°F, 73°F, and 95°F. The first temperature of the mixture identification will be the temperature at which the test was conducted.

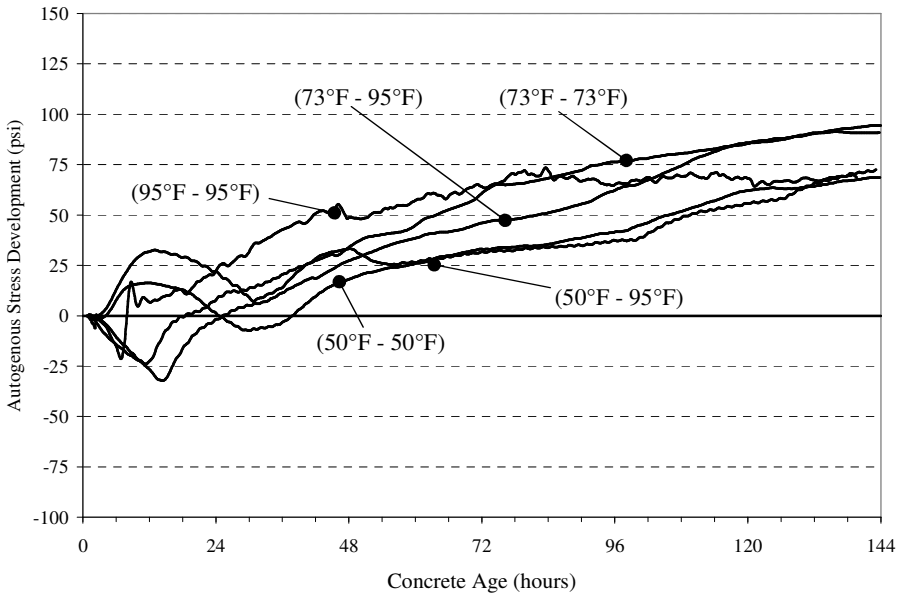


**Figure C-1:** Test results of the control mixture from the isothermal rigid cracking frame (Mix ID = CTRL)

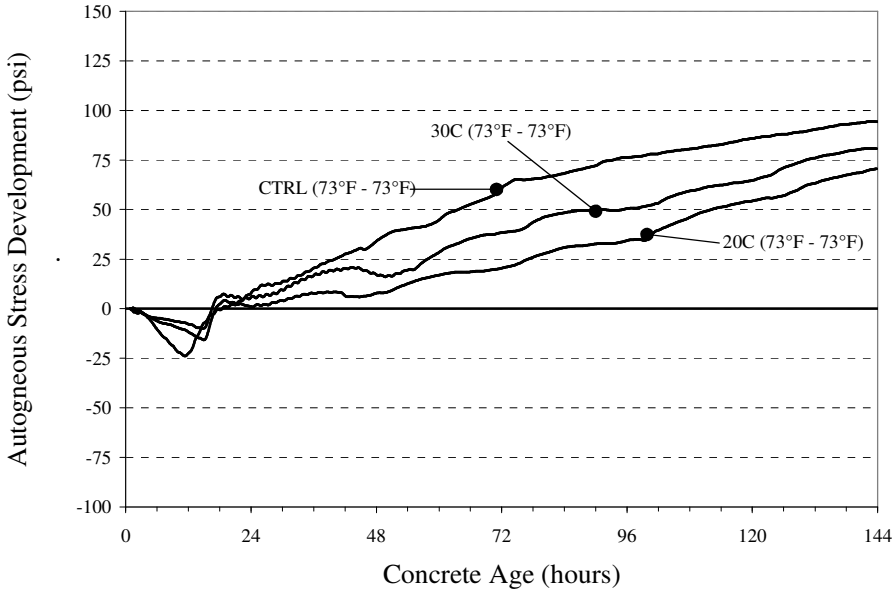


**Figure C-2:** Test results of the Class C fly ash mixture from the isothermal rigid cracking frame (Mix ID = 30C and 20C)

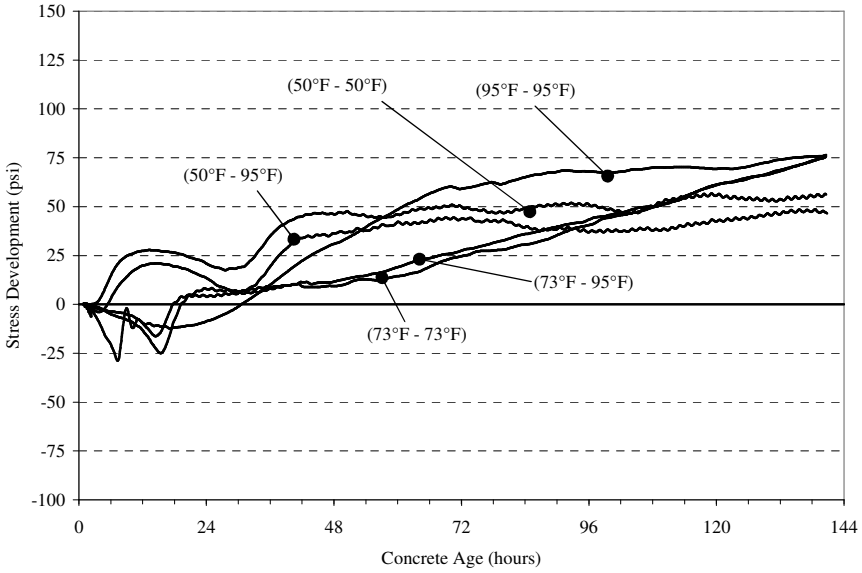


**Figure C-3:** Test results of the 30% GGBF slag mixture from the isothermal rigid cracking frame (Mix ID = 30SG)

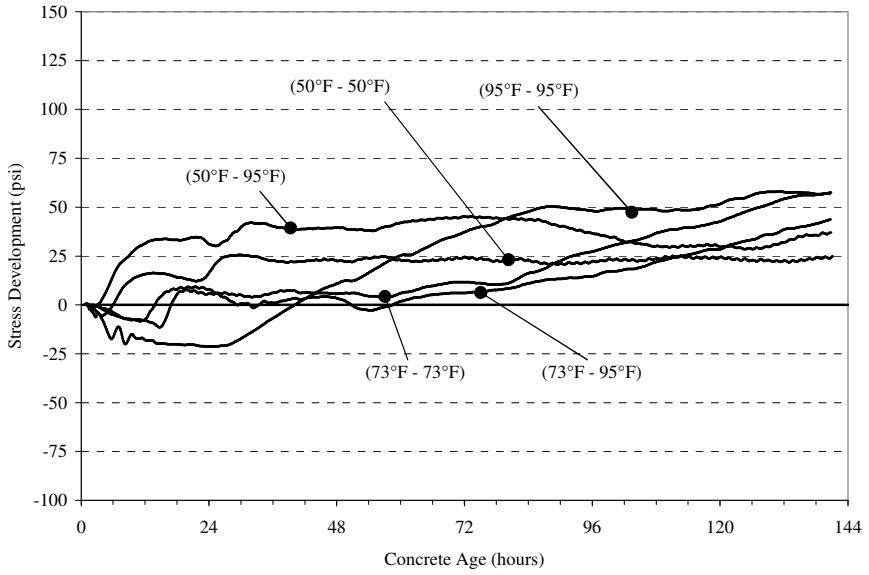


**Figure C-4:** Test results of the 50% GGBF slag mixture from the isothermal rigid cracking frame (Mix ID = 50SG)

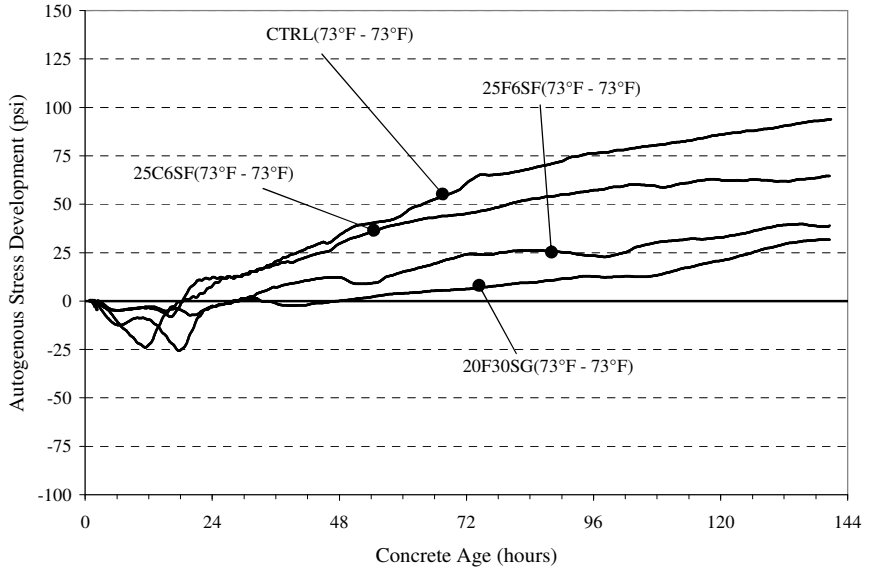


**Figure C-5:** Test results of the ternary mixtures from the isothermal rigid cracking frame (Mix ID = 25C6SF, 25F6SF, and 20F30SG)

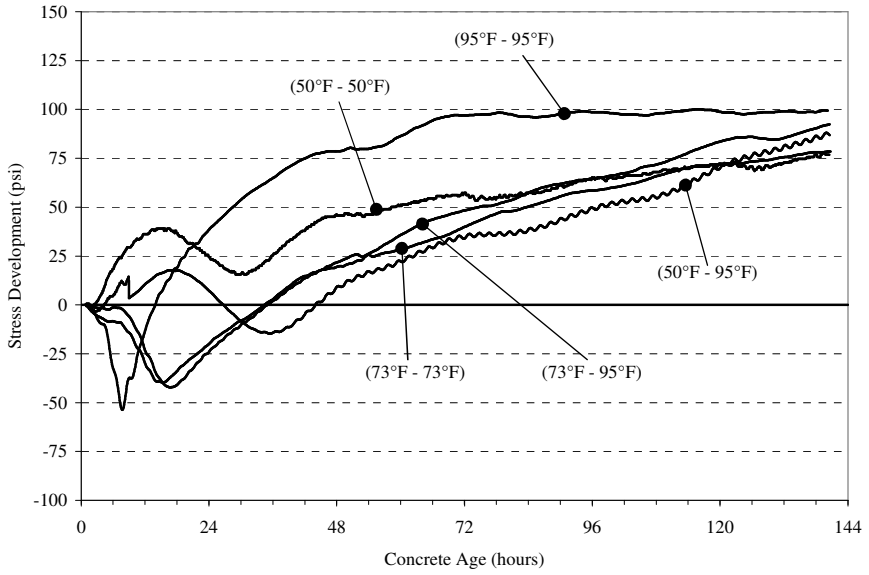


**Figure C-6:** Test results of the low water-to-cement ratio mixture from the isothermal rigid cracking frame (Mix ID = WC38)

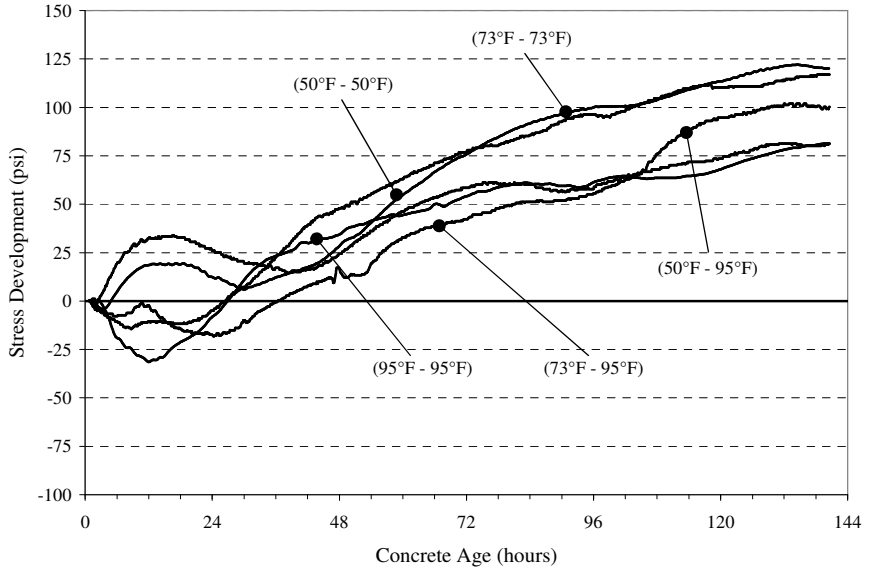


**Figure C-7:** Test results of the Type III cement mixture from the isothermal rigid cracking frame (Mix ID = TYPE3)

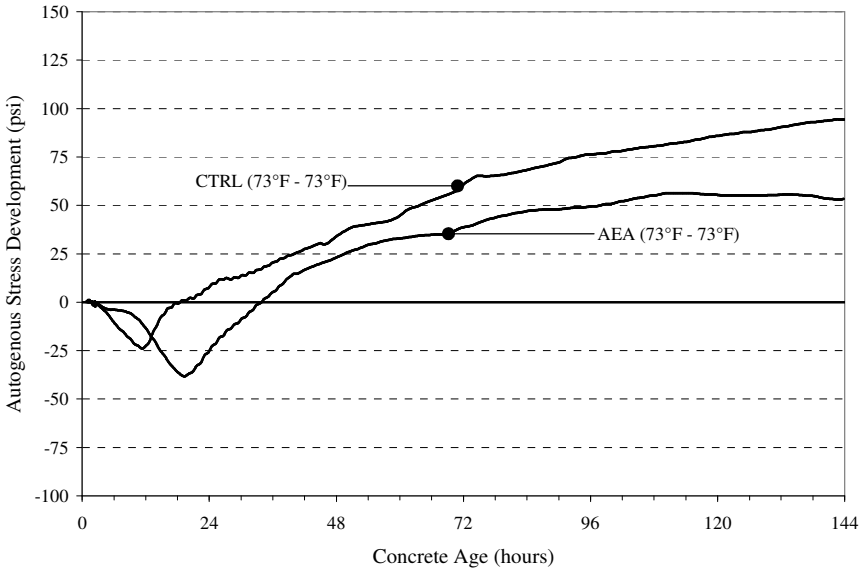


**Figure C-8:** Test results of the air entrained mixture from the isothermal rigid cracking frame (Mix ID = AEA and CTRL)

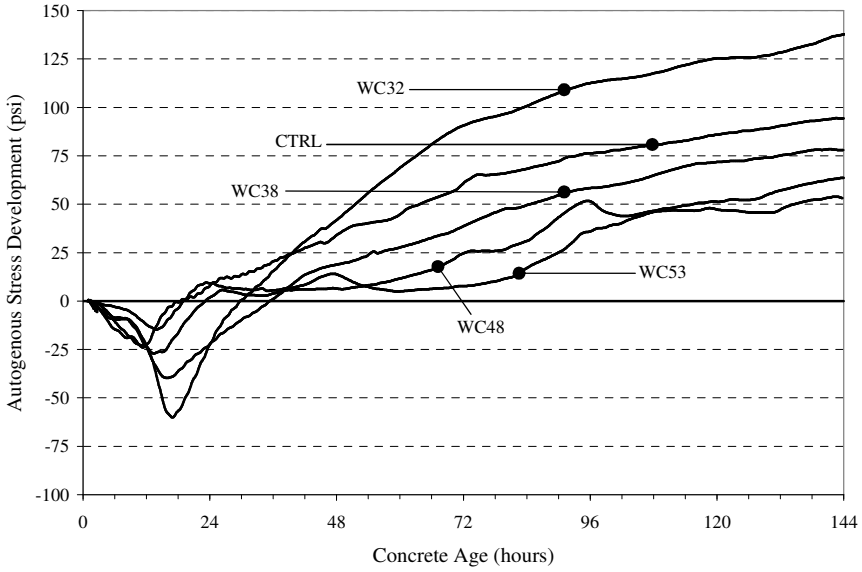


**Figure C-9:** Test results of the varied water-to-cement ratio mixtures from the isothermal rigid cracking frame (Mix ID = CTRL, WC32, WC38, WC48, and WC53)

## APPENDIX D

## HYDRATION PARAMETERS

**Table D-1:** List of hydration parameters

| Mix ID | Wall Thickness meters | Activation Energy J/mol | Tau hours | Beta | Alpha (Ultimate) | Hu J/kg |
|---|---|---|---|---|---|---|
| CTRL | 1.0 | 27,944 | 13.542 | 1.171 | 0.796 | 513,000 |
| 30C | 1.0 | 35,050 | 30.300 | 1.047 | 0.764 | 515,100 |
| 20C | 1.0 | 34,150 | 18.950 | 1.241 | 0.679 | 514,400 |
| 30SG | 1.0 | 36,300 | 20.850 | 0.877 | 0.821 | 497,345 |
| 50SG | 1.0 | 38,900 | 28.440 | 0.665 | 0.879 | 486,960 |
| 25C6SF | 1.0 | 34,500 | 23.820 | 1.144 | 0.701 | 515,000 |
| 25F6SF | 1.0 | 33,150 | 19.100 | 1.283 | 0.690 | 440,000 |
| 20F30SG | 1.0 | 34,000 | 25.650 | 1.108 | 0.856 | 355,460 |
| WC32 | 1.0 | 29,800 | 12.000 | 1.310 | 0.660 | 513,000 |
| WC38 | 1.0 | 29,400 | 12.542 | 1.251 | 0.716 | 513,000 |
| WC48 | 1.0 | 34,944 | 14.514 | 0.917 | 0.838 | 513,000 |
| WC53 | 1.0 | 34,944 | 14.961 | 0.899 | 0.870 | 513,000 |
| TYPE3 | 1.0 | 28,940 | 12.074 | 1.203 | 0.847 | 467,900 |
| AEA | 1.0 | 32,370 | 14.528 | 1.313 | 0.692 | 513,000 |